11th International Conference on Photo-Excited Processes and Applications –
ICPEPA 11

September 10-14, 2018

Vilnius, Lithuania

Programme Book of Abstracts

www.icpepa11.com

Contents

Welcome message

Dear Colleagues,

Welcome to 11th International Conference on Photo-Excited Processes and Applications – ICPEPA 11 which is waiting for you in Vilnius, Lithuania on September 10-14, 2018.

We attracted the conference to our capital to provide you with another opportunity to share new results and ideas on fundamentals of laser-matter interaction, photo-excited processes and application. Together with the Program Committee, we tried to expand the scope of the conference beyond just "laser processing." You will hear here more presentations on nanophotonics, plasmonics or spectroscopy.

I hope you will also find time for networking and establishing new contacts in a relaxing environment, as well as exploring our city and country with their long and diverse history.

Lasers and Lithuania – similarities are not only in the first letter of both words. Lasers is a fingerprint of the country and became the third religious after Christianity and basketball.

Vilnius is a city with old traditions in lasers, laser spectroscopy and technologies. Our city just recently raised the goal to become ***"the world capital of lasers"***. The ICPEPA11 conference is one of our activities seeking the goal. We provide you with the opportunity to visit leading laser companies and research laboratories, discuss with local laser people and hope you will recognise we are on the right way.

Cardially welcome you to ICPEPA 11, to Vilnius, capital of Lithuania.

Chair of ICPEPA 11
Gediminas Račiukaitis

Organizers and acknowledgments

Congress organizers

Center for Physical Sciences and Technology

CENTER
FOR PHYSICAL SCIENCES
AND TECHNOLOGY

Vilnius University

VILNIAUS UNIVERSITETAS · 1579 · UNIVERSITAS VILNENSIS

CONGRESS SECRETARIAT

CREATIVA

Gedimino ave. 24, Vilnius, Lithuania
+370 603 78930
info@creativa.lt
www.creativa.lt

Committees

CONFERENCE CHAIR

Gediminas Raciukaitis, Department of Laser Technologies, Center for Physical Sciences and Technology, Lithuania

LOCAL ORGANISING COMMITTEE

Valdas Sirutkaitis, Department of Quantum Electronics & Laser Research Center, Vilnius University, Lithuania

Arūnas Krotkus, Department of Optoelectronics, Center for Physical Sciences and Technology, Lithuania;

Audrius Dubietis, Department of Quantum Electronics & Laser Research Center, Vilnius University, Lithuania;

Gediminas Niaura, Department of Organic Chemistry, Center of Physical Sciences and Technology, Lithuania;

Mindaugas Gedvilas, Department of Laser Technologies, Center of Physical Sciences and Technology, Lithuania;

Mangirdas Malinauskas, Laser Research Center, Vilnius University, Lithuania;

Domas Paipulas, Department of Quantum Electronics & Laser Research Center, Vilnius University, Lithuania;

Paulius Gečys, Department of Laser Technologies, Center of Physical Sciences and Technology, Lithuania;

Romualdas Trusovas, Department of Laser Technologies, Center of Physical Sciences and Technology, Lithuania

OUR GLOBAL AMBASSADORS

Leonid Zhigilei, Department of Materials Science and Engineering, University of Virginia, USA;

Saulius Juodkazis, Swinburne Center for Micro-Photonics, Swinburne University, Australia;

Alexandr Ovsianikov, Institute of Materials Science and Technology, Vienna University of Technology (TU Wien), Austria;

Vygantas Mizeikis, Research Institute of Electronics, Shizuoka University, Japan

STEERING PANEL

Chunlei Guo, University of Rochester, USA;

Peter Hess, University of Heidelberg, Germany;

Ion N. Mihailescu, National Institute for Lasers, Plasma and Radiation Physics, Romania;

Aaron Peled, Holon Institute of Technology, Israel;

Jørgen Schou, Technical University of Denmark, Denmark;

Koji Sugioka, RIKEN, Japan;

Yasuyuki Tsuboi, Osaka City University, Japan;

Leonid Zhigilei, University of Virginia, USA

ICPEPA 11 INTERNATIONAL ADVISORY COMMITTEE

Salvatore Amoruso, University of Napoli Federico II, Italy;

Saulius Juodkazis, Swinburne University of Technology, Australia;

Jack Yoh, Seoul National University, South Korea;

Micha Asscher, Hebrew University, Israel;

Peter Balling, University of Århus, Denmark;

Nadezhda Bulgakova, Institute of Termophysics SB RAS – Novosibirsk, Russia / HiLASE Centre, Institute of Physics ASCR – Dolni Brezany, Czech Republic;

Anna Paola Caricato, University of Salento, Italy;

Ya Cheng, Shanghai Institute of Optics and Fine Mechanics, China;

Valentin Craciun, National Institute for Lasers, Plasma and Radiation Physics, Romania;

Philippe Delaporte, CNRS/University Aix-Marseille, France;

Thomas Dickinson, Washington State University, USA;

Maria Dinescu, National Institute for Lasers, Plasma and Radiation Physics, Romania;

Mindaugas Gedvilas, Center for Physical Sciences and Technology, Vilnius, Lithuania;

David Geohegan, Oak Ridge National Laboratory, Oak Ridge, TN, USA;

Richard Haglund Jr., Vanderbilt University, USA;

Jürgen Ihlemann, Laser-Laboratorium Göttingen e.V. (LLG), Göttingen, Germany;

Sergey I. Kudryashov, Lebedev Physical Institute, Moscow, Russia;

Thomas Lippert, Paul Scherrer Institute, Switzerland;

Yongfeng Lu, University of Nebraska Lincoln, USA;

Mangirdas Malinauskas, Vilnius University, Lithuania;

Paolo Maria Ossi, Politecnico di Milano, Italy;

Jürgen Reif, Brandenburg University of Technology, Cottbus, Germany;

Carmen Ristoscu, National Institute for Lasers, Plasma and Radiation Physics, Romania;

Pere Serra, Department of Applied Physics and Optics, University of Barcelona, Spain;

Razvan Stoian, Laboratoire Hubert Curien, University Jean-Monnet, Saint-Etienne, France;

Emmanuel Stratakis, Institute of Electronic Structure and laser (IESL), Foundation for Research and Technology-Hellas (FORTH), Greece;

Zygmunt Szymanski, Department of Laser Technology Applications, Institute of Fundamental Technological Research, Poland;

Tetsuo Tsuchiya, National Institute of Advanced Industrial Science and Technology, Tsukuba, Ibaraki, Japan

Acknowledgments

Organizers would like to express their gratitude to all those who have generously contributed to the Scientific Programme:

General sponsor:

Lietuvos mokslo taryba

Silver sponsor:

EKSPLA

LIGHT CONVERSION

Conference sponsors:

LIDARIS LDT Service

OPTOGAMA

femtika

Student award sponsor:

TRUMPF

One coffee break is sponsored by:

HAMAMATSU PHOTON IS OUR BUSINESS

Supported by:

Go Vilnius

Timetable

Monday, September 10

17:00–19:00		Registration		
19:00–21:00		Welcome reception		

Tuesday, September 11

Plenary session – session chair: Gediminas Raciukaitis

09:45-10:30 **Plenary Lecture**	TU-PL-1	Photonic Crystal Devices for Bio-Sensing and LiDAR Applications	**Toshihiko Baba**	Yokohama National University, Japan
10:30–11:00		**Coffee break**		

Fundamentals – session chair: Leonid Zhigilei

11:00-11:30 **Invited**	TU-IN-1	Relaxation cascade of laser-excited nonequilibrium electrons in solids	**Baerbel Rethfeld**	Technical University Kaiserslautern, Germany
11:30-11:50	TU-O-1	Ultrafast laser excitation of dielectrics: Measuring and modeling the transient optical properties	Peter Balling	Aarhus University, Denmark
11:50-12:10	TU-O-2	From high field plasmonics to laser driven shock kick-off: variety of ablation scenarios and navigation between them	Nail Inogamov	Landau Institute for Theoretical Physics of Russian Academy of Sciences (RAS), Russia & Dukhov Research Institute of Automatics (VNIIA), Russia
12:10-12:30	TU-O-3	Transport properties of liquid metals and semiconductors from molecular-dynamics simulation with Kubo-Greenwood formula	Kirill Migdal	Dukhov Research Institute of Automatics & Landau Institute for Theoretical Physics, Russia
12:30-12:50	TU-O-4	Nonthermal melting in Si controlled by ultrashort laser pulses	Tobias Zier	University of Kassel, Germany
12:50-13:10	TU-O-6	Electron excitation rates and saturation effects in laser-excited solids resolved by time-dependent density functional theory	Thibault J.-Y. Derrien	Institute of Physics of the Czech Academy of Sciences, Czech Republic & Max Planck Institute for Structure and Dynamics of Matter (MPSD), Germany
13:10-14:00	**Lunch**			

Highly efficient laser ablation – session chair: Chunlei Guo

14:00-14:30 **Invited**	TU-IN-2	Making Metals Transparent for White Light by Surface Plasmons	**Ru-Wen Peng**	Nanjing University, China
14:30-14:45	TU-O-7	Ultrafast laser nanofabrication of advanced nanophotonic structures	Aleksandr Kuchmizhak	Far Eastern Federal University, Russia & Russian Academy of Science, Russia
14:45-15:00	TU-O-8	Efficient Laser Scanning Ablation Procedure for Ultrafast Surface Structuring	Mindaugas Gedvilas	Center for Physical Sciences and Technology, Lithuania
15:00-15:15	TU-O-9	High-throughput ultrashort laser micromachining by MHz-THz pulse bursts	Sergey Kudryashov	ITMO university, Russia, Lebedev Physical Institute, Russia, & Far Eastern Branch of RAS, Russia
15:15-15:30	TU-O-10	Near-THz bursts of pulses –governing surface ablation mechanisms for laser material processing	Jaka Mur	University of Ljubljana, Slovenia
15:30-15:45 **Student**	TU-O-11	From the bulk to thin films: On the interplay of photomechanical and photothermal ablation induced within gold by ultrafast laser radiation	Markus Olbrich	Laserinstitut Hochschule Mittweida, Germany
15:45-16:00	TU-O-12	Vector vortex beams generated by q-plates as a versatile route to direct femtosecond laser surface structuring	Salvatore Amoruso	Università di Napoli Federico II, Italy & Complesso Universitario di Monte S. Angelo, Italy
16:00-16:30	**Coffee break**			

X-ray – session chair: Gediminas Raciukaitis

16:30-17:00 **Invited**	TU-IN-3	Modulation of Light with Metasurfaces and Phase Change Materials	**Hamza Kurt**	TOBB University of Economics and Technology, Turkey
17:00-19:00	**Poster session 1 (odd numbers)**			
19:00	**A visit to Light Conversion company and selected laboratories at Laser Research Center of Vilnius University**			

Wednesday, September 12

08:00	**Morning coffee**			
		PLD – session chair: Aaron Peled		
08:15-08:45 Invited	WE-IN-1	Laser-induced Forward Transfer (LIFT) of 3D micro-structures	**Gert-Willem Römer**	University of Twente, The Netherlands
08:45-09:00	WE-O-1	Temperature effects in synthesis of metal nanostructures by pulsed laser deposition: Comparison of substrate heating and post-annealing	Alexander V. Bulgakov	Institute of Physics of the Czech Academy of Sciences, Czech Republic & Kutateladze Institute of Thermophysics SB RAS, Russia
09:00-09:15	WE-O-2	Short laser pulses excited processes: Applications to nanobiomedicine	Ion N. Mihailescu	National Institute for Lasers, Plasma and Radiation Physics, Romania
09:15-09:30	WE-O-3	Large optical nonlinearity in gold nanoparticle films made by PLD	James G Lunney	Trinity College Dublin, Ireland
09:30-09:45	WE-O-4	Thin films for solar cells produced by pulsed laser deposition	Jørgen Schou	Technical University of Denmark, Denmark
09:45-10:00	WE-O-5	One- and three-dimensional analysis of colliding laser-induced plumes	Ikurou Umezu	Konan University, Japan
10:00-10:15	WE-O-6	10B-enriched neutron conversion layers deposited by pulsed laser deposition at different wavelengths	Anna Paola Caricato	University of Salento-Lecce, Italy & National Institute of Nuclear Physics (INFN) - Sezione di Lecce, Italy
10:15-10:30 Student	WE-O-7	Surface microstructuring over wide area on nickel plating by laser-Induced back deposition in ambient air	Kazuki Koda	DENSO CORPORATION, Japan & Osaka University, Japan
10:30-11:00	**Coffee break**			
		3D printing – session chair: Yongfeng Lu		
11:00-11:30 Invited	WE-IN-2	Three-dimensional μ-Printing: An enabling Technology	**Georg von Freymann**	Technische Universität Kaiserslautern, Germany
11:30-11:45	WE-O-8	Continuous 3D Writing for Stich-Free 3D Meso-Scale Laser Printing	Mangirdas Malinauskas	Vilnius University, Lithuania
11:45-12:00	WE-O-9	Simple method for birefringence imaging of natural and laser fabricated polymers	Reo Honda	Tokyo Institute of Technology, Japan
12:00-12:15 Student	WE-O-10	3D printed Polarization Micro-Optics: Fresnel Rhomb printed on an optical fiber	Andrea Bertoncini	King Abdullah University of Science and Technology (KAUST), Saudi Arabia
12:15-12:30	WE-O-11	Laser Printing of Functional Resonant Dielectric Nanoparticles	Sergey Makarov	ITMO University, Russia
12:30-13:00 Invited	WE-IN-3	Complex and hybrid 3D printed microoptics	**Harald Giessen**	University of Stuttgart, Germany
13:00-14:00	**Lunch**			
14:00-17:30	**Excursion Vilnius old town & Trakai castle**			
19:00	**Banquet in Palace of the Grand Dukes of Lithuania (Cathedral square 4, Vilnius) in old town**			

Thursday, September 13

08:00	**Morning coffee**			
		Graphene and carboneous materials – session chair: Mangirdas Malinauskas		
08:15-08:45 Invited	TH-IN-1	Two-photon polymerization for three-dimensional assembly of aligned carbon nanotubes	**Yong Feng Lu**	University of Nebraska-Lincoln, USA
08:45-09:00 Student	TH-O-1	Laser-induced graphene ablation and graphene oxide reduction for application as electrodes in thin-film transistors	Maren Kasischke	Ruhr Universität Bochum, Germany
09:00-09:30	TH-O-3	Laser-Induced Processes in Nanotechnology	Wolfgang Kautek	University of Vienna, Austria
09:30-09:45	TH-O-4	Force Sensor Fabrication by AgNWs Film using 532nm Pulses Laser	Wen-Tse Hsiao	National Applied Research Laboratories, Taiwan
09:45-10:00	TH-O-5	Threshold fluence of femtosecond laser ablation for metals	Masaki Hashida	Kyoto University, Japan
10:00-10:15 Student	TH-O-6	Time-resolved investigation of laser-induced damage fatigue of single layer dielectric coatings	Linas Smalakys	Vilnius University, Lithuania

10:15-10:30	TH-O-7	Determination of material parameters for modelling of ultra-short pulse ablation threshold in transparent, dielectric material	Marco Jupe	Laser Zentrum Hannover e.V., Germany
10:30-11:00	**Coffee break**			
		Simulation of photo-excited processes – session chair: Peter Balling		
11:00-11:30 Invited	TH-IN-2	Ultrafast Laser-Induced Surface and Bulk Nanostructuring: Similarities Revealed by Electromagnetic Modeling	**Jean-Philippe Colombier**	University of Lyon, France
11:30-11:50	TH-O-8	Large-scale atomistic simulations of the generation of nanoparticles and surface nanostructuring by short pulse laser ablation in liquids	Leonid V. Zhigilei	University of Virginia, USA
11:50-12:10	TH-O-10	Ultrafast dynamics of non-equilibrium electrons and strain generation under femtosecond laser irradiation of Nickel	George Tsibidis	IESL-FORTH, Greece
12:10-12:30	TH-O-11	Model for UV induced CdS nanoparticle formation in a polymer matrix	Nikita Bityurin	Institute of Applied Physics Russian Academy of Sciences, Russia
12:30-13:00 Invited	TH-IN-3	Intense femtosecond laser interaction with aqueous solutions for X-ray, THz wave, and ultrasound emission	**Koji Hatanaka**	Research Center for Applied Sciences, Academia Sinica, Taiwan
13:00-14:00	**Lunch**			
		LIPSS – session chair: Saulius Juodkazis		
14:00-14:30 Invited	TH-IN-4	Periodic phase-change structures in silicon: Control and formation mechanism	**Jan Siegel**	Instituto de Óptica, IO-CSIC, Spain
14:30-14:45	TH-O-12	Formation of Highly-regular LIPSS on Cr Under Condition of Strong Ablation	Iaroslav Gnilitskyi	NoviNano Inc., Ukraine & University of Modena and Reggio Emilia (UNIMORE), Italy
14:45-15:00	TH-O-13	Ultrafast microscopy in resolving femtosecond laser-induced surface structuring	Chunlei Guo	University of Rochester, USA & Changchun Institute of Optics, Fine Mechanics, and Physics, China
15:00-15:15 Student	TH-O-14	Control of femtosecond laser induced periodic nanostructures by changing dielectric constant of polymers on Ti surface	Naoki Shinohara	Osaka University, Japan
15:15-15:30 Student	TH-O-15	Laser fabrication of Si nanosheets via nanoplasmonic self-organization in liquid CS2	Irina Saraeva	Lebedev Physical Institute, Russia
15:30-15:45 Student	TH-O-16	Ablation suppression of titanium surface interacted with two color double-pulse beam of femtosecond laser	Keisuke Takenaka	Osaka University, Japan
15:45-16:00	TH-O-17	Nanometer-Precision Measurement of Surface Morphology Change Induced by Femtosecond Laser Ablation	Shuntaro Tani	The University of Tokyo, Japan
16:00-16:30		**Coffee break**		
		Bio-medical applications – session chair: Gediminas Raciukaitis		
16:30-17:00 Invited	TH-IN-5	The functional roles of vibronic coupling in biological light harvesting	**Jürgen Hauer**	Technische Universität München, Germany
17:00-19:00		**Poster session 2 (even numbers)**		
19:00	**A visit to Ekspla company and Department of Laser Technologies of FTMC**			

Friday, September 14

08:00		**Morning coffee**		
		Nanotechnologies – session chair: Sergey Kudryashov		
08:15-08:45 Invited	FR-IN-1	Nano-scale Laser Printing on Template Optical Metasurfaces	**Anders Kristensen**	Technical University of Denmark, Denmark
08:45-09:00	FR-O-1	Laser patterning of metal cylinders for roll to toll application	Klaus Zimmer	Leibniz Institute of Surface Engineering (IOM), Germany
09:00-09:15	FR-O-2	Growth of regular micro-pillars arrays on steel by polarization-controlled laser interference patterning	Bogdan Voisiat	Technische Universität Dresden, Germany
09:15-09:30	FR-O-3	Versatile surface structuring using cylindrically polarized femtosecond laser beams	George Tsibidis	IESL-FORTH, Greece & University of Crete, Greece

09:30-0945	FR-O-4	Optical elements for synchroton X-ray and THz beamlines	Saulius Juodkazis	Swinburne University of Technology, Australia & the Victorian Node of the Australian National Fabrication Facility, Australia
09:45-10:00	FR-O-5	Photodeposition of Nanometric Thin Films from Bio-Chromophores	Aaron Peled	Holon Institute of Technology (HIT), Israel
10:00-10:15 Student	FR-O-6	Qualitative and Quantitative Investigation of Free-Form fs Laser Made Structures to Intense Ultrafast Laser Radiation	Linas Jonušauskas	Vilnius University, Faculty of Physics, Laser Research Center
10:15-10:30	FR-O-7	Dicing of soda-lime glass with elliptical Bessel beam	Paulius Gečys	Center for Physical Sciences and Technology, Lithuania
10:30-11:00	**Coffee break**			
Photo-excited processes & spectroscopy – session chair: Salvatore Amoruso				
11:00-11:30 Invited	FR-IN-2	Optical probing of charge carrier motion dynamics in disordered, heterogeneous organic and hybrid materials	**Vidmantas Gulbinas**	Center for Physical Sciences and Technology, Lithuania
11:30-11:45	FR-O-8	Luminescent carbon dots synthesized by the laser ablation in liquid	Justyna Chrzanowska-Giżyńska	Polish Academy of Sciences, Poland
11:45-12:00	FR-O-9	Interaction of femtosecond white light continua generated by different wavelengths in bulk transparent media	Mikas Vengris	Vilnius University, Lithuania
12:00-12:15	FR-O-10	High-quality CsPbBr3 nanolasers fabricated by spray forming	Anatoly Pushkarev	ITMO University, Russia
12:15-12:30	FR-O-11	Photonic Crystal Microchip Laser	Kęstutis Staliūnas	Institucio Catalana de Reserca i Estudis Avancats (ICREA), Spain, Universitat Politecnica Catalunya (UPC), Spain
12:30-13:00	FR-IN-3	Spectroscopy in Flatland	**Sejeong Kim**	University of Technology Sydney (UTS), Australia
13:00-14:00	**Lunch**			
Laser generation of nanoparticles – session chair: Mindaugas Gedvilas				
14:00-14:30 Invited	FR-IN-4	Nanofabrication of metallic structures by femtosecond laser-induced photoreduction	**Atsushi Ono**	Shizuoka University, Japan
14:30-14:45	FR-O-12	Up-scaling for manipulation of particle properties on the nano- an sub-micrometer scale by laser irradiation in liquids	Marcus Lau	TRUMPF Laser- und Systemtechnik GmbH, Germany
14:45-15:00	FR-O-13	Laser Induced Quantum Dots generation	Iaroslav Gnilitskyi	University of Modena and Reggio Emilia, Italy
15:00-15:15 Student	FR-O-14	Laser-ablative fabrication of hybrid meta-dielectric nanoparticles via laser-assisted heterogeneous condensation	Irina Saraeva	Lebedev Physical Institute, Russia
15:15-15:30	FR-O-15	Nanosecond Laser Treatment of Thin Gold Film on ITO Glass	Evaldas Stankevičius	Center for Physical Sciences and Technology, Lithuania
15:30-15:45	FR-O-16	Magneto-optical Faraday effect of waveguide structures fabricated inside silica xerogels containing magnetic nanoparticles	Seisuke Nakasima	Shizuoka University, Hamamatsu, Shizuoka, Japan
15:45-16:00	FR-O-17	Optical Properties of the Solar Cells with Nanostructures Formed by XeCl Excimer Laser	Mitsuhiro Kusaba	Osaka Sangyo University, Japan
16:00	**Awards and closing of the conference**			

POSTERS

P1 Student	Synthesis of Acceptor Doped ZnO Films by Inductively-Coupled Plasma-Assisted Pulsed-Laser Deposition	Hayato Tsukuda	Nihon University, Japan
P2	Thin WB_x and $W_xTi_{1-x}B_2$ films deposited by combined magnetron sputtering and pulsed laser deposition technique	Tomasz Moscicki	Institute of Fundamental Technological Research, Polish Academy of Science, Poland
P3 Student	Optimizing copper profiles for open circuit voltage boost in Cu_2ZnSnS_4 solar cells by pulsed laser deposition	Mungunshagai Gansukh	Technical University of Denmark, Denmark
P4	An optical method for determination of the mass thickness of thin gold films with arbitrary morphology	Sergey V. Starinskiy	S.S. Kutateladze Institute of Thermophysics SB RAS, Novosibirsk, Russia
P5 Student	In situ laser-induced codeposition of metals for fabrication of non-enzymatic sensor materials	Alexandra Smikhovskaia	Saint Petersburg State University, Russia
P6 Student	Influence of ambient gas on microstructure formation on Ni surface by laser-Induced back deposition	Kazuki Koda	DENSO CORPORATION, Japan & Osaka University, Japan
P7	Investigation of optical and electrical properties of Sc-doped ZnO thin films deposited by co-sputtering	Alexander Axelevitch	Holon Technological Institute (HIT), Israel
P8	Tailoring diamond's optical properties via direct femtosecond laser nanostructuring	Miguel Martínez-Calderón	CEIT-IK4, Spain
P9 Student	Effect of surface roughness on the ultra-short pulsed laser ablation fluence threshold of zinc and steel	Hasib Mustafa	University of Twente, the Netherlands
P10	Effects of the repetition rate on femtosecond laser induced periodic surface structures on silicon	Jijil JJ Nivas	Università di Napoli Federico II, Italy & CNR-SPIN UOS Napoli, Italy
P11	Control of femtosecond laser-induced periodic surface structures on Ni	Taek Yong Hwang	Korea Institute of Industrial Technology, South Korea
P12 Student	Investigation of large-area femtosecond laser-induced periodic surface nanostructuring of metals	Marek Stehlík	HiLASE Centre, Institute of Physics of the Czech Academy of Sciences, Za Radnicí 828, 25241 Dolní Břežany, Czech Republic
P13 Student	Ultrashort laser non-Gaussian pulse induced temperature field dynamics	Alexander Fedotov	Belarusian State University, Minsk, Belarus
P14	Electron-phonon coupling after ultrashort laser-excitation in gold	Sebastian T. Weber	Technische Universitaet Kaiserslautern, Germany
P15 Student	The resolution study of the 3D printer EOSINT M280 for iron-based powders	Ada Steponavičienė	Center for Physical Sciences and Technology, Vilnius, Lithuania
P16	Design of fs-laser writable borate glasses for photonic devices	Jan Siegel	Instituto de Optica-CSIC
P17	Selective surface modification on PEDOT:PSS films for planar heater fabrication using short and long laser wavelengths	Wen-Tse Hsiao	Instrument Technology Research Center, National Applied Research Laboratories, Taiwan
P18	A micro sensor fabricated on bipod structure using 355 nm pulsed UV laser for evaluating the deformation by scattering light	Kuo-Cheng Huang	Instrument Technology Research Center, National Applied Research Laboratories, Taiwan
P19	Laser surface texturing of copper and variation of the wetting response with the laser pulse fluence	Elaheh Allahyari	Dipartimento di Fisica Ettore Pancini, Università di Napoli Federico II
P20 Student	Optimization of P3 Laser Process in CIGS Thin-Film Solar Cells	Edgaras Markauskas	Center for Physical Sciences and Technology, Vilnius, Lithuania

Tuesday, 11th of September, 17:00-19:00 (odd numbers).

Thursday, 13th of September, 17:00-19:00 (even numbers).

Presenters are requested to be close to their posters during the whole allocated session.

POSTERS

P21 Student	New laser assisted method for copper circuit fabrication on dielectrics	Karolis Ratautas	Center for Physical Sciences and Technology, Vilnius, Lithuania
P22	Delamination of GaN coating from sapphire substrate using femtosecond laser lift-off technique	Domas Paipulas	Laser Research Center, Vilnius University, Lithuania
P23	Graphene formation in wood by 1064 nm laser irradiation	Romualdas Trusovas	Center for Physical Sciences and Technology
P24 Student	Dynamic Optical Properties of Graphene Layers with Different Preparation and Morphology	Erika Rajackaitė	Kaunas University of Technology, Institute of Materials Science
P25	Analysis of ultrafast optical properties and morphology of diamond-like carbon nanocomposites with aluminium nanoparticles	Domantas Peckus	Kaunas University of Technology, Lithuania
P26	Formation of laser-induced periodical surface structures on multilayer graphene with femtosecond pulses	Tatsiana Smirnova	Scientifi c-Practical Material Research Centre, National Academy of Sciences of Belarus, Belarus & Belarusian State University, Belarus
P27	Comparative single-shot femtosecond laser ablation of solid surfaces in air and liquid environments	Sergey Kudryashov	ITMO University, Russia & P.N. Lebedev Physical Institute, Russia
P28 Student	Single- shot pulse ablation of silicon by ultrashort laser pulses of varying duration	Nikita Smirnov	P.N. Lebedev Physical Institute, Russian Academy of Sciences, Russia
P29 Student	Laser ablation of material surfaces by ultrashort pulses of varying duration	Nikita Smirnov	P.N. Lebedev Physical Institute, Russian Academy of Sciences, Russia
P30 Student	Femtosecond laser micro-processing of thin films using diffractive optical elements	Sofia F. Umanskaya	P.N. Lebedev Physical Institute, Russian Academy of Sciences, Russia, Samara National Research University, Russia, & National Research Nuclear University MEPHi, Russia
P31 Student	Temporally and spatially resolved investigations on resonant-infrared ablation of organic materials caused by ultrafast mid-IR laser radiation	Markus Olbrich	Laserinstitut Hochschule Mittweida, Germany
P32 Student	Case study on the dynamics of ultrafast excitation of gold thin films and bulk PMMA by ultrafast pump-probe reflectometry and ellipsometry	Markus Olbrich	Laserinstitut Hochschule Mittweida, Germany
P33 Student	Efficient picosecond laser ablation on cylindrical surfaces	Mantas Gaidys	Center for Physical Sciences and Technology, Vilnius, Lithuania
P34 Student	Fabrication of scanned three-dimensional object by efficient laser ablation	Augustinas Skirsgilas	Center for Physical Sciences and Technology, Vilnius, Lithuania
P35 Student	Rapid and high-quality 3D fabrication by efficient ultrashort laser ablation	Andrius Žemaitis	Center for Physical Sciences and Technology, Vilnius, Lithuania
P36 Student	Photosensitive naturally derived resins toward optical 3D printing	Edvinas Skliutas	Laser Research Center, Vilnius University, Lithuania
P37	Large-Scale 3D microstructured scaffolds fabricated by direct laser writing out of biocompatible polymers	Sima Rekštytė	Laser Research Center, Vilnius University, Lithuania
P38	3D polymeric microstructures for micro-actuation and environmental sensing fabricated by direct laser writing technique	Mae Nishimura	Research Institute of Electronics, Shizuoka University, Japan
P39 Student	Lithography of True 3D Ceramic Structures on the Microscale	Viktorija Padolskytė	Laser Research Center, Vilnius University, Lithuania & Femtika Ltd., Lithuania
P40 Student	Investigation of mechanical properties of polymeric microstructures using glass microcantilevers	Titas Tičkūnas	Laser Research Center, Vilnius University, Lithuania
P41 Student	Fabrication and surface engineering of silicon nanocrystals by laser-induced processes in liquid	Natalie Tarasenka	B.I. Stepanov Institute of Physics Minsk, Belarus

POSTERS

P42 Student	Photocatalytic TiO_2-based fine particles synthesized by pulsed-laser ablation in $SrCl_2$ solution	Shu Kaiya	Nihon University, Japan
P43 Student	Laser generation of photoactive nanoparticles	Alina Georgiana Ilie	National Institute for Lasers, Plasma and Radiation Physics, Romania & University of Bucharest, Romania
P44 Student	Laser ablative hybrid Si-Au nanoparticles	Anastasia Ivanova	P.N. Lebedev Physical Institute, Russian Academy of Sciences, Russia & National Research Nuclear University MEPhI, Russia
P45 Student	Fs/ps pulsewidth-dependent yield of Au, Ag and Si nanoparticles	Irina Saraeva	P.N. Lebedev Physical Institute, Russian Academy of Sciences, Russia
P46 Student	Micro-Sampling of Biological Tissue by Substrate-Mediated Laser Ablation: Toward Spatially-Resolved Proteomics at μm Scale	Tony Maulouet	Université Lille 1 - PhLAM/Prism, France
P47	Contact laser surgery of oncological tumors with a minimum of dissemination of tumor in the operating field on the basis of the technology of the absorbing layer at the tip of quartz fiber	Nikita Bityurin	Institute of Applied Physics, Russian Academy of Sciences, Russia
P48	2D mesoscale colloidal crystal patterns on polymer substrates due to control of wettability of materials by UV treatment	Nikita Bityurin	Institute of Applied Physics, Russian Academy of Sciences (IAP RAS), Russia
P49	Patterning of photoinduced nanocomposites by focused laser beam: a model	Nikita Bityurin	Institute of Applied Physics, Russian Academy of Sciences, Russia
P50	In-situ monitoring of evolution of optical properties of UV LED irradiated polymer-based photoinduced nanocomposites	Anton A. Smirnov	Institute of Applied Physics, Russian Academy of Sciences, Russia
P51	Nanopattern formation by local laser annealing of diblock copolymer (BCB) films	Klaus Zimmer	Leibniz Institute of Surface Engineering, Leipzig, Germany
P52	Control of wettability on PLLA surface by femtosecond laser irradiation for development of advanced implant devices	Yuji Sato	Joining and Welding Research Institute, Osaka University, Japan
P53 Student	Fabrication of elastomeric structures via stereolithography and optimization of their biocompatibility	Giedrė Grigalevičiūtė	Laser Research Center, Vilnius University, Lithuania
P54	Nanometric z-profiling of Bio-chromophore layers by DRLS	Aaron Peled	Holon Institute of Technology, Israel
P55 Student	Antibacterial effect of nanostructured silicon	Alena Nastulyavichus	P.N. Lebedev Physical Institute, Russian Academy of Sciences, Russia
P56 Student	Nanosecond and femtosecond laser ablation of silver films of variable thickness	Alena Nastulyavichus	P.N. Lebedev Physical Institute, Russian Academy of Sciences, Russia
P57 Student	Femtosecond laser fabrication, spectral characterization and modelling of plasmonic nanostructures	Nikolay Busleev	Lebedev Physical Institute, Russia & Samara National Research University, Russia
P58 Student	High-efficiency fabrication of geometric phase spiral phase plates by femtosecond laser	Jian-Guan Hua	State Key Laboratory of Integrated Optoelectronics, Jilin University, China
P59 Student	High-throughput ablative pulsed-laser pattering of various nanoplasmonic films	Pavel A. Danilov	P.N. Lebedev Physical Institute, Russia
P60	Colloidal particle lens arrays-assisted surface nano-patterning by two-coloured femtosecond pulses. The effect of delay time between the pulses of different frequencies	Andrey Afanasiev	Institute of Applied Physics, Russian Academy of Sciences, Russia

POSTERS

P61 Student	How uniform is uniform – Characterisation and optimisation of structures fabricated by Direct Laser Interference Patterning	Mikhael El-Khoury	Fraunhofer-Institut für Werkstoff- und Strahltechnik (IWS), Dresden, Germany
P62	Laser fabrication of optical components for THz radiation	Simonas Indrišiūnas	Center for Physical Sciences and Technology, Vilnius, Lithuania
P63	Direct laser writing and etching of high aspect ratio structures in fused silica using different etchants	Simas Butkus	Laser Research Center, Vilnius University, Lithuania
P64	Recording of diffraction elements in fused silica by the deep focused femtosecond pulses	Valdemar Stankevič	Center for Physical Sciences and Technology, Vilnius, Lithuania & ELAS Ltd., Lithuania
P65 Student	Femtosecond laser micromachining of glass samples in air, water and various solutions (NaCl, KOH)	Lina Mačernytė	Laser Research Center, Vilnius University, Lithuania
P66 Student	Application of asymmetrical Bessel-like laser beams for glass processing	Juozas Dudutis	Center for Physical Sciences and Technology, Vilnius, Lithuania
P67	Direct laser writing of photonic microstructures for spatial light filtering using Gaussian and Bessel beams	Vytautas Purlys	Laser Research Center, Vilnius University, Lithuania & Femtika Ltd., Lithuania
P68	Fabrication of perfect absorber metasurface structures by direct laser write technique and their post-fabrication tuning	Subhashri Chatterjee	Research Institute of Electronics, Shizuoka University, Japan
P69	Numerical Study on Power Absorption Distribution of Powders in Selective Laser Melting	Tomomasa Ohkubo	Tokyo University of Technology, Japan
P70	In situ X-ray observation of pure-copper layer formation with blue direct diode laser	Yuji Sato	Joining and Welding Research Institute, Osaka University, Japan
P71 Student	Laser microwelding application for wire to flat geometry of dissimilar materials in electromechanical components	Mahdi Amne Elahi	University of Luxembourg, Luxembourg
P72 Student	Investigation on autogenous laser welding of copper to aluminium	Karthik Mathivanan	University of Luxembourg, Luxembourg
P73	Pulse length and shape in two-photon excited theranostics	Jaka Mur	Jožef Stefan Institute, Ljubljana, Slovenia
P74	Application of laser induced breakdown spectroscopy to femtosecond laser micromachining of glass by use of single pulses and pulse trains	Ona Balachinaitė	Laser Research Center, Vilnius University, Lithuania
P75	Characterization of latent 3D laser exposure patterns in photoresist using photoluminescence quenching	Edy Yulianto	Research Institute of Electronics, Shizuoka University, Japan
P76 Student	Active tuning of surface plasmon resonance by controlling interparticle distance of gold nanoparticles	Ayana Mizuno	Shizuoka University, Japan
P77 Student	Control of expansion processes by counter shock waves during pulsed laser ablation	Keita Katayama	Graduate school of Natural Science, Konan University, Japan
P78 Student	Impact of the wall roughness on the quality of micrometric nozzles manufactured from fused silica by hybrid laser processing	Vidmantas Tomkus	Center for Physical Sciences and Technology, Vilnius, Lithuania
P79	The approximations of Boltzmann transport equation for modelling of ultrafast photoconductive terahertz antennas	Gediminas Šlekas	Vilnius Gediminas Technical University, Lithuania & Center for Physical Sciences and Technology, Vilnius, Lithuania
P80	Microstructure and mechanical properties of parts obtained by Direct Metal Laser Sintering	Genrik Mordas	Center for Physical Sciences and Technology, Vilnius, Lithuania
P81	Infrared-laser precipitation of Dy-Yb codoped SrF_2 nanocrystals in glass and emission enhancement	Ki-Soo Lim	Chungbuk National University, Republic of Korea
P82	Spatial-temporal dynamics of vortex light bullet at femtosecond filamentation in Kerr media	Olga Fedotova	Scientific Practical Materials Research Centre of NAS of Belarus, Belarus & Belarusian State University, Belarus

POSTERS

P83 Student	Forming accelerating light beams with phase masks fabricated from glass	Mykolas Karpavičius	Laser Research Center, Vilnius University, Lithuania
P84 Student	Structuring of geometric phase microoptics via 3D laser nanolithography	Simonas Varapnickas	Laser Research Center, Vilnius University, Lithuania
P85	Direct laser writing of spin-orbital angular momentum coupler microstructures	Ryosuke Shoyama	Research Institute of Electronics, Shizuoka University, Japan
P86 Student	From stealth dicing at 1342 nm to diamond nanostructuring at 224 nm: emerging opportunities for a new mode-locked laser	Ernestas Kuodys	Center for Physical Sciences and Technology, Vilnius, Lithuania
P87 Student	Photonic crystals for visible wavelength via physical vapour deposition	Darius Gailevičius	Vilnius University, Lithuania & Femtika Ltd., Lithuania
P88	Influence of the third order nonlinearity on the instabilities in the synchronously pumped optical parametric oscillator	Viktorija Tamulienė	Laser Research Center, Vilnius University, Lithuania
P89	BBO crystal for characterization of mid-infrared laser pulses	Gintaras Tamošauskas	Laser Research Center, Vilnius University, Lithuania
P90 Student	Simultaneous ultrabroad-band nonlinear interactions in polycrystalline ZnS and ZnSe	Rosvaldas Šuminas	Laser Research Center, Vilnius University, Lithuania
P91 Student	Filamentation of femtosecond mid-infrared pulses in crystalline silicon	Agnė Marcinkevičiūtė	Laser Research Center, Vilnius University, Lithuania
P92 Student	Tuneable z-scan setup as a versatile tool to improve the efficiency of PDT and high resolution 3D printing	Wolfgang Steiger	Institute of Materials Science and Technology, TU Wien, Austria. Austrian Cluster for Tissue Regeneration
P93	Nonlinear response of and energy deposition in bulk silicon and germanium driven by intense femtosecond laser	Tzveta Apostolova	Institute for Nuclear Research and Nuclear Energy, INRNE-BAS, Sofi a, Bulgaria
P94	Fabrication of carbonaceous pattern based on liquid polymer and laser	Yong-Won Ma	Pusan National University

General information

General information

Congress Venue

Radisson Blu Hotel Lietuva****
Konstitucijos Ave. 20, Vilnius

Largest conference venue and hotel in the heart of Vilnius Conveniently located near the city's historic and business districts, this Vilnius hotel overlooks Old Town and the river. The 291 comfortable rooms include Free high-speed, wireless Internet, and the on-site Riverside Restaurant serves international specialties while the hotel bars provide creative cocktails and light snacks. Guests can also enjoy the fitness center, sauna and beauty salon.

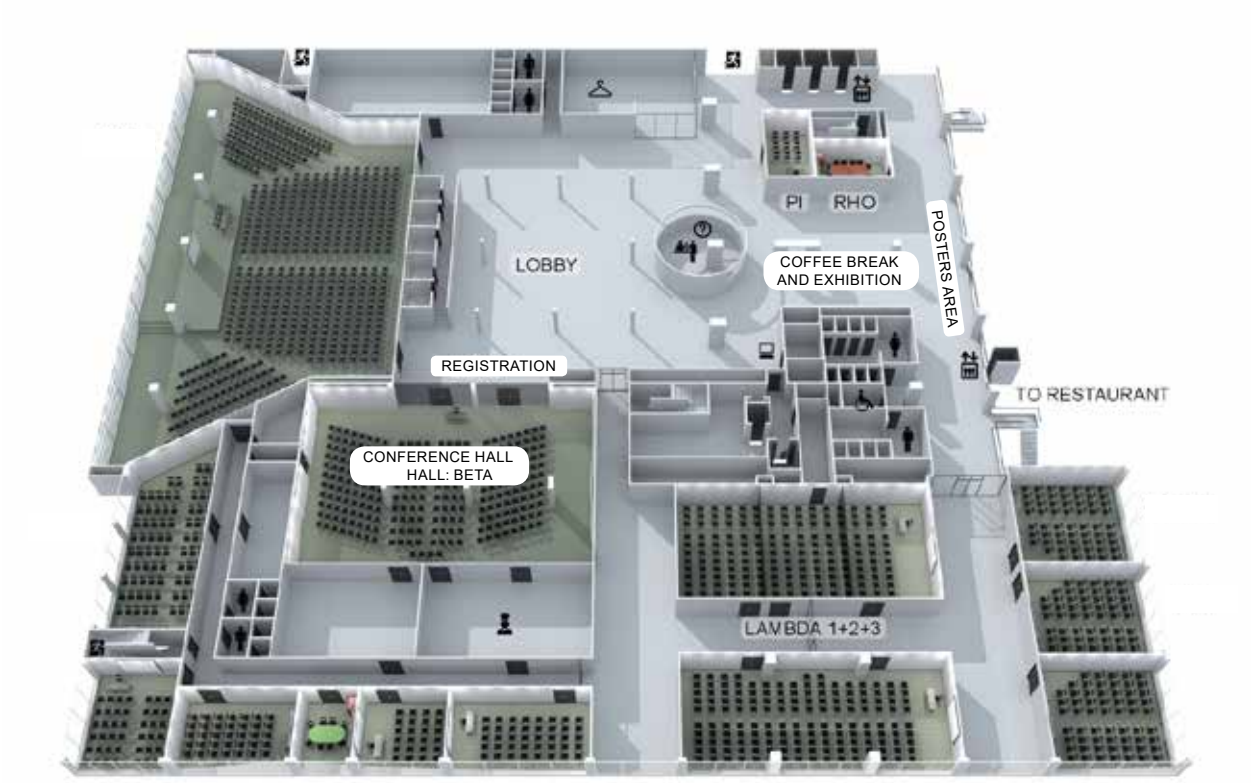

Transport options

GETTING TO THE CENTRE OF THE CITY:

By bus:
No. 1 AIRPORT-RAILROAD AND BUS STATION
Runs every 40-50 minutes. First bus leaves from the airport at 05:49AM, the last one at 22:23PM;

No. 3G AIRPORT-CENTER-FABIJONIŠKĖS
Runs every 8-10 minutes. First bus leaves from the airport a 05:22 AM, the last one leaves at 23:11 PM;

No. 88 AIRPORT-KONSTITUCIJOS PR.
Runs every16-17 minutes. First bus leaves from the airport a 05:16 AM, the last one leaves at 01:39 PM.

Bus times are available at bus stops or on the website www.stops.lt
Once you have boarded public transportation, you can purchase a one way ticket from the driver that costs 1 euro. You need to mark the paper ticket at one of the several small red metal ticket validators found on the stands in the bus or by placing it in the yellow electronic ticket validator.

By train:
Distance from the airport to Vilnius Railway station is about 5 km, the journey takes up to 8 minutes. Trains run approximately every 40 minutes. The schedule can be found at www.litrail.lt. Tickets can be purchased on the train or at Vilnius Railway Station. Train timetable is available on www.litrail.lt

By taxi:
Next to the airport there is a taxi rank. There are always plenty of taxis there. You can also call a taxi by phone or to book a taxi at Vilnius Tourist Information Centre (Airport Arrival Hall). Taxi booking and information www.etaksi.lt.

General information

Lunches

Lunches are served in Restaurant “Riverside”, ground floor.

Tuesday (September 11)	13:00-14:00
Wednesday (September 12)	13:00-14:00
Thursday (September 13)	13:00-14:00
Friday (September 14)	13:00-14:00

Coffee breaks

Coffee breaks will be served in the lobby of the Conference Centre of Radisson Blu Hotel Lietuva.

Tuesday (September 11)	10:30-11:00 / 16:00-16:30
Wednesday (September 12)	from 08:00 / 10:30-11:00
Thursday (September 13)	from 08:00 / 10:30-11:00 / 16:00-16:30
Friday (September 14)	from 08:00 / 10:30-11:00

Language

The official language of the conference is English.

No – smoking

Smoking in the congress center is strictly forbidden.

Mobile phones

Delegates are kindly requested to set their mobile phones on silent mode in the Hall where scientific sessions are being held.

Cloakroom

A cloakroom is at participants’ disposal.

Registration information

Registration and hospitality desks opening hours

DAY	TIME
September 10	17:00-19:00
September 11	08:00-19:00
September 12	08:00-14:00
September 13	08:00-19:00
September 14	08:00-17:00

Admission

The participant name badge will be provided at the registration desk. All participants are requested to wear the badge throughout the conference. Only badge holders will be admitted to the sessions.

Scientific information

Oral presentations

Technical Information for Oral Presentations

All presentation slots should include a few minutes for questions and answers (Q&A). Time allocation for presentations:

- plenary speaker – 45 minutes (40 min for your presentation, 5 min for Q&A);
- invited speakers – 30 minutes (25 min for your presentation, 5 min for Q&A);
- other oral speakers – 15 minutes (12 min for your presentation, 3 min for Q&A).

Uploading your Presentation

Oral presentations can be presented either from your own laptop or uploaded on the

Conference room.

For speakers presenting from own laptops connections are available that accommodate MacBooks (lightning port) and PCs (HDMI, VGA). Please bring a backup version of your presentation file, e.g. on a USB memory stick, which can be used for uploading directly to computer.

If you would prefer not to bring a laptop, you can upload your presentation onto conference room from a USB memory stick well before the session. Room technical helpers will be available to assist with uploading your presentations.

Please test that your presentation is working before the session. Please retrieve your laptop or memory stick immediately after your presentation

.

Technical Information for Poster Presenters

- Poster size: A0 (841 mm × 1189 mm, 33.11 in × 46.811 in).
- Orientation: portrait.
- Drawing-pins and Scotch tapes will be provided to attach your poster to the board.
- Posters will be displayed in the Poster area.
- All posters (odd and even numbers) should be set up on Tuesday, 11th of September before the beginning of the first poster session at 17:00.
- The official poster sessions are on:
  - Tuesday, 11th of September, 17:00-19:00 (odd numbers).
  - Thursday, 13th of September, 17:00-19:00 (even numbers).
  - Presenters are requested to be close to their posters during the whole allocated session.
  - **Six best student poster will be selected by a jury.**
  - There will be refreshments provided during the poster sessions.
  - All posters (odd and even numbers) should be removed on Thursday, 13th of September after the end of the second poster session at 19:00 and before the end of the conference (Friday, 14th of September, 16:00). Any material remaining after this time will be disposed of.

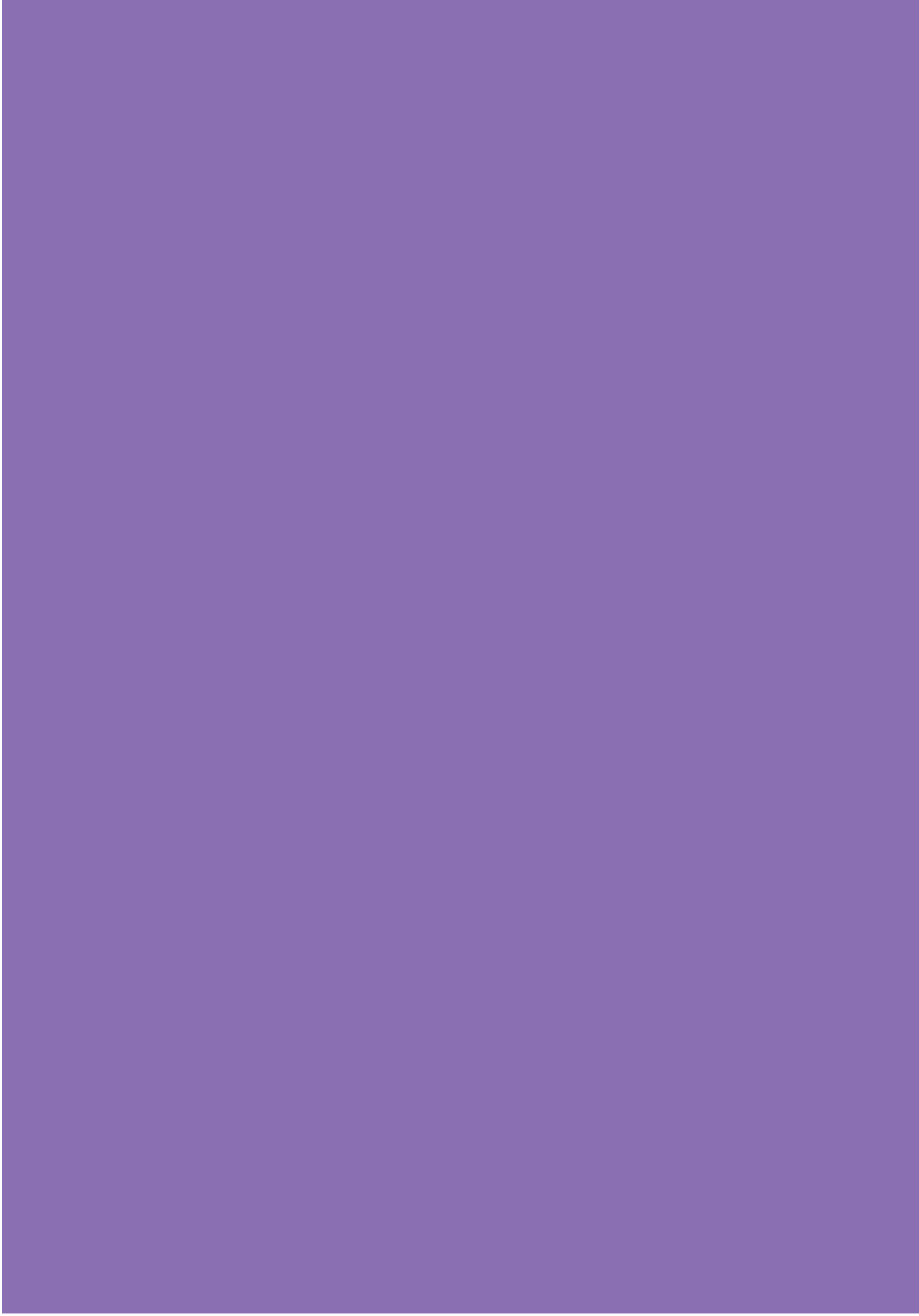

Speakers

Invited speakers

PLENARY SPEAKER

- **Toshihiko Baba** (Yokohama National University, Japan)
  Photonic Crystal Devices for Bio-Sensing and LiDAR Applications

INVITED SPEAKERS

- **Hamza Kurt** (TOBB University of Economics and Technology, Turkey)
  Modulation of Light with Metasurfaces and Phase Change Materials
- **Sejeong Kim** (University of Technology Sydney (UTS), Australia)
  Spectroscopy in Flatland
- **Harald Giessen** (University of Stuttgart, Germany)
  Complex and hybrid 3D printed microoptics
- **Anders Kristensen** (DTU, Lyngby, Denmark)
  Nano-scale Laser Printing on Template Optical Metasurfaces
- **Yongfeng Lu** (Department of Electrical Engineering University of Nebraska-Lincoln, USA)
  Two-photon polymerization for three-dimensional assembly of aligned carbon nanotubes
- **Ru-Wen Peng** (Nanjing University, China)
  Making metals transparent for white light by surface plasmons
- **Jan Siegel** (CSIC, Madrid, Spain)
  Periodic phase-change structures in silicon: Control and formation mechanism
- **Baerbel Rethfeld** (Technical University Kaiserslautern, Germany)
  Relaxation cascade of laser-excited nonequilibrium electrons in solids
- **Vidmantas Gulbinas** (Center for Physical Sciences and Technology, Vilnius, Lithuania)
  Optical probing of charge carrier motion dynamics in disordered, heterogeneous organic and hybrid materials
- **Gert-Willem Römer** (Chair of Laser Processing, University of Twente, The Netherlands)
  Laser-induced Forward Transfer (LIFT) of 3D micro-structures
- **Jean-Philippe Colombier** (Hubert Curien laboratory, University of St Etienne, France)
  Ultrafast Laser-Induced Surface and Bulk Nanostructuring: Similarities Revealed by Electromagnetic Modeling

- **Georg von Freymann** (University of Kaiserslautern, Germany)
  3D µ-printing – An enabling technology
- **Atsushi Ono** (Shizuoka University, Japan)
  Nanofabrication of metallic structures by femtosecond laser-induced photoreduction
- **Jürgen Hauer** (TU Munich, Germany)
  The functional roles of vibronic coupling in biological light harvesting
- **Koji Hatanaka** (Research Center for Applied Sciences, Academia Sinica, Taipei, Taiwan)
  Intense femtosecond laser interaction with aqueous solutions for X-ray, THz wave, and ultrasound emission

Social programme

10 SEPTEMBER

19:00-22:00 Get together
Venue: Conference venue hotel (Radisson BLU hotel Lietuva, Konstitucijos Ave. 24, Vilnius)

Get Together evening will take place in SKY BAR which is located on the top floor Radisson BLU Hotel Lietuva. You will have a chance to enjoy snacks and drinks with your colleagues and admire Vilnius view up above.

12 SEPTEMBER

14:00-17:30 Tour to Trakai
Meeting point: Conference venue hotel reception (Radisson BLU hotel Lietuva, Konstitucijos Ave. 24, Vilnius)

Trakai is the old capital of Lithuania situated 29 kilometers west of Vilnius between hills, forests and lakes. The town is famous for its picturesque landscape and the magnificent Castle of Trakai which is located on the island of the lake Galvė and is the only one water castle in Eastern Europe. The castle was build as a defensive fortress against the Teutonic knights in the end of the 14th century. The legendary past of the town makes it one of the most attractive tourist's destinations in Lithuania. Trakai is also known for Karaites (a community of people speaking the Turkic language), who have lived here since the 14 th century and preserved their traditions, language and religion. During the Tour to Trakai you will visit the Medieval Castle where the museum of the Lithuania's History is established.

19:00 - 23:00 Banquet
Venue: Palace of the Grand Dukes of Lithuania (Katedros ave. 4, Vilnius) in old town

The reconstructed Palace of the Grand Dukes of Lithuania, the former political, diplomatic, cultural center of the State, was one of the most famous in Europe in the 15th-17th centures and was demolished in the beginning of the 19th century. This Palace is excellent located just in the heart of Vilnius, within the confines of Lower Castle.

Part of the reconstructed Palace of the Grand Dukes in Vilnius Lower Castle officially transferred to the Museum. In the reconstructed Palace of the Grand Dukes of Lithuania there are two exhibition tour routes directly related to the historical functions of this residence. The first tour will show the historical and architectural development of the palace by highlighting the ancient ruins still in place, excavated artifacts and by using models and iconographic materials. The second tour route will bring the visitors into the ceremonial halls, which have been reconstructed in such a way as to show the evolution of architectural styles – from the late Gothic to the Renaissance to the early Baroque.

Palace of the Grand Dukes of Lithuania
(Cathedral Square 4, Vilnius)

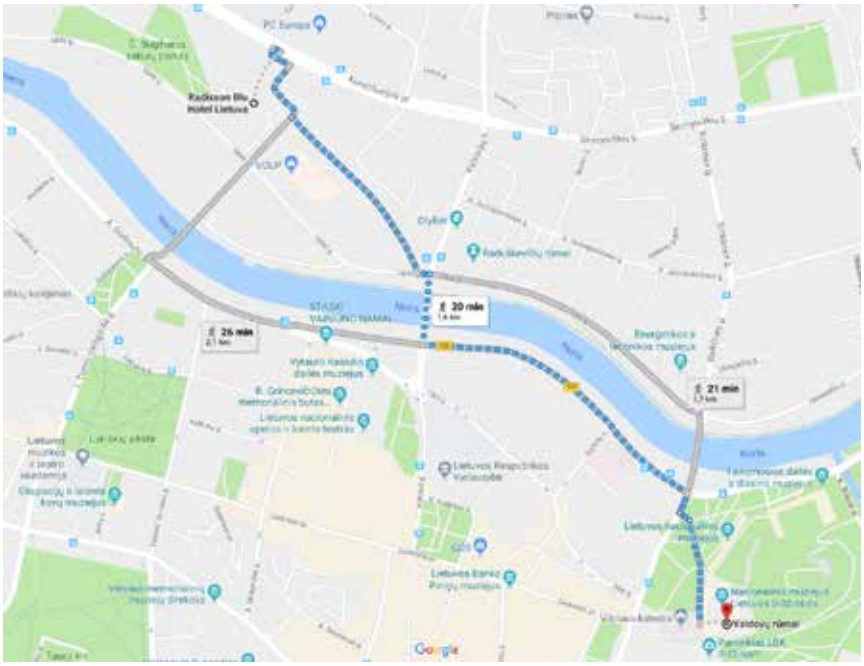

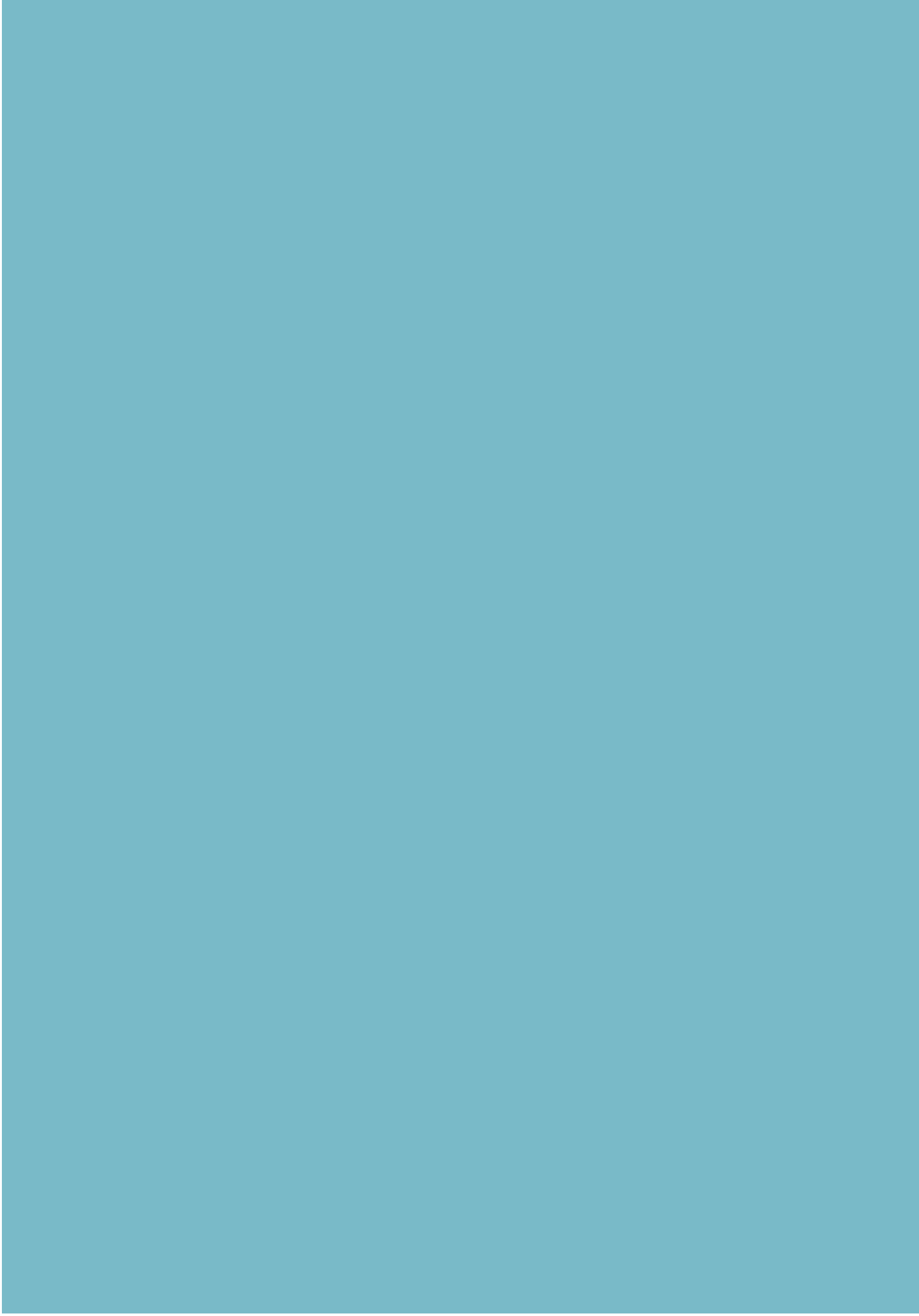

Book of abstracts

TU-PL-1

Photonic Crystal Devices for Bio-Sensing and LiDAR Applications

Toshihiko Baba

Yokohama National University, 79-5 Tokiwadai, Hodogayaku, Yokohama 240-8501, Japan
Corresponding author: baba-toshihiko-zm@ynu.ac.jp

Photonic bandgap in photonic crystals (PCs) has been anticipated to create some novel and practical applications. In these years, III-V semiconductor and Si photonics processings have been matured so that they achieve robust point defect nanolasers [1] and slow-light waveguides [2] in a PC slab. Among various applications studied so far for these devices, this presentation particularly focuses on biosensing and LiDAR.

High-sensitivity biosensing is available by exploiting GaInAsP PC nanolasers. Similar to the resonance wavelengths of passive cavities, nanolasers shift their lasing wavelengths when biomolecules are adsorbed [3]. Different from passive cavities', however, this behaviour of nanolasers arises not only from the change of environmental index but also from an iontronic effect, in which the surface charge of biomolecules modifies the electronic band profile of the semiconductor [4,5]. This phenomenon allows ultrasensitive detection of biomarker proteins suitable from a detection limit beyond the present standard methods' such as ELISA. It also allows a very simple detection via the emission intensity change if lower sensitivity is acceptable [6].

LiDAR is a hot topic in these years as a 3D sensor for autonomous vehicles, robots and drones. Here, compactness, low-cost mass productivity, and nonmechanical are the key, and Si photonics is a candidate platform that satisfies these requirements. Optical phased arrays are studied extensively as nonmechanical beam steering devices, while an alternative approach is using a doubly-periodic PC waveguide [7-9]. Thanks to the slowlight effect, it radiates a light beam whose radiation angle is sensitively changed by a small wavelength and index variation. WDM concept is also effective for wide-angle and parallel beam steering [10]. FMCW-type LiDAR will become possible by integrating a FM modulator and balanced photodiodes as well as the beam steering device working as a Tx and Rx optical antenna [11].

[1] S. Kita, K. Nozaki, et al., IEEE J. Sel. Top. Quantum Electron. 17, 1632 (2011).
[2] T. Baba, Nature Photon. 2, 465 (2008).
[3] T. Baba, MRS Commun. 5, 555 (2015).
[4] K. Watanabe, Y. Kishi, S. Hachuda, et al., Appl. Phys. Lett. 106, 021106 (2015).
[5] T. Watanabe, Y. Saijo, Y. Hasegawa, K. Watanabe, et al., Opt. Express 25, 24469 (2017).
[6] K. Watanabe, M. Nomoto, et al., Biosensors & Bioelectron., (2018, in press).
[7] K. Kondo, T. Tatebe, S. Hachuda, H. Abe, et al., Opt. Lett. 42, 4990 (2017).
[8] H. Abe, M. Takeuchi, G. Takeuchi, et al., Opt. Express 26, 9389 (2018).
[9] G. Takeuchi, Y. Terada, M. Takeuchi, H. Abe, H. Ito and T. Baba, Opt. Express 26, 11529 (2018).
[10] H. Ito, T. Tatebe, H. Abe and T. Baba, Conf. Laser and Electro-Opt., SM2B.5 (2018).
[11] Y. Furukado, H. Abe, Y. Hinakura and T. Baba, SPIE Photonics West, 10539-4 (2018).

TU-IN-1

Relaxation cascade of laser-excited nonequilibrium electrons in solids

Baerbel Rethfeld, Anika Rämer, Sebastian Weber, Nils Brouwer

Department of Physics and Research Center OPTIMAS, Technische Universitaet Kaiserslautern, Germany
Corresponding author: rethfeld@physik.uni-kl.de

During femtosecond laser irradiation of solids, mainly the electrons in the material gain energy. Free electrons in the conduction band of a metal can directly absorb photons. In semiconductors and dielectrics, on the other hand, a band gap has to be overcome first, before further energy gain from the laser beam is possible. These absorption processes transfer the electronic system to a state of strong thermodynamic nonequilibrium.

In the case of band-gap materials, electron-electron impact ionization may promote additional electrons to the conduction band, while Auger-like recombination processes with holes in the valence band may decrease the density of free carriers. All these processes can be understood as relaxation processes acting towards a new thermodynamic equilibrium between the density of electron-hole pairs and the energy density of the system. We analyze the different relaxation processes with the help of full Boltzmann-type collision integrals [1]. We also present, how such kinetic nonequilibrium calculations can be simulated with the help of a multiple rate equation system [2,3].

Our results reveal the different timescales of the considered relaxation processes. Usually, intraband thermalization is the fastest of these processes. Depending on excitation strength and material, excited electrons may establish a new Fermi distribution of elevated temperature on a femtosecond timescale [4]. In case of several excited electron bands, these temperatures equilibrate due to interband energy exchange. Additionally, particles have to be exchanged between the bands in order to establish a joint chemical potential of all electrons. Finally, ultrafast electron-phonon collisions lead to the temperature relaxation of hot electrons and the initially cold lattice. The energy transfer due to these collisions is completed on rather long picosecond timescales, while the collisions themselves occur on a femtosecond timescale. These collisions, therefore, also influence the relaxation processes within the electronic system. We show examples of the various relaxation processes, discuss their timescales and present examples of their mutual influence.

[1] N. Brouwer and B. Rethfeld, Phys. Rev. B **95**, 245139 (2017).

[2] B. Rethfeld, Phys. Rev. Letters **92**, 187401 (2004).

[3] A. Rämer, PhD Thesis TU Kaiserslautern, ISBN 978-3-8439-3208-0, Verlag Dr. Hut 2017.

[4] B.Y. Mueller and B. Rethfeld, Phys. Rev. B **87**, 035139 (2013).

TU-O-1

Ultrafast laser excitation of dielectrics: Measuring and modeling the transient optical properties

Søren H. Møller[1], Sebastian T. Andersen[1], Thomas Winkler[2], Lasse Haahr-Lillevang[1], Cristian Sarpe[2], Bastian Zielinski[2], Nadine Götte[2], Arne Senftleben[2], Thomas Baumert[2], and Peter Balling[1*]

[1]Department of Physics and Astronomy, Aarhus University, Ny Munkegade 120, DK-8000 Aarhus C, Denmark.
[2]Institute of Physics and CINSaT, University of Kassel, Heinrich-Plett-Strasse 40, D-34132 Kassel, Germany
Corresponding author: balling@phys.au.dk

The excitation of transparent dielectric materials by ultrashort laser pulses has been investigated since the invention of short-pulse lasers [1]. The process is initiated by strong-field excitation of electrons from the valence band (VB) to the conduction band (CB), and these electrons then open up for new processes. First, they can be further excited (intraband) while the laser is still on; this is sometimes described as "electron heating" due to inverse Bremsstrahlung. The newly created CB electrons change the optical properties of the sample, which acquires metal-like nature: high (transient) reflectivity and absorption of the light in the electron plasma (which is the optical signature of the intraband excitation). As some of the CB electrons acquire sufficient energy, a new process becomes possible: a high-energy electron can collide with an electron from the VB and impart sufficient energy for it to be excited to the CB, while the high-energy electron is left in a lower-energy state of the CB. The net effect is thus an increased CB-electron density, and since the mechanism has the potential to increase the excitation rapidly, it is sometimes coined "avalanche excitation".

The transient optical properties during excitation can be measured in variations of pump-probe experiments, where a strong pump pulse initiates the excitation process and a second (weaker) pulse measures signatures of the time-dependent refractive index of the excited material. An obvious quantity to measure is the transient reflectivity, which samples the surface properties, while the bulk excitation can also be measured, e.g. in spectral interferometry experiments [2-6]. The observations are generally reproduced by simulations of the excitation using the multi-rate-equation model [7], modified to incorporate all the processes described qualitatively above [8,9].

This presentation will provide an overview of the current understanding of short-pulse excitation of dielectrics and include a description of recent results, reporting a surprising observation of *transient coherent optical amplification* in excited dielectrics [6]. The amplification factor depends non-linearly on the probe-pulse energy and is thus attributed to two-photon stimulated emission based on population inversion between the bottom of the CB and the top of the VB. The gain occurs after a few hundred femtoseconds, consistent with a relaxation of the carriers to the band edge in combination with a carrier-induced band-gap shrinkage. The gain persists at pump-probe delays exceeding several tens of picoseconds [6].

[1] P. Balling and J. Schou, *Reports on Progress in Physics*, **76**, 036502 (2013).
[2] K. Wædegaard, D. B. Sandkamm, A. Mouskeftaras, S. Guizard, and P. Balling, Europhysics Letters **105**, 47001 (2014).
[3] L. Haahr-Lillevang, K. Wædegaard, D. Sandkamm, A. Mouskeftaras, S. Guizard, P. Balling, Appl. Phys. A **120**, 1221 (2015).
[4] T. Winkler, C. Sarpe, N. Jelzow, L. Haahr-Lillevang, N. Götte, B. Zielinski, P. Balling, A. Senftleben, and T. Baumert, Appl. Surf. Sci. **374**, 235-242 (2016).
[5] M. Garcia-Lechuga, L. Haahr-Lillevang, J. Siegel, P. Balling, S. Guizard, and J. Solis, Phys. Rev. B **95**, 214114 (2017).
[6] T. Winkler, L. Haahr-Lillevang, C. Sarpe, B. Zielinski, N. Götte, A. Senftleben, P. Balling, and T. Baumert, Nature Physics **14**, 74-79 (2018).
[7] B. Rethfeld, Phys. Rev. Lett. **92**, 187401 (2004).
[8] B. H. Christensen and P. Balling, Phys. Rev. B **79**, 155424 (2009).
[9] K. Wædegaard, D. B. Sandkamm, L. Haahr-Lillevang, K. G. Bay, and P. Balling, Applied Physics A **117**, 7-12 (2014).

TU-O-2

From high field plasmonics to laser-driven shock kick-off: variety of ablation scenarios and navigation between them

Sergey Anisimov[1], Nail Inogamov[1,2*], Viktor Khokhlov[1], Kirill Migdal[2,1], Yurii Petrov[1,3], Vadim Shepelev[4,1], Vasilii Zhakhovsky[2,1]

[1]Landau Institute for Theoretical Physics of RAS, Akademika Semyonova St., 1A, 142432, Chernogolovka, Moscow region, Russia [2]Dukhov Research Institute of Automatics (VNIIA), Sushchevskaya St., 22, 127055, Moscow, Russia [3]Moscow Institute of Physics and Technology, Institutskiy Lane, 9, 141700, Dolgoprudny, Moscow region, Russia [4]Institute for Computer-Aided Design of Russian Academy of Sciences (RAS), Vtoraya Brestskaya 19/18, Moscow 123056, Russia
Corresponding author: nailinogamov@gmail.com

Laser technologies based on laser ablation are widely used in modern high-tech industry. Ablation differs qualitatively, e.g., remember about (1) particle acceleration by ultra-intense 10^{22} W/cm^2 laser action, (2) NIF and production of hot plasma corona, (3) thermomechanical kick-off ablation by ultrashort pulses, (4) high field plasmonics, (5) single atom removal ablation in ultra-multi-shot regime using 100s MHz repetition rates when delay between successive bursts becomes just a few nanoseconds.

Main parameters defining these huge qualitative differences are: photon energy *hv* (from hard x-ray in XFELs to soft x-ray/EUV and to infrared lasers and down to THz sources), fluence, duration, number of shots, repetition rate, diameter of a spot on surface (from submicron to many microns), beam structure (from Gaussian to non-Gaussian spatial distributions of intensity on a surface), target configurations (bulk targets, thin or thick films, free-standing or supported films, laminates), target materials (there is a special group of refractory metals). There are critical values of these parameters separating qualitatively different regimes, e.g. if absorbed energy overcomes ablation threshold, then the ratio of electron-ion temperature equilibration time to acoustic time scale defines change from thermomechanical to evaporative ablation; while the value *hv* is insignificant for this change.

In the report, we will present practically significant new results relating to:

(R1) in the regime (3) the lateral spreading of heat along a thin metal film during a time interval, when separation of a film from substrate lasts, is important only for small spots, less than 400 nm in diameter;

(R2) mechanisms of film separation qualitatively differ depending on film thickness and duration of a pulse; it is surprising that nevertheless, the final solidified solitary structures created by diffraction limited laser action are similar;

(R3) we present the limit which bounds applicability of the law $r_{thr}^2 = R^2 \log F_c/F_{thr}$ following from fluence distribution of a Gaussian beam $F=F_c \exp(-r^2/R^2)$, here is F_c central fluence, R is e-radius of a Gaussian beam, is r_{thr} radius of a hole in a film. The law which changes the dependence $r_{thr}^2 \sim \log$ is also presented.

(R4) Structuring of a film by high field plasmonics ablation is described.

(R5) Nanoparticles formation by ablation in the liquid is discussed.

The work is supported by Russian Foundation for Basic Research (grant 16-08-01181-a).

TU-O-3

Transport properties of liquid metals and semiconductors from molecular-dynamics simulation with Kubo-Greenwood formula

Kirill Migdal[1,2], Vasily Zhakhovsky[1,2], Alexey Yanilkin[1,3], Yury Petrov[2,3] and Nail Inogamov[1,2]

[1]Dukhov Research Institute of Automatics (VNIIA), Sushchevskaya St., 22, 127055, Moscow, Russia
[2]Landau Institute for Theoretical Physics, Akademika Semyonova St., 1A, 142432, Chernogolovka, Moscow region, Russia 3Moscow Institute of Physics and Technology, Institutskiy Ln., 9, 141700, Dolgoprudny, Moscow region, Russia
Corresponding author: migdal@vniia.ru

Intensive nano- or femtosecond laser irradiation of metals and semiconductors produces the surface temperatures higher than 3000 K [1]. Hydrodynamic modeling of nanosecond fragmentation of such materials is feasible if the reflectivity and heat conductivity coefficients, usually determined from experiments, are available. However, there are insufficient temperature dependent data for some materials including titanium and silicon. On the other hand, a timescale of femtosecond laser heating is so short for hydrodynamic expansion of the thin surface layer. The hot and dense state of the material in this layer is also challenging to study using the experimental techniques such as the electrical explosion of wires or films [2]. Thus, calculations of electronic transport properties in such conditions are required.

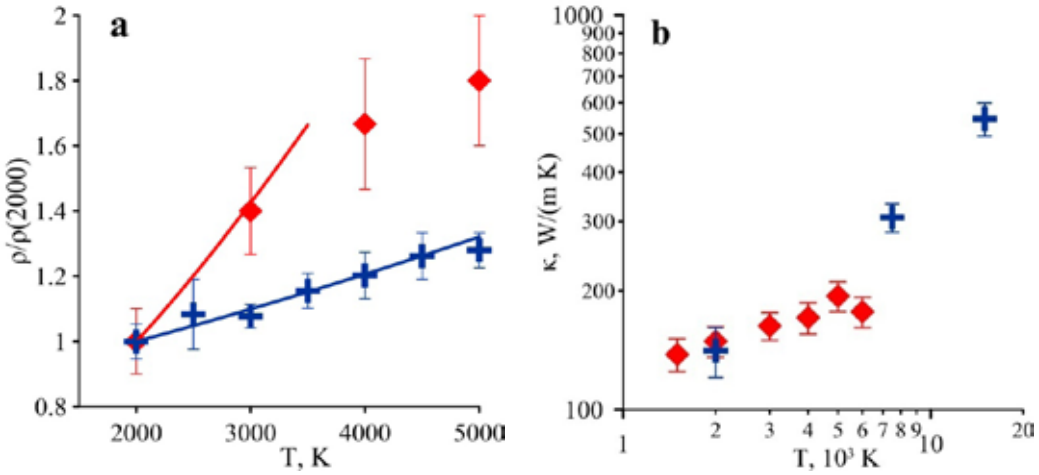

Fig. 1 (a) Electrical resistivity of copper ρ (diamonds) with respect to its value at T=2000 K ρ(2000). The resistivity of titanium is shown by crosses. The solid lines correspond to the experimental data approximations given in [2]. (b) Heat conductivity of copper κ in two-temperature state at the fixed pressure of 105Pa is shown by diamonds. Conductivity at the fixed density of 8 g/cc is presented by crosses.

We used classical and quantum molecular dynamics in conjunction with the Kubo-Greenwood theory to reproduce the states of several materials, including aluminum, copper, gold, silicon and titanium, along with their liquid-vapour coexistence curves or at equilibrium volume for 300 K. The calculated transport coefficients of copper and titanium are shown in figure 1. KM, VZh, YuP and NI are supported by the Russian Fund for Basic Researches (grant No 16-20-00864).

[1] N. A. Inogamov, V. V. Zhakhovsky, V. A. Khokhlov, Yu. V. Petrov and K. P. Migdal, Electron Solitary Nanostructures Produced by Ultrashort Laser Pulse, Nanoscale Res. Lett., 11, 177-189 (2016).
[2] G. R. Gathers, Dynamic methods for investigating thermophysical properties of matter at very high temperatures and pressures, Rep. Prog. Phys., 49, 341-396 (1986).

TU-O-4

Nonthermal melting in Si controlled by ultrashort laser pulses

Tobias Zier, Eeuwe S. Zijlstra, and Martin E. Garcia

Theoretical Physics, University of Kassel, Heinrich-Plett-Strasse 40, 34132 Kassel, Germany
Corresponding author: zier@uni-kassel.de

Recent developments showed that femtosecond-laser pulses are an ideal tool to address and/or manipulate properties in the matter since pulse durations are comparable to typical time scales of atomic motions in molecules and solids. In general, the excitation of crystalline material by an intense ultrashort laser pulse creates extreme nonequilibrium conditions within the solid. The optical energy of such excitation is, due to the high difference in mass of electrons and atoms, mainly deposited in the electronic system. Therefore one can induce electronic temperatures in materials of several 10000 K, whereas the atomic system remains almost unaffected near room temperature. Such an immense change in the electronic system has a direct influence on the bonding properties of the material, which feeds the idea of manipulating and controlling the crystalline structure by ultrashort laser pulses. In silicon, a femtosecond-laser excitation induces a weakening of the interatomic bonds, so-called bond softening. As a consequence, for moderate excitation below any damage threshold, the atoms start to oscillate collectively around their equilibrium positions [1,2]. For pulse intensities, which are high enough that bonds become unstable or even break, the crystalline structure disorders within hundreds of femtoseconds after the laser excitation [3–6]. In order to find a way of controllability of this phenomena, we intensively studied the atomic motion during the nonthermal melting process. Our results indicate that is very crucial for a possible control mechanism to minimize or even stop the laser-induced atomic acceleration due to the bond breaking. Since the acceleration strength varies between the different q-points within the Brillouin zone for a given laser strength [6], this does not appear to be a simple task. In this framework of ultrafast excitations, we studied theoretically the possibility to control the atomic motion during the ultrafast melting process in silicon. Our results show that although melting is a stochastic process in thermodynamical equilibrium, some coherences are preserved or even created in the laser-excited nonthermal case, which can be used to suppress the atomic acceleration that causes nonthermal melting. In particular, we could demonstrate that the crystalline structure stays intact following this approach.

[1] E. S. Zijlstra, A. Kalitsov, T. Zier, and M. E. Garcia, “Squeezed thermal phonons precurse nonthermal melting of silicon as a function of fluence”, Phys. Rev. X **3**, 011005 (2013).
[2] T. Zier, E. S. Zijlstra, and M. E. Garcia, “Silicon before the bonds break”, Appl. Phys. A **117**, 1 (2014).
[3] C. V. Shank, R. Yen, and C. Hirlimann,“Time-resolved reflectivity measurements of femtosecond-optical-pulse–induced phase transitions in silicon”, Phys. Rev. Lett. **50**, 454 (1983).
[4] H. W. K. Tom, G. D. Aumiller, and C. H. Brito-Cruz, “Time-resolved study of laser-induced disorder of Si surfaces”, Phys. Rev. Lett. **60**, 1438 (1988).
[5] K. Sokolowski-Tinten, C. Blome, C. Dietrich, A. Tarasevitch, M. Horn von Hoegen, D. von der Linde, A. Cavalleri, J. Squier, and M. Kammler, “Femtosecond x-ray measurement of ultrafast melting and large acoustic transients”, Phys. Rev. Lett. **87**, 225701 (2001).
[6] T. Zier, E. S. Zijlstra, M. E. Garcia, ”Quasimomentum-Space Image for Ultrafast Melting of Silicon”, Phys. Rev. Lett. **116**, 153901 (2016).
[7] E. S. Zijlstra, A. Kalitsov, T. Zier, and M. E. Garcia, “Fractional diffusion in silicon”, Adv. Mater **25**, 5605 (2013).
[8] T. Zier, E. S. Zijlstra, A. Kalitsov, I. Theodonis, and M. E. Garcia, “Signatures of nonthermal melting”, Struct. Dyn. **2**, 054101(2015).
[9] E S. Zijlstra, T. Zier, B. Bauerhenne, S. Krylow, P. M. Geiger, and M. E. Garcia, “Femtosecond-laser-induced bond breaking and structural modifications in silicon, TiO2, and defective graphene: an ab initio molecular dynamics study”, Appl. Phys. A **114**, 1 (2014).

TU-O-6

Electron excitation rates and saturation effects in laser-excited solids resolved by time-dependent density functional theory

Thibault J.-Y. Derrien[1,2,*], Nicolas Tancogne-Dejean[2,3], Vladimir P. Zhukov[1], Heiko Appel[2], Angel Rubio[2,3,4], Nadezhda M. Bulgakova[1]

[1]HiLASE Centre, Institute of Physics of the Czech Academy of Sciences, Za Radnici 828/5, 25241 Dolni Brezany, Czech Republic,
[2]Max Planck Institute for Structure and Dynamics of Matter (MPSD), Luruper Chaussee 149, 22761 Hamburg, Germany,
[3]Center for Free-Electron Laser Science, Luruper Chaussee 149, 22761 Hamburg, Germany,
[4]Center for Computational Quantum Physics, Flatiron Institute, 162 Fifth Avenue, New York, NY 10010, USA
*Corresponding author: derrien@fzu.cz

Predicting the energy absorbed by bandgap materials upon ultrashort pulse laser irradiation remains an open challenge in developing further the applications of pulsed lasers [1]. Although silicon is one of the most studied materials, its properties in a highly excited non-equilibrium state remain poorly known. A wealth of processes triggered by intense laser light such as transient change of optical properties [2], variable light scattering [3], and excitation-dependent energy relaxation [4] make it difficult to achieve a satisfactory description and hence to predict laser modification of bandgap materials. To analyze the available experimental data, it is necessary to account for the spatiotemporal variation of the optical response of materials, which strongly depends on the transient electron density. To perform this task with a reasonable computational cost, simplified descriptions are usually employed to describe the transient excitation of the electrons where several parameters, such as non-linear probabilities of light absorption, effective free electron mass, and collision frequency can be adjusted [2,5]. In the perturbative regime, multiphoton ionization rates are usually taken from the available experimental measurements [6]. At higher intensities, the Keldysh theory is commonly used to address the transition from the multi-photon to tunnelling ionization, while it also requires assumptions on the effective electron mass and band structure [7].

In this work, we employ time-dependent density functional theory (TD-DFT) to compute laser excitation of bulk silicon without introducing free parameters. The conduction band electron density, the total electron current and the electron energy are calculated as functions of time, laser intensity, photon wavelength, electric field strength, pulse duration, and carrier-envelope phase. The results demonstrate the possibility to calculate the non-linear photoionization rates from first principles and to identify the regimes where the Keldysh theory is qualitatively valid. In such regimes, the number of excited electrons scales with the square of the laser vector potential. However, our results show that increasing the laser pulse duration leads to a saturation of the excited electron density, whereas the absorbed electron energy keeps increasing. We show that, beyond the validity of the Keldysh theory, the TD-DFT simulations enable to derive photoionization rates in solids that is of paramount importance for a realistic description of high-power laser modification of dielectric and semiconductor materials.

[1] D. Grojo *et al.*, *Phys. Rev. B* **88**, 195135 (2013)
[2] K. Sokolowski-Tinten & D. von der Linde, *Phys. Rev. B* **61**, 2643-2650 (2000)
[3] E. V. Zavedeev *et al.*, *Laser Phys.* **26**, 016101 (2016)
[4] T. Sjodin *et al.*, *Phys. Rev. Lett.* **81**, 5664-5667 (1998)
[5] T. Y. Choi and C. P. Grigoropoulos, *J. Appl. Phys.* **92**, 4918-4925 (2002)
[6] A. D. Bristow *et al.*, *Appl. Phys. Lett.* **90**, 191104 (2007)
[7] V. E. Gruzdev, Phys. Rev. B **75**, 205106 (2007)

TU-IN-2

Making Metals Transparent for White Light by Surface Plasmons

Ru-Wen Peng*, and Mu Wang

National Laboratory of Solid State Microstructures, School of Physics, and Collaborative Innovation Center of Advanced Microstructures, Nanjing University, Nanjing 210093, China
Corresponding author: rwpeng@nju.edu.cn

Bulk metals are naturally opaque to light due to the large index mismatch between metals and dielectrics. Making metals transparent for white light, which could achieve various fascinating applications in optoelectronics, has been expected for a long period. In this talk, we present our recent work on making structured metals transparent for white light via surface excitations, such as surface plasmons. First, we show that periodic, quasiperiodic, and disordered metallic gratings can become transparent and completely antireflective for extremely broadband electromagnetic waves at oblique incidence. Second, we significantly develop oblique metal gratings transparent for broadband electromagnetic waves (including optical waves and terahertz ones) under normal incidence. In the third, we present that the principles of broadband transparency for structured metals can be extended from one-dimensional metallic gratings to two-dimensional cases. Moreover, similar phenomena are found in sonic artificially metallic structures, which present the transparency for broadband acoustic waves. These investigations provide guidelines for developing novel broadband metamaterials and have potential applications on transparent conducting panels, antireflective conducting solar cells, broadband acoustic imaging and sensing, and so on.

[1] Xian-Rong Huang, Ru-Wen Peng, and Ren-Hao Fan, "Making metals transparent for white light by spoof surface plasmons", *Phys. Rev. Lett.* (2010) 105, 243901.
[2] R. H. Fan, Ru-Wen Peng, Xian-Rong Huang, Jia Li, Yongmin Liu, Qing Hu, Mu Wang, and Xiang Zhang, "Transparent metals for ultrabroadband electromagnetic waves", *Advanced Materials* (2012) 24, 1980.
[3] R. H. Fan, L. H. Zhu, R. W. Peng, X. R. Huang, D. X. Qi, X. P. Ren, Q. Hu, and Mu Wang, "Broadband antireflection and light-trapping enhancement of plasmonic solar cells", *Phys. Rev. B* (2013) 87, 195444.
[4] R. H. Fan, J. Li, R. W. Peng, X. R. Huang, D. X. Qi, D. H. Xu, X. P. Ren, and Mu Wang, "Oblique metal gratings transparent for broadband terahertz waves", *Appl. Phys. Lett.* (2013) 102, 171904.
[5] Dong-Xiang Qi, Ren-Hao Fan, Ru-Wen Peng, Xian-Rong Huang, Ming-Hui Lu, Xu Ni, Qing Hu, and Mu Wang, "Multiple-band transmission of acoustic wave through metallic gratings", *Appl. Phys. Lett.* (2012) 101, 061912.
[6] D. X. Qi, Y. Q. Deng, D. H. Xu, R. H. Fan, R. W. Peng, Z. G. Chen, M. H. Lu, X. R. Huang, and Mu Wang, "Broadband enhanced transmission of acoustic waves through serrated metal gratings", *Appl. Phys. Lett.* (2015) 106, 011906.
[7] X. P. Ren, R. H. Fan, R. W. Peng, X. R. Huang, D. H. Xu, Yu Zhou, and Mu Wang, "Non-periodic metallic gratings transparent for broadband terahertz waves", *Phys. Rev. B* (2015) 91, 045111.
[8] Dong Liu, Ren-Hao Fan, Hao Jing, Ru-Wen Peng, Xian-Rong Huang, and Mu Wang, manuscript submitted (2018).

TU-O-7

Ultrafast laser nanofabrication of advanced nanophotonic structures

Aleksandr Kuchmizhak[1,2]

[1]School of Natural Sciences, Far Eastern Federal University, Vladivostok, Russia
[2]Institute of Automation and Control Processes, Far Eastern Branch, Russian Academy of Science, Vladivostok 690041, Russia
Corresponding author: alex.iacp.dvo@mail.ru

In past decades, direct processing of different noble-metal materials using short- and ultrashort laser pulses has become a matured technology allowing rapid prototyping of various nanotextured morphologies. Pulse repetition rate of the commercially available laser systems used in the nanotexturing experiments enters sub-GHz range ensuring extremely fast material processing at speed reaching several cm^2 per second. From the other hand, laser nanofabrication with a "structured light", specially designed laser beams with a complex intensity profile allowing specific conditions of energy deposition into the irradiated materials become a hot topic in the area of laser nanofabrication. Here, an overview of recent results related to direct fabrication of various micro- and nanoscale structures and surface textures using short and ultrashort laser pulses is presented. First, we present the results on the formation of chiral surface nanoneedles under noble-metal films ablation with "perfect" vortex beams having a variable topological charge as well as specially designed spiral beams [1,2] discussing the underlying formation mechanisms and the ability to tune the structure's chirality (Fig.1(a)). Then, we present the method allowing the fabrication of various isolated plasmonic nanostructures with a porous inner structure via the ablation of the nitrogen-doped noble-metal films [3]. The proposed method allows to precisely tune the porosity of the produced structures through the control over the nitrogen content in the irradiated noble-metal films (Fig.1(b)). Several applications of the presented laser-printed nanostructures and nanotextures in a plasmon-mediated structural color generation [4], biosensing based on surface-enhanced spectroscopy effects [5], etc. are also discussed.

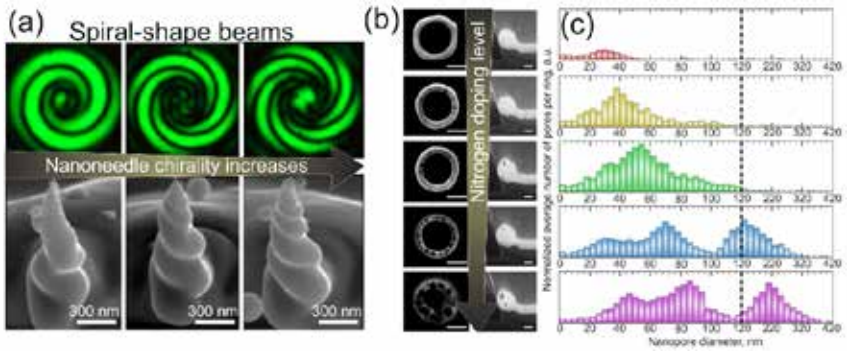

Fig. 1 (a) Focal-plane intensity distribution of the DOE-generated spiral-shape beams having a various number of spiral arms (top row) as well as corresponding chiral nanoneedle printed on the surface of 500-nm thick Ag film with such beams. (b) Normal-view SEM images of the isolated 900-nm diameter nanorings (left column) and corresponding cross-sectional FIB cuts (right column) of the nanoring wall showing the position and the average size of the nanopores. (c) Averaged distribution of nanopore diameters inside the fabricated microrings.

[1] S. Syubaev, A. Zhizhchenko, A. Kuchmizhak, A. Porfirev, E. Pustovalov, O. Vitrik, Yu. Kulchin, S. Khonina, S. Kudryashov. Direct laser printing of chiral plasmonic nanojets by vortex beams. *Opt. Express* **25**, 10214-10223 (2017).
[2] S. Syubaev, A. Nepomnyashchiy, E. Mitsai, E. Pustovalov, O. Vitrik, S. Kudryashov, A. Kuchmizhak, Fabrication of porous microrings via laser printing and ion-beam post-etching, *Appl. Phys. Lett.* **111** (8), 083102 (2017).
[3] X.W. Wang, A.A. Kuchmizhak, D. Storozhenko, S. Makarov, S. Juodkazis A. Author, B. Author, C. Author, Single-step laser plasmonic coloration of metal films. *ACS Appl. Mater. Interfaces* **10,** 1422–1427 (2018).

TU-O-8

Efficient Laser Scanning Ablation Procedure for Ultrafast Surface Structuring

Mindaugas Gedvilas*, Andrius Žemaitis, Mantas Gaidys, Paulius Gečys, Gediminas Račiukaitis

Center for Physical Sciences and Technology, Savanoriu Ave. 231, LT-02300 Vilnius, Lithuania
Corresponding author: mgedvilas@ftmc.lt

Ultra-short laser pulses have shown their applicability for high-quality laser micromachining of semiconductors, metals and insulators in technological, scientific and medical applications. However, its usage is limited by the low ablation rates at which material is removed. The experimental/theoretical works clarifying the optimization of the ablation rate by selection particular laser fluence emerged a decade ago [1, 2]. Later, the efficient laser ablation has been wildly investigated by the several scientific groups. However, there are only a few attempts of investigation of ablation rate by taking into account incubation effect and saturation of ablation depth for multi-pulse irradiation [3]. Here we present the theoretical and experimental studies of laser ablation taking into account the incubation phenomenon and the saturated ablation depth for multi-pulse treatment. The new model of plane surface ablation has been created for the scanned laser beam. Picosecond laser pulses were applied to ablate the target material at various beams scanning speeds and laser spot sizes. The experiment of laser ablation on copper by various processing parameters sets demonstrates, that optimal point for efficient ablation can be predicted by the proposed theoretical model.

The new model of plane surface ablation by parallel scanned lines over the flat target material has been created in this work. The main purpose of the new proposed model is theoretically to calculate the ablated volume per pulse of the scanned laser beam by taking into account the incubation phenomenon and saturation of ablation depth for multi-pulse ablation. The experiments of rectangular cavity ablation have been conducted in order to confirm modelling results. The picosecond laser (Atlantic, Ekspla) has been used for ablation of copper. The processing parameters: scanning speed, the distance between scanned lines and spot size on the sample has been varied in order to reach maximum removal rate. The array of rectangular cavities with depth-dependant on the processing parameters was ablated. The ablation rate was evaluated from the averaged depth of cavities taken from measured profiles at different processing parameters. The experimental and modelling results show the optimal processing parameters for maximum available ablation rate: scanning speed and beam spot radius. The efficient ablation is reached because of a combination of all factors influencing material removal rate. The experiment data results have a good agreement with numerical calculation results of a new proposed model. The laser ablated cavity with the removal rate of 330 μm^3/pulse has been performed by using 130 µJ laser pulse energy at 100 kHz repetition rate.

The new proposed model of plane surface ablation which takes into account the ablation threshold and penetration depth decrease with increasing number of laser pulses per spot has been created in this work. Model is in good agreement with experiment. The removal rate of 0.15 mm^3/(min·W) has been achieved for the copper target.

[1] G. Raciukaitis, M. Brikas, M. Gedvilas, Efficiency Aspects in Processing of Metals With High-Repetition-Rate Ultra-Short-Pulse Lasers, *Proc. ICALEO* 176–184 (2008).
[2] G. Račiukaitis, M. Brikas, P. Gečys, B. Voisiat, M. Gedvilas, Use of High Repetition Rate and High Power Lasers in Microfabrication: How to Keep the Efficiency High?, *J. Laser Micro Nanoen.* **4**, 186–191 (2009).
[3] G. Raciukaitis, M. Brikas, P. Gecys, M. Gedvilas, Accumulation effects in laser ablation of metals with high-repetition- rate lasers, *Proc. SPIE* **7005**, 70052L–70052L–11 (2008).

TU-O-9

High-throughput ultrashort laser micromachining by MHz-THz pulse bursts

Sergey Kudryashov[1,2,3,*] Pavel Danilov[2,3], Nikita Smirnov[2], Andrey Ionin[2], Andrey Samokhvalov[1], Eduard Ageev[1], Vadim Veiko[1], Alexey Porfirev[3,4], Oleg Vitrik[3], Alex Kuchmizhak[3], Svetlana Khonina[4]

[1] ITMO University, 49 Kronverksky prospect, 191107 St. Petersburg, Russia
[2] Lebedev Physical Institute, 53 Leninsky prospect, 119991 Moscow, Russia
[3] Institute of Automation and Control Processes, Far Eastern Branch of RAS, 5 Radio st., 690041 Vladivostok, Russia
[4] Image Processing Systems Institute – Branch of the FSRC "Crystallography and Photonics" RAS, 151 Molodogvardeyskaya st., 443001 Samara, Russia
* Corresponding author: sikudryashov@corp.ifmo.ru, sikudr@sci.lebedev.ru

High-throughput laser micromachining by ultrashort (femto-picosecond) laser pulses was explored in terms of optimal pulsewidth and fluence [1], efficient power utilization via beam multiplexing using diffractive optical elements [2] and ultrafast laser scanning speeds in order to employ the available multi-MHz repetition rates [3]. The underlying physical processes and ablation mechanisms were overviewed [1-5].

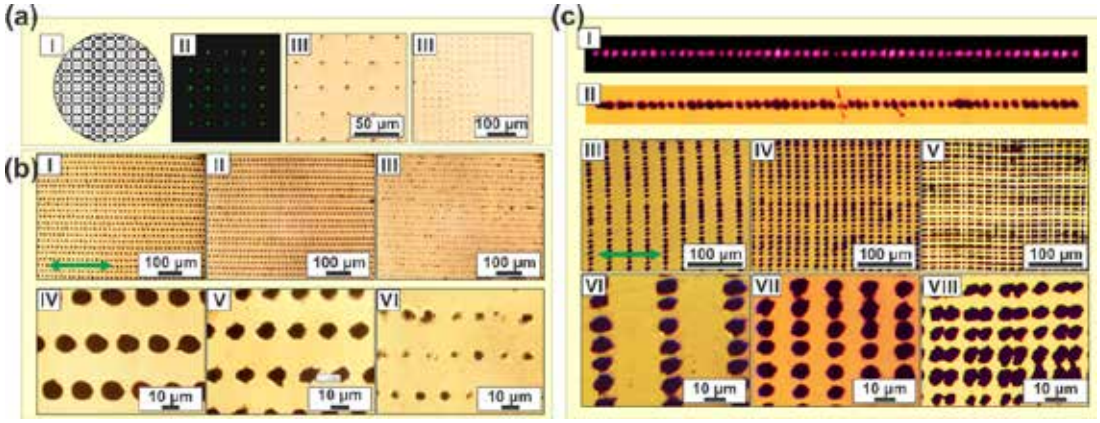

Fig. 1 Examples of Mega-element per second DOE-mediated rates of femtosecond-laser patterning of thin plasmonic films.

Optimal pulse separation in their trains and bursts (MHz-THz) was explored using our pump/probe [5] and double-pump [6] fs-laser ablation studies, indicating the most efficient operation window for various ablation mechanisms, emerging on different – from sub-ps till sub-ns – temporal scales [7].

This work was supported by Russian Science Foundation (grant #16-12-10165).

[1] I. Artyukov, D. Zayarniy, A. Ionin, S. Kudryashov, S. Makarov, Relaxation phenomena in electronic and lattice subsystems on iron surface during its ablation by ultrashort laser pulses, *JETP Letters* **99**, 51-55 (2014).
[2] A. Kuchmizhak, A. Porfirev, S. Syubaev, P. Danilov, A. Ionin, O. Vitrik, Yu. Kulchin, S. Khonina, S. Kudryashov, Multi-beam pulsed-laser patterning of plasmonic films using broadband diffractive optical elements, *Optics Letters* **42**, 2838-2831(2017).
[3] A. Ionin, A. Ivanova, R. Khmel'nitskii, Yu. Klevkov, S. Kudryashov, N. Mel'nik, A. Nastulyavichus, A. Rudenko, I. Saraeva, N. Smirnov, D. Zayarny, A. Baranov, Milligram-per-second femtosecond laser production of Se nanoparticle inks and ink-jet printing of nanophotonic 2D-patterns, *Applied Surface Science* **436**, 662-669 (2018).
[4] X. Wang, A. Kuchmizhak, X. Li, S. Juodkazis, O. Vitrik, Yu. Kulchin, V. Zhakhovsky, P. Danilov, A. Ionin, S. Kudryashov, A. Rudenko, N. Inogamov, Laser-induced Translative Hydrodynamic Mass Snapshots: non-invasive characterization and predictive modeling via mapping at nanoscale, *Phys Rev Applied* **8**, 044016 (2017).
[5] S. Kudryashov, A. Ionin, Multi-scale dynamics of front-side femtosecond laser heating, melting and ablation of thin supported aluminum film, *International Journal of Heat & Mass Transfer* **99**, 383-390 (2016).
[6] E. Ageev, V. Bychenkov, A. Ionin, S. Kudryashov, A. Petrov, A. Samokhvalov, V. Veiko, Double-pulse femtosecond laser peening of aluminum alloy AA5038: effect of inter-pulse delay on transient optical plume emission and final surface micro-hardness, *Applied Physics Letters* **109**, 211902 (2016).
[7] A. Ionin, S. Kudryashov, A. Samokhin, Material surface ablation produced by ultrashort laser pulses, *Physics-Uspekhi* **60**, 149-160 (2017).

TU-O-10

Near-THz bursts of pulses –governing surface ablation mechanisms for laser material processing

Jaka Mur[1*], Rok Petkovšek[1]

[1]University of Ljubljana, Faculty of Mechanical Engineering, Aškerčeva 6, SI-1000 Ljubljana, Slovenia
Corresponding author: jaka.mur@fs.uni-lj.si

RRecent advances in ultra-short pulsed laser source development have attracted a lot of attention to the bursts of pulses, as high average powers and pulse energies have become available. Bursts are obtained either by splitting a single pulse [1,2] or by grouping consequent pulses together [3–5]. Different approaches have shown similar results (i.e. significantly lower ablation threshold) albeit explained with different physical mechanisms, such as heat accumulation [4], incubation [6], or ablation-cooling [3].

Bursts of pulses at near-THz repetition rates (up to 440 GHz) were generated via series of birefringent crystals. We have hypothesised that a THz burst exhibits a similar interaction with the material as a proportionally longer single pulse, which is in disagreement with recent results of other groups on metal processing applications [2]. We have used a NIR laser emitting 1.5 ps pulses and have compared the surface effect of a single pulse to a near-THz burst of 2-16 pulses with variable repetition rates. Ablation efficiency was observed as a measure of the total throughput as well as the resulting structure quality (surface roughness, signs of heat-related processes). Five different materials were investigated (copper, Kapton, LTCC, Al2O3, and Kovar) with results showing a uniform tendency that an increased burst duration reduces the ablation efficiency at constant burst energy. Signs of surface melting were observed on copper at longer burst durations, similarly as a longer single pulse would have behaved.

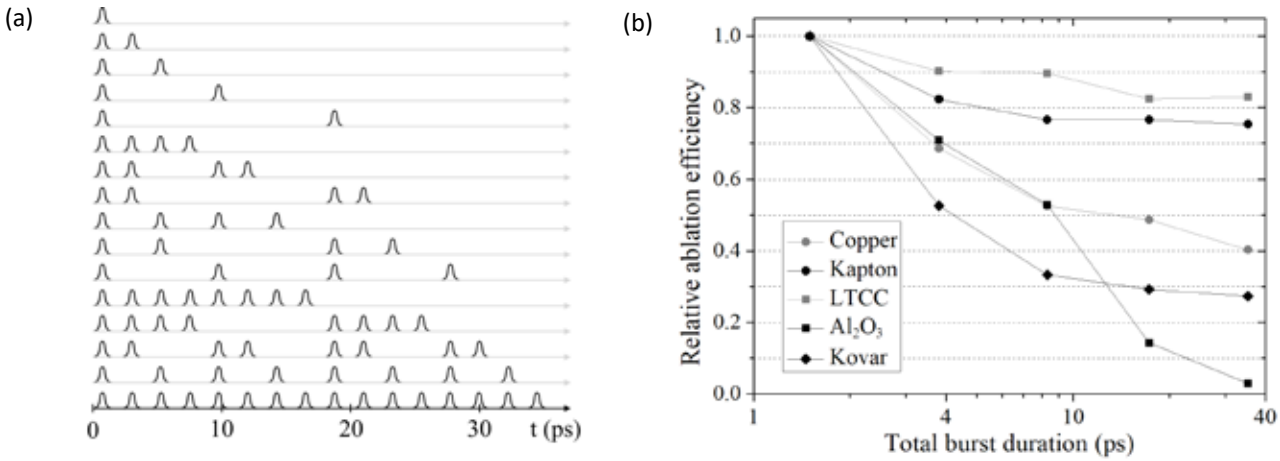

Fig. 1: (a) Different temporal distributions of pulses within bursts as used in experiments. (b) Graph of ablation efficiency as a function of burst duration at 440 GHz repetition rate of subpulses.

Near-THz bursts of pulses enable an increase of overall energy delivered to the material under an assumption that a laser source is natively capable of operation at given conditions. We have demonstrated that splitting a single pulse into a burst of 2-16 subpulses does not increase the ablation efficiency nor the final structure quality as longer bursts, in general, behave similarly to a single, proportionally longer pulse.

[1] A. Okhrimchuk, S. Fedotov, I. Glebov, V. Sigaev, and P. Kazansky, Sci. Rep. **7**, 16563 (2017).
[2] C. Gaudiuso, G. Giannuzzi, A. Volpe, P. M. Lugarà, I. Choquet, and A. Ancona, Opt. Express **26**, 3801 (2018).
[3] C. Kerse, H. Kalaycıoğlu, P. Elahi, B. Çetin, D. K. Kesim, Ö. Akçaalan, S. Yavaş, M. D. Aşık, B. Öktem, H. Hoogland, R. Holzwarth, and F. Ö. Ilday, Nature **537**, 84 (2016).
[4] J. Mur, L. Pirker, N. Osterman, and R. Petkovšek, Opt. Express **25**, 26356 (2017).
[5] J. Mur, J. Petelin, N. Osterman, and R. Petkovšek, J. Phys. Appl. Phys. **50**, 325104 (2017).
[6] N. Lasemi, U. Pacher, L. V. Zhigilei, O. Bomatí-Miguel, R. Lahoz, and W. Kautek, Appl. Surf. Sci. **433**, 772 (2018).

TU-O-11

From the bulk to thin films: On the interplay of photomechanical and photothermal ablation induced within gold by ultrafast laser radiation

Markus Olbrich*, Theo Pflug, and Alexander Horn

Laserinstitut Hochschule Mittweida, Schillerstraße 10, 09648 Mittweida, Germany
Corresponding author: molbrich@hs-mittweida.de

Irradiating metals films with single pulsed ultrafast laser radiation two distinguishable ablation mechanism are induced in dependence of the applied fluence, so-called photomechanical and photothermal ablation [1]. While photomechanical ablation is caused by the induced rarefaction and shock waves resulting in spallation of layers of molten material, photothermal ablation is mainly determined by phase explosion requiring higher fluences of the laser radiation compared to photomechanical ablation in general. Therefore, these two mechanisms are also associated with the so-called low and high fluence regime [2], or gentle and strong ablation regime [3]. Whether photomechanical or photothermal ablation represents the dominant ablation process depends on several parameters, like thermophysical parameters of the metal such as the electron-phonon coupling time and the thermal conductivity as well, or material parameters like the film-thickness and the material of the substrate. Furthermore, the induced rarefaction and shock waves are reflected partially in case of a mismatch of the wave impedance between the film and the substrate and may cause secondary photomechanical ablation or even photothermal ablation at the rear side of the film. These ablation processes at the rear side induced by only irradiating the film at the front side with ultrafast laser radiation represents a key parameter in understanding ablation of thick gold films [4] but has to be taken into account also for thin films.

Therefore, in this work, several films of gold consisting of a different film thickness (20 nm – 2 µm) are irradiated with ultrafast laser radiation (800 nm, 40 fs) in dependence on the applied fluence. The topology of the induced ablation structures in regard of the ablation depth as well as the diameter of the structures, and from that derived ablation threshold, are discussed in competitive comparison with hydrodynamic modelling [5], and temporally and spatially resolve measurements [6] (Fig. 1).

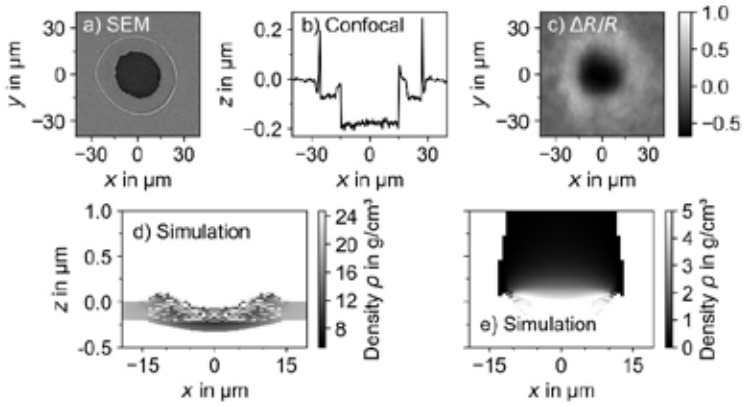

Fig. 1 a) SEM and b) confocal micrograph of the obtained ablation structure, c) spatially resolved relative change of reflectance for a delay time of 50 ps, calculated spatial density distribution of d) solid and liquid gold as well of e) vapour and plasma for a delay time of 50 ps; all for a thin film of gold (200 nm) irradiated with single pulsed ultrafast laser radiation (800 nm, 40 fs, 7 J/cm²)

[1] L.V. Zhigilei, Z. Lin, D.S. Ivanov, E. Leveugle, W.H. Duff, D. Thomas, C. Sevilla, S.J. Guy, in *Laser-Surface Interactions for New Materials Production*, ed. by A. Miotello, P.M. Ossi (Springer Berlin Heidelberg Berlin, Heidelberg, 2010), p. 43
[2] R. Le Harzic, D. Breitling, M. Weikert, S. Sommer, C. Fhl, F. Dausinger, S. Valette, C. Donnet, E. Audouard, *Appl. Phys. A* **80**, 1589 (2005)
[3] M. Olbrich, E. Punzel, R. Roesch, R. Oettking, B. Muhsin, H. Hoppe, A. Horn, *Appl. Phys. A* **122**, 648 (2016)
[4] M. Olbrich, T. Pflug, A. Horn, *App. Surf Sci, in preparation*
[5] M.E. Povarnitsyn, N.E. Andreev, E.M. Apfelbaum, T.E. Itina, K.V. Khishchenko, O.F. Kostenko, P.R. Levashov, M.E. Veysman, *Appl. Surf. Sci.* **258**, 9480 (2012)
[6] T. Pflug, J. Wang, M. Olbrich, M. Frank, A. Horn, *Appl. Phys. A* **124**, 17572 (2018)

TU-O-12

Vector vortex beams generated by q-plates as a versatile route to direct femtosecond laser surface structuring

Jijil JJ Nivas[1,2], Elaheh Allahyari[1,2], Filippo Cardano[1], Andrea Rubano[1], Rosalba Fittipaldi[3], Antonio Vecchione[3], Domenico Paparo[4], Lorenzo Marrucci[1,4], Riccardo Bruzzese[1,2], Salvatore. Amoruso[1,2]

[1]Dipartimento di Fisica "Ettore Pancini", Università di Napoli Federico II, Via Cintia, 80126 Napoli, Italy.
[2]CNR-SPIN UOS Napoli, Complesso Universitario di Monte S. Angelo, Via Cintia, 80126 Napoli, Italy.
[3]CNR-SPIN, UOS Salerno, Via Giovanni Paolo II 132, 84084 Fisciano,Italy.
[4]National Research Council, Institute of Applied Science & Intelligent Systems (ISASI) 'E. Caianiello',
Via Campi Flegrei 34, 80078 Pozzuoli (NA), Italy.
Corresponding author: salvatore.amoruso@unina.it,amoruso@fisica.unina.it

Complex light beams with spatially variant state of polarization are receiving increasing attention thanks to the large variety of new possibilities in a wide range of applications, including, e.g., microscopy, lithography, optical trapping, information technology and material processing [1]. Recently, optical cylindrical vector beams with fs pulse duration has been demonstrated as an effective laser surface fabrication method for the generation of patterns with axial symmetry (e.g., azimuthal, radial, spiral, etc.) [2-4], thanks to their numerous spatially-variant state of polarization. In this communication, we report on our ongoing research on direct femtosecond laser surface structuring with vector vortex beams (VVB) generated by q-plates. A q-plate is an optical device formed by a thin layer of liquid crystals, whose optic axes form a singular pattern with a topological charge *q* [5].

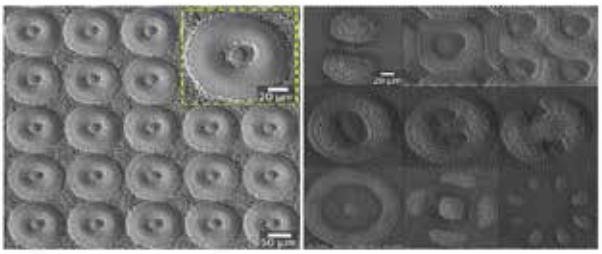

Fig. 1 Left: periodic surface structure obtained by step scan repeating a unit cell produced by a VVB with annular spatial intensity distribution. Right: examples of different unit cell achieved by optical retardation tuning and filtering of singular VVB.

We generate a large class of fs VVB with various q-plates (e.g. topological charge q=1/2, 1, 3/2, 2, 5/2) characterizing the corresponding surface patterns. In this communication, we will present a variety of surface structures achieved by exploiting VVB both in static (i.e. consecutive laser pulses on the same point) and step scan (i.e. gradual variation of irradiation point after a given number of pulses on a selected site) conditions. The variety of surface structures and their intriguing characteristics will be illustrated and discussed to demonstrate that VVB generated by q-plates can offer a versatile route to direct fs laser surface structuring. Finally, the use of surface structures as a feasible and reliable way to characterize intense fs complex beams in the focal region will also be addressed.

[1] J. Secor, R. Alfano, S. Ashrafi, *Complex Light* (IOP Publishing Ltd, 2017).
[2] K. Lou et al., *Femtosecond Laser Processing by Using Patterned Vector Optical Fields*, Sci. Rep. **3**, 2281 (2013).
[3] J. JJ Nivas et al., *Direct Femtosecond Laser Surface Structuring with Optical Vortex Beams Generated by a q-plate*, Sci. Rep. **5**, 17929 (2015).
[4] G.D. Tsibidis et al., *Ripple formation on nickel irradiated with radially polarized femtosecond beams*, Opt. Lett. **40**, 5172 (2015).
[5] L. Marrucci, et al., "Optical Spin-to-Orbital Angular Momentum Conversion in Inhomogeneous Anisotropic Media", Phys. Rev. Lett. 96, 163905 (2006).

TU-IN-3

Modulation of Light with Metasurfaces and Phase Change Materials

Ahmet Ozer[1], Hasan Kocer[2], Hamza Kurt[1,*]

[1]TOBB University of Economics and Technology, Department of Electrical and Electronics Engineering, Sogutozu Ave. 43, Ankara, Turkey
[2]Medical Supply and Maintenance Center, Dogu Ave. 1, Ankara, Turkey
Corresponding author: hkurt@etu.edu.tr

In various novel optical applications based on metasurfaces which were recently proposed to control amplitude, phase, and polarization of the light, the components that transmit light in one only direction [1,2] and whose behavior can be tuned by excitation have become an important requirement. In this study, we propose and numerically demonstrate modulation of light transmission mechanism in metasurface configuration that consists of an array of trapezoidal shaped silver (Ag) on a sapphire substrate in the mid-infrared spectrum. The unit cell of the proposed metasurface and the metasurface array are seen in Figs. 1(a) and 1(b), respectively. As a result of numerical parametric analysis of the unit cell utilizing the 3D finite-difference-time-domain method, the optimum values of the parameters where asymmetric transmission is strong and wideband are determined as p = 3.0 µm, a = 1.0 µm, b = 2.0 µm and h = 1.0 µm.

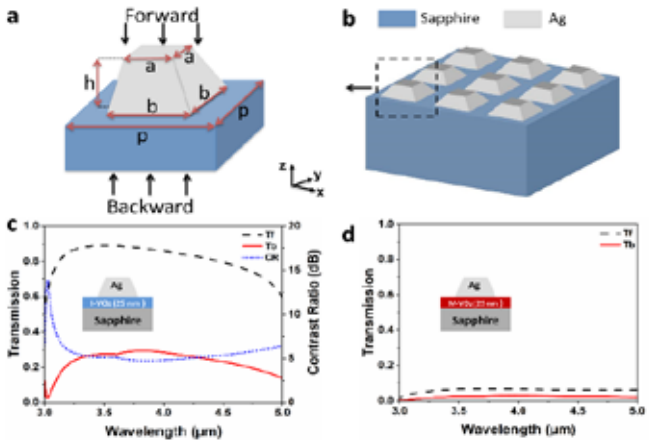

Fig. 1 (a) Unit cell of the proposed metasurface. (b) Metasurface array. Transmission spectra under forwarding (T_f) and backward (T_b) illuminations at (c) insulator and (d) the metallic state of VO_2. (In (c), CR is the contrast ratio expressed by $10\log(T_f / T_b)$).

Then, we focus on how to bring tunable behavior so that the optical behavior of the structure changes with an external stimulus. To achieve this goal, we add an ultra-thin (~λ/150) 25 nm phase change material (made of vanadium dioxide, VO_2) between the trapezoidal layer and the substrate as seen in the inset of Figs. 1(c) and 1(d). Hence, we show that the optical behavior can be switched in the mid-infrared region as shown in Figs. 1(c) and 1(d). While forward propagating light is promoted, and backward one is suppressed in the insulator phase of VO_2, light propagation in both directions are almost eliminated when VO_2 is in the metallic phase as shown in Fig. 1(d).

[1] B. Tang, Z. Li, F. Callewaert and K. Aydin, Broadband asymmetric light transmission through tapered metallic gratings at visible frequencies, *Sci. Rep.*, **6**, 39166 (2016).
[2] B. Shen, R. Polson and R. Menon, Broadband asymmetric light transmission via all-dielectric digital metasurfaces, *Opt. Express*, **23**, 20961–20970 (2015).

WE-IN-1

Laser-induced Forward Transfer (LIFT) of 3D micro-structures

Gert-Willem **Römer**[1], Matthias Feinaeugle[1], Ralph Pohl[1,2]

[1]Chair of Laser Processing, Department of Mechanics of Solids, Surfaces & Systems (MS[3]), Faculty of Engineering Technology, University of Twente, Drienerlolaan 5, 7522NB, Enschede, The Netherlands
[2]Demcon B.V., Institutenweg 25, 7521PH, Enschede, The Netherlands
Corresponding author: g.r.b.e.romer@utwente.nl

Laser-induced Forward Transfer (LIFT) is a promising direct-write Additive Manufacturing technique, which allows transferring various materials selectively and has the potential to print 3D micro-structures [1-3]. In the LIFT process, the donor material to be printed consists of a thin film, which is supported by a carrier substrate, see Fig. 1. The carrier substrate is transparent to the incident laser wavelength. When a pulsed laser beam is focused on the carrier–donor interface the absorbed laser energy ejects the donor material onto a receiving substrate. The latter is usually referred to as the receiver. Besides in the liquid phase, the donor material can also be transferred in solid phase [4]. This work presents methods, tools and results of LIFT-printing copper and gold 3D structures and their potential applications.

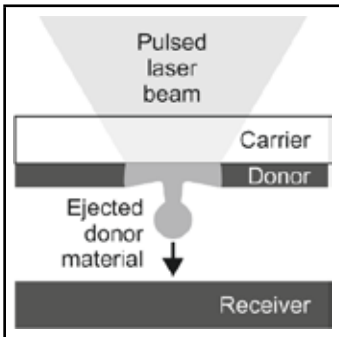

Fig. 1 Schematic of Laser-induced Forward Transfer (LIFT).

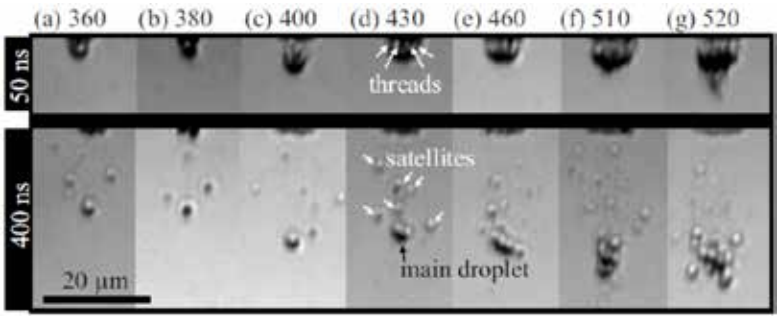

Fig. 2 Ejection events (droplets) originating from a 200nm copper donor film at different peak fluence levels [mJ/cm^2], using a 7ps Yb:YAG laser source [1]. The ejection events were recorded at time instances of 50 ns (top graph) and 400 ns (bottom graph) with respect to the time instance of the first visible deformation of the donor layer. Image (d), top graph, shows liquid threads (see arrows) between the donor layer and the droplet during the ejection process. When threads break up, satellites are formed (see arrows) resulting in debris on the receiver.

For example, it was found that controlling the fluence levels allows to control the velocity and size of droplets, see Fig. 2. However, next to the main droplet, also multiple smaller droplets, also referred to as “satellites”, are ejected. The latter result in debris on the receiver. It was found that after 50 ns, the ejected droplet is partly attached to the liquefied donor by thin “threads” (top graph in Fig. 2), which break up at a later stage in the process (bottom graph in Fig. 2), causing the satellites.

[1] A. Piqué, P. Serra (Eds.), *Laser Printing of Functional Materials: 3D Microfabrication, Electronics and Biomedicine*, Chapter 17 (Wiley-VCH Verlag, 2018).
[2] R. Pohl, *Laser-induced forward transfer of pure metals - Towards 3D printing*, PhD thesis, University of Twente, The Netherlands (2015).
[3] J. Luo, R. Pohl, L. Qi, G.R.B.E. Römer, C. Sun, D. Lohse, C.W. Visser. Printing Functional 3D Microdevices by Laser-Induced Forward Transfer, *Small* **13**, 1602553 (2017).
[4] R. Pohl, M. Jansink, G.R.B.E. Römer, Solid-phase laser-induced forward transfer of variable shapes using a liquid-crystal spatial light modulator. *Appl. Phys. A* **120**, 427 (2015).

WE-O-1

Temperature effects in synthesis of metal nanostructures by pulsed laser deposition: Comparison of substrate heating and post-annealing

Alexander V. Bulgakov[1,2*], Sergey V. Starinskiy[2], Yuri G. Shukhov[2]

[1]HiLASE Centre, Institute of Physics of the Czech Academy of Sciences, Za Radnicí 828, 25241 Dolní Břežany, Czech Republic
[2]Kutateladze Institute of Thermophysics SB RAS, Lavrentyev Ave. 1, 630090 Novosibirsk, Russia
Corresponding author: bulgakov@fzu.cz

Pulsed laser ablation (PLD) is a well-established technique for producing nanostructured materials, in particular, high-purity metal nanoparticles. The film growth temperature is shown to be a key process parameter to control the film morphology [1, 2]. On the other hand, post-annealing of thin metal films is an efficient method for surface engineering allowing to change the particle size, shape and structure [3]. However, the temperature effects during and after PLD are still poorly understood, a direct correlation between the two methods of nanostructure formation is missing, and the control of the sizes of PLD-produced nanoparticles remains a challenge. In this work, we report experimental results on comparison of the morphology of nanostructured films produced in two PLD regimes, (a) a substrate kept at an enhanced temperature T_s (in the range 300-800 °C) during PLD and (b) post-annealing at the same temperature for films deposited at room temperature. Gold and silver films were deposited with the mass thickness h_m in the range 3-8 nm. We demonstrate that the final film morphology, for both synthesis ways, is mainly governed by a combination of the two parameters, T_s and h_m (typical SEM images are shown in Fig. 1). Various mechanisms underlying film structuring in different PLD regimes such as nucleation, particle surface diffusion and evaporation, island coalescence, assembling of preformed small clusters, solid-state dewetting, and Ostwald ripening are discussed. Ways to control the particle size distributions under PLD conditions are also discussed.

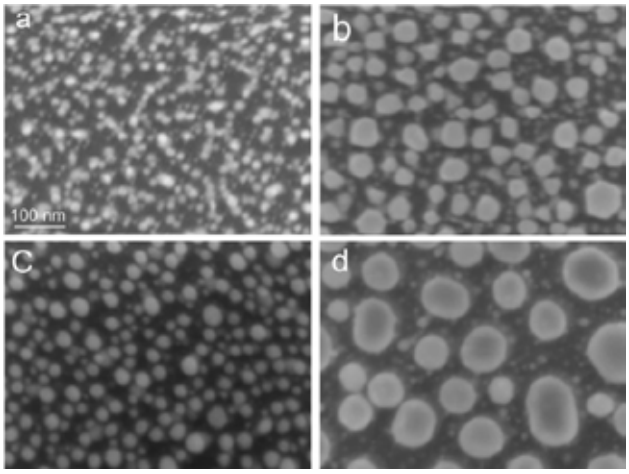

Fig. 1. SEM images of gold nanostructured films produced by PLD onto silicon substrates at 800 °C (a, b) and at room temperature with post-annealing at 800 °C (c, d) for the mass-averaged film thicknesses of 3 nm (a, c) and 7 nm (b, d).

[1] P. Kumar, M.G. Krishna, A.K. Bhatnagar, A.K. Bhattachara, Dynamic force microscopy study of the microstructural evolution of pulsed laser deposited ultrathin Ni and Ag films. *J. Mater. Res*. 23, 1826-1839 (2008).
[2] S.V. Starinskiy, Yu.G. Shukhov, A.V. Bulgakov, Dynamics of pulsed laser ablation of gold in vacuum in the regime of nanostructured film synthesis. *Tech. Phys. Lett*. 42, 411-414 (2016).
[3] A. Kosinova, O. Kovalenko, L. Klinger, E. Rabkin, Mechanisms of solid-state dewetting of thin Au films in different annealing atmosphere. *Acta Materialia* 83, 91-101 (2015).

WE-O-2

Short laser pulses excited processes: Applications to nanobiomedicine

Ion N. Mihailescu

National Institute for Lasers, Plasma and Radiation Physics, POB MG-36, Magurele, Ilfov, Romania
Corresponding author e-mail: ion.mihailescu@inflpr.ro

Basic principles of short laser pulses excited processes are introduced, and new recent results in the synthesis of biomaterials in the form of thin films and nanoparticles are reviewed. Deposited layers were optimized based upon the results of physical-chemical investigations, while biocompatibility, bioactivity and biodegradation were assessed by *in-vitro* tests.

Coating of implants with composite alendronate (AL)-HA by MAPLE was demonstrated to enhance human osteoblasts proliferation and differentiation, while inhibiting osteoclasts growth, with benefic effects for the treatment of bone diseases. MAPLE thin films of calcium alendronate monohydrate, octacalcium phosphate, or CaAL·H_2O / OCP composite on Titanium substrates showed that the presence of calcium alendronate in the coatings dramatically inhibits proliferation, differentiation and activity of osteoporotic osteoclast.

A compositional gradient was obtained by Combinatorial-MAPLE (C-MAPLE) by synchronous laser vaporization of two targets. Levan and oxidized levan cryogenic targets were used for the transfer under protection by MAPLE and assemble a two-compound biopolymer film structure. FTIR micro-spectroscopy confirmed the existence of a composition gradient all along the sample. *In-vitro* cell culture assays illustrate characteristic responses of cells to specific surface locations. Attached cells were in direct proportion with oxidized levan concentration.

C-MAPLE was applied to synthesize crystalline gradient thin films of Sr-substituted hydroxyapatite (Sr-HA) and Zolendronate modified hydroxyapatite (ZOL-HA). The inhibitory action of ZOL on osteoclast viability and activity was more efficient than Sr, with an improved role in osteoblast proliferation and viability. C-MAPLE allows modulating the composition of the films and hence the promotion of bone growth and the inhibition of bone resorption.

C-MAPLE has been extended to deposit adherent thin films with a gradient composition of SrHA and β-ZnTCP on Ti substrates. The response of co-cultured osteoblasts and osteoclasts was modulated by the graded composition as a function of the relative content of SrHA and β-ZnTCP. The presence of SrHA inhibits osteoclasts viability and differentiation, while β-ZnTCP had a beneficial action of the mineralization process. Intermediate compositions, with SrHA and β-ZnTCP, combine the positive effects on osteoblasts with the inhibitory one on osteoclasts and opens the way for the biofabrication of materials with tailored capability, via laser processing parameters, in order to enhance and accelerate bone repair.

Our conclusion is that thin films prepared by pulsed laser techniques were identical in chemical composition, structure, morphology, and most likely functionality with the base material, as proved by physical-chemical characterization and *in-vitro* testing.

[1] “Biomimetic Coatings by Pulsed Laser Deposition”, Ristoscu Carmen and Ion N. Mihailescu, Pages 163-191, “Laser Technology in Biomimetics”, Volker Schmidt, Maria Regina Belegratis , (Eds.), 2013, Basics and Applications, Series: Biological and Medical Physics, Biomedical Engineering, Springer-Verlag Heidelberg, New York, Dordrecht, London 2013

[2] “Biomaterial thin films by soft pulsed laser technologies for biomedical applications”, Ion N. Mihailescu, Adriana Bigi, Eniko Gyorgy, Carmen Ristoscu, Felix Sima, Ebru Toksoy Oner, Chapter 11 in “Lasers in Materials Science” (SLIMS 2012 Proceedings), Springer Series Materials in Science, vol. 191, Eds. P.M. Ossi, M. Castillejo, L. Zhigilei, ISBN 978-3-319-02897-2 (2014) pp. 271-291

[3] ”Protected Laser Evaporation/ Ablation and Deposition of Organic/Biological Materials : Thin Films Deposition for Nanobiomedical Applications”, Gianina-Florentina Popescu-Pelin, Carmen Ristoscu, Maria Badiceanu, Ion N. Mihailescu, Chapter 3 - Laser Ablation - From Fundamentals to Applications, InTechOpen, ISBN : 978-953-51-3700-9, Edited by Tatiana E. Itina, pp. 57-79, (2017)

[4] ”New bio-active, antimicrobial and adherent coatings of nanostructured carbon double-reinforced with silver and silicon by Matrix-Assisted Pulsed Laser Evaporation for medical applications” L. Duta, C. Ristoscu, G.E. Stan, M.A. Husanu, C. Besleaga, M.C. Chifiriuc, V. Lazar, C.Bleotu, F. Miculescu, N. Mihailescu, E. Axente, M. Badiceanu, D. Bociaga, Ion N. Mihailescu, Applied Surface Science, Vol. 441, p. 871-883, May 31 2018

[5] ”Gradient coatings of strontium hydroxyapatite/zinc β-tricalcium phosphate as a tool to modulate osteoblast/osteoclast response”, Boanini E, Torricelli P., Sima F., Axente E., Fini M., Mihailescu I.N., Bigi A.; Journal of Inorganic Biochemistry; 183, pp 1-8, 2018

WE-O-3

Large optical nonlinearity in gold nanoparticle films made by PLD

Inam Mirza[1, 3], David McCloskey[1], James G.Lunney[1]

[1]School of Physics, Trinity College Dublin, Dublin 2, Ireland
[2]HiLASE Centre, Institute of Physics ASCR, v.v.i., Za Radnicí 828, 25241 Dolní Břežany, Czech Republic
Corresponding author: jlunney@tcd.ie

Materials with large, and fast, third order nonlinear optical response find applications in optical telecommunication, optical data storage and digital information processing, where optical modulation of the optical phase is required [1]. There have been multiple reports of strong non-linear effects in thin metallic nanoparticle films, including, non-linear refraction [2], and saturable absorption [3]. In this work, the Z-scan technique, using femtosecond (fs) laser pulses at 1480 nm, was used to measure the nonlinear optical properties of gold (Au) nanoparticle (NP) films made by both nanosecond (ns) and fs pulsed laser deposition (PLD) in vacuum [4]. Typical films had particle sizes ranging from 5-10 nm, shown in Fig.1 (a). At irradiance levels of 10^{12} W $m^{-2,}$ the ns-PLD films displayed induced absorption with $\beta = 4\times10^{-5}$ m W^{-1}, and a negative lensing effect with $n_2 = -4.7\times10^{-11}$ m^2 W^{-1}, with somewhat smaller values for the fs-PLD films. These values of n_2 imply a very large change in the real part of the refractive index and point to the need to take account of nonlinear changes of the Fresnel coefficients and multiple beam interference when dealing with Z-scan measurements on nanoscale films. Following this approach, the Z-scan observations were analysed to determine the effective complex refractive index of the NP film at high irradiance. It appears that at high irradiance the NP film behaves as a metal, while at low irradiance it behaves as a low-loss dielectric (Fig1 (b)). Thus it is conjectured that the mechanism for high optical non-linearity in these films is a dielectric-to-metal transition due to laser-driven electron tunnelling between nanoparticles. Experiments are underway to confirm this conjecture.

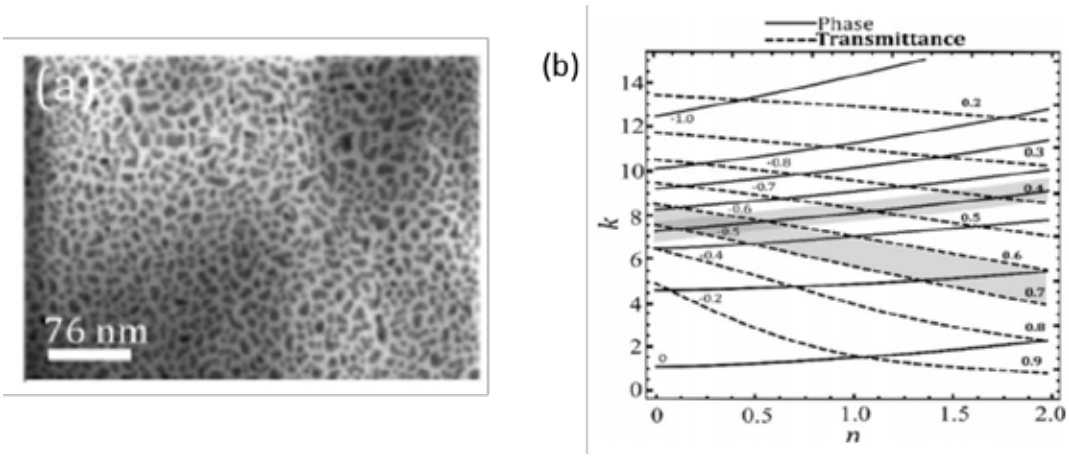

Fig 1 (a) SEM image of a typical film of PLD deposited Au particle on a SiO_2 substrate. (b) Map of *n* and *k* values corresponding to different measured values of transmission and phase in Z-scan technique.

[1] D. Cotter, R. J. Manning, K. J. Blow, A. E. Kelly, D Nesset, I. D. Phillips, A. J. Poustie, and D. C. Rodgers, *Science* **286,** 1523 (1999).
[2] E. Xenogiannopoulou, P. Aloukos, S. Couris, E. Kaminska, A. Piotrowska, and E. Dynowska, *Opt. Commun*. **275**, 217 (2007).
[3] W. T. Wang, D. Y. Guan, G. Yang, G. Z. Yang, Y. L. Zhou, H. B. Lu, and Z. H. Chen, *Thin Solid Films* **471**, 86 (2005).
[4] I. Mirza, G. O'Connell, J. J. Wang and J. G. Lunney, *Nanotechnology* **25**, 1455 (2018).

WE-O-4

Thin films for solar cells produced by pulsed laser deposition

Jørgen Schou, Mungunshagai Gansukh and Stela Canulescu

DTU Fotonik, Technical University of Denmark, DK-4000 Roskilde, Denmark
Corresponding author: josc@fotonik.dtu.dk

Silicon solar cells are presently dominant for harvesting solar energy because of the well-known production technology which ensures inexpensive and reliable cells with a module efficiency up to 20 %. Since silicon has an indirect band gap, its absorption is so low that a cell requires a layer up to 200 µm silicon for sufficient light absorption.

During the latest decades, new thin-film semiconductor cells with a four-component absorber, CIGS ($CuI_xGa_{1-x}Se_2$) or CZTS (Cu_2ZnSnS_4) have emerged as promising candidates for solar energy. The materials have a direct absorption, and the absorber works perfectly with a thickness of 1-2 µm, and CIGS-cells have recently reached an efficiency exceeding 20%.

These four-component materials, in particular, CZTS, are difficult to produce since the stoichiometry for the most efficient absorbers are different from the nominal composition mentioned above, i.e. Cu-poor and Zn rich. In addition, the number of defects in the absorber has to be so low that the charge carriers can reach the electrodes before being trapped at the defects.

Pulsed Laser Deposition (PLD) is a well-known technique by which the stoichiometry of a complex target can be transferred to a film with the same composition on a substrate. It is therefore straightforward to apply PLD to these chalcogenides materials. However, it turned out that the films produced by PLD were usually Cu-rich in contrast to the desired Cu-poor condition. At low fluence, it was possible to obtain a Cu-poor composition for CZTS such that a cell of more than 5 % efficiency could be produced. Also, the usual problem for PLD, large droplets, could be reduced at low fluence.

The underlying physics of the behavior of the film composition as a function of laser fluence for a number of chalcogenides will be discussed in terms of the physical properties of the materials, in particular, the cohesive energy.

WE-O-5

One- and three-dimensional analysis of colliding laser-induced plumes

Ikurou Umezu[1], Toshiki Kinoshita[2], Hiroshi Fukuoka[2], Keita Katayama[3], Yuki Horai[3], Tamao Aoki[1], Takehito Yoshida[4] and Minoru Yaga[5]

[1]Department of Physics, Konan University, Kobe 658-8501, Japan
[2]National Institute of Technology, Nara College, Nara 639-1080, Japan
[3]Graduate School of Natural Science, Konan University, Kobe 658-8501, Japan
[4]National Institute of Technology, Anan College, Anan 774-0017, Japan
[5] Department of mechanical system engineering, University of the Ryukyus, Nishihara 903-0213, Japan

Corresponding author: unezu@center.konan-u.ac.jp

Formation of the shock wave is essential for pulsed laser ablation in background gas. Deep understanding of the effects of the collision of two plumes and counter shock wave will lead to the preparation of novel complex nanoparticles. Effects of a head-on collision on two laser ablation plumes in background gas are revealed by observation of plume expansion dynamics and three-dimensional simulation. Si and Ge targets were set parallel to each other and irradiated simultaneously by two YAG lasers in He background gas. The results of plume emission intensity as a function of time and position are shown in Fig. 1. The stagnation and backward movements of the plumes due to the collision are observed at 500 and 3000 Pa respectively. The results of three-dimensional flow calculation at 3000 Pa for plume density and pressure derivative are shown in Fig.2. These results indicate that the backward movement is due to the collision of the plume with counter shock wave [1]. In the present paper, we analyze the effect of the counter shock wave by a one-dimensional model and three-dimensional simulation. According to the one-dimensional model, the velocity of the plume after a collision with the counter shock wave is determined by shock impedances of ahead and behind of contact front. They are a function of a ratio of specific heat, acoustic velocity and pressure ratio of ahead to behind of counter shock front. The change in the velocity of the plume by collision is discussed in terms of shock impedance. The velocity of shock wave reduces with increasing background gas pressure and increases the shock impedance of the background gas region. This is the origin of backward movement of plume after collision with counter shock wave. In conclusion, we clarified effect of counter shock wave on expansion dynamics of plume. These results indicate that plume expansion dynamics of colliding plumes, which is important for the formation of the novel complex nanoparticle, can be varied by using shock wave.

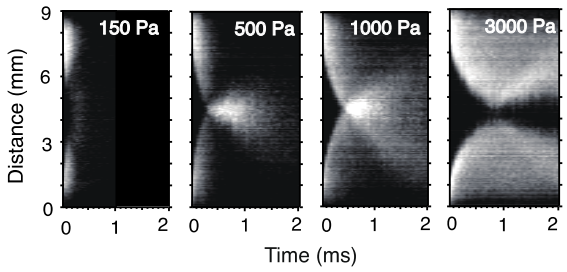

Fig.1. Contour plots of plume emission intensity.
Upper and lower sides are Ge and Si plumes, respectively.

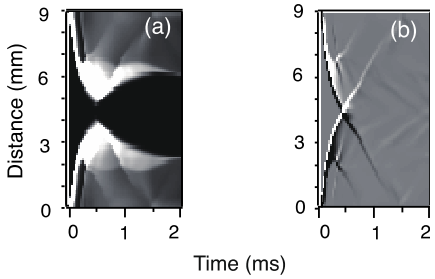

Fig.2 The results of computer simulation of (a) plume density and (b) pressure derivative at 3000 Pa.

[1] K. Katayama, Y. Hourai, H. Fukuoka, T. Kinoshita, T. Yoshida, T. Aoki, I. Umezu, Appl. Phys. A. **124**, 045328, 2018

WE-O-6

10B-enriched neutron conversion layers deposited by pulsed laser deposition at different wavelengths

Anna Paola Caricato[1,2], Gianluca Quarta[1,2,3], Maurizio Martino[1,2], Daniela Manno[1,2,3], Antonio Serra[1,2,3], Antonella Lorusso[1,2], Alessio Perrone[1,2], Lucio Calcagnile[1,2,3]

[1]Department of Mathematics and Physics "Ennio De Giorgi"-University of Salento-Lecce
[2]National Institute of Nuclear Physics (INFN) -Sezione di Lecce
[3]CEDAD (Centro of Applied Physics, Dating and Diagnostics)-Department of Mathematics and Physics "Ennio De Giorgi"-University of Salento-Lecce
Corresponding author: annapaola.caricato@unisalento.it

Neutron detection has an important role in many disciplines in science, industry and medicine. Neutron detectors are typically based on a conversion reaction in which neutrons interact with a nucleus to produce secondary charged particles, which are detected. The most used converter element is ^{3}He, but its availability is decreasing. For this reason, recently, a lot of research effort is devoted to studying and developing alternative materials, new technologies and methods for neutron detection.

In this study, we explore the potentialities of the laser ablation technique (PLD) for the deposition of ^{10}B enriched films in order to realize a neutron converter which can potentially be adapted to the different existing charge particles detectors.

In this respect, ^{10}B-enriched neutron conversion layers have been deposited ablating boron carbide (B_4C) targets with different laser wavelengths 266 nm (fourth harmonic of the Nd:YAG), 248 nm and 193 nm (KrF and ArF gas mixture respectively of a multigas excimer laser) on different substrates (silica, (100) Si, Kapton, Al).

The films have been characterized by many different diagnostic techniques SEM, TEM, XRD, Raman, AFM and IBA.

The analyses have highlighted that the laser wavelength and power density strongly influence the films properties and qualities in terms of deposition rate, crystalline structures (Fig. 1), stoichiometry and morphology.

In particular, the fourth harmonic of the Nd:YAG laser revealed to be the best choice in depositing B_4C films providing very smooth films, a congruent transfer of the material from target to the substrate and high deposition rates respect to excimer lasers.

All these results are discussed in terms of the characteristics and properties of the target material and laser sources and the peculiarity of the deposition process.

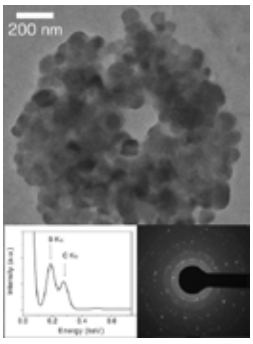

Figure 1 Typical results obtained on films deposited by Nd:YAG laser: TEM image, SEM-EDX spectrum and electron diffraction pattern.

WE-O-7

Surface microstructuring over wide area on nickel plating by laser-Induced back deposition in ambient air

Kazuki Koda[1,2], Ryosuke Izumi[1], Hirokazu Imai[1], Masahiro Tsukamoto[3]

[1]Sensor & Semiconductor Packaging R & D Div, DENSO CORPORATION, 1-1 Showa-cho, Kariya, Aichi 448-8661, Japan
[2]Department of Mechanical Engineering, Graduate School of Engineering, Osaka University, 1-1 Yamadaoka, Suita Osaka 565-0871, Japan
[3]Joining and Welding Research Institute, Osaka University, 11-1 Mihogaoka, Ibaraki, Osaka 567-0047, Japan
Corresponding author: kazuki_kouda@denso.co.jp

Microstructuring on a metal surface is a key technique to strengthen adhesion between polymer and metal by anchor effect and to improve sensitivity by plasmon resonance [1]. It is necessary to form a microstructure in a certain area for practical applications, and it is suggested that back deposition induced by laser plume in the ambient air could form microstructure over a wide area on a metal surface by laser scanning[2, 3]. However few studies have focused on wide area microstructuring by this method.

In this report, the formation process and shape controlling of microstructure by laser scanning were investigated by comparing microstructure formed by fixed point irradiation and laser scanning. In experiments, nanosecond laser was irradiated on the nickel plating by changing the fluence, the hatching distance and the number of irradiation and surface topography were analyzed by Scanning Electron Microscope (SEM) and Scanning Transmission Electron Microscopy (STEM).

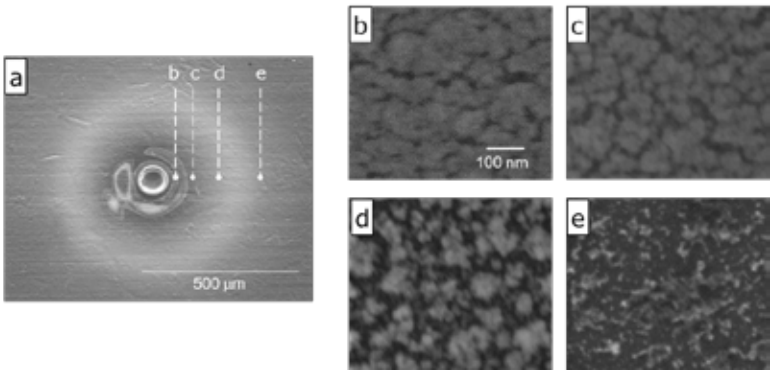

Fig. 1 (a) Low-magnification image of surface SEM observation. (b~e) High-magnification images of fig. 1(a).

Fig. 1 shows surface SEM images on the Ni surface. The wavelength, the pulse duration, the fluence and the number of shots were 1064 nm, 6 ns, 5 J/cm^2, 100 times, respectively. Fig. 1(a) shows a low-magnification image and Fig. 1(b)-(e) show the high-magnification images corresponding to Fig. 1(a). A dense structure was formed as near the irradiated area. Results in this experiments, It was suggested that the concentration of the plume influences the shape distribution of microstructure and the hatching distance of the laser is an important factor in the formation of a wide range of microstructure.

[1] W. Kiefer, A. P. Mazzolini, and P. R. Stoddart, Nanostructures and nanostructured substrates for surface-enhanced Raman scattering (SERS), *Raman Spectros* **38**, 1538 (2007).
[2] K.Koda, W. Kobayashi, H. Imai, and M. Tsukamoto, Formation of microstructures on Ni film surface by nanosecond laser irradiation, *Applied Physics A* **124**, 227 (2018).
[3] A. Pereira, P. Delaporte, M. Sentis, A. Cros, W. Marine, A. Basillais, A. L. Thomann, C. Leborgne, N. Semmar, P. Andreazza, and T. Sauvage, *Thin Solid Films* **453**, 16 (2004).

WE-IN-2

Three-Dimensional µ-Printing: An Enabling Technology

Julian Hering[1], Christina Jörg[1], Erik H. Waller[1], Georg von Freymann[1,2*]

[1]Physics Department and research center OPTIMIAS, Technische Universität Kaiserslautern, 67663 Kaiserslautern, Germany
[2]Fraunhofer Institute for Industrial Mathematics ITWM, 67663 Kaiserslautern, Germany
Corresponding author: georg.freymann@physik.uni-kl.de

During the last years, direct laser writing via two-photon absorption has reached a level of maturity and ease of application that it can be considered as 3D printing on the micron scale. This technology is still developing towards higher resolution and increasing speed of fabrication. Among the recent technological achievements are the fields of super-resolution lithography and spatial-light-modulator based lithography as well as novel materials for direct laser writing [1,2]. Applications span from bio-templating over metamaterials to photonic quantum simulators.

In this presentation, I will give an overview over our recent progress regarding spatial-light-modulator based direct laser writing and steps towards bio-based as well as metallic resists. Spatial-light-modulators allow for precise tuning of the point-spread-function and enable studies of the spatio-temporal proximity effect in direct-laser-writing [3].

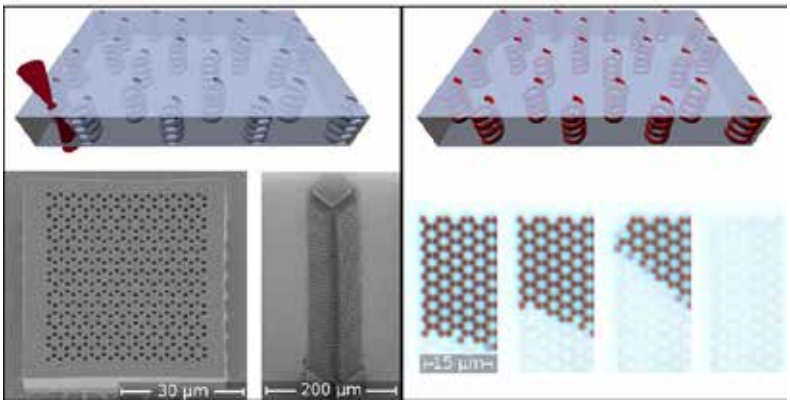

Figure 1: Direct laser written photonic quantum simulators: Hollow waveguides are infiltrated after development with higher-index material to enable waveguiding in this set of evanescently coupled waveguides [5].

I will further discuss selected applications, e.g., transport phenomena arising in aperiodic deterministic photonic structures as well as in photonic topological insulators (see Fig. 1). We observe transport phenomena ranging from lateral Anderson localization of light [4] to topologically protection. Here, we especially study the influence of time-dependent defects on topologically protected edge modes [5].

[1] J. K. Hohmann, M. Renner, E. H. Waller, and G. von Freymann, Three-Dimensional µ-Printing: An Enabling Technology, *Adv. Optical. Mater.* **3**, 1488 (2015)
[2] Erik H. Waller and Georg von Freymann, From photo-induced electron transfer to 3D metal microstructures via direct laser writing, *Nanophotonics* (2018)
[3] Erik H. Waller and Georg von Freymann, Spatio-temporal proximity characteristics in 3D µ-printing via multi-photon-absorption, *Polymers* **8**, 297 (2016)
[4] M. Renner and G. von Freymann, Spatial correlations and optical properties in three-dimensional deterministic aperiodic structures, *Scientific Reports* **5**, 13129 (2015).
[5] C. Jörg, F. Letscher, M. Fleischhauer, and G. von Freymann, Dynamic defects in photonic Floquet topological insulators, *New Journal of Physics* **19**, 083003 (2017)

WE-O-8

Continuous 3D Writing for Stitch-Free 3D Meso-Scale Laser Printing

Linas Jonušauskas[1,2], Tomas Baravykas[1,2], Darius Gailevičius[1,2], Sima Rekštytė[1], Saulius Juodkazis[3], Mangirdas Malinauskas[1*]

[1]Vilnius University, Faculty of Physics, Laser Research Center, Sauletekio Ave. 10, Vilnius, Lithuania
[2] Femtika Ltd., Saulėtekio Ave. 15, LT-10224, Vilnius, Lithuania
[3]Swinburne University of Technology, Victoria 3122, Hawthorn, Australia
Corresponding author: mangirdas.malinauskas@ff.vu.lt

In this work, we present an approach of synchronizing linear positioning and galvano-scanning for continuous writing based 3D optical printing of mesoscale structures out of lithographic materials. In such configuration, linear stages provide nearly limitless (up to tens of cm) working areas (volumes) and stitch-free final structures, while galvano-scanners allow achieving linear translation velocities in the range of mm/s-cm/s without sacrificing nano-scale positioning accuracy. We achieve normalized throughput-to-resolution reaching up to 32 722 voxels/s (employing NA=1.4 objective individual voxels corresponding to ≈0.34 μm^3 of polymerized volumes). The versatility of such an approach is demonstrated by fabricating multi-scale object with freely movable internal micro-parts as shown in Fig. 1.

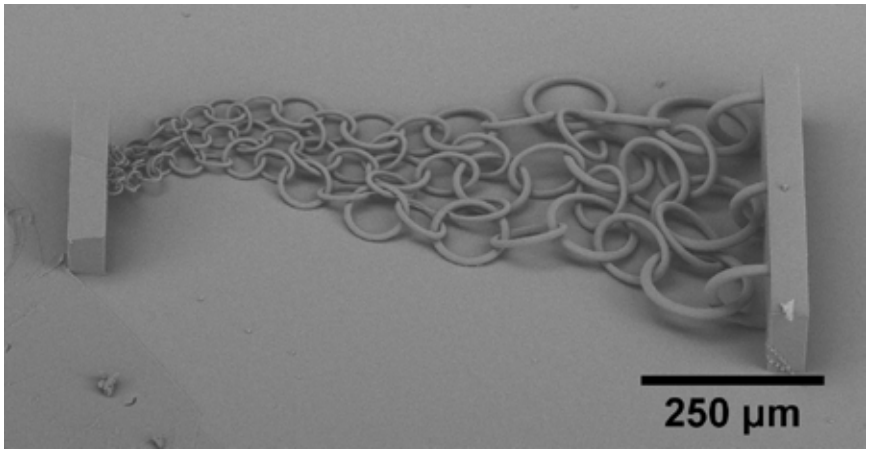

Fig. 1 An SEM image of a mesoscale chain-mail of SZ2080 made by continuous 3D direct laser writing lithography. It is 1 mm long gradient structure varying from 5 μm to 100 μm individual ring diameter and was printed in 25 min. Note the self-intertwined object was flexible and drifted freely during the wet developing process.

The proposed method's versatility was additionally validated by manufacturing mm-scale microoptical elements with μm-scale accuracy and characterized their optical performance. Finally, mm-scale 3D photonic crystals consisting of 10k rods (arranged to form a homogeneous lattice with 1.25M individual unit cells) were made and proved their functions as spectral-sensitive flat spatial-filters for beam quality improvement.

[1] M. Malinauskas *et al*., Ultrafast-laser micro/nano-structuring of photo-polymers: a decade of advances. *Phys. Rep.* **533**, 1 (2013).
[2] J.K. Hohmann *et al*., Three-Dimensional μ-Printing: An Enabling Technology. Adv. Opt. Mater. **3**, 1488 (2015).
[3] M. Malinauskas *et al*., Ultrafast laser processing of materials: from science to industry. *Light: Sci. Appl*. **5**, e16133 (2016).
[4] L. Jonusauškas *et al*., Optical 3D printing: bridging the gaps in the meso-scale. *J. Opt.* **20**, 053001 (2018);
[5] W. Chu *et al.*, Centimeter-Height 3D Printing with Femtosecond Laser Two-Photon Polymerization. Adv. Mater. Techn. **in press**.
[6] L. Jonušauskas *et al*., Mesoscale ultrafast laser 3D lithography: throughput in voxels-per-second. *Proc. SPIE* **in press**.
[7] L. Jonušauskas *et al*., **in preparation**.

WE-O-9

Simple method for birefringence imaging of natural and laser fabricated polymers

R. Honda[1], M. Ryu[1], J. Morikawa[1], S. Chatterjee[2], E. Yulianto[2], V. Mizeikis[2], T. Katkus[3], S. Juodkazis[3]

[1]Tokyo Institute of Technology, Meguro-ku, Tokyo 152-8550, Japan
[2]Research Institute of Electronics, Shizuoka University, 3-5-1 Johoku, Naka-ku, Hamamatsu, 432-8561, Japan
[3]Swinburne University of Technology, John St., Hawthorn 3122 Vic, and Melbourne Centre for Nanofabrication, ANFF, 151 Wellington Rd., Clayton 3168 Vic, Australia

Simple ($2k) setup based on crossed polarisers and a liquid crystal retarder was made to image birefringence. For materials which have distinct orientation such as fibres or polymerised linear patterns this measurement provides a fast and easy mapping of retardance and, hence, birefringence, Δn, when thickness of sample, d, is known. Due to a spectrally broadband transmissivity of liquid crystals, this setup is applicable over the entire visible spectral range. For the best performance, red, green, or blue colour filters with 10 nm bandwidth were used for the corresponding spectral RGB cannel of the image. Detection limit of retardance Δnd/λ (λ is the wavelength) was around 2x10-4 as measured from the four averaged pixels of a 480 x 640 VGA pixel image in the region outside the silk fibre.

Samples of silk of two different varieties were used as examples of bio-polymers with linear molecular ordering as well as laser polymerised structures built up from linear structures fabricated at high-repetition-rate of 82 MHz, when thermal polymerisation has a considerable contribution. Photo-polymer SZ2080 with 0.5wt% photoinitiator 4,4'-bis(diethylamino)-benzophenone was used. Laser writing/printing was made with 800 nm wavelength, 100 fs duration pulses at different focusing and sample scanning conditions using microscope objective lens focusing. Influence of linearly polarised E-field and its coupling with the writing direction [1] was investigated on a cumulative retardance for multi-layered 3D structures. We also applied magnetic field during laser writing/printing using Nd:magnets (Nd2Fe14B) with the remanent magnetization B ≈ 1.3 Tesla. Coupling of the linearly polarised E-field of light and magnetic field at the sample plane, where photo-excited charge transport and E-field-ordered polymerisation is taking place, were analysed for optical birefringence at visible wavelengths and for the orientational effects in absorbance at the fingerprinting IR spectral range. This setup can also be used to quantify stress-induced retardance [2] in 3D printed workpieces.

Keywords: birefringence, silk, polymerisation by direct laser writing, 3D printing

References:

1. S. Rekštytė, T. Jonavičius, D. Gailevičius, M. Malinauskas, V. Mizeikis, E.G. Gamaly, S. Juodkazis, Nanoscale precision of 3D polymerization via polarization control, Advanced Optical Materials 4(8), 1209-1214 (2016).
2. R. Meguya, D. Linklater, W. Hart, A. Balčytis, E. Skliutas, M. Malinauskas, D. Appadoo, Y.-R. E. Tan, E. P. Ivanova, J. Morikawa, S. Juodkazis, 3D printed polarizing grids for IR-THz synchrotron radiation, J. Opt. 20 035101 (2018).

WE-O-10

3D printed Polarization Micro-Optics: Fresnel Rhomb printed on an optical fiber

Andrea Bertoncini, Carlo Liberale

Biological and Environmental Science and Engineering (BESE), King Abdullah University of Science and Technology (KAUST), Thuwal 23955 6900, Saudi Arabia
Corresponding author: carlo.liberale@kaust.edu.sa

Here we show the use of Direct Laser Writing (DLW) for the fabrication of a polarization optics element, a Fresnel Rhomb (FR), integrated onto a polarization-maintaining (PM) optical fiber to obtain a miniaturized on-fiber source of circularly polarized light. The Fresnel Rhomb is a prism in which light experiences two total internal reflections at a precisely tuned incidence angle so that the phase shift difference between *s* and *p* polarizations at the output of the prism is 90° [1]. The FR acts as a quarter waveplate and features a very broad spectral range because it is not based on material birefringence. The designed micro-structure (total height 320 µm) is composed of two main parts (see fig. 1a): a collimating microlens and an FR, oriented at 45 deg with respect to the axis of PM fiber, to convert linear polarization to a circular one. We used a DLW 3D printer based on two-photon lithography (Photonic Professional GT, Nanoscribe GmbH) to print the designed micro-structure with IP-S (Nanoscribe GmbH) on top of a PM panda fiber (PM780-HP, Thorlabs). By measuring the Stokes parameters of the output beam with the classical "quarter waveplate - polarizer" method, we demonstrate the obtaining of an almost pure circularly polarized beam in the whole spectral bandwidth of the PM fiber (770-1100 nm).

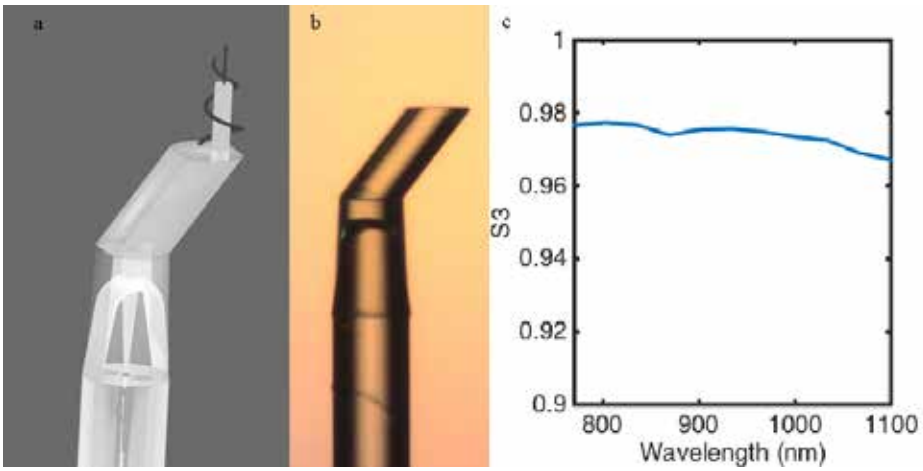

Fig. 1. a) Sketch of the designed microstructure. A linearly polarized beam exits from the PM fiber (bottom part), is collimated by a lens (in the middle) and is transformed to a circularly polarized beam by the Fresnel Rhomb (top part); b) Optical image of the microfabricated structure on top of the PM optical fiber; c) Measured normalized S3 Stokes parameter which indicates almost pure circularly polarized beam in the whole spectral bandwidth of the PM fiber.

[1] A. Fresnel (1832) "Mémoire sur les modifications que la réflexion imprime à la lumière polarisée" (Memoir on the alterations that reflection imparts to polarized light), *Mémoires de l'Académie des sciences de l'Institute de France*, vol. 11, pages 373-434)

WE-O-11

Laser Printing of Functional Resonant Dielectric Nanoparticles

Sergey Makarov[1]

[1]ITMO University, Department of Nanophotonics and Metamaterials, 197101 Saint Petersburg, Russia;
Corresponding author: s.makarov@metalab.ifmo.ru

The study of both linear and nonlinear effects in all-dielectric resonant nanophotonic structures is a hot topic of research that employs strong electric and magnetic field enhancements due to dipole and multipole Mie responses, accompanied by low losses [1,2]. Herein we review our recent achievements in the field of laser printing of resonant dielectric nanoparticles with enhanced light-emitting characteristics. Namely, we will discuss enhanced photoluminescence [3,4], second harmonics generation [5], and Raman scattering [6] from the printed nanoparticles possessing Mie resonances in the visible range. These recent developments pave the way for the high-throughput fabrication of nanoscale light emitters with various functionality: from efficient light frequency conversion to nanothermometry.

[1] A. Kuznetsov et al. Science 354, aag2472 (2016)
[2] I Staude, J Schilling, Nature Photonics 11(5), 274 (2017)
[3] E Tiguntseva, et al. Nano Letters 18 (2), 1185-1190 (2018)
[4] SV Makarov, et al. Nano Letters 18 (1), 535-539 (2018)
[5] SV Makarov, et al. Nano Letters 17 (5), 3047-3053 (2017)
[6] GP Zograf, et al. Nano Letters 17 (5), 2945-2952 (2017)

WE-IN-3

3D Printing of Complex Microoptics

Harald Giessen*, Simon Ristok, Ksenia Weber, Michael Schmid, Simon Thiele, Alois Herkommer

[1]4th Physics Institute, Institute for Technical Optics, and Research Center SCoPE, University of Stuttgart, 70569 Stuttgart, Germany
Corresponding author: giessen@physik.uni-stuttgart.de

Microoptics has a plethora of applications, ranging from miniature endoscopes in hospitals to beam shaping or imaging. 3D printing with a femtosecond laser and two-photon polymerization allows for manufacturing optical elements directly after their design with an optical CAD program on a computer, with a resolution better than 100 nm and high accuracy and reproducibility.

The talk is showing the first experimental results and discusses the different possibilities and perspectives. Triplett microscope objectives of only 100 µm diameter with excellent imaging properties, fitting into the inside of a syringe, are becoming available with this technology and can be useful for medical applications as well as for novel sensors or inspection methods.

Merging this technology with metasurfaces and plasmonics in order to achieve active and switchable optical systems will be discussed.

Fig. 1 (a) 3D printed complex microoptical microobjective on the optical fiber. (b) A miniature endoscope inserted into the syringe.

[1] T. Gissibl et al., Optica **3**, 448 (2016).
[2] T. Gissibl et al., Nature Communications **7**, 11763 (2016).
[3] T. Gissibl et al., Nature Photonics **10**, 554 (2016).
[4] S. Thiele et al., Opt. Lett. **41**, 3029 (2016).
[5] S. Thiele et al., Science Advances **3**, e1602655 (2017).

TH-IN-1

Two-photon polymerization for three-dimensional assembly of aligned carbon nanotubes

Ying Liu,[1] Wei Xiong,[2] Li Jia Jiang,[1] Yun Shen Zhou,[1] Da Wei Li,[1] Lan Jiang,[3] Jean-François Silvain,[4] Yong Feng Lu[1]*

[1]Department of Electrical and Computer Engineering, University of Nebraska-Lincoln, Lincoln, NE 68588-0511 (USA) [2]Wuhan National Laboratory for Optoelectronics, Huazhong University of Science and Technology, 1037 Luoyu Road, Wuhan 430074 (China)
[3]School of Mechanical Engineering, Beijing Institute of Technology, Beijing, 100081 (China)
[4]Institut de Chimie de la Matière Condensée de Bordeaux, Avenue du Docteur Albert Schweitzer F-33608 Pessac Cedex, (France)
Corresponding author: ylu2@unl.edu

Precise assembly of carbon nanotubes (CNTs) in arbitrary 3D space with proper alignment is critically important and desirable for CNT applications but still remains as a long-standing challenge. Using the two-photon polymerization (TPP) technique, it is possible to fabricate 3D micro/nanoscale CNT/polymer architectures with proper CNT alignments in desired directions, which is expected to enable a broad range of applications of CNTs in functional devices. To unleash the full potential of CNTs, it is strategically important to develop TPP-compatible resins with high CNT concentrations for precise assembly of CNTs into 3D micro/nanostructures for functional device applications. We investigated a thiol grafting method in functionalizing multiwalled carbon nanotubes (MWNTs) to develop TPP-compatible MWNT-thiol-acrylate (MTA) composite resins (Fig. 1). The composite resins developed had high MWNT concentrations up to 0.2 wt%, over one order of magnitude higher than previously published work. Significantly enhanced electrical and mechanical properties of the 3D micro/nanostructures were achieved. Precisely controlled MWNT assembly and strong anisotropic effects were confirmed. Microelectronic devices made of the MTA composite polymer were demonstrated. The nanofabrication method can achieve controlled assembly of MWNTs in 3D micro/nanostructures, enabling a broad range of CNT applications, including 3D electronics, integrated photonics, and micro/nanoelectromechanical systems (MEMS/NEMS).

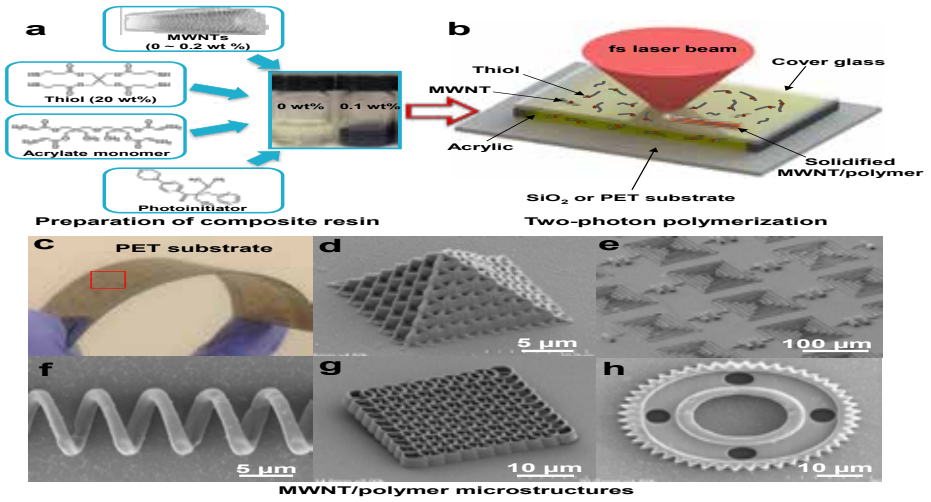

Fig. 1 3D micro/nanofabrication based on MTA composite resins by TPP lithography. (a) The experimental procedure in preparing MTA composite resins. **(**b) Experimental setup of TPP fabrication.

TH-O-1

Laser-induced graphene ablation and graphene oxide reduction for application as electrodes in thin-film transistors

Maren Kasischke[1], Stella Maragkaki[1], Ersoy Subasi[2], Claudia Bock[3], Evgeny L. Gurevich[1], Ulrich Kunze[2] and Andreas Ostendorf[1*]

[1]Ruhr University Bochum, Faculty of Mechanical Engineering, Applied Laser Technologies, Bochum, Germany
[2]Ruhr University Bochum, Faculty of Electrical Engineering and Information Technology, Electronic Materials and Nanoelectronics, Bochum, Germany
[3]Ruhr University Bochum, Faculty of Electrical Engineering and Information Technology, Microsystems Technology, Bochum, Germany

Corresponding author: andreas.ostendorf@ruhr-uni-bochum.de

Graphene and graphene-based materials have a high potential as thin-film electrodes, e.g. for thin-film transistors (TFTs), due to their optical transparency and low sheet resistance. For this purpose, clean and well-defined microstructures of the graphene material and an effective graphene oxide (GO) reduction are necessary. However fabrication of such microstructures is difficult due to handling and machining problems. Femtosecond lasers are versatile tools for controlled ablation and modification of thin-films. Here we present femtosecond laser processing of two different carbon-based materials. First, selective structuring of single graphene layers and its application as source and drain electrodes in TFTs are shown (see Fig. 1 (a)). The performance of TFTs is improved by graphene patterning in vacuum, as compared to patterning in air, due to reduction of debris in the transistor channel. Secondly, reduction of GO layers is investigated (see Fig. 1 (b)). Self-organized periodic structures appear on GO surfaces upon processing at fluences slightly higher than the fluence needed for reduction of the GO [1]. The laser-induced structuring of graphene is analyzed with scanning electron microscopy and atomic force microscopy while the reduction of GO is identified by sheet resistance measurements, Raman and X-ray photoelectron spectroscopy.

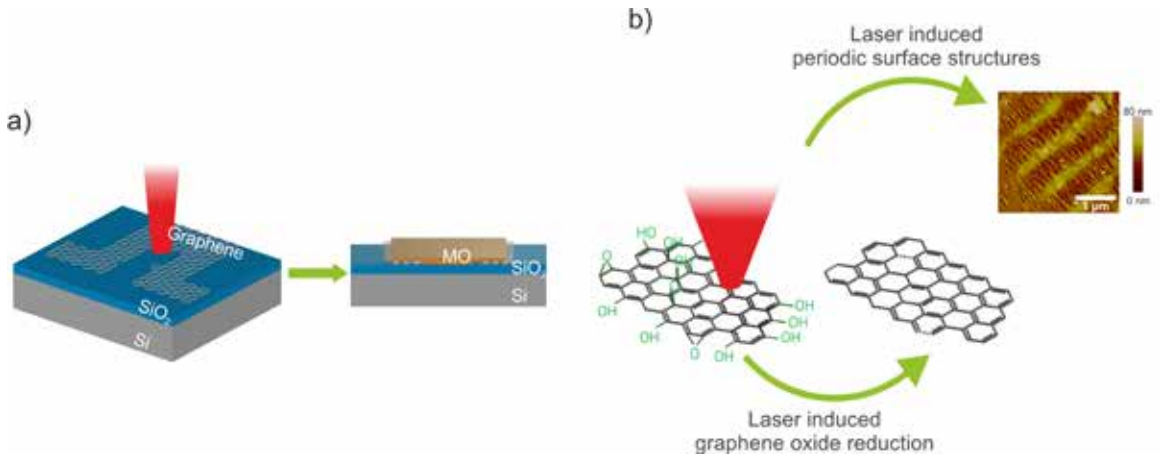

Fig. 1 (a) SEM images of single pulse graphene ablation at different fluences
(b) Laser-induced graphene oxide reduction and nano-patterning [1].

[1] M. Kasischke, S. Maragkaki, S. Volz, A. Ostendorf, E. L. Gurevich, Simultaneous nanopatterning and reduction of graphene oxide by femtosecond laser pulses. *Appl Surf Sci* **445,** 197-203 (2018).

TH-O-3

Laser-Induced Processes in Nanotechnology

Aida Naghilou, Martin Pfaffeneder-Kmen, Ignacio Falcon-Casas, Niusha Lasemi, Oskar Armbruster, Ulrich Pacher, Evgeniya Paulis, Tristan Nagy, Leonid V. Zhigilei, Wolfgang Kautek

[1]University of Vienna, Department of Physical Chemistry, Vienna, Austria
[2] University of Virginia, Department of Materials Science & Engineering, Charlottesville, VA 22904-4745, USA
Corresponding author: wolfgang.kautek@univie.ac.at

Research in physical chemistry and nanotechnology at interfaces is presented. This includes femtosecond far field investigations with bandwidth-limited [1-6], temporally shaped pulses, and electrochemical in-situ techniques in graphene nanosheet synthesis [7,8]. Further, deterministic nanostructuring of solids such as e.g. nanojets, hot electron electrochemistry, and the laser generation of colloids for medical applications [9-11] are discussed. High-resolution depth profiling by laser-induced break-down spectroscopy (LIBS) is being developed for industrial applications [12-14].

Finally, apertureless scanning near-field nanolithography with a femtosecond Yb-doped fiber laser oscillator (Fig. 1) was demonstrated to be based on non-thermal electromagnetic energy transfer [15-17].

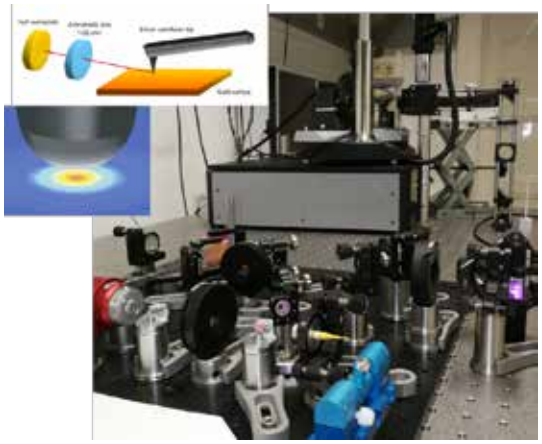

Fig. 1 Apertureless scanning near-field nanolithography with a femtosecond Yb-doped fiber laser oscillator.

[1] W. Kautek and O. Armbruster, Springer Series in Materials Science 191 (2014) 43-66.
[2] M.V. Shugaev, C. Wu, O. Armbruster, A. Naghilou, N. Brouwer, D.S. Ivanov, T.J.-Y. Derrien, N.M. Bulgakova, W. Kautek, B. Rethfeld, L.V. Zhigilei, MRS Bulletin 41 (2016) 960–968.
[3] O. Armbruster, A. Naghilou, M. Kitzler, W. Kautek, J. Phys. Chem. C 119 (2015) 22992−22998.
[4] O. Armbruster, A. Naghilou, M. Kitzler, W. Kautek, Appl. Surf. Sci. 396 (2017) 1736–1740.
[5] A. Naghilou, O. Armbruster, W. Kautek, Appl. Surf. Sci. 418 (2017) 487-490.
[6] M. Forster, C. Huber, O. Armbruster, R. Kalish, W. Kautek, Diam. Rel. Mat. 74 (2017) 114–118.
[7] M. Pfaffeneder-Kmen, F. Bausch, G. Trettenhahn, W. Kautek, J. Phys. Chem. C 120 (2015) 15563–15568.
[8] M. Pfaffeneder-Kmen, I. Falcon Casas, A. Naghilou, G. Trettenhahn, W. Kautek, Electrochim. Acta 255 (2017) 160-167.
[9] N. Lasemi, U. Pacher, C. Rentenberger, O. Bomati Miguel, W. Kautek, ChemPhysChem 18 (2017) 1118–1124.
[10] N. Lasemi, U. Pacher, L.V. Zhigilei, O. Bomati-Miguel, R. Lahoz, W. Kautek, Applied Surface Science 433 (2018) 772–779.
[11] N. Lasemi, O. Bomati Miguel, R. Lahoz, V.V. Lennikov, U. Pacher, C. Rentenberger, W. Kautek, ChemPhysChem (2018) DOI: 10.1002/cphc.201701214.
[12] T. Nagy, U. Pacher, A. Giesriegl, L. Soyka, G. Trettenhahn, W. Kautek, Appl. Surf. Sci. 302 (2014) 184–188.
[13] E. Paulis, U. Pacher, M.J.J. Weimerskirch, T.O. Nagy, W. Kautek, Appl. Phys. A 123 (2018) 790.
[14] U. Pacher, M. Dinu, T.O. Nagy, R. Radvan, W. Kautek, Spectrochim. Acta B 146 (2018) 36-40
[15] C. Huber, A Trügler, U. Hohenester, Y. Prior, W Kautek, Phys. Chem. Chem. Phys. 16 (2014) 2289-2296.
[16] C. Huber, Y. Prior, W. Kautek, Meas. Sci. Technol. 25 (2014) 075604-075610.
[17] I. Falcon Casas and W. Kautek, in "Laser micro-nano-nanomanufacturing and 3D microprinting", A. Hu (Ed.), Springer, in press. „Apertureless scanning near-field optical lithography".

TH-O-4

Force Sensor Fabrication by AgNWs Film using 532nm Pulses Laser

Ching-Ching Yang, Yi-Cheng Lin, Min-Wei Hung, Hsin-Yi Tsai, Kuo-Cheng Huang, Wen-Tse Hsiao*

Instrument Technology Research Center, National Applied Research Laboratories, Hsinchu 30076, Taiwan
Corresponding author: wentse@narlabs.org.tw

The silver nanowire (AgNWs) [1,2] thin film is regarded as an emerging conductive material in recent years and has the advantages of high transmittance, low resistivity, stretchability, flexibility and cost-effective. In general, AgNWs thin film is now widely used to fabricate the electronic components, such as transistors [3], detectors [4], touch sensors [5,6], and supercapacitors [7,8]. Especially in the applications of the touch panel industry, AgNWs thin film is expected to become an ideal replacement material for the indium tin oxide (ITO) [9] thin film. In the study, the pulses laser system with 532 nm laser (NANIO 532-10-V, InnoLas Laser GmbH, Germany) and a 2-axis laser scanner (SS-II-15, Raylase AG, Germany) was adopted and a focus shifter inside the scanner can be used to adjust the focus range from +10 mm to −10 mm in Z-direction. The telecentric focusing lens with a focal length of 100 mm and the scanning area of 54 × 54 mm^2 were used in the processing. In addition, the force sensor was made of the polyimide substrate with the AgNWs thin film, and its thickness is 2 µm, and the size is 1.8× 1.8 cm. In order to obtain the optimal micromachining effect, the force sensors with the different linewidths (100, 300 and 500 µm) were developed on the substrate surface by laser direct writing (LDW) technique. Moreover, the output power of the laser is 2 watts, and the pulse repetition frequency is 40 kHz at different scanning speeds (800, 1,000 and 1,200 mm/s). The schematic of the experimental setup used for force sensor electrode patterning was shown in Fig. 1 and force testing platform was built to evaluate the laser ablation quality of force sensor shown in Fig. 1 (d). From the experimental results, it can be known that the faster the scanning speed of laser ablation, the smaller the pulse overlap. It means the edge of force sensor will gradually be serrated (i.e. sawlike) and obtain higher oxidation degree. Moreover, the resistance value from the force sensor will increase to affect the force sensing efficiency.

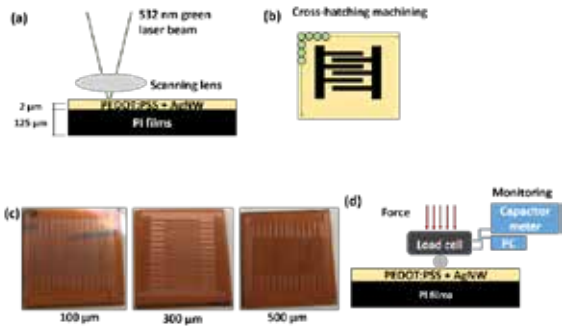

Fig. 1 (a) The schematic of the experimental setup used for force sensor making, (b) machining path planning, (c) the force sensors with the different linewidths (100, 300 and 500 µm), and (d) touch panel testing platform for force evaluation.

[1] K.M. Lin, R.L. Lin, W.T. Hsiao, Y.C. Kang, C.Y. Chou, Y.Z. Wang, Effects of the structural properties of metal oxide/Ag/metal oxide multilayer transparent electrodes on their optoelectronic performances, *Journal of Materials Science: Materials in Electronics*, **28**, 12363-12371 (2017).
[2] C. H. Liu, X. Yu, Silver nanowire-based transparent, flexible, and conductive thin film, *Nanoscale Research Letters*, **6**, 75-82 (2011).
[3] L.G.S. Albano, M.H. Boratto, O. Nunes-Neto, C.F.O. Graeff, Low voltage and high frequency vertical organic field effect transistor based on rod-coating silver nanowires grid electrode, *Organic Electronics*, **50**, 311-316 (2017).
[4] A. Kumar, P. Karadan, H.C. Barshilia, Synthesis of silver nanowires towards the development the ultrasensitive AgNWs/SiNPLs hybrid photodetector and flexible transparent conductor, *Materials Science in Semiconductor Processing*, **75**, 239-246 (2018)
[5] Y.M. Kim, J.W. Kim, Silver nanowire networks embedded in urethane acrylate for flexible capacitive touch sensor, *Applied Surface Science*, **363**, 1-6 (2016).
[6] M. Cann, M.J. Large, S.J. Henley, D. Milne, T. Sato, H. Chan, I. Jurewicz, A.B. Dalton, High-performance transparent multi-touch sensors based on silver nanowires, *Materialstoday Communications*, **7**, 42-50 (2016).
[7] W. Alshammari, D.S. Patil, S.A.Pawar, J.C. Shin, Silver nanowires-copper sulfide core/shell nanostructure for electrochemical supercapacitors, *Materialstoday Chemistry*, **5**, 72-80 (2017).
[8] P. Pattananuwat, P. Thammasaroj, W. Nuanwat, J. Qin, P. Potiyaraj, One-pot method to synthesis polyaniline wrapped graphene aerogel/silver nanoparticle composites for solid-state supercapacitor devices, *Materials Letters*, **217**, 104-108 (2018).
[9] S.F. Tseng, W.T. Hsiao, K.C. Huang, D. Chiang, Mi.F. Chen, C.P. Chou, Laser scribing of indium tin oxide (ITO) thin films deposited on various substrates for touch panels, *Applied Surface Science,* **257**, 1487-1494 (2010).

TH-O-5

Threshold fluence of femtosecond laser ablation for metals

Masaki Hashida[1], Mitsuhiro Kusaba[2], Fumitaka Nigo[2], Takeshi Nagashima[3], Akinori Irizawa[4], Hitoshi Sakagami[5], Amany Gouda[5], Shunsuke Inoue[1], Yuki Furukawa[1], Shuji Sakabe[1]

[1] Institute for Chemical Research, Kyoto University, Gokasyo, Uji, Kyoto, 611-0011, Japan
[2] Department of Electronics, Osaka Sangyo University, 3-1-1 Nakagaito, Daito, Osaka 574-8530, Japan.
[3] Faculty of Science and Engineering, Setsunan University, 17-8 Ikeda-Nakamachi, Neyagawa, Osaka 572-8508, Japan
[4] The Institute of Scientific and Industrial Research, Osaka University, 8-1 Mihogaoka , Ibaraki, Osaka 567–0047, Japan
[5] National Institute for Fusion Science, Toki, Gifu 509-5292, Japan
Corresponding author:hashida@laser.kuicr.kyoto-u.ac.jp

To achieve laser nano-fabrication much smaller size than that of diffraction limit, the knowledge of the laser-matter interaction is important, especially for producing the LIPSS on a solid surface. For femtosecond lasers, LIPSS can be produced on the metal surface irradiated by a laser pulse (and terahertz waves) fluence adjusting to a little higher than the ablation threshold. The periodicity of LIPSS has been down to λ/13[1)]- λ/25[2)] for the various wavelength λ of electro-magnetic fields (see Fig. 1). Therefore the ablation threshold might be one of the key issues to discuss physics of the laser-matter interaction. In this study, the ablation threshold has been measured precisely and compiled all data published for metals[3)]. We found that the nonlinear absorption on the metal surface irradiated by femtosecond laser pulses is an important role for determined the ablation threshold.

Femtosecond laser ablation of Ti by short-pulse laser irradiation (800 nm/40 fs) is studied in the laser fluence range of 70 mJ/cm^2 to 500 mJ/cm^2. To determine the ablation threshold, the ablation rate dependence on laser fluence is precisely measured. Multishot ablation threshold of titanium is found to be 74m J/cm^2 in which value is good agreement with that reported previously by another group. To discuss the ablation mechanism, all the ablation thresholds for metals previously published are plotted as a function of work function (see Fig. 2) and melting temperature. We found that the ablation thresholds correlated with a work function of metals. Experimental data suggested that the femtosecond laser ablation is mainly due to multiphoton absorption and optical field ionization.

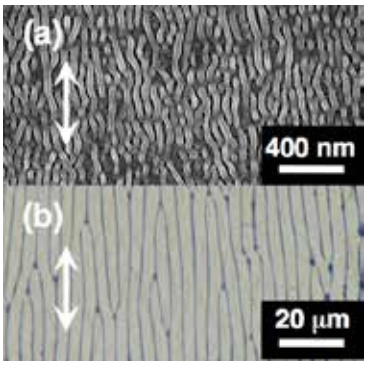

Fig. 1 SEM images of surface structures on (a) titanium produced by femtosecond double-pulse irradiation (LIPSS periodicity λ/13)[1)] and (b) silicon produced by linearly polarized terahertz waves of which wavelength of 85mm (LIPSS periodicity λ/25)[2)]. The white arrow shows the laser polarization direction for the double pulsed beam.

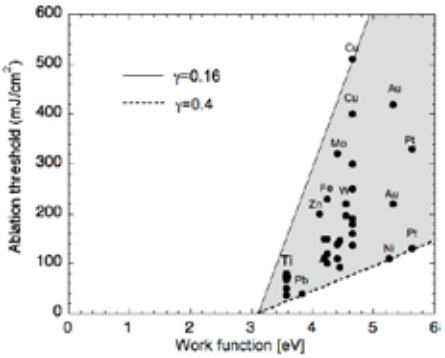

Fig. 2 Dependence of the ablation threshold on work function for metals,

This research was partially supported by a Grant-in-Aid for Scientific Research (C) (25420728, JP16K06745) from MEXT, Japan, supported by NEDO, NIFS Collaborative Research Program (NIFS17KNTS053), and the Collaborative Research Program of Institute for Chemical Research, Kyoto University(grant 2018-6).

1) M. Hashida, L. Gemini, T. Nishii, Y. Miyasaka, H. Sakagami, M. Shimizu *et al*., J. Laser Micro/ Nanoeng. **9**, 234-237(2014).
2) A. Irizawa, S. Suga, T. Nagashima, A. Higashiya, M. Hashida, S. Sakabe, Appl. Phys. Lett. **111**, 251602(2017).
3) M. Hashida, Y. Miyasaka, T. Nishii, M. Shimizu, S. Inoue, S. Sakabe., Electron. Communi. Jpn. **99**, 88(2016).

TH-O-6

Time-resolved investigation of laser-induced damage fatigue of single layer dielectric coatings

Linas Smalakys[1*], Balys Momgaudis[1], Mikas Vengris[1], Robertas Grigutis[1], Andrius Melninkaitis[1]

[1]Vilnius University, Faculty of Physics, Laser Research Center, Saulėtekio Ave. 10, Vilnius, Lithuania
[*]Corresponding author: linas.smalakys@ff.vu.lt

The decrease of laser-induced damage threshold (LIDT), when exposed with a high number of laser pulses, is a well-known phenomenon in most dielectrics. In the femtosecond regime, this fatigue is usually attributed to the accumulation of laser-induced lattice defects. Generation of such defects in SiO_2 was thoroughly investigated during the past few decades: intense laser pulse ionizes the material, the resulting electrons are converted into self-trapped excitons at a time scale of 150 fs, which, at room temperature, are then converted to permanent color centers [1]. Subsequent laser pulses can re-ionize laser-induced color centers. Thus the total number of generated electrons increases with each subsequent pulse [2]. However, little is known about the fatigue and accumulation mechanisms in oxides with much lower band gaps which are commonly used for thin film production. Previous experiments suggest the existence of laser-induced states [3], however, the information about their origin and characteristic features is extremely scarce.

In this work, a unique approach combining digital holography and time-resolved spectroscopy was employed in order to investigate the existence of laser-induced lattice defects in single layer dielectric coatings deposited by IBS process. Two-dimensional numerical model based on the finite-difference-time-domain (FDTD) method was developed in order to numerically simulate the pump-probe geometry of digital holography experiments and decouple ultra-fast processes overlapping in both space and time. Spectral information about laser-induced lattice defects from time-resolved spectroscopy experiments was employed to determine the system of rate equations required to simulate the dynamics of the electronic subsystem. The results of this work provided valuable insights into the probable cause of LIDT fatigue in thin film coatings.

[1] S. Guizard, P. Martin, G. Petite, P. D'Oliveira, P. Meynadieri, Time-resolved study of laser-induced colour centres in SiO2. *J. Phys. Condens. Matter* **8**, 1281–1290 (1996).
[2] L. A. Emmert, M. Mero, W. Rudolph, Modeling the effect of native and laser-induced states on the dielectric breakdown of wide band gap optical materials by multiple subpicosecond laser pulses. *J. Appl. Phys.* **108**, 1–7 (2010).
[3] M. Mero, A. J. Sabbah, J. Zeller, W. Rudolph, Femtosecond dynamics of dielectric films in the pre-ablation regime. *Appl. Phys. A Mater. Sci. Process.* **81**, 317–324 (2005).

TH-O-7

Determination of material parameters for modelling of ultra-short pulse ablation threshold in transparent, dielectric material

Marco Jupé, Detlev Ristau
Laser Zentrum Hannover e.V., Hollerithallee 8, 30419 Hannover, Germany

With respect to material structuring, the ablation of dielectric materials is an important issue. To limit the damage zone during the material processing, the applied energy densities are close to the damage threshold. In theoretical descriptions of these processes, the excitation of the valence band electrons is calculated. Generally, a combination of photoionization (multiphoton and tunnel ionization) and avalanche ionization is used. Especially the Keldysh theory is based on the assumption that the material has a crystalline structure. Often, this theory is also used for amorphous solids. However, several parameters are not defined for amorphous dielectrics. For instance, amorphous materials do not have a well-defined band structure. Also, the model of the effective mass of the electrons is established on a periodic structure. Nevertheless, these parameters are utilized in calculations for amorphous structures. Especially the effective mass of the electrons is a pure fitting parameter. In this presentation, different theoretical and experimental approaches are discussed determining the respective parameters. For the theoretical calculation, the concept of the virtual coater has been established. This approach combines transport and atomistic thin film growth simulations as well as ab-initio methods which enable the electronic structure to be calculated. The virtual coater includes the specific growth conditions, which influence the atomistic structure, and consequently, the electronic and optical properties. Because of fundamental problems experienced when calculating the effective mass in non-periodical solids, an experimental approach is applied. Here, quantized nanolaminates are deposited and evaluated experimentally.

Finally, the extracted parameters are used to calculate the ablation threshold of hafnia or tantala. The results are verified by experimental studies.

TH-IN-2

Ultrafast Laser-Induced Surface and Bulk Nanostructuring: Similarities Revealed by Electromagnetic Modeling

Jean-Philippe Colombier[1*], Anton Rudenko[1], Hao Zhang[1], Cyril Mauclair[1], Tatiana Itina[1], Florence Garrelie[1], Razvan Stoian[1]

[1]Univ Lyon, UJM-Saint-Etienne, CNRS, IOGS, Laboratoire Hubert Curien UMR5516, F-42023 St-Etienne, France

Corresponding author: jean.philippe.colombier@univ-st-etienne.fr

Progress in manufacturing, energy conversion or transportation is closely tied up to the ability to manipulate bulk and surface material properties at the nanoscale. The interaction of intense ultrashort laser pulses with rough surfaces and inhomogeneous volumes offers the possibility to localize light beyond the diffraction limit, presenting a real potential of direct nanostructuring with spatial order and tunable physical characteristics by optical means. Laser Induced Periodic Surface Structures (LIPSS) with periodicity varying from near laser wavelength down to sub-100 nm scale, has been reported on a large variety of solid materials. As well, the formation of bulk nanogratings in dielectrics upon irradiation with multiple femtosecond-laser pulses share some strong similarities with LIPSS although their formation mechanisms have been the subject of speculation and intensive debate throughout the decade. To explain this “universal mechanism of self-organization”, the role of surface and bulk roughness distributions will be discussed based on 3D electrodynamic simulations, first principles approaches and hydrodynamic processes [1]. A complex but similar electromagnetic origin, mainly induced by scattering and defined by the spatial coherence of the laser field [2], predicts a spatially-ordered energy deposition for periodic surface and bulk structuring. More precisely, simulations reveal the associated roles of a coherent superposition of far-field scattered waves with refracted waves and local near-field enhancement [3]. This indicates that the control of the underlying mechanisms is achievable through reaching a detailed elucidation of the electromagnetic response of irradiated materials.

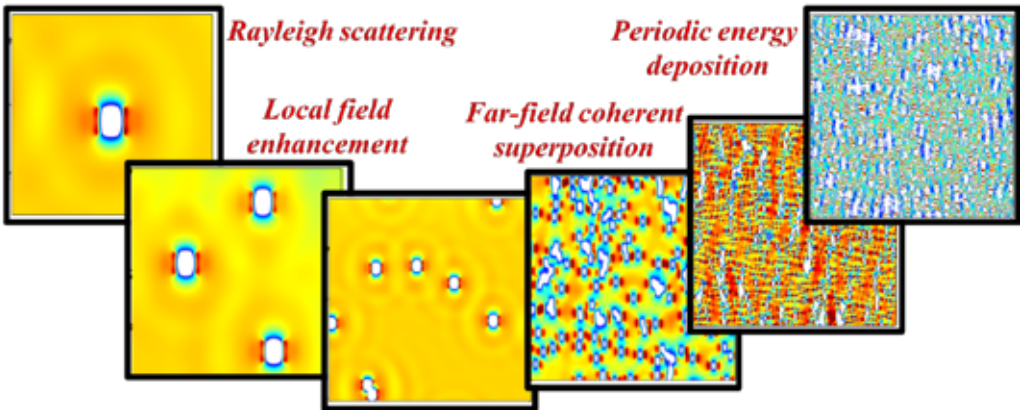

Fig. 1 Simulations of electromagnetic processes involved in laser-induced self-organization of material as a function of roughness concentration evolution.

[1] A. Rudenko, J.P. Colombier, S. Höhm, A. Rosenfeld, J. Krüger, J. Bonse, T.E. Itina, Spontaneous periodic ordering on the surface and in the bulk of dielectrics irradiated by ultrafast laser: a shared electromagnetic origin, *Scientific reports* 7 (1), 12306 (2017).

[2] H. Zhang, J.P. Colombier, C. Li, N. Faure, G. Cheng, R. Stoian, Coherence in ultrafast laser-induced periodic surface structures, *Physical Review B* 92, 174109 (2015).

[3] X. Sedao, A. Abou Saleh, A. Rudenko, T. Douillard, C. Esnouf, S. Reynaud, C. Maurice, F. Pigeon, F. Garrelie, J.-P. Colombier, Self-Arranged Periodic Nanovoids by Ultrafast Laser-Induced Near-Field Enhancement, *ACS Photonics* 5 (4) 1418-1426 (2018).

TH-O-8

Large-scale atomistic simulations of the generation of nanoparticles and surface nanostructuring by short pulse laser ablation in liquids

Cheng-Yu Shih, Maxim V. Shugaev, Chengping Wu, and Leonid V. Zhigilei

University of Virginia, Department of Materials Science and Engineering, 395 McCormick Road, Charlottesville, VA 22904, USA
Corresponding author: *lz2n@virginia.edu*

In this presentation, we report the results of large-scale molecular dynamics simulations aimed at revealing the key processes that control the surface morphology and nanoparticle size distributions generated by pulsed laser ablation in liquids [1-4]. The simulations of Ag and Cr targets irradiated in water are performed with an advanced computational model combining a coarse-grained representation of the liquid environment and an atomistic description of laser interaction with metal targets. One of the interesting predictions of simulations performed at sufficiently high laser fluences, in the regime of phase explosion, is the emergence of Rayleigh–Taylor and Richtmyer–Meshkov hydrodynamic instabilities at the interface between ablation plume and superheated water, leading to the formation of nanojets and emission of large droplets into cold water environment, Fig. 1. The droplets are rapidly quenched and solidified into nanoparticles featuring complex microstructure and metastable phases. Rapid nucleation and growth of small nanoparticles in the metal–water mixing region and the breakup of the hot metal layer into larger droplets due to the hydrodynamic instabilities represent two distinct mechanisms of the nanoparticle formation that yield nanoparticles of two different size ranges. This computational prediction is related to experimental observations of bimodal nanoparticle size distributions in short pulse laser ablation experiments.

Fig. 1: Snapshot from a large-scale atomistic simulations of laser ablation of an Ag target in water illustrating two distinct mechanisms of nanoparticle generation:
(1) Rayleigh-Taylor instability at the interface between the ablation plume and water leading to nano-jetting and generation of large (10s of nm) nanoparticles;
(2) rapid nucleation and growth of smaller (≤ 10 nm) nanoparticles in a low-density water-metal mixing region.

[1] M. V. Shugaev, C.-Y. Shih, E. T. Karim, C. Wu, L. V. Zhigilei, Generation of nanocrystalline surface layer in short pulse laser processing of metal targets under conditions of spatial confinement by solid or liquid overlayer, *Appl. Surf. Sci.* **417**, 54-63, 2017.
[2] C.-Y. Shih, C. Wu, M.V. Shugaev, and L.V. Zhigilei, Atomistic modeling of nanoparticle generation in short pulse laser ablation of thin metal films in water, *J. Colloid Interface Sci.* **489**, 3-17, 2017.
[3] C.-Y. Shih, M. V. Shugaev, C. Wu, and L. V. Zhigilei, Generation of subsurface voids, incubation effect, and formation of nanoparticles in short pulse laser interactions with bulk metal targets in liquid: Molecular dynamics study, *J. Phys. Chem. C* **121**, 16549-16567, 2017.
[4] C.-Y. Shih, R. Streubel, J. Heberle, A. Letzel, M. V. Shugaev, C. Wu, M. Schmidt, B. Gökce, S. Barcikowski, and L. V. Zhigilei, Two mechanisms of nanoparticle generation in picosecond laser ablation in liquids: The origin of the bimodal size distribution, *Nanoscale* **10**, 6900-6910, 2018.

TH-O-10

Ultrafast dynamics of non-equilibrium electrons and strain generation under femtosecond laser irradiation of Nickel

George D.Tsibidis[1]

[1]Institute of Electronic Structure and Laser (IESL), Foundation for Research and Technology (FORTH), N. Plastira 100, Vassilika Vouton, 70013, Heraklion, Crete, Greece
E-mail: * tsibidis@iesl.forth.gr

We present a theoretical study of the ultrafast electron dynamics in transition metals of large electron-phonon coupling constant using ultrashort pulsed laser beams. The significant influence of the dynamics of produced nonthermal electrons to electron thermalisation and electron-phonon interaction is thoroughly investigated for various values of the pulse duration (i.e. from 10fs to 2.3ps). The theoretical model elaborates firstly on possible transient changes of optical parameters during irradiation due to the presence of the non-equilibrium electrons and the modification of the electron distribution function in a material characterized by a variable electron density of states around the Fermi energy. The model correlates the role of nonthermal electrons, relaxation processes and induced stress-strain fields. Simulations are presented by choosing Nickel (Ni) as a test material to compute electron-phonon relaxation time due to its large electron-phonon coupling constant. We demonstrate that the consideration of the aforementioned factors leads to significant changes compared to the results the traditional Two Temperature Model (TTM) provides (Fig.1a). The proposed model predicts a large increase of the stress (~20%, at early times) (Fig.1b) and a substantially (~33%) smaller damage threshold (Fig.1c)and which firstly underlines the role of the nonthermal electron interactions and secondly enhances its importance with respect to the precise determination of laser specifications in material micromachining techniques.

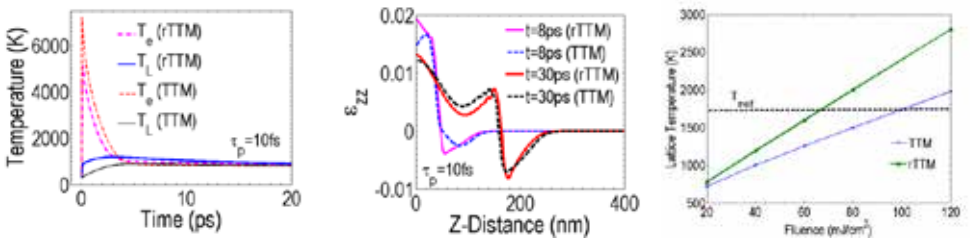

Fig. 1. (a) Electron and Lattice temperatures for revised model (rTTM) and classical TTM, (b) Strain along z-axis at two different times computed by rTTM and TTM (τp=10fs, Ep =40mJ/cm2, 800nm laser wavelength, R0=15μm), (c) Lattice temperature at different fluences.

Acknowledgement: The authors acknowledge financial support from the following EU-funded projects: (i) MouldTex (under the H2020 framework programme for research and innovation under Grant Agreement: 768705) and (ii) LinaBiofluid (under the H2020 framework programme for research and innovation under Grant Agreement No. 665337).

References

[1] G. D. Tsibidis, Applied Physics A, 124,311 (2018).
[2] G. D. Tsibidis, Applied Physics Letters, 104, 051603 (2014).

TH-O-11

Model for UV induced CdS nanoparticle formation in a polymer matrix

Nikita Bityurin*, and Anton A. Smirnov

Institute of Applied Physics Russian Academy of Sciences, 46, Ul'yanov str., 603950, Nizhny Novgorod, Russia
Corresponding author: bit@ufp.appl.sci-nnov.ru

Self-assembly of species that originated from light-induced precursor destruction can result in nanoparticle formation within the polymer matrix. The optical properties of such photoinduced nanocomposites usually drastically differ from those of the initial materials. This provides an opportunity for patterning of the initially homogeneous material because the nanoparticles are formed only within the irradiated domains. Most of the previously published papers used CdS precursors, which are not soluble in the polymer matrix. In this case, the nanoparticles are formed within the precursor islands in the matrix, and the process resembles one occurring within the grains of powder. Recently, some good soluble CdS precursors, in particular $[Cd(N(SCNEt_2)_2)_2]$ (TEDBCd), have been reported [1]. In [2] the PMMA film containing TEDBCd was irradiated by an ultraviolet light emitting diode (UV LED) with the central wavelength of 365 nm at different fixed temperatures and at different fixed intensities. The authors of [2] *in situ* followed the evolution of absorbance at the wavelength of 405 nm where the film initially is transparent. The main result is that at a given temperature, the effect of UV radiation on the sample is determined by the exposure (dose) rather than the light intensity and the irradiation time separately. The presented paper aims at constructing a model of semiconductor particle growth initiated by the light-induced destruction of the good soluble precursor molecules and fitting this model to the experimental data of paper [2], estimating the most important parameters of the process. The photoinduced formation of CdS nanoparticles is a complicated process that includes the photo-mediated destruction of the precursor molecules followed by a diffusion-assisted growth of nanoclusters. The exposure dependence of the absorbance can be understood as suggesting that the precursor destruction is the limiting stage here. The feature of the growing semiconductor nanoparticles is that rather small particles do not absorb radiation at the particular wavelength because of the quantum confinement, and the extinction cross section of sufficiently large particles, whose dielectric function is close to that of the bulk material, is proportional to the volume of the particle. The theory also takes into account the finite thickness of the sample and the nonlinear effects of radiation shielding. The exposure dependence of the process allows application of the mathematical approach developed in [3] and successfully used in investigations on photoinduced species as Ti^{3+}centers in TiO_2 gel and TiO_2 gel-based organic-inorganic hybrids [4]. This approach is further developed allowing to obtain an analytical expression for the experimentally measured time-dependent absorbance at different wavelengths, including the wavelength of irradiation and the wavelengths at which the initial absorption can be neglected.

The work is supported by the Russian Science Foundation (Grant No. 14-19-01702).

[1] A.A. Smirnov, A. Afanasiev, N. Ermolaev and N. Bityurin, LED induced green luminescence in visually transparent PMMA films with CdS precursor, Opt. Mater. Express. **6**(1), 290-295 (2016)

[2] A.A. Smirnov, A. Afanasiev, S. Gusev, D. Tatarskiy, N. Ermolaev and N. Bityurin, Exposure dependence of the UV initiated optical absorption increase in polymer films with a soluble CdS precursor and its relation to the photoinduced nanoparticle growth, Opt. Mater. Express, 8(6), 1603-1612 (2018)

[3] N. Bityurin, "UV etching accompanied by modifications. Surface etching," Appl. Surf. Sci. 138-139, 354-358 (1999)

[4] N. Bityurin, A.I. Kuznetsov, A. Kanaev, Kinetics of UV induced darkening of titanium – oxide gels, Appl. Surf. Sci., 248, 86-90 (2005)

TH-IN-3

Intense femtosecond laser interaction with aqueous solutions for X-ray, THz wave, and ultrasound emission

Koji Hatanaka[1,2,3*]

1 Research Center for Applied Sciences, Academia Sinica, Nankang, Taipei 11529, Taiwan
2 College of Engineering, Chang Gung University, Guishan, Taoyuan 33302, Taiwan
3 Dept. of Materials Sci. and Eng., National Dong Hwa University, Shoufeng, Hualien 97401, Taiwan
Corresponding author: kojihtnk@gate.sinica.edu.tw

Photon emission induced by intense femtosecond laser-matter interaction such as X-ray and THz wave is independently expected for various types of applications from industry to security control and so on. X-ray or ultrasound emission from aqueous solutions have been extensively studied so far [1-3], while targets for THz wave emission, in particular, are limited to solids, and there have been no reports with water until recently [4,5].

Furthermore, combination usages of such X-ray and THz wave pulses are highly expected for further applications [6] though reports on their simultaneous emission are still quite limited except one paper with gas cluster targets in a vacuum chamber [7]. In this presentation, simultaneous emission/detection of X-ray and THz wave from aqueous solution flow irradiated by focused femtosecond laser pulses in the air will be introduced.

[1] F. C. P. Masim, *et al.*, **ACS Photonics**, **3**, 2184 (2016)
[2] W. –H. Hsu, *et al.*, **Opt. Express**, **25**, 24109 (2017).
[3] F. C. P. Masim, *et al.*, **Opt. Express**, **25**, 19497 (2017).
[4] Q. Jin, *et al.*, **Appl. Phys. Lett**.. **111**, 071103 (2017)
[5] I. Dey, *et al*., **Nature Commun. 8**, 1184 (2017).
[6] X. C. Zhang, *et al.*, **Nature Photonics, 11**, 16 (2017).
[7] A. Balakin, *et al.*, **IEEE Trans. Terahertz Sci. Tech.**, **7**, 70 (2017).

TH-IN-4

Periodic phase-change structures in silicon: Control and formation mechanism

Yasser Fuentes-Edfuf[1], Mario Garcia-Lechuga[1], Daniel Puerto[1], Camilo Florian[1], Adianez Garcia-Leis[2], Santiago Sanchez-Cortes[2], Javier Solis[1] and Jan Siegel[1]

[1] Laser Processing Group, Instituto de Óptica, IO-CSIC, Serrano 121, 28006, Madrid, Spain
[2] Instituto de Estructura de la Materia, CSIC, Serrano 121, 28006, Madrid, Spain
Corresponding author: j.siegel@csic.es

Laser-induced periodic surface structures (LIPSS) are a universal phenomenon observed in metals, semiconductors and dielectrics upon irradiation with short and ultrashort laser pulses. They manifest as self-assembled sub-wavelength surface structures with different symmetries that depend on the processing parameters and are typically formed via ablation [1]. We report a different type of LIPSS in silicon, which is based on melting / rapid solidification and leads to the formation of high-precision phase-change nanograting structures that consist of alternating amorphous and crystalline lines. By means of a fine control of the processing parameters, all three dimensions of a single fringe can be tuned over a wide range. The fabrication strategy can also be extended into two dimensions by scanning the laser beam over the sample surface (c.f. Fig. 1 (a-e)) [2].

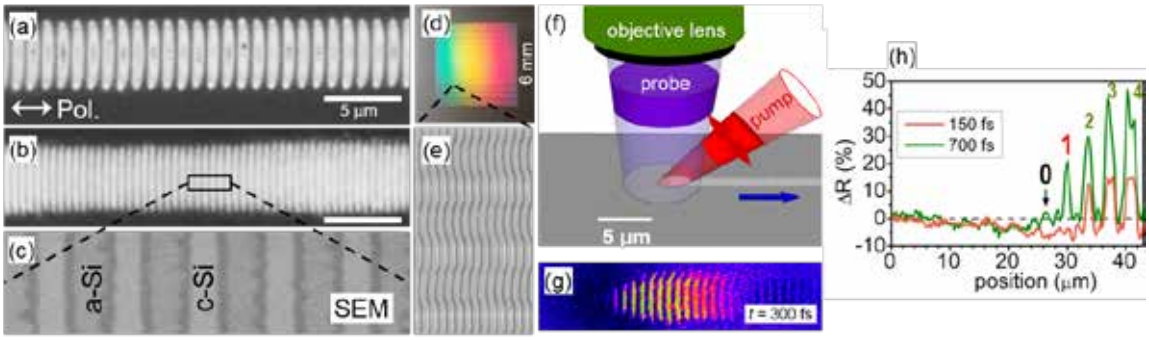

Figure 1 : (a-b) Optical micrographs of self-organized amorphous fringes with different periods written on the surface of crystalline silicon. (c) SEM image of the region marked in (b). (d) Colour photograph of a fabricated area grating (6 × 6 mm), illustrating wavelength-dependent diffraction. (e) Optical micrograph in the reflection of the region marked in (d). (f) Experimental configuration employed for moving-spot femtosecond microscopy, yielding (g) time-resolved images at certain delays t after the arrival of the pump pulse, which are analyzed (h) in order to clarify the formation dynamics of amorphous-crystalline LIPSS.

We also introduce an experimental strategy to clarify the mechanism responsible for the formation of phase-change LIPSS, based on a time-resolved measurement, namely moving-spot femtosecond microscopy [3], which is able to spatially and temporally resolve the birth and growth of individual fringes, as illustrated in Fig. 1 (f-h). We show that the formation process is initiated by free electron generation, leading to thermal and non-thermal melting, liquid phase overheating and rapid solidification into the amorphous phase. [3]. The applicability of the writing strategy and the monitoring technique to other materials is discussed, together with potential applications.

[1] J. Bonse, S. Höhm, S. Kirner, A. Rosenfeld, J. Krüger, Laser-Induced Periodic Surface Structures – a Scientific Evergreen, IEEE J. Sel. Top. Quantum Electron. 23, 9000615 (2016).
[2] Y. Fuentes-Edfuf, M. Garcia-Lechuga, D. Puerto, C. Florian, A. Garcia-Leis, S. Sanchez-Cortes, J. Solis and J. Siegel, Coherent scatter-controlled phase change grating structures in silicon using femtosecond laser pulses, Scientific Reports 7, 4594 (2017).
[3] M. Garcia-Lechuga, D. Puerto, Y. Fuentes-Edfuf, J. Solis and J. Siegel, Ultrafast Moving-Spot Microscopy: Birth and Growth of Laser-Induced Periodic Surface Structures, ACS Photonics 3, 1961–1967 (2016).

TH-O-12

Formation of Highly-regular LIPSS on Cr Under Condition of Strong Ablation

Iaroslav Gnilitskyi[1,2], Maxim V. Shugaev[3], Leonardo Orazi[2] and Leonid V. Zhigilei3

[1]NoviNano Inc., Lviv, 79021, Ukraine
[2]DISMI, University of Modena and Reggio Emilia (UNIMORE), Reggio Emilia, 42121, Italy
[3]University of Virginia, Department of Materials Science and Engineering, Charlottesville, VA 22904-4745, USA
Corresponding author: iaroslav.gnilitskyi@novinano.com

The first observation of laser-induced periodic surface structures (LIPSS) dates back to 1965 [1]. These structures are already used and have a potential to be applied in various fields, including improving adhesive properties [2], decreasing coefficient of friction (COF) [3] and many others. Although LIPSS are commonly produced by repetitive irradiation of the same area by multiple laser pulses in the regime of surface melting and resolidification, recent reports demonstrate the formation of LIPSS in nearly single pulse irradiation regime at laser fluences well above the ablation threshold [4]. Usage of this regime substantially improves the quality of the produced surface structures as well as processing speed. In this study we present results of both computational and experimental study targeted at revealing the mechanisms responsible for LIPSS generation in the regime of strong ablation [5].

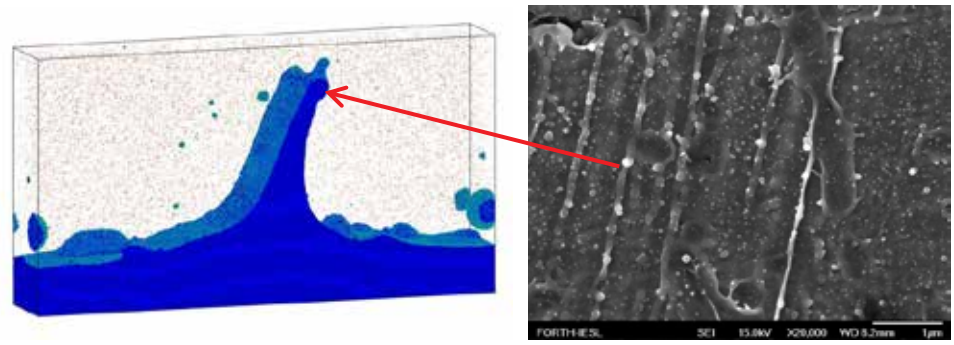

Fig. 1 (a) The final shape of protrusion predicted in a large-scale atomistic simulation [5] and (b) an SEM image of the processed area.

Surface morphology observed in experiments (Fig. 1b) is in a quite good agreement with the results of large-scale molecular dynamics simulations (Fig. 1a). The SEM image of the processed area shows thin lines with large distance between them, which match the shape of the protrusion revealed in modeling. Presence of several droplets on top of these lines further supports the simulation results, where these droplets are observed to form during decomposition of elongated liquid walls transiently generated in the course of the spatially modulated ablation [5].

[1] M. Birnbaum, J. Appl. Phys. 36, 3688-3689 (1965).
[2] G. Rotella, L. Orazi, M. Alfano, S. Candamano, and I. Gnilitskyi, CIRP J. Manuf. Sci. Technol. 18, 101 (2017).
[3] I. Gnilitskyi, F. Rotundo, I. Pavlov, S. Ilday, C. Martini, F.O. Ilday and L. Orazi Trib. Int. 99 67–76 (2016).
[4] I. Gnilitskyi, V. Gruzdev, N. M. Bulgakova, T. Mocek, and L. Orazi, Appl. Phys. Lett., 109, 143101 (2016)
[5] M. V. Shugaev, I. Gnilitskyi, N. M. Bulgakova, and L. V. Zhigilei, Phys. Rev. B 96, 205429 (2017

TH-O-13

Ultrafast microscopy in resolving femtosecond laser-induced surface structuring

R. Fang[1], A.Y. Vorobyev[1], M. ElKabbash[1], Subhash C. Singh[1,2], and Chunlei Guo[1,2,*]

[1]The Institute of Optics, University of Rochester, Rochester, New York 14627, USA
[2]Changchun Institute of Optics, Fine Mechanics, and Physics, Changchun, China
Corresponding author: guo@optics.rochester.edu

Despite extensive studies of femtosecond laser-material interactions, even the simplest morphological responses following femtosecond pulse irradiation have not been fully resolved. Past studies provided only partial dynamics. Here, we introduce a zero-background and high-contrast optical imaging technique [1], through which we capture the complete temporal and spatial evolution of femtosecond laser-induced morphological surface structural dynamics of metals from start to finish, i.e., from transient initial surface fluctuations, through melting and ablation, until the end of resolidification. We find that the transient surface structures first appear at a delay time on the order of 100 ps, and this is attributed to ablation driven by pressure relaxation in the surface layer. Evolution of surface structural formation at different length scales is individually resolved and the sequence of their appearance changes with laser fluence. The cooling and entire resolidification, observed here for the first time, are shown to occur slower than previously predicted by two orders of magnitude. We examine and identify mechanisms for each of the dynamic steps. The visualization and controlling surface morphological structural dynamics not only have fundamental importance to understand fs laser-induced material responses but also pave the path for designing new material functionalities through surface structuring.

[1] R.Fang, A.Y. Vorobyev, and C. Guo, Light: Science & Applications **6**, e16256 (2017).

TH-O-14

Control of femtosecond laser-induced periodic nanostructures by changing dielectric constant of polymers on Ti surface

Masahiro Tsukamoto[1], Yuji Sato[1], Naoki Shinohara[2], Keisuke Takenaka[3], Satoru Asai[3], Godai Miyaji[4]

[1] Joining and Welding Research Institute, Osaka University, 11-1 Mihogaoka, Ibaraki, Osaka, 567-0047, Japan
[2] Department of Mechanical Engineering, Osaka University, 1-1 Yamadaoka, Suita, Osaka, 565-0871, Japan
[3] Graduate School of Engineering, Osaka University, 1-1 Yamadaoka, Suita, Osaka, 565-0871, Japan
[4] Graduate School of Engineering, Tokyo University of Agriculture and Technology, 2-24-16 Naka-cho, Koganei-shi, Tokyo, 184-8588, Japan
Corresponding author: tukamoto@jwri.osaka-u.ac.jp

Titanium (Ti) is one of useful biomaterials in metals, because of its high corrosion resistance and strength. Femtosecond laser was used to form periodic nanostructures on Ti surface. The period of the periodic nanostructures on Ti surface under atmospheric (air) condition was about 70 to 80 % of the laser wavelength. However, the mechanism of the periodic nanostructures formation by femtosecond laser irradiation has not been clarified yet. We focused on surface plasmon polariton (SPP) model to explain this cause. In this model, high electron density region was formed on a Ti surface by laser irradiation. Then, standing wave was generated at the boundary between high electron density region and Ti surface. The wavelength of the standing wave depended on the dielectric constant of interface medium. This model suggested that the period of the periodic nanostructures could be varied due to the wavelength of the standing wave. In this study, experiments using three kinds of polymers were conducted to change the dielectric constant on a Ti surface. The schematic diagram of femtosecond laser irradiation on a Ti surface through polymer is shown in Fig 1. They were Polylactide (PLA), Polyethylene terephthalate (PET) and polymethyl methacrylate (PMMA). Dielectric constants of PLA, PET and PMMA films were 2.5, 3.0 and 3.4, respectively [2, 3]. The femtosecond laser irradiated on Ti surface through polymer. The wavelength, repetition rate and pulse duration of the femtosecond laser were 800 nm, 1 kHz and 150 fs, respectively. The periods of the periodic nanostructures under air, PLA, PET and PMMA contact condition were 600 nm, 475 nm, 440 nm and 380 nm, respectively. It was found that the period of the periodic nanostructures could be controlled by changing dielectric constant of the polymer on Ti surface.

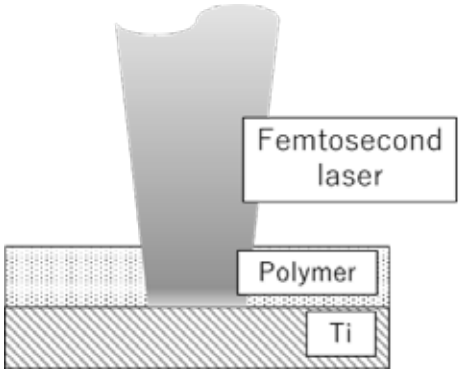

Fig. 1 Schematic diagram of the experimental setup

[1, 2] Y. Sato, M. Tsukamoto, et al., Applied Physics A **122,** 184(2016).
[3] K. Takenaka, M. Tsukamoto, et al., Applied Physics A **124**, 410(2018).

TH-O-15

Laser fabrication of Si nanosheets via nanoplasmonic self-organization in liquid CS_2

I.N. Saraeva,[1] S.I. Kudryashov,[1,2] L. V. Nguyen,[1,3] D. A. Kirilenko,[2,4] P. N. Brunkov,[2] A.A. Rudenko,[1] N. N. Melnik,[1] R. A. Khmelnitsky,[1] A. L. Shakhmin,[5] A.A. Nastulyavichus,[1] N. I. Busleev,[1] A. V. Semencha,[5] A. A. Ionin,[1] E. R. Tolordava,[6] Y. M. Romanova[6]

[1]Lebedev Physical Institute, Leninsky Prospect 53, 119991 Moscow, Russia
[2]ITMO University, Kronverkskiy Prospect 49, 197101 St. Petersburg, Russia
[3]Institute of Physics and Technology, Institutskiy Pereulok 9, 141700 Dolgoprud-ny, Russia
[4]Ioffe Institute, Politekhnicheskaya Street 26, 194021 St. Petersburg, Russia
[5]Peter the Great Polytechnic University, Politekhnicheskaya Street 29, 195251 St. Petersburg, Russia
[6]N. F. Gamaleya Federal Research Centre of Epidemiology and Microbiology, Gamalei Street 18, 123098 Moscow, Russia
Corresponding author: insar@lebedev.ru

Large-scale surface arrays of ultra-thin (< 30 nm) amorphous Si 2D-nanosheets were produced on a Si(100) wafer (Figure 1b, inset) under the 5-mm thick carbon disulfide (CS_2) layer by 10-ps, IR-laser (λ≈1030 nm) pulses. Such nanosheets demonstrate the broad low mid-IR transmittance and the high content of sulfur, carbon and oxygen in the surface layer and are of potential use for anti-fouling coatings and in optoelectronic, nanophotonic and sensing applications. Such structures appear via the interfacial vapor/plume bubble-mediated redeposition of Si ablation nanoplumes from the regular trenches and sulfur-containing products of carbon disulfide decomposition in the bubble. Numerical modelling indicates the nanoplasmonic origin of the Si nanosheets, self-limited both in the 100-nm periods and the sub-micron heights. The period of the nanoripples Λ ≈ 0.1 μm can be explained in terms of the laser-induced surface plasmon resonance (SPR) of the photoexcited Si with the high SPR wavenumber k = 1/2Λ ~ 4-5 μm^{-1}.

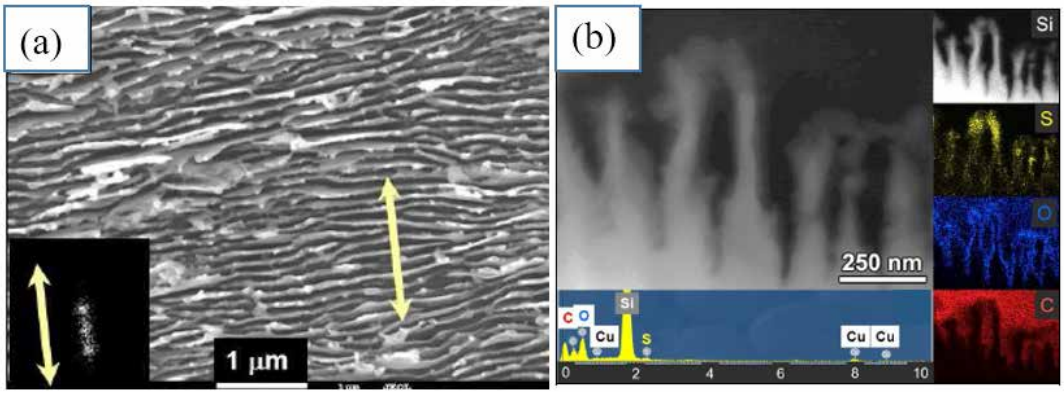

Fig. 1 (a) SEM image of the surface Si nanosheets with its 2D-FFT spectrum (inset); the yellow arrows indicate the laser polarization. (b) Cross-sectional HRTEM image of Si nanosheets with the corresponding EDX-acquired elemental composition along with the 10-keV EDX spectrum. The copper appears due to the copper sample holder.

This work was supported by the Russian Science Foundation (project no. 18-15-00220)

[1] R. Li, X.-F.; Zhang, C.-Y.; Li, H.; Dai, Q.-F.; Lan, S.; Tie, S.-L. Formation of 100-nm Periodic Structures on a Titanium Surface by Exploiting the Oxidation and Third Harmonic Generation Induced by Femtosecond Laser Pulses. Opt. Express 2014, 22, 28086−28099.
[2] Nathala, C. S. R.; Ajami, A.; Ionin, A. A.; Kudryashov, S. I.; Makarov, S. V.; Ganz, T.; Assion, A.; Husinsky, W. Experimental Study of Fs-Laser Induced sub-100-nm Periodic Surface Structures on Titanium. Opt. Express 2015, 23, 5915−5929

TH-O-16

Ablation suppression of titanium surface interacted with two color double-pulse beam of femtosecond laser

Keisuke Takenaka[1], Masahiro Tsukamoto[2], Masaki Hashida[3], Shinichiro Masuno[2], Shuji Sakabe[3], Shunsuke Inoue[3], Yuki Furukawa[3], Satoru Asai

[1]*Graduate School of Engineering, Osaka University, 1-1 Yamadaoka, Suita, Osaka, 565-0871, Japan*
[2]*Joining and Welding Research Institute, Osaka University, 11-1 Mihogaoka, Ibaraki, Osaka, 567-0047, Japan*
[3]*Institute for Chemical Research, Kyoto University, Gokasyo, Uji, Kyoto, 611-0011, Japan*
Corresponding author: takenaka@jwri.osaka-u.ac.jp

It has been reported that laser ablation of titanium (Ti) is suppressed by single color double pulse beam irradiation of femtosecond lasers[1]. However, the mechanism of suppression is under debated, and we need further investigation. In this study, we have demonstrated laser ablation experiment of Ti with a double-pulse beam of two-color laser in time delays of Δt = -700 - 700 ps for investigating the influence on ablation suppression effect by changing the combination of delay time and fluence of two color beam. The double pulse beam consists of a fundamental pulse (150 fs, λ = 800 nm) and a second harmonic pulse (> 150 fs, λ = 400 nm). A positive delay time indicates 800 nm pulse irradiated first then 400 nm pulse irradiated after that and a negative delay time indicates 400 nm pulse irradiated in advance and 800 nm pulse later. The laser diameters and these center positions for two-color double pulse beam at the irradiation position were adjusted to be equal to ϕ= 25 μm ($FWe^{-1}M$) and collinearly aligned, respectively.

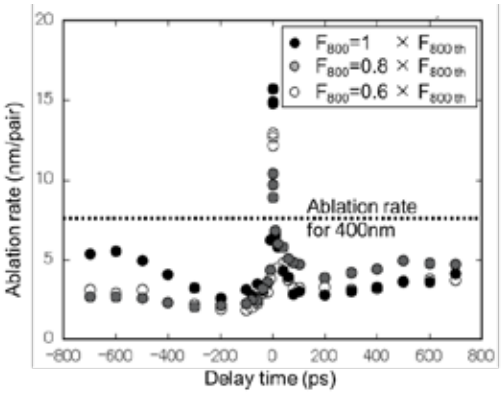

Fig. 1 Relationship between laser fluence and ablation rate with 400 or 800 nm single-pulse beam

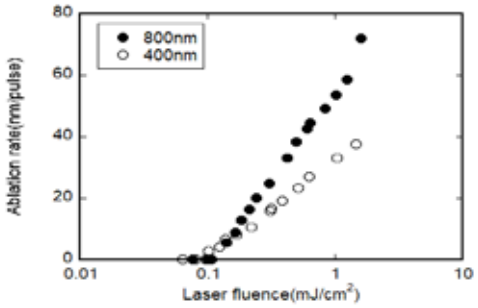

Fig. 2 Relationship between delay time and ablation rate with two color double-pulse beam

Figure 1 shows the dependence of the ablation rate on the fluence for irradiating 800nm pulse or 400m pulse individually. The ablation threshold was identified at F_{400th} = 109 mJ/cm² for 400 nm pulse and F_{800th} = 90 mJ/cm² for 800 nm pulse. Figure 2 shows the result of two color double-pulse beam irradiation. The 400nm pulse fluence F_{400} was kept $1.6F_{400th}$ (ablation rate for 400 nm pulse was 8.7 nm/pulse), and the 800nm-pulse fluence F_{800} had values of 1, 0.8, $0.6F_{800th}$. The ablation rate of Ti was drastically decreased at delay times of -200ps. We found that the ablation suppression at Δt = -200 ps with two color double pulse beam was more enhanced than that for single color double pulse beam. The result suggests that the material processing with ultrafine resolution much smaller than the diffraction limit (STED like processing) might be realized.

This research was partially supported by a Grant-in-Aid for Scientific Research (C) (JP16K06745) from MEXT, Japan, and supported by NEDO.

[1] Y. Furukawa, R. Sakata, K. Konishi, K. Ono, S. Matsuoka, K. Watanabe, *et al.*, Appl. Phys. Lett. **108**, 264101(2016).

TH-O-17

Nanometer-Precision Measurement of Surface Morphology Change Induced by Femtosecond Laser Ablation

Shuntaro Tani[1*], Yohei Kobayashi[1]

[1] University of Tokyo, Institute for Solid State Physics, Kashiwa-no-ha 5-1-5, Chiba, 277-8581, Japan
Corresponding author: stani@issp.u-tokyo.ac.jp

Laser processing using femtosecond laser pulses has been emerging as a powerful tool for micromachining and surface functionalization owing to its precise processing capability, and the understanding of light-matter interactions is of great importance for the optimization of the processes. One major challenge is to understand how the surface morphology of a target affects the interactions and the laser ablation processes. Especially, pulses after the first shot experience changes in the surface morphology, which are induced by the prior pulses in multi-shot irradiation [1]. To investigate the relation between the surface morphology and the laser ablation processes during multi-shot irradiation, we developed an in-situ three-dimensional depth profile measurement system with nanometer precision, which enabled pulse-by-pulse monitoring of the surface morphology changes during multi-shot irradiation [2].

The experimental system consisted of a 1-kHz femtosecond laser, and a white-light interferometry microscope, which was synchronized with the regenerative amplifier. The Ti:sapphire regenerative amplifier provided 50-fs laser pulses with a center wavelength of 800 nm. Figure 1 shows changes in a depth profile of a copper plate induced by femtosecond laser pulse irradiation at a fluence of 1 J/cm^2. The target began to swell for the first pulse and then was ablated and roughened as the number of pulses increased. Notably, the changes in the depth profile less than a few tens of nanometers were precisely measured, and the changes strongly depended on the original surface morphology and the laser fluence. We performed systematic measurements on the changes in depth profile as a function of laser fluence and the number of irradiated pulses with various material, and conclude that laser-induced embrittlement of a target material plays a decisive role to determine the ablation rate during multiple-pulse irradiation.

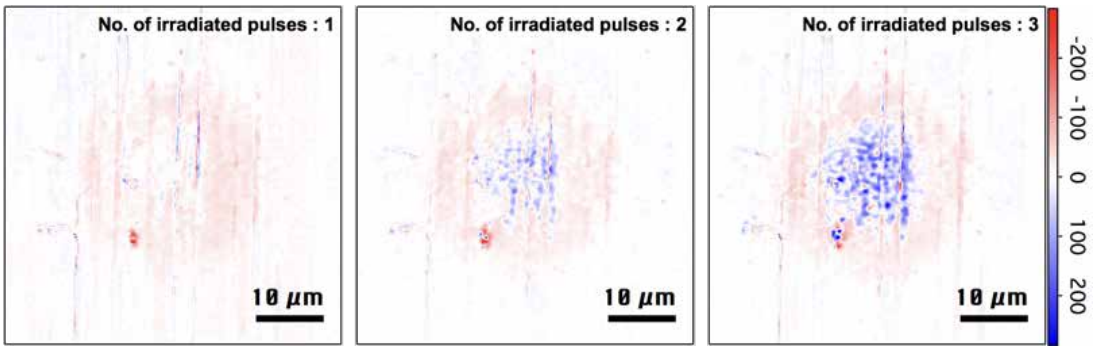

Fig. 1 Changes in-depth profile induced by femtosecond laser pulse irradiation at a fluence of 1 J/cm^2 on a copper plate.

[1] A.Y. Vorobyev, C. Guo, "Enhanced absorptance of gold following multipulse femtosecond laser ablation," Phys. Rev. B **72**, 195422 (2005)
[2] S. Tani, Y. Kobayashi, "Pulse-by-pulse depth profile measurement of femtosecond laser ablation on copper," Appl. Phys. A, **124**:265 (2018)

TH-IN-5

The functional roles of vibronic coupling in biological light harvesting

Jürgen Hauer[1*]

[1]Professur für Dynamische Spektroskopien, Fakultät für Chemie, Technische Universität München, Lichtenbergstr. 4, D- 85748, Garching b. München, Germany
*Corresponding author: juergen.hauer@tum.de

In π-conjugated chain molecules such as carotenoids, the coupling between electronic and vibrational degrees of freedom is of central importance.[1] It governs both dynamic and static properties, such as the timescales of excited state relaxation as well as absorption spectra. I will present a model, which treats vibronic dynamics in carotenoids on four electronic states in a physically rigorous framework. This model explains all features previously associated with the intensely debated S*-state. Additionally, we are able to incorporate findings from pump-deplete-probe experiments, which were incompatible to any pre-existing model.[2]

Besides clarifying features in transient absorption spectra of isolated carotenoids, vibronic coupling also explains the ultrafast transfer rates between carotenoids and bacteriochlorophylls in the natural peripheral light-harvesting antenna complex (LH2) of purple photosynthetic bacteria. Its energy transfer dynamics are an ideal testing ground for models on a structure-function relationship due to the well-determined molecular structure and ultrafast energy deactivation of LH2. The initial carotenoid-to-bacteriochlorophyll energy transfer step after visible light excitation was long considered to follow the Förster mechanism, even though observed transfer times as short as 40 femtoseconds are hard to accommodate by Förster theory, as the moderate coupling strengths found in LH2 suggest much slower transfer within this framework. I will present data on LH2 from *Phaeospirillum molischianum*, with special regards to the split Qx-band in this system.[3] Vibronically mediated transfer explains both the ultrafast carotenoid-to-B850 transfer and the almost complete lack of transfer to B800. These results are beyond Förster-theory, which predicts an almost equal partition between the two channels.

[1] T. Polivka, V. Sundstrom, Dark excited states of carotenoids: Consensus and controversy. *Chem. Phys. Lett.* 2009, **477**, 1-11
[2] V. Balevičius, D. Abramavicius, T. Polívka, A. Galestian Pour, J. Hauer, A Unified Picture of S* in Carotenoids. *J. P. C. Lett.* **7**, 3347-3352 (2016).
[3] E. Thyrhaug *et al.*, Carotenoid-to-bacteriochlorophyll energy transfer through vibronic coupling in LH2 from Phaeosprillum molischianum. *Photosynth. Res.*, **135**, 45-54 (2017).

FR-IN-1

Nano-scale Laser Printing on Template Optical Metasurfaces

Airidas Žukauskas[1], Xiaolong Zhu[1], Søren Raza[1], Mehdi K. Hedayati[1], Uriel Levy[2], N. Asger Mortensen[3], Anders Kristensen[1*]

[1] DTU Nanotech, Technical University of Denmark, 2800 Kongens Lyngby, Denmark
[2] Department of Applied Physics, The Hebrew University of Jerusalem, Jerusalem 91904, Israel
[3] Center for Nano Optics & Danish Institute for Advanced Study, University of Southern Denmark, DK-5230 Odense M, Denmark
Corresponding author: anders.kristensen@nanotech.dtu.dk

This paper describes the digital printing of optical metasurfaces for ink-free colour decoration and flat optics, by holographic laser post-writing on nano-textured optical metasurfaces [1].

Our optical metasurfaces are based on the concepts of both localized surface plasmon resonances (LSPR) [2,3], and high-index dielectrics [4] compatible with technologies for high volume manufactured plastic products [5]. The optical metasurfaces are formed by nanoimprinting a surface texture comprising nanoscale cylinders. By subsequent deposition of a thin film of metal or high index dielectric, isolated nano-disks are formed on top of the cylinders, while a continuous film is formed on the substrate surface in between the cylinders. The nano-scale disks and corresponding holes in the continuous film form optical resonators. The master-original for the square-centimeter nano-texture is realized by means of fast e-beam writing [6]. The nanotextured plasmonic metasurface may be covered with a transparent protective coating, which can withstand the daily life handling.

Laser post-writing can modify disks and holes, and hence the optical resonances [4,7]. Laser pulses induce transient local heat generation that leads to melting and reshaping of the imprinted nanostructures. This enables flexible definition and alignment of optical components on high volume manufactured plastic products [8]. Our approach offers a printing speed of 1 ns per pixel (in a raster scan), resolution up to 127,000 dots per inch (DPI) and power consumption down to 0.3 nJ per pixel.

[1] X. Zhu et al., *Nano Today*, 19, 7-10 (2018)
[2] J. S.Clausen et al., *Nano Letters*, 14, 4499-4504, (2014).
[3] A. Kristensen et al., *Nature Reviews Materials* 2, 16088, (2016).
[4] X. Zhu et al., *Science Advances*, 3(5), e1602487, (2017).
[5] E. Højlund-Nielsen et al., *Adv. Mater. Technol.,* 1600054, **(2016).**
[6] E. Højlund-Nielsen et al., *Microelectronic Engineering*, 121, 104-107, **(2014).**
[7] X. Zhu et al., *Nature Nanotechnology*, 11, 325-329, **(2016).**
[8] M. S. Carstensen et al., *ACS Photonics*, in press (2018); arXiv:1708.05571v1

FR-O-1

Laser patterning of metal cylinders for roll to toll application

Pierre Lorenz[1,*], Lukas Bayer[1], Nikos Kehagias[2], Klaus Zimmer[1]

[1] Leibniz Institute of Surface Engineering (IOM), Permoserstraße 15, 04318 Leipzig, Germany
[2] Nanotypos, VEPE Technopoli Thessalonikis, Building C2, 55535, Pylea, Thessaloniki, Greece
Corresponding author: pierre.lorenz@iom-leipzig.de

The large area and seamless (360°) laser patterning of nickel sleeves for roll-to-roll application was performed using ps-laser radiation with different wavelengths to realize diverse structures like hierarchically organized dot pattern, line structures and free-formed 3D structures (see Fig. 1). The hierarchical patterns were produced by overlapping of pattern structures produced by IR- (λ = 1064 nm) and UV- laser radiation λ= 355 nm), respectively. The concept of overlapping of patterns written with different spot size allows the fabrication of complex µm-scaled structures with aspect ratio larger than 1 and lateral sizes down to 5 µm (see Fig. 1 b). The line, as well as the 3D free-formed, was produced by defined scanning of the laser beam over the Ni sleeve (see Fig. 1 c). The fabricated structures were embossed in silicone for SEM imaging and were transferred in a roll to roll process into ormocere-based photoresist with high surface energy deposited on polymer foil. The structures were analyzed by optical and scanning electron microscopy (SEM). The surface morphology and the roughness were measured by white light interference microscopy (WLIM). Furthermore, the influence of the moulded hierarchical pattern on the contact angle was measured.

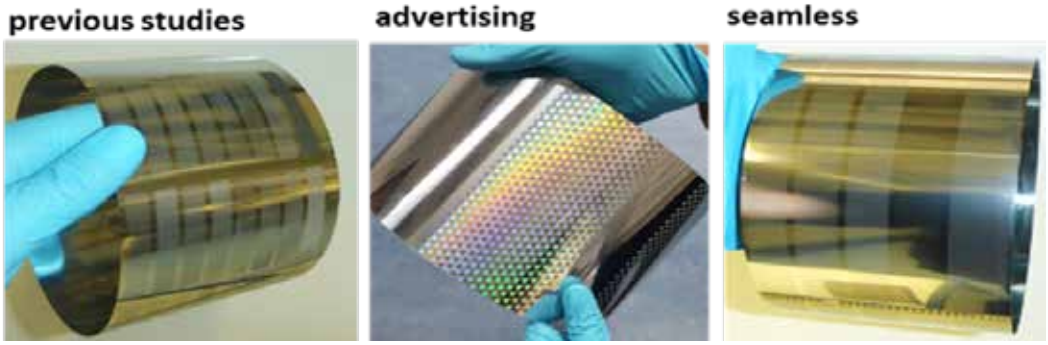

(a)

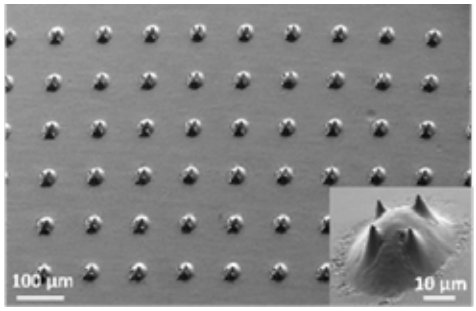

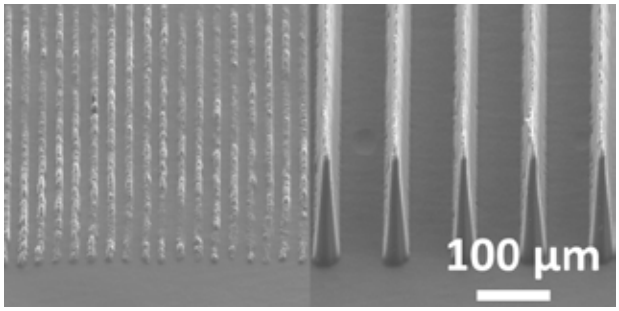

(b) (c)

Fig. 1 (a) Optical images of exemplary laser structures Ni sleeves and SEM images of silicone moulding of (b) hierarchic structures as well as of (c) different line structures on a Ni sleeve

FR-O-2

Growth of regular micro-pillars arrays on steel by polarization-controlled laser interference patterning

Bogdan Voisiat[1], Christoph Zwahr[1], Andreas Rank[1], S. Alamri[2], Andrés Fabián Lasagni[1,2]

[1]Institute for Manufacturing Technology, Technische Universität Dresden, George-Baehr-Str.3c, 01069 Dresden, Germany
[2]Fraunhofer-Institut für Werkstoff- und Strahltechnik IWS, Winterbergstr. 28, 01277 Dresden, Germany
Corresponding author: bogdan.voisiat@tu-dresden.de

Since the global market is getting more and more competitive, surface micro-structuring of various products is becoming more popular in many industrial sectors, in order to increase the effectiveness of their functionality or to provide better aesthetic look. In order to produce such surface structures, versatile, fast and cost-effective fabrication methods are needed. A very attractive method capable of producing micro-/nanometer sized periodic structures on large areas with just a single laser shot is Direct Laser Interference Patterning (DLIP) [1]. This technology enables to use high power laser systems to produce micro- and/or nanostructured surfaces on larger areas at high throughput. However, the biggest drawback of this technique is the lack of availability to control the shape of the formed structures. This is because the optical parameters, distribution and number of the interfering beams predefine the shape of the interference profile.

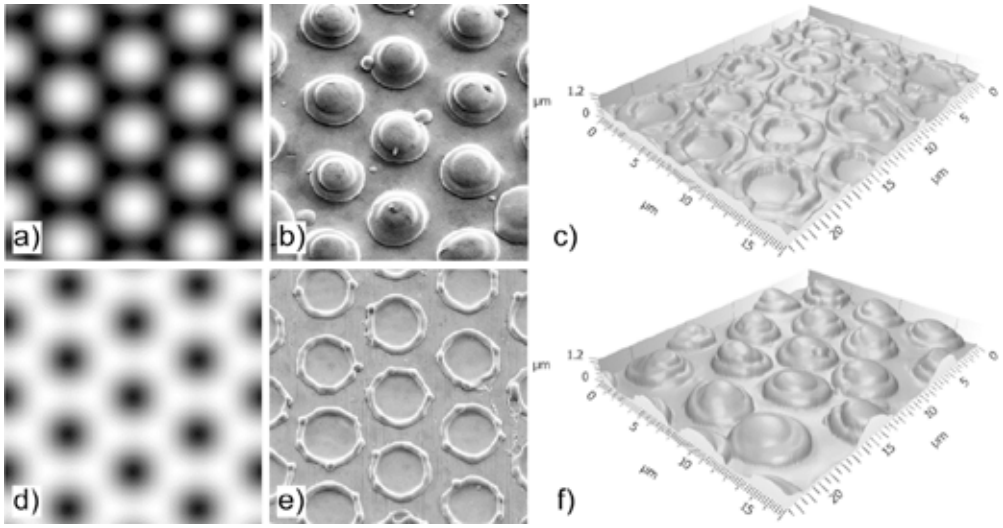

Fig. 1. Ordinary (a) and inverted (d) intensity profiles produced by interference of 3 laser beams and scanning electron microscope (b, e), confocal microscope (c, f) micrographs of the fabricated structure using corresponding intensity profiles.

In this work, an optical setup providing the ability to change the intensity distribution of the interference pattern by manipulating the polarization of the interfering beams is presented. This configuration is used to change a 3-beam interference pattern, consisting of periodically distributed round-shaped intensity peaks, into identical inversed intensity profile. This inverted profile is used to pattern steel samples, which leads to the formation of micro-sized pillars. The growth mechanism of these pillars is discussed in detail.

[1] A. F. Lasagni, D. Benke, T. Kunze, M. Bieda, S. Eckhardt, T. Roch, D. Langheinrich, J. Berger, Bringing the Direct Laser Interference Patterning Method to Industry: a One Tool-Complete Solution for Surface Functionalization. *J. Laser Micro Nanoeng.* **10,** 340–344 (2015).

FR-O-3

Versatile surface structuring using cylindrical vector femtosecond laser beams

Evangelos Skoulas[1,2*], George Tsibidis[1,2],Emmanuel Stratakis[1,2]
[1]Institute of Electronic Structure and Laser (IESL), Foundation for Research and Technology (FORTH), N. Plastira 100
[2] Materials Science and Technology Department, University of Crete, 71003 Heraklion, Greece
Corresponding author: skoulasv@iesl.forth.gr

We report on a new, scalable method to fabricate at single-step, highly ordered, multi-directional, complex surface structures that mimic the unique morphological features of certain species found in nature. Advanced surface structuring was realized utilizing the unique and versatile angular profile and the electric field symmetry of cylindrical vector (CV) femtosecond laser beams. It is concluded that, highly controllable, periodic structures exhibiting sizes at nano-, micro- and dual-scale micro/nano scales can be directly written on metal surfaces upon line and large area scanning with radially and azimuthally polarized beams. Depending on the irradiation parameters, new and more complex multi-directional nanostructures, inspired by the Shark's skin morphology, as well as superhydrophobic dual-scale structures mimicking the Lotus' leaf water repellent properties can be attained. It is concluded that the versatility and features variations of structures formed upon scanning with CV beams is by far superior to those obtained via laser processing with linearly polarized beams. More important, by exploiting the capabilities offered by fs CV optical fields, the present technique can be further extended to fabricate even more complex and unconventional structures. We believe that our approach provides a new concept in laser processing of materials, which can be further exploited for expanding the breadth and novelty of potential applications.

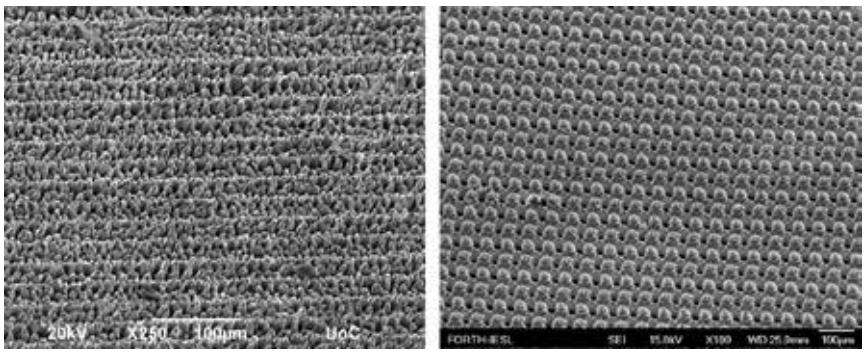

Fig. 1 (a) High aspect ration spike formation on staineless steel surface, (b) Spot by spot hierarchical surface stractures on nickel, utilized via cylindrically polarized femtosecond laser pulses.

[1] G. D. Tsibidis, E. Skoulas, and E. Stratakis, "Ripple formation on nickel irradiated with radially polarized femtosecond beams," *Opt. Lett.*, vol. 40, no. 22, p. 5172, 2015.
[2] E. Skoulas, A. Manousaki, C. Fotakis, and E. Stratakis, "Biomimetic surface structuring using cylindrical vector femtosecond laser beams," *Sci. Rep.*, vol. 7, no. November 2016, p. 45114, 2017.

FR-O-4

Optical elements for synchroton X-ray and THz beamlines

Raghuram Dharmavarapu[1,2,3], Soon Hock Ng[1,2], Stefan Lundgaard[1,2], Shanti Bhattacharya[3], Saulius Juodkazis[1,2]

[1]Swinburne University of Technology, John St., Hawthorn 3122 Vic, Australia
[2]Melbourne Centre for Nanofabrication, the Victorian Node of the Australian National Fabrication Facility, 151 Wellington Rd., Clayton 3168 Vic, Australia
[3]Centre for NEMS and Nanophotonics (CNNP), Department of Electrical Engineering, Indian Institute of Technology Madras, Chennai 600036, India

As free electron lasers with ultrashort 10-100 fs X-ray pulses of high brightness become more widely available at synchrotron facilities, specially designed optical elements for investigation of dynamics of light-matter interaction on ultra-short time scales become required. In such experiments, modification of the sample induced by an ultra-short optical excitation pulse (pump) are probed with ultra-short X-ray pulses. One geometry investigated here numerically is a realisation of a flat optical element that generates an optical vortex with doughnut intensity and Bessel beam generators. A versatile method using two optical elements was adopted in this work [1]. The first element realises the required intensity profile while the second circular grating generates the Bessel beam with engineered axial intensity distribution. We discuss the main challenges in achieving tight focusing, approaching a numerical aperture of 0.5 required for laser structuring of crystals and glasses by Bessel pulses [2].

For mid-IR and THz synchrotron sources there is a need for fabrication of flat optical elements to impart angular momentum to the transmitted light. We use a metamaterials approach to combine electric and magnetic resonances and supress back reflection. This together with high efficiency of vortex generation in transmission are realised by lithography and plasma etching of Si. Modeling and experimental results will be presented.

Since the optical elements for long wavelengths do not require high spatial resolution, three dimensional (3D) printing using direct laser writing or projection exposure are possible solutions [2]. Plasma etching of Si, which is transparent in the IR-THz spectral range was investigated using different recipes and a sacrificial polymeric mask.

Keywords: optical elements, direct laser writing, synchroton, free electron laser, THz

References:

1. R. Dharmavarapu, S. Juodkazis, S. Bhattacharya, Engineering the axial intensity of Bessel beams, arXiv:1711.00576 (2017).
2. M. Mikutis, T. Kudrius, G. Šlekys, D. Paipulas, S. Juodkazis, High 90% efficiency Bragg gratings formed in fused silica by femtosecond Gauss-Bessel laser beams, Optical Materials Express 3(11),1862-1871 (2013).
3. R. Meguya, D. Linklater, W. Hart, A. Balčytis, E. Skliutas, M. Malinauskas, D. Appadoo, Y.-R. E. Tan, E. P. Ivanova, J. Morikawa, S. Juodkazis, 3D printed polarizing grids for IR-THz synchrotron radiation, J. Opt. 20 035101 (2018).

FR-O-5

Photodeposition of Nanometric Thin Films from Bio-Chromophores

Simona Alexandra Popescu and Aaron Peled*

Holon Institute of Technology(HIT), Engineering Faculty, Photonics Laboratory, 52 Golomb Str. Holon, Israel 5810210
Corresponding author: *peled@hit.ac.il

Photodeposited organic materials, with z-axis nanometer depth well-resolved spatial patterns of organic materials, were created directly on PMMA substrates from bio-chromophores solutions see Fig. 1(a). The irradiation was carried out with various types of incoherent and coherent sources in the UV-Visible spectrum. As experimental sources of this work, we used Chlorophyll pigments solutions in Ethanol extracted from leaves of *Red Rubin Ocimum Basilicum* plants, to produce typically, bleached organic-nanolayers with thickness up to about 200 nm. The bio-organic material deposition patterns were obtained for a green laser wavelength of 532 nm in excess of a fluence threshold of F_{th} ~ 16 J/cm^2, as shown in Fig. 1(b). The chromophores optical spectral identification and characterization of the liquid plant extracts was performed by UV-VIS Optical Absorption and Fluorescence using PMMA optical cells of 1 cm optical path length and 4-5 ml volume samples. Optical Absorption Spectra were recorded in the whole wavelength range of 300-800 nm. Fluorescence measurements were performed by exciting with various RGB Lasers, Fiber Halogen Tungsten lamp and Xenon UV-VIS lamp. For the deposited layers morphology investigation, spatial profiles and thickness diagnostic measurements were carried out by the optical microscopy differential scattering light intensity DSLI method [1] with a custom imaging setup coupled to a Zooming Optical Microscope equipped with a CMOS camera. To augment the DSLI investigation and calibrate experimentally the patterns absolute thickness, an SEM investigation was also performed. The samples illumination for the DSLI procedures was provided by a diffused LED illuminator, and the scattered light images were acquired by the CMOS Camera setup and transferred to a PC with appropriate image processing analyzing software. The photodeposited patterns on the substrates were inspected by the Zooming Optical Microscope, providing wide field spatial observation capabilities with lateral x-y magnifications up to about x40 and the DSLI technique gave z-thickness resolutions down to about 5 nm.

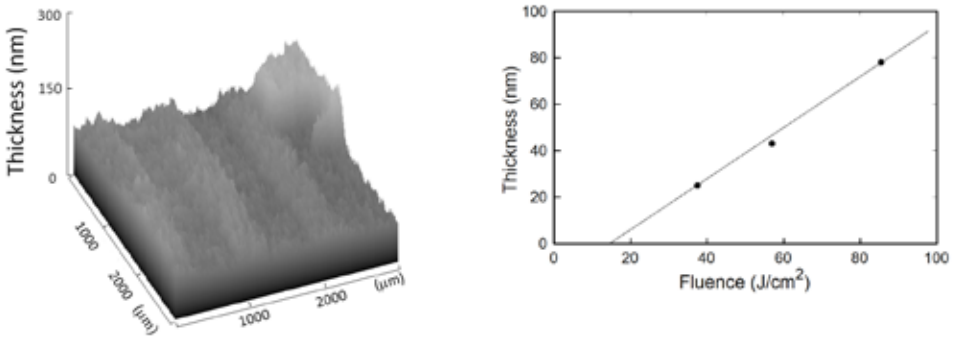

Fig. 1. (a) 3D pattern of photodeposited bio-material by laser irradiation. (b) The plot of the deposited layers average thickness vs fluence obtained from photodepositiom with the Green Laser

[1] S.A.Popescu and A. Peled, "Nanometric z-profiling of photodeposited Bio-Chromophores layers by the DSLI method", 4th International Symposium on Nanotechnology from Academia to Industry, NTAI-2018, 5-May 2018, HIT Holon, Israel.

FR-O-6

Qualitative and Quantitative Investigation of Free-Form fs Laser Made Structures to Intense Ultrafast Laser Radiation

Linas Jonušauskas[1,2], Laurynas Čekanavičius[1], Agnė Butkutė[1], Mangirdas Malinauskas[1]
[1]Vilnius University, Faculty of Physics, Laser Research Center, Saulėtekio Ave. 10, Vilnius LT-10223, Lithuania
[2]Femtika Ltd. Saulėtekio Ave. 15, Vilnius LT-10224, Vilnius, Lithuania
Corresponding author: linas@femtika.lt

3D Laser Lithography (3DLL) is a powerful technique to produce structures for various functional applications [1], including integrated microoptics [2, 3]. However, the spread of this technology is limited in applications requiring intense laser radiation (optical communications, multiphoton imaging, direct fiber processing, fiber lasers, etc.), as there is very little knowledge on how resilient are the polymeric fs laser made free-form microstructures. In this work, we design and apply a method for combined qualitative and quantitative investigation of Laser Induced Damage Threshold (LIDT) of free-form polymeric structures. The laser beam is sequentially focused to an array of 3DLL produced objects [Figure 1 (a)]. The radiation fluence is varied from row-to-row changing LIDT probability in the range from 0% to 100%. This way a statistical measurement is carried out. The results are interpreted by linear approximation in the dynamic range of optical damage probability yielding LIDT value. Additionally, as damage to the structure is determined both by optical imaging and SEM, the morphology of laser-induced deterioration can be evaluated, adding a qualitative aspect to the investigation [Figure 1 (b)]. SU8, OrmoClear, SZ2080 and other materials suitable for 3DLL are tested in this manner, showing the superb optical resilience of hybrid non-photosensitized SZ2080.

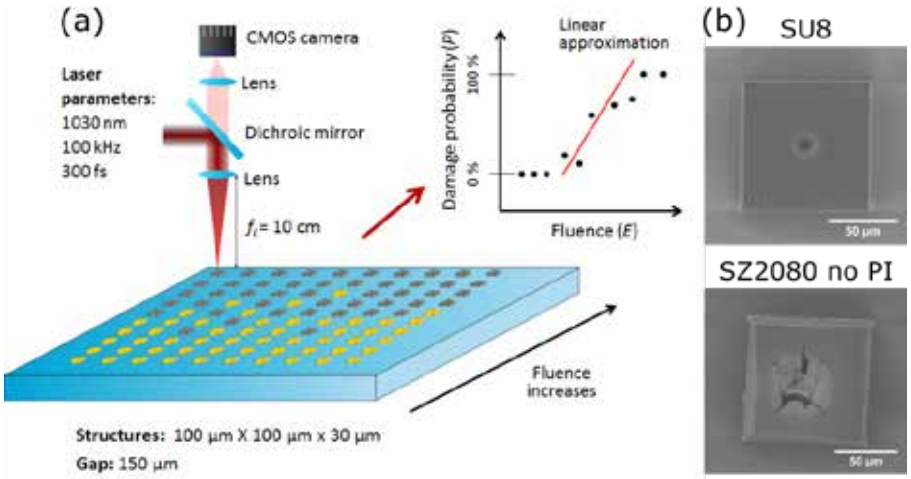

Fig. 1 (a) – schematics of LIDT measurement of 3DLL produced structures. The laser is focused to targets with fluence varying from row-to-row enabling statistical evaluation of LIDT. (b) – SEM images of targets made out of organic SU8 (top) and hybrid organic-inorganic SZ2080 without photoinitiator (PI), showing that the organic material is burned through, while the hybrid one is melted and cracked.

[1] L. Jonušauskas, S. Juodkazis, M. Malinauskas, Optical 3D printing: bridging the gaps in the mesoscale, *J. Opt.* **20**, 053001 (2018).
[2] A. Žukauskas, V. Melissinaki, D. Kaškelytė, M. Farsari, M. Malinauskas, Improvement of the Fabrication Accuracy of Fiber Tip Microoptical Components via Mode Field Expansion, *J. Laser Micro. Nanoen.* **9**(1), 68-72 (2014).
[3] T. Gissibl, S. Thiele, A. Herkommer, H. Giessen, Sub-micrometre accurate free-form optics by three-dimensional printing on single-mode fibres, *Nat. Commun.* **7**, 11763 (2016).

FR-O-7

Dicing of soda-lime glass with elliptical Bessel beam

Juozas Dudutis, Rokas Stonys, Paulius Gečys*
Center for Physical Sciences and Technology, Savanoriu Ave. 231, LT-02300 Vilnius, Lithuania
Corresponding author: p.gecys@ftmc.lt

In the case of high volume production, laser scribe and brake method could be the only alternative to conventional glass processing techniques. To minimize the separation force elongated modifications along the whole glass thickness are desirable. Such modifications can be generated by applying axicon-generated Bessel beams. In our previous research, we found that elliptical oblate tip of the axicon can induce central core ellipticity, which was the cause of transverse crack propagation in the dominant direction [1]. We could also control the Bessel beam ellipticity by tilting the axicon perpendicular to its optical axis [2]. Also, the intensity pattern asymmetry can be induced by filtering the spatial frequencies of the generated beam [3,4].

In this work, we demonstrate the possibility to optimize the glass dicing process by controlling the axicon-generated Bessel beam ellipticity. We investigated single-shot modifications in 1 mm thickness glass samples followed by dicing experiments. We found that Bessel beam ellipticity is essential for glass dicing process. Such beam generates intra-volume modifications with transverse crack propagation in dominant direction. The orientation of these modifications parallel to the dicing direction, as shown in Fig. 1, gives significant advantages in terms of processing speed, glass breaking force and fractured edge roughness.

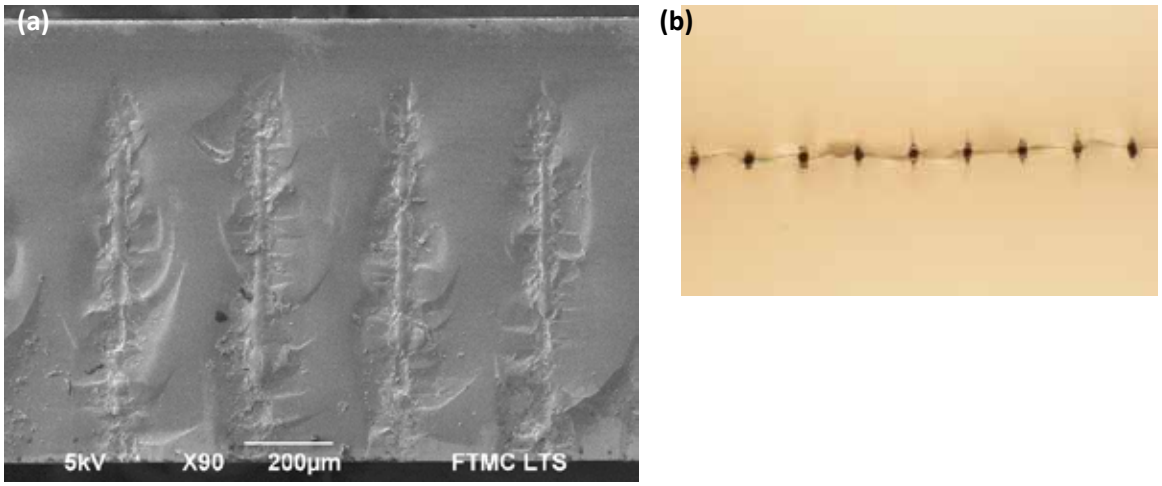

Fig. 1 Elliptical Bessel beam induced modifications in the glass. (a) Cleaved glass sample when elliptical Bessel beam induced transverse cracks are orientated parallel to dicing direction. (b) Top-view of laser diced glass before mechanical separation.

[1] J. Dudutis, P. Gečys, G. Račiukaitis. Non-ideal axicon-generated Bessel beam application for intra-volume glass modification, *Opt. Express*, **24**., 28433–28443, 2016.
[2] J. Dudutis, R. Stonys, G. Račiukaitis Aberration-controlled Bessel beam processing of glass, *Opt. Express*, **26**., 3627–3637, 2018.
[3] R. Meyer, M. Jacquot, R. Giust, J. Safioui, L. Rapp, L. Furfaro, et al. Single shot ultrafast laser processing of high-aspect ratio nanochannels using elliptical Bessel beams, *Opt. Lett*., **42**., 4307–4310, 2017.
[4] R. Meyer, R. Giust, M. Jacquot, J.M. Dudley, F. Courvoisier, R. Meyer, et al. Submicron-quality cleaving of glass with elliptical ultrafast Bessel beams, *Appl. Phys. Lett*., 231108., 2017.

FR-IN-2

Optical probing of charge carrier motion dynamics in disordered, heterogeneous organic and hybrid materials

Vidmantas Gulbinas
[1]Center for Physical Sciences and Technology, Sauletekio Ave. 3, LT-10257, Vilnius, Lithuania
Corresponding author: vidmantas.gulbinas@ftmc.lt

Organic bulk heterojunction photovoltaic solar cells now achieve a power conversion efficiency of >10%. Because of the complex morphology of active layers of these devices, charge separation mechanism and properties of subsequent motion of free charge carriers are intricate and still remain not clearly understood. Charge carrier traps play a very important role in carrier extraction and recombination. Trapping states reduce average carrier mobility, and trapped carriers create recombination centers. Therefore a clear understanding of the origin, properties and possibilities to control trap states is an important task in the further development of the organic solar cell technology.

We used several optical and optoelectrical investigation techniques, including those with ultrafast time-resolution, to address the carrier motion and trapping dynamics in bulk heterojunction (BHJ) solar cells fabricated from polymer donors and fullerene or organic molecule acceptors. Optical probing of the electric field dynamics by means of electric-field-induced second harmonic generation [1] was used to examine the motion of charge carriers with subpicosecond time resolution. Conventional transient photocurrent and modified time-delayed collection field (TDCF) technique gave us information on the carrier extraction at longer times.

Investigation of the carrier motion dynamics revealed dispersive carrier motion with decreasing in time carrier mobility, which shows that charge carriers gradually occupy low energy states and may also meet spatial obstacles. 1 sun steady state illumination does not affect mobility on a picosecond timescale, however, illumination increases mobility at long times, indicating that at least fraction of carrier trapping states become occupied.

Modified TDCF technique, enabled us to identify two types of traps: energy and spatial traps. Spatial traps are associated with dead ends in the intermixed donor-acceptor blend. Both types of traps lead to the slow-down of charge extraction and to enhanced recombination and associated performance losses. These effects were observed in addition to the dispersive behavior that is characteristic of charge motion in energetically disordered media. Deep traps are populated by carriers under cell operation at 1 sun irradiation, which leads to faster carrier extraction, however also enhances geminate and nongeminate recombination.

[1] A. Devižis, A. Serbenta, K. Meerholz, D. Hertel, V. Gulbinas, Phys. Rev. Lett. 2009, 103, 027404.

FR-O-8

Luminescent carbon dots synthesized by the laser ablation in liquid

Justyna Chrzanowska-Giżyńska[1*], Artur Małolepszy[2], Slawomir Błonski[1], Leszek Stobinski[2], Zygmunt Szymanski[1]

[1] Institute of Fundamental Technological Research, Polish Academy of Sciences, Pawinskiego 5B, 02-106 Warsaw, Poland
[2] Faculty of Chemical and Process Engineering, Warsaw University of Technology, Warynskiego 1, 00-645 Warsaw, Poland
Corresponding author: jchrzan@ippt.gov.pl

Fluorescent carbon nanoparticles with diameters of 2 to 8 nm called Carbon-Dots (CDots) are widely used for purposes of fluorescent imaging, mainly of cells and tissues [1]. Their most remarkable property is the excitation-dependent photoluminescence emission. Although the origin of luminescence from carbon nanoparticles is still not fully understood there is rising evidence that it is extrinsic fluorescence resulting from surface states. The close relationship between functional groups of ligands attached to the CDots surface and carbon dots luminescence has been demonstrated in several studies [2].

In this paper, the results of synthesis of the luminescent carbon dots performed by interaction of a nanosecond laser pulse with the suspension of expandable graphite flakes in various liquids like triethanolamine (TEA), ethylenediamine (EDA), polyethylene glycol (PEG) and PEG-diamine are presented. All suspensions after laser irradiation consisted of CDots that exhibited typical strong broadband photoluminescence with a maximum dependent on the excitation wavelength. This photoluminescence originates from the functional groups attached to the surface of nanoparticles during the laser processing in appropriate liquids. Since the quantum efficiency of obtained CDots depends on these functional groups, several liquids containing different functional groups like hydrocarbon or amine chains are used in the experiments, and the results are compared and analysed.

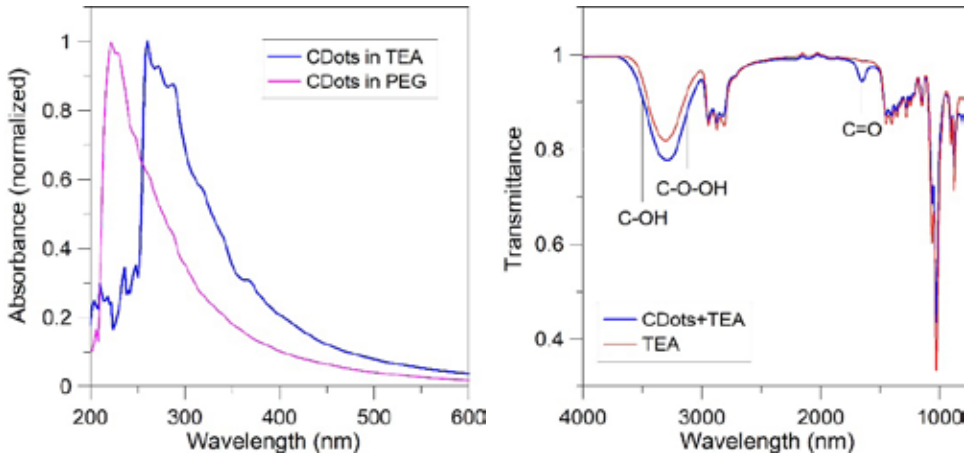

Fig. 1 (a) Absorbance of CDots in PEG 200 and TEA. (b) FTIR spectrum of CDots in TEA and pure TEA

The effect is already seen in Fig.1a, where the differences in absorbance of CDots synthesized in PEG 200 and TEA, are shown. CDots synthesized in PEG show a strong absorption peak located at 220 nm, associated with the transition π–π* of aromatic C–C bonds while CDots in TEA show peaks at 260, 270, and 288 and 365 nm from different transitions are observed.

[1] O. S. Wolfbeis, An overview of nanoparticles commonly used in fluorescent bioimaging. Chem. Soc. Rev.**44**, 4743-4768 (2015)
[2] R. Jelinek, Carbon Quantum Dots. Synthesis, Properties and Applications (Springer, 2017)

FR-O-9

Interaction of femtosecond white light continua generated by different wavelengths in bulk transparent media

Mikas Vengris[1], Lukas Rimkus[1], Augustas Čepėnas[1], Gintaras Tamošauskas[1], Nail Garejev[1], Audrius Dubietis[1]

[1]Vilnius University, Faculty of Physics, Laser Research Center, Sauletekio Ave. 10, Vilnius, Lithuania
Corresponding author: mikas.vengris@ff.vu.lt

White light continuum (WLC) generated in cubic nonlinear media is a widely investigated topic, because it provides insight into fundamental aspects of light self-action in cubic nonlinear media. WLC can also be used for generating interesting spatiotemporal light structures called X-pulses and is widely applied in laser technology as a seed source for optical parametric amplifiers and time-resolved spectroscopy, as a broadband femtosecond probe light source (see ref. [1] for a recent review).

In this study, we present an investigation into the possibility of extending the spectral range of WLC generated by Yb:KGW laser in sapphire by using a two-colored pump pulse, the fundamental output (1030 nm) and second harmonic (515 nm). The WLC bandwidth can be extended when two pulses arrive at a nonlinear medium with 1 ps or larger delay. However, when they overlap in time, the WLC intensity exhibits complicated dependence on the relative delay of the pulses, with continuum generation completely inhibited at certain delays. We present a detailed investigation of this behaviour, with WLC spectra, output power and beam track in the crystal recorded as a function of delay between two frequencies (data sample shown in Fig.1).

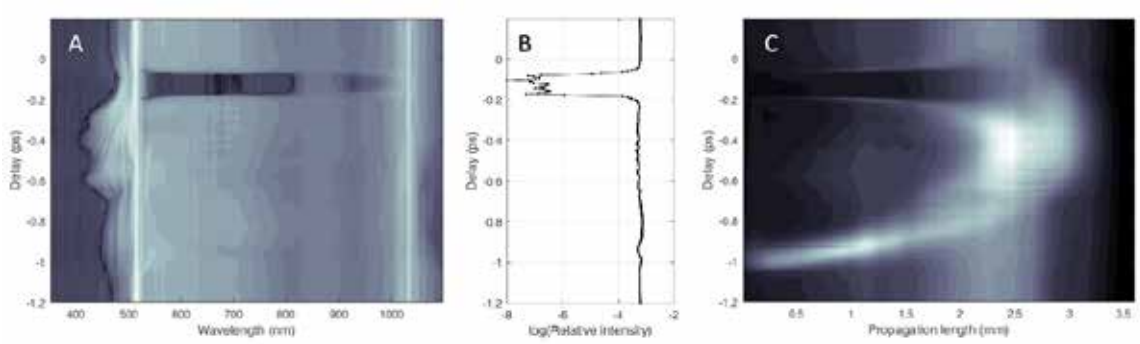

Fig. 1 WLC spectrum (A), a relative intensity at 660 nm (B) and beam profile in the nonlinear medium (C) as a function of delay between 1030 nm and 515 nm pulses when 1030 nm pulse is above, and 515 nm pulse is below WLC generation threshold.

Interestingly, the extinguishment of WLC is extremely fast and occurs within 20 fs of delay change between the two pump pulses. In addition, even the pulse energies 10x below the continuum threshold are capable of inhibiting the WLC generation by a powerful pulse of a different wavelength. In the case when the intensities of both beams are below WLC threshold, a combined effect has been observed, when WLC lights up at a certain delay between the pulses. Such complex behaviour poses a challenge for a model able to explain experimental observations.

[1] A. Dubietis, G. Tamošauskas, R. Šuminas, V.Jukna, A. Couairon, Ultrafast supercontinuum generation in bulk condensed media. *Lith. J. Phys*. **57**, 113-157 (2017).

FR-O-10

High-quality $CsPbBr_3$ nanolasers fabricated by spray forming

Anatoly Pushkarev[1], Filipp Komissarenko[1], Denis Sannikov[2], Anton Zasedatelev[2], Vidas Pakštas[3], Pavlos Lagoudakis[2], Anvar Zakhidov[1], Sergey Makarov[1]

[1]ITMO University, Department of Nanophotonics and Metamaterials, 197101 Saint Petersburg, Russia;
[2]Skolkovo Institute of Science and Technology, Moscow, Russia;
[3]Center for Physical Sciences and Technology, Saulėtekio Ave. 3, LT-10257 Vilnius, Lithuania.
Corresponding author: anatoly.pushkarev@metalab.ifmo.ru

Since the breakthrough reports dedicated to the utilization of $MAPbI_3$ material for efficient photoconversion in solar cells, researchers working in the field of organic electronics and dielectric nanophotonics have been discovering new applications of lead halide perovskites. One of the recent cutting-edge applications is perovskite nanowires (NWs) generating laser emission in the broad spectral range 420-800 nm [1,2] that can be exploited for the development of photonic chips capable of super fast information processing. Although such nanowires have already demonstrated lasing with very low excitation threshold 0.22-40 μJ cm-2, high cavity quality factor (Q = 1500-3600) and short radiative decay (τ ≈ 20 ps), there are some problems with their fabrication and operation stability as well as many questions regarding the mechanism of their functioning. The issue related to the production of the nanowires stems from the methods of synthesis presented in the literature. To the best of our knowledge they can be grown as a dense nanoforest onto substrates covered by PEDOT:PSS thin film in an alcohol solution or by means of metal halides thermal coevaporation in an argon atmosphere. Further optical characterization and practical application of the individual nanolasers requires their separation and careful transfer to the auxiliary substrate. The reshaping caused to the nanowires (especially very long ones with lengths larger than 10 μm) during these procedures dramatically decreases their performance. Furthermore, the wet synthesis presented in previous works was conducted in the N_2-filled glove box for 12-24 h that makes it non-convenient for large-scale fabrication.

Herein we report the rapid production of separated nanowires on a glass substrate at ambient conditions. $CsPbBr_3$ in DMSO was spray formed (Fig. 1a) onto the substrates and then treated with antisolvent vapor to give the wide dispersion of the NWs with lengths from 5 to 50 μm and different aspect ratio. SEM images of the samples revealed the formation of well-shaped objects with orthorhombic facets (Fig. 1b). Their XRD patterns also confirmed the existence of the orthorhombic phase (Fig. 1c). The measured under pulsed laser excitation (λ = 400 nm, τ = 100 fs) 11 μm nanowire showed laser generation with high Q = 2200 and relatively low excitation threshold (Fig. 1d).

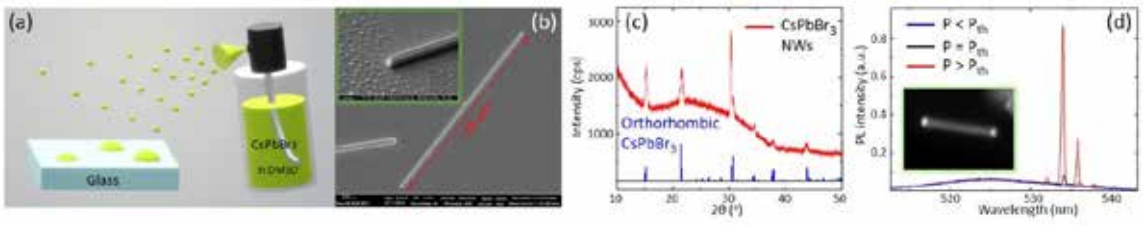

Fig. 1 (a) Scheme of spray forming;(b) SEM images of NWs; (c) XRD spectrum of NWs; (c) PL spectra showing the lasing.

[1] H. Zhu et al., Nature Mater.14, 636 (2015).
[2] K. Park et al., J. Phys. Chem. Lett. 7 3703 (2016).

FR-O-11

Photonic Crystal Microchip Laser

K. Staliunas[1,2], D.Gailevicius[3], V. Koliadenko[4], V. Taranenko[4], V. Purlys[3], M. Peckus[3]

[1]Institucio Catalana de Reserca i Estudis Avancats (ICREA), Barcelona, Spain
[2]Department of Physics, Universitat Politecnica Catalunya (UPC), Barcelona, Spain
[3]Laser Research Center, Vilnius University, Vilnius, Lithuania
[4]Institute of Applied Optics, NAS of Ukraine, Kyiv, Ukraine
Corresponding author: kestutis.staliunas@icrea.cat

Microchip lasers (and generally most micro-sized lasers, like diode lasers, edge emitting lasers or VCELS) being extremely compact and efficient sources of coherent radiation, suffer from one drawback: the low spatial quality of the emitted beam. Only at low power emission regimes (close to the generation threshold), the microchip lasers can emit the beams and pulses of reasonable spatial quality. Every attempt to increase the emission power, by increasing the pump power, or by increasing the pumping area, leads to the deterioration of the spatial quality of the beams, equivalently to large angular divergence, and results to lower brightness of the radiation. The conventional lasers usually contain the spatial filtering elements within the resonator. In microlasers, the spatial filtering is very problematic.

We proposed that the use of the specially designed intracavity Photonic Crystals can substantially improve the spatial quality of the emission of such microlasers, in particular of microchip laser. The Photonic Crystals were recently shown to provide the spatial filtering functionality [1]. Both the 1D filtering, as well as axisymmetric 2D filtering, were experimentally demonstrated. The positioning of such Photonic Crystals spatial filters inside the cavity of microchip lasers enabled to decrease the divergence of the radiation at high power regimes, and eventually to increase the brightness of emitted radiation. Presently we demonstrated enhancement of the brightness approximately 3 times due to intracavity photonic crystal spatial filtering, or, equivalently, we achieved a single-transverse-mode emission of approximately 3 times higher emission powers [2].

The reported results are presently limited by fabrication restrictions and imperfections of Photonic Crystals spatial filters, and potentially can be improved with the advance of the fabrication technologies. We will present the basic physical idea of the microchip lasers with intracavity spatial filtering [2], and the recent advances of this idea.

[1] L. Maigyte and K. Staliunas, Spatial filtering with photonic crystals, *Appl. Phys. Rev.* **2,** 011102 (2015).
[2] D. Gailevicius, V. Koliadenko, V. Purlys, M. Peckus, V. Taranenko, and K. Staliunas, “Photonic Crystal Microchip Laser“, Scientific Reports, **6**, 3417 (2016)

FR-IN-3

Spectroscopy in Flatland

Sejeong Kim[1], Milos Toth[1], Igor Aharonovich[1]

[1]Institute of Biomedical Materials and Devices (IBMD), Faculty of Science, University of Technology Sydney, Ultimo, NSW, 2007, Australia
Corresponding author: Sejeong.Kim-1@uts.edu.au

Single-photon emitters (SPEs) are key resources for many quantum technologies including quantum computation and quantum communications. To date, the most investigated solid state SPE systems are epitaxial quantum dots that operate primarily at cryogenic temperatures, and colour centres in solids. Despite years of research, the existing systems remain inadequate for practical applications, and the search is on for high-performance quantum emitters. In 2015, the SPE platform expanded to two-dimensional (2D) materials. In 2016, hexagonal boron nitride (hBN) emerged as a compelling 2D host of SPEs [1].

SPEs in hBN are promising because they are bright, with more than a million counts per second at room temperature, optically stable at ambient conditions, fully polarized and with a narrow zero photon line (ZPL) [2-3]. Furthermore, hBN is a wide bandgap material, which guarantees optical transparency in the visible and IR spectral regions. These factors make this material an outstanding candidate for quantum nanophotonics with diverse promising applications.

Here we discuss fundamental characteristics of SPEs in hBN including temperature and strain dependency. On the device fabrication front, we discuss coupling emitters to the Plasmonic and optical resonators.

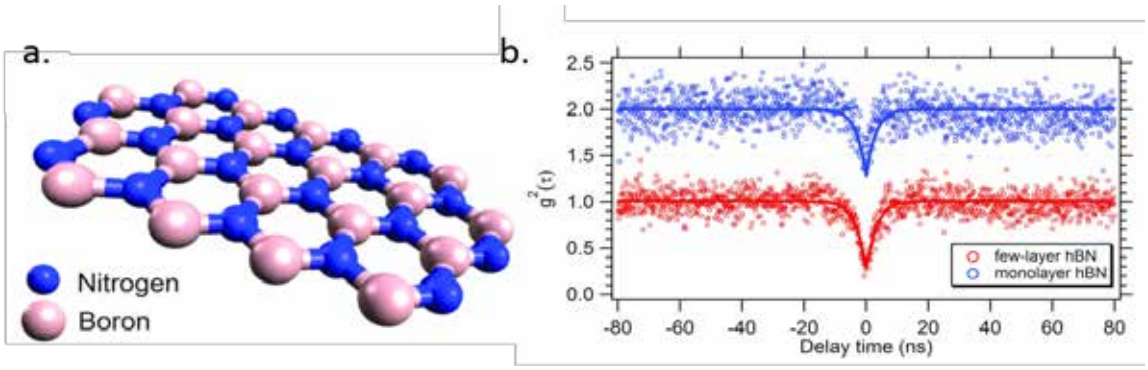

Fig. 1 (a) Schematic illustration of a hBN monolayer. (b) Antibunching curves from hBN [2].

[1] I. Aharonovich, M. Toth, Quantum emitters in two dimensions, Science **358**, 170-171 (2018).
[2] T. T. Tran, K. Bray, M. J. Ford, M. Toth, I. Aharonovich, Quantum emission from hexagonal boron nitride monolayers, Nature Nanotechnology **11**, 37-41 (2016).
[3] M. Kianinia, B. Regan, S. A. Tawfik, T. T. Tran, M. J. Ford, I. Aharonovich, M. Toth, Robust solid-state quantum system operating at 800 K, ACS Photonics 4, 768-773 (2017).

FR-IN-4

Nanofabrication of metallic nanostructures by femtosecond laser-induced photoreduction

Atsushi Ono[1*], Seiya Toriyama[2], Masato Sumiyoshi[1], and Vygantas Mizeikis[1]

[1]Graduate School of Engineering, Department of Electronics and Materials Science, Shizuoka University, 3-5-1 Johoku, Naka-ku, Hamamatsu 432-8561
[2]Graduate School of Science and Technology, Shizuoka University
Corresponding author: ono.atsushi@shizuoka.ac.jp

Photons coupled with electron oscillations in metal excite surface plasmons, and enhanced electric field is generated at the metal surface. A metallic nanostructure with a distinct shape and arrangement exhibits resonant coupling of surface plasmons in the ultraviolet to the near-infrared region and has the potential for a variety of applications to imaging, lithography, optoelectronic devices, and biosensors [1, 2]. Our group established a fabrication technique for metallic nanostructures by laser-induced metal reduction techniques. Direct laser writing technique with metal-ion photoreduction draws an arbitrary pattern of metal [3]. Although the usual technique for the patterning of metal requires a multi-step procedure involving photolithography, metal deposition, and lift-off or etching, this technique essentially involves a single fabrication step. Furthermore, the diffractive resolution limit is overcome by the transition process with multi-photon absorption induced by femtosecond laser irradiation. The initial material, developed for this study, is a photo-reducing agent containing silver ions. Nonlinear optical exposure by the focused Ti:Sapphire laser beam leads to local photoreduction reaction of silver ions in the irradiated area. By translating the laser focus, various structures, such as silver gratings were fabricated.

Figure 1(a) shows the schematic image of laser-induced metal reduction. Silver nitrate is dissolved in polymer material consisted with carboxyl radical. The carboxyl radical emits an electron by photon absorption, and the silver ion is reduced to silver. Figure 1(b) shows SEM image of line and space of silver pattern. Irradiated laser power is set to 5 mW. Scan speed is 3.0 µm/sec. Line period is 1 µm. Clear silver lines are patterned by this laser-induced photoreduction technique. This silver patterning on the polymer is applied for the development of flexible plasmonic devices, a flexible electric circuit, and so on.

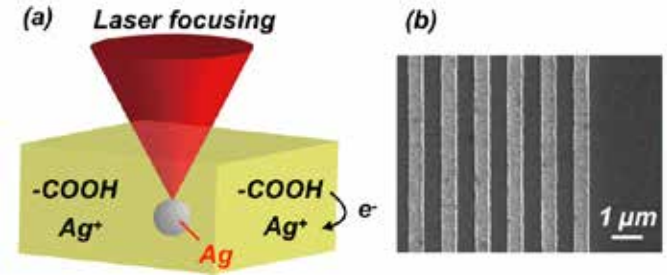

Fig. 1 (a) Schematic image of laser-induced photoreduction. (b) Fabricated silver lines with 1 µm pitch. Line width is about 500 nm.

[1] Optical Properties of Nanostructured Random Media, edited by V. M. Shalaev (Springer, Berlin, 2002).
[2] Near-Field and Surface Plasmon Polaritons, edited by S. Kawata et al. (Springer, Berlin, 2001).
[3] T. Tanaka, et al., Appl. Phys. Lett. 88, 081107 (2006).

FR-O-12

Up-Scaling for Manipulation of Particle Properties on the Nano- and Sub-Micrometer Scale by Laser Irradiation in Liquids

Marcus Lau, Ulf Quentin

TRUMPF Laser- und Systemtechnik GmbH, Johann-Maus-Straße 2, 71254 Ditzingen, Germany
Corresponding author: marcus.lau@trumpf.com

The reports of the possibilities to change particle properties by pulsed laser irradiation in liquids are manifold. First reported by Henglein and Fojtik [1], this method has proven not only to change sizes of the irradiated particles [2], but also their chemical composition [3]. A free liquid jet is beneficial for an optimized and scalable particle irradiation process [4]. Utilizing this set-up enables up-scaling of laser fragmentation [4] and laser melting [5] when sufficient laser power is available [6]. The specific power input and number of pulses per particle can be derived what enables balancing of the process. This experimental design also allows determination of the laser fluence correlated process window for the particle processing, due to confinement of the particles in the liquid jet. This gives access to scaling parameters to increase the throughput with sufficient laser power, what will be presented here.

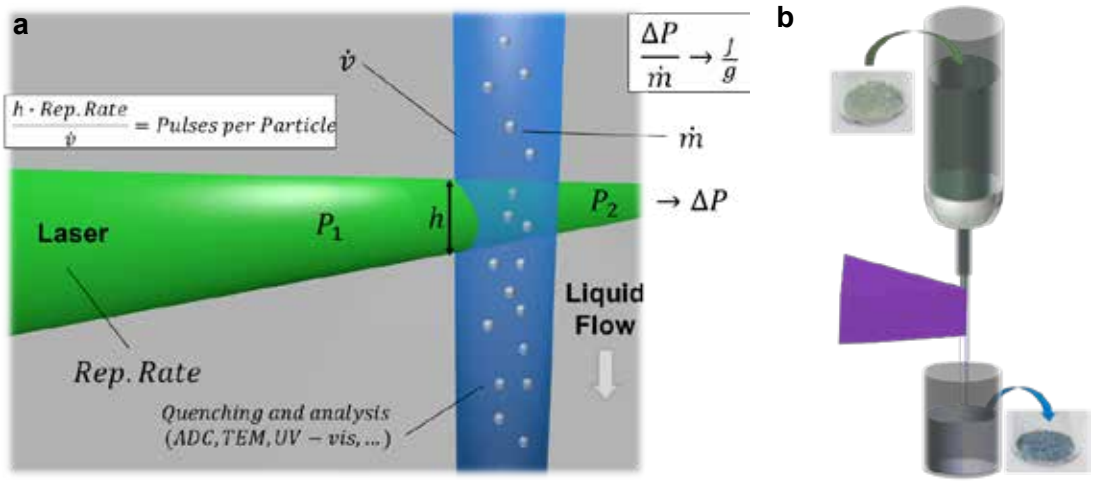

Fig. 1 (a) Illustration of the particles in a liquid jet irradiated with a laser beam correlated with key figures required for process characterization and up-scaling. (b) Illustration of the liquid jet reactor illuminated with a focused line beam optic for up-scaling [7].

[1] A. Fojtik, A. Henglein, Laser ablation of films and suspended particles in a solvent: formation of cluster and colloid solutions, *Ber. Bunsenges. Phys. Chem.* **97**, 252–254 (1993).
[2] Y. Tamaki, T. Asahi, H. Masuhara, Tailoring nanoparticles of aromatic and dye molecules by excimer laser irradiation, *Appl. Surf. Sci.* **168**, 85-88 (2000).
[3] Y. Ishikawa, Y. Shimizu, T. Sasaki, N. Koshizaki, Boron carbide spherical particles encapsulated in graphite prepared by pulsed laser irradiation of boron in liquid medium, *Appl. Phys. Lett.* **91**, 161110 (2007).
[4] M. Lau, S. Barcikowski, Quantification of mass-specific laser energy input converted into particle properties during picosecond pulsed laser fragmentation of zinc oxide and boron carbide in liquids, *Appl. Surf. Sci.* **348**, 22-29 (2015).
[5] M. Lau, A. Ziefuss, T. Komossa, S. Barcikowski, Inclusion of supported gold nanoparticles into their semiconductor support, *Phys. Chem. Chem. Phys.* **17** 29311-29318 (2015).
[6] M. Lau, *Laser Fragmentation and Melting of Particles* (MatWerk, Springer, 2016).
[7] M. Lau, T. Straube, V. Aggarwal, U. Hagemann, B. de Oliveira Viestel, N. Hartmann, T. Textor, H. Lutz, J. Gutmann, S. Barcikowski, Gradual modification of ITO particle's crystal structure and optical properties by pulsed UV laser irradiation in a free liquid jet, *Dalton Trans.* **46** 6039-6048 (2017).

FR-O-13

Laser-Induced Quantum Dots Generation

Leonardo Orazi[1], Francesco Antolini[2], Barbara Reggiani[1], Iaroslav Gnilitskyi[1,3]

[1]University of Modena and Reggio Emilia, Department of Sciences and Methods for Engineering, Via Amendola 2, 42122 Reggio Emilia, Italy.
[2]ENEA, Fusion and Nuclear Security Dept., Photonics Micro and Nanostructures Laboratory Via E. Fermi 45, 00044 Frascati (Rome), Italy
[3]NoviNnano Inc., 79000, Lviv, Ukraine
Corresponding author: leonardo.orazi@unimore.it

The present work will deal with the formation of the micro Quantum Dots in polymer films for photonics applications by picosecond laser pulses. Prior works in the literature indicate that laser can be effectively used to induce the selective formation of QDs in polystyrene, TOPAS® and PMMA films loaded with CdS precursors [1]. Despite this, it is not clear if the formation mechanism is photo-thermally [1] or photo-chemically [2,3] driven. In this work, preliminary results of MILEDI project [4] will be presented and discussed. The aim of the project is to selectively pattern polymeric films in order to obtain both red and green QDs based pixels (Fig. 1a) and to correlate this generation with laser treatment parameters. The laser source is operated in the near UV range in the ps regime in order to minimise thermal diffusive effects.

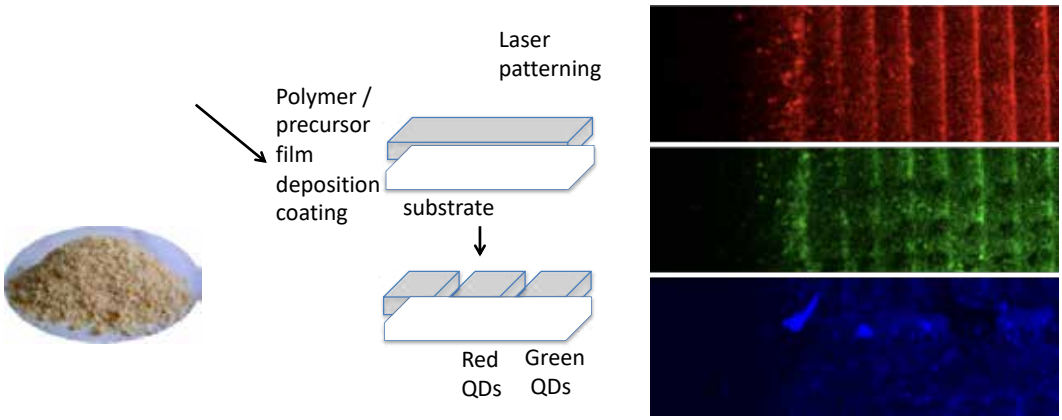

Fig. 1 (a) Patterning process. (b) Preliminary photoluminescence results
Analysis of the QDs generation will be obtained indirectly by photoluminescence analysis (Fig. 1b).

[1] F. Antolini et al., Laser-induced nanocomposite formation for printed nanoelectronics. *Mater Lett* **60(8),** 1095-1098 (2006).
[2] Račiukaitis, G.et al, Formation of quantum dots from precursors in polymeric films by ps-laser. *Proc SPIE*, 8607,815696 (2013)
[3] A. K. Bansal et al., In situ formation and photo patterning of emissive quantum dots in small organic molecules. *Nanoscale* **7,** 11163-11172 (2015).
[4] www.miledi-h2020.eu/

FR-O-14

Laser-ablative fabrication of hybrid meta-dielectric nanoparticles via laser-assisted heterogeneous condensation

I. N. Saraeva,[1]* N. V. Luong,[1,2] S. I. Kudryashov[1,3]A. A. Ionin,[1] A. A. Rudenko,[1] R. A. Khmelnitsky,[1] D. A. Zayarny,[1] D. H. Tung,[4] P. V. Duong,[4] P. H. Minh[4]

[1] Lebedev Physical Institute, Leninskiy prospect 53, 119991 Moscow, Russia
[2] Moscow Institute of Physics and Technology (State University) Institutskiy per. 9, Dolgoprudnyi, Moscow Region 141700, Russia
[3] ITMO University, Kronverkskiy prospect 49, 197101 St. Petersburg, Russia
[4] Institute of Physics, Vietnam Academy of Science and Technology, 18 Hoang Quoc Viet, Cau Giay, Hanoi, Vietnam
Corresponding author: insar@lebedev.ru

Hybrid metal-dielectric/semiconductor NPs combine the unique properties of both plasmonically-resonant metal NPs and the polaritonically-resonant high-index dielectric or semiconductor nano- and (sub)microparticles, demonstrating both electrical and magnetic multipolar resonances, suitable for diverse advanced applications as basic elements for precise sensing devices, ultrafast light switches, non-linear optical elements etc. [1 – 2]. In our work we report the facile synthesis of colloidal Se@Au (Fig. 1), Si@Au, Si@Ag (Fig. 2) NPs via ns IR (λ = 1040 nm, pulse width τ = 120 ns, E ≈ 1 mJ, repetition rate ~ 80 kHz) through laser ablation of bulk targets in 0.03 mM aqueous solutions of chloroauric acid ($HAuCl_4$) and silver nitrate ($AgNO_3$) or in metal NPs colloids. The resulting NPs, prepared at different laser intensities were analysed in terms of their extinction coefficients in the form of hydrosols by UV-vis spectroscopy and as deposits by scanning electron microscopy and energy-dispersive X-ray spectroscopy.

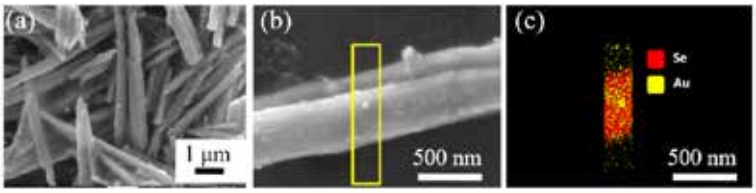

Fig. 1 SEM-images of Au-decorated Se nanorods (a, b); the corresponding elemental composition by EDX spectroscopy (c).

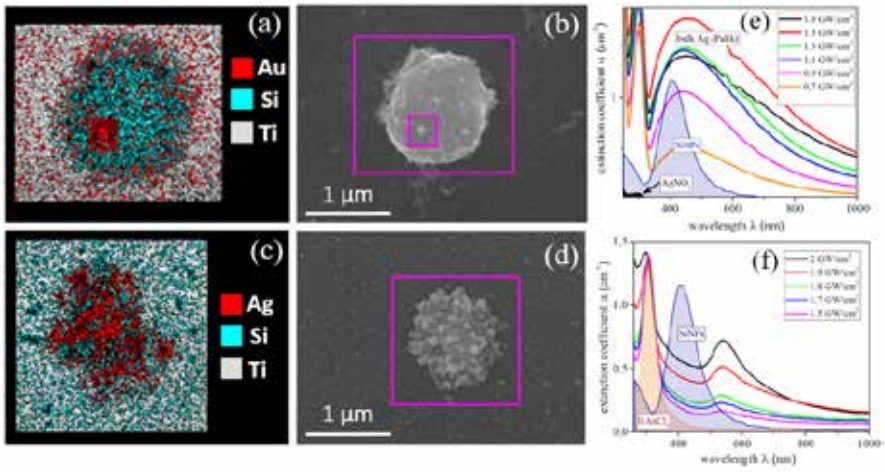

Fig. 2 Dry deposits of Si@Au (a, b) and Si@Ag (c, d) NPs: SEM images (b, d) and the elemental analysis by EDX spectroscopy (a, c).

[1] R. E. Noskov, A. E. Krasnok, Y. S. Kivshar, Nonlinear metal–dielectric nanoantennas for light switching and routing, New Journal of Physics, 14 093005 (2012).
[2] D. A. Zuev, S. V. Makarov, I. S. Mukhin, V. A. Milichko, S. V. Starikov, I. A. Morozov, I. I. Shishkin, A. E. Krasnok, P. A. Belov, Fabrication of Hybrid Nanostructures via Nanoscale Laser-Induced Reshaping for Advanced Light Manipulation, Adv. Mater., 28, 3087–3093 (2016).

FR-O-15

Nanosecond Laser Treatment of Thin Gold Film on ITO Glass

Evaldas Stankevičius[1*], Mantas Garliauskas[1], Lukas Laurinavičius[1], Romualdas Trusovas[1], Nikolai Tarasenko[2], Rasa Pauliukaitė[1] and Gediminas Račiukaitis[1]

[1]Center for Physical Sciences and Technology, Savanoriu Ave. 231, LT-02300 Vilnius, Lithuania
[2]Stepanov Institute of Physics of National Academy of Sciences of Belarus, Nezavisimosti Ave. 68, 220072 Minsk, Belarus
Corresponding author: estankevicius@ftmc.lt

Indium tin oxide (ITO) films on glass or quartz substrates often used as an electrode surface due to their prominent characteristics such as good electrical conductivity and wide electrochemical working window, as well as low-cost. ITO electrode modified with Au NPs possesses a faster electron transfer rate and larger current response than the bare ITO electrode. Therefore, such electrodes could be applied for the creation of highly sensitive and selective future sensors. It is highly desired to develop a simple and effective method to synthesise AuNPs on a solid support as a highly electroactive electrode. An excellent alternative strategy for one-step and useful fabrication of AuNPs on ITO electrodes directly can be the thermal treatment of thin gold coatings on ITO glass. These methods have an advantage versus drop-casting deposition as they do not use colloidal solutions and the generation of AuNPs occurs directly on the desired surface. The main advantages of nanosecond laser processing are the submicron treatment accuracy, the low thermal impact to the substrate and surrounding areas and the selective generation of nanoparticles on desired place and shape of the surface [1].

The example of SEM images of generated Au NPs when the thickness of the gold coating on ITO glass is 3 nm, 5 nm and 20 nm are shown in Figure 1d-f. The micrographs clearly indicate that the size and density of generated Au NPs depend on the gold film thickness.

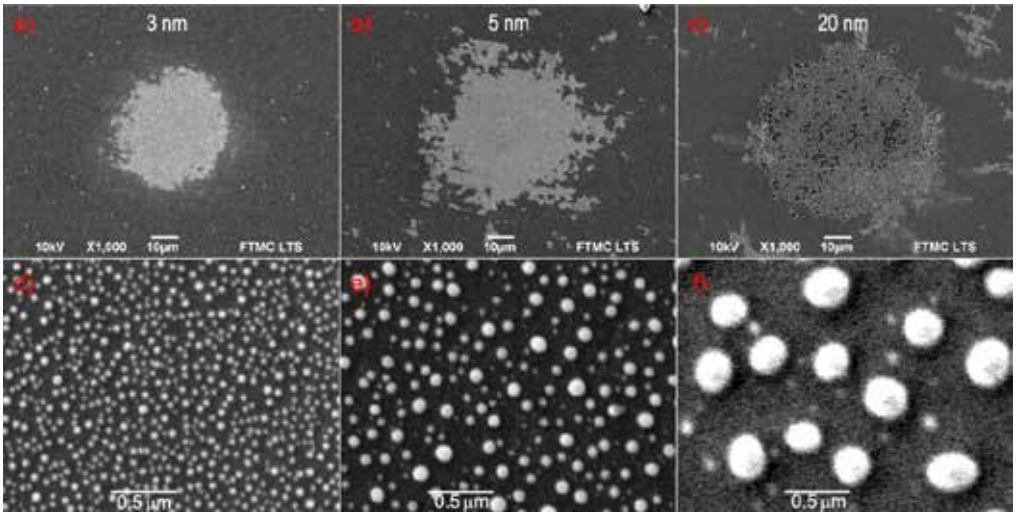

Figure 1. SEM micrographs of Au coatings affected by single laser pulse when coatings thickness are 3 nm (a, d), 5 nm (b, e) and 20 nm (c, f). The laser processing parameters in all cases were the same (laser pulse energy – 40 µJ, laser energy density – 505 mJ/cm^2, peak pulse intensity – 14 MW/cm^2, pulse duration – 35 ns, beam diameter – 142 µm).

Here, simple one-step generation of gold nanoparticles on ITO glass using nanosecond laser will be presented and the electrochemical properties of the gold modified ITO electrodes by the detection of the ascorbic acid will be analysed.

1. Y. Lin, T. Zhai, and X. Zhang, "Nanoscale heat transfer in direct nanopatterning into gold films by a nanosecond laser pulse," Opt. Express **22**, 8396-8404 (2014).

FR-O-16

Magneto-optical Faraday effect of waveguide structures fabricated inside silica xerogels containing magnetic nanoparticles

*S. Nakashima[1)2)], R. Okabe[1)], R. Mizutani[3)], K. Sugioka[2)], and A. Ishida[1)]

1) Shizuoka University, Hamamatsu, Shizuoka, Japan, 2) Advanced Science Institute
*nakashima.seisuke@shizuoka.ac.jp
Keywords: magneto-optical effect, glass, femtosecond laser, localized surface plasmon resonance

Optical waveguide structures containing functional nanoparticles (NPs) have considerable potential for use in photonic microdevices. A variety of functional NPs, such as metal, semiconductor, dye molecules, and magnetic NPs were combined with optical waveguide structures, suggesting that novel and micro-sized active waveguide devices can be realized.[1] In particular, waveguide structures containing magnetic NPs exhibit magneto-optical Faraday effect.[2] In this paper, waveguide structures were fabricated by using fs laser inside transparent silica xerogels doped with magnetite nanoparticles (NPs), and Faraday rotation angles for the propagated light through the waveguides were evaluated. Water-soluble magnetite NPs were synthesized using co-precipitation method. The sol-gel reactions using (3-aminopropyl)triethoxysilane and the aqueous solution of magnetite NPs were performed to prepare silica xerogels. Observations of microstructures and absorption spectra suggest that magnetite NPs were successfully dispersed into xerogels without agglomeration. Magnetic field dependences of Faraday rotation angles for the obtained xerogels exhibit ferrimangetic behaviors after subtracting the contributions of substrates and diamagnetic xerogels. As the increase in the NPs concentration, the saturated rotation angle becomes higher.

Magnetization curves were also measured using superconducting quantum interference devices. Ferrimagnetic behavior agrees with the results of Faraday rotation measurement. Significantly small coercive fields in both measurements indicate that the magneto-optical responses are due to magnetite NPs with no aggregation. After annealing process at 150 °C, femtosecond-laser beam was focused inside the xerogels to fabricate optical waveguide structures. The laser pulses were focused inside the samples through the bottom glass, and horizontally scanned. In the irradiated area, refractive-index changes were observed at scanning speed slower than 250 µm/s. Propagated light images were successfully observed in some conditions. By comparing intensity profiles of the spots, we found that the most intense propagated light was obtained in the case of using pulse energy of 4.6 nJ and scanning speed of 150 µm/s. Evaluation of Faraday rotation angles was performed for the propagated light and ferromagnetic saturation behaviors were observed in different concetrations of magnetite NPs.

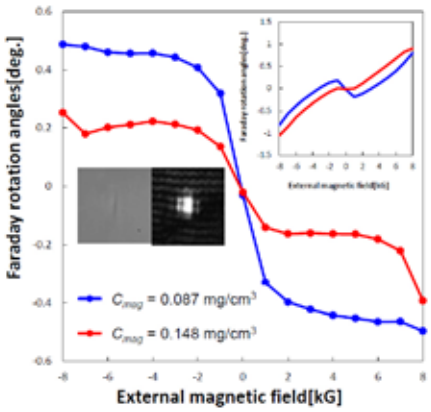

Fig. 1 Faraday rotation angles as a function of magnetic field measured for the propagated light through waveguides in magnetite-doped xerogels.

References

1) S. Nakashima, T. Tanaka, A. Ishida, K. Mukai, Appl. Phys. A, 123, 723 (2017).
2) S. Nakashima, K. Sugioka, K. Tanaka, M. Shimizu, Y. Shimotsuma, K. Miura, K. Midorikawa, and K. Mukai, Opt. Express, 20, 28191 (2012).
different transitions are observed.

FR-O-17

Optical Properties of the Solar Cells with Nanostructures Formed by XeCl Excimer Laser

Mitsuhiro Kusaba[1], Fumitaka Nigo[1], Masaki Hashida[2,3] and Shuji Sakabe[2,3]

[1] Department of Electronics, Information and Communication Engineering, Osaka Sangyo University, 3-1-1 Nakagaito, Daito, Osaka 574-8530, Japan.
[2] ICR Kyoto University, Gokasho, Uji, Kyoto 611-0011, Japan.
[3] Department of Physics, Graduate School of Science, Kyoto University, Kitashirakawa, Sakyo, Kyoto 606-8502, Japan.
Corresponding author: kusaba@eic.osaka-sandai.ac.jp

The solar cells with laser-induced periodic surface structure (LIPSS) have been investigated using a XeCl excimer laser with an oscillation wavelength of 308 nm and pulse width (FWHM) of 20.6 ns. The sample was the mono-crystalline silicon solar cell with the surface formed pyramidal structures of 1 to 10 mm high and fixed on the accurate positioning stage. The laser fluence was controlled using an attenuator that comprised a polarizer and half-wave plate. After the laser was passed through a mask, the beam profile in which the length of 8 mm with homogeneous intensity distribution and the width of 70 mm with Gaussian distribution ($FWe^{-1}M$) was obtained. The laser energy with the stability of 12% and the number of pulses were adjusted in the range of 0.16 to 0.70 J/cm^2 and 2 to 42 shots. The laser irradiated the area of 2 cm × 2 cm on the sample by controlling the stage. Figure 1 shows the SEM image of the solar cell irradiated with the laser fluence of 0.41 J/cm^2 and the shot number of 42 shots. The nanostructures with the periodic length of 200 nm to 300 nm were observed on the surface of the pyramidal structures. Figure 2 shows the reflection spectra in the region between 200 nm and 800 nm for the solar cell with the nanostructures, the solar cell with the pyramidal structures and flat silicon. It is found that the reflectances around 500 nm were decreased by adding the nanostructures to the surface of the pyramidal structures. It is known that the diffuse transmittance of Si depends on the surface roughness [1]. Therefore, this result will suggest that the increase of the diffuse transmittance of the solar cells by the addition of the nanostructures causes the decrease of the reflectance.

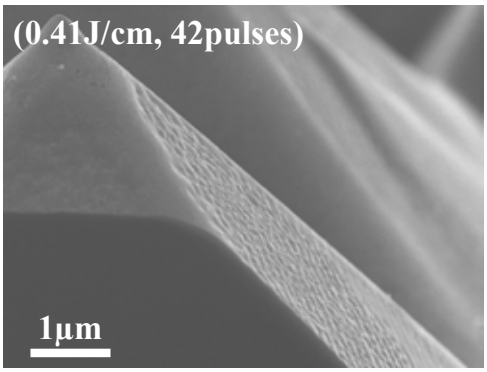

Fig. 1 SEM image of the solar cell with the nanostructures.

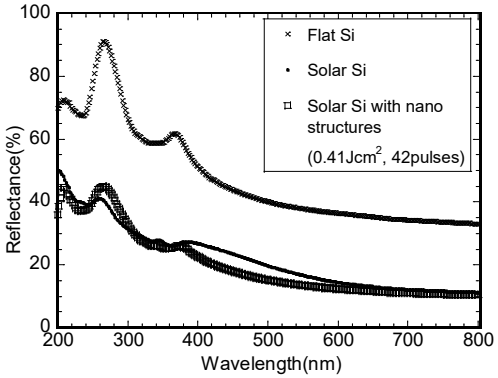

Fig. 2 Reflection spectra of the solar cell and flat Si.

This work was supported by the Collaborative Research Program of Institute for Chemical Research, Kyoto University (grant 2018-6).

[1] O. Isabella, J. Krc, M. Zeman, Appl. Phys. Lett., **97**, 101106(2010).

P1

Synthesis of Acceptor Doped ZnO Films by Inductively-Coupled Plasma-Assisted Pulsed-Laser Deposition

Hayato Tsukuda[1], Satoshi Kurumi[2], Ken-ichi Matsuda[2], Kaoru Suzuki[2]

[1]Graduate School of Electrical Engineering, College of Science and Technology, Nihon University
[2]Department of Electrical Engineering, College of Science and Technology, Nihon University
1-8-14 Kanda-Surugadai, Chiyoda-ku, Tokyo 101-8308 Japan
csha18023@g.nihon-u.ac.jp

Wide-gap semiconducting films have contributed to the development of functional devices such as transistors with high-voltage capability acting and ultraviolet emitting diodes. Among them, ZnO has expected as an ultraviolet emission device because of large exciton energy, and the direct band gap of 3.37 eV [1]. In order to attract much more attention to the wide-gap semiconductor, it is necessary to develop the film growth and impurity doping techniques [2]. Therefore, we examine to synthesize ZnO films for ultraviolet emission devices by pulsed-laser deposition (PLD). In that fabrication it, we tried to dope N_2 and O_2 atoms in the films by plasma-assisted processes during film depositing. The ZnO films were produced as below. Mixing ZnO powder (SOEKAWA CHEMICALS, Purity 99.99%) and P_2O_5 powder for the PLD target was pressed at 80 kN for 30 minutes. The target and an Al_2O_3 (0001) substrate were mounted on a vacuumed chamber. A focused Nd:YAG laser beam (LOTIS, LS2147, wavelength: 355 nm, fluence: 1.2 J/cm^2, pulse width = 20 ns, repetition frequency = 10 Hz) was irradiated to the target and ablation plumes were generated from a laser beam spot on the target. N_2 gas as an acceptor source for ZnO was introduced to ablation plumes via inductively-coupled plasma (ICP) generator which connected with the chamber. To enhance N doping efficiency, N_2 plasma, which generated by the ICP generator (13.56 MHz, 50 W), was injected to the ablation plumes. The emission spectra of the ablation plumes near the plasma injecting spot was measured by a CCD spectrometer (EPP 2000-UVN-SR-50, wavelength 300 nm to 800 nm). Fig. 1 shows the emission spectra of the ablation plumes and ICP particles. The emission peak at 355 nm was due to Nd: YAG laser beam. Emission from Zn (Zn I: 334 nm) and O (O I: 465, 480 and 496 nm) were observed in all the spectra. As shown in Fig. 1(b), emission lines of 526, 559, 598, 639 and 783 nm were attributed to O_2. In N_2 plasma assisted condition, emission from N_2 was observed (Fig. 1(c)). The existence of ablation plumes and plasma particles in the same place were expected to increase carrier implantation efficiency.

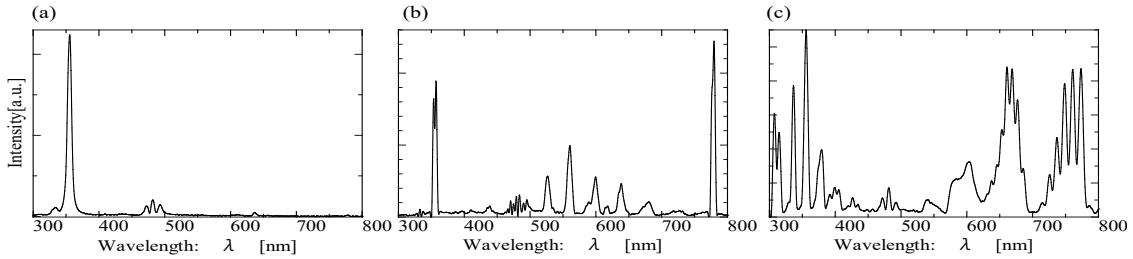

Fig. 1 Emission spectra of ICP and ablation plums. (a) Normally PLD. (b) Oxygen plasma assist. (c) Nitrogen plasma assist.

[1] A. Tsukazaki, M. Kubota, A. Ohtomo, T. Onuma, K. Ohtani, H. Ohno, S.F. Chichibu, M. Kawasaki, Jpn. J. Appl. Phys., **44**, 643 (2005).
[2] T. Uehara, S. Kurumi, K. Takase, and K. Suzuki, Appl. Phys. A, **101**, 723 (2010).

P2

Thin WB_x and $W_xTi_{1-x}B_2$ films deposited by combined magnetron sputtering and pulsed laser deposition technique

Justyna Chrzanowska-Giżyńska[1], Piotr Denis[1], Rafał Psiuk[1], Hanna Słomińska[1], Ion Mihailescu[2], Carmen Ristoscu[2], Tomasz Mościcki[1], Zygmunt Szymański[1]

[1]Institute of Fundamental Technological Research, Polish Academy of Sciences, Pawinskiego 5B, 02-106 Warsaw, Poland
[2]Natioal Institue for Lasers, Plasma and Radiation Physics, Bucharest, Romania

Corresponding author: jchrzan@ippt.pan.pl

The development of high-speed tools requires materials having high hardness, good chemical and thermal stability. Diamond and cubic boron nitride are the hardest materials currently used, but still, they have some drawbacks like the requirement of the high temperature-high pressure conditions during the synthesis process. Therefore, the topic of new superhard materials is still under the consideration of scientists. One of the materials considered to be superhard are compounds of transition metals and light elements like B, N, O, C. Among such materials, tungsten borides are known for high hardness [1] and wear resistance [2], and their properties change significantly depending on the chemical and phase composition.

In this paper, the results of WB_x and $W_xTi_{1-x}B_2$ films deposited by combined magnetron sputtering and pulsed laser deposition technique are presented. The experimental setup is presented in Fig. 1. In the case of WB_x films, pure boron target was sputtered by the magnetron, and pure tungsten target was ablated by laser impulse, and in the case of $W_xTi_{1-x}B_2$ films, the W_2B_5 target was sputtered by the magnetron, and the TiB_2 target was ablated by laser impulse. The deposited films have a high hardness exceeding 40 GPa. The chemical composition of deposited films was adjusted by sputtering power and laser fluence, and the Ti dopping supported the formation of boron-rich phases. Moreover, the effect of substrate temperature in the range from 23 °C to 700 °C was investigated.

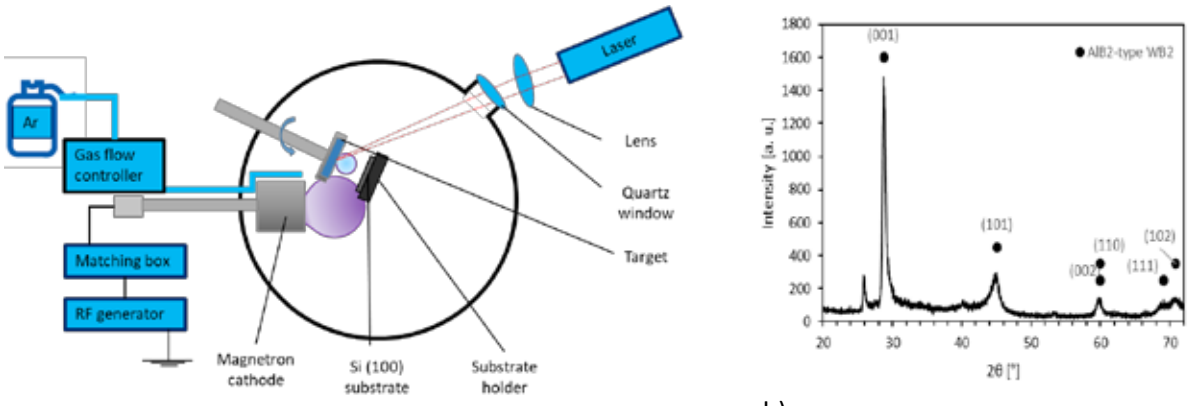

Fig. 1 (a) The experimental setup. (b) An example of the XRD pattern of the deposited film.

Acknowledgement: This work was supported by the NCN (National Science Centre) Research Project 2015/19/N/ST8/03928

[1] X. -Y. Cheng, X. -Q. Chen, D. -Z. Li, Y. -Y. Li, Computational materials discovery: the case of the W-B system, Acta Cryst. C C70 85-103 (2014)
[2] C. Jiang, Z. Pei. Y. Liu, J. Xiao, J. Gong, C. Sun, Preparation and characterization of superhard AlB_2-type WB_2 nanocomposite coatings, Phys. Status Solidi A 210 (6) 1221-1227 (2013)

P3

Optimizing copper profiles for open circuit voltage boost in Cu_2ZnSnS_4 solar cells by pulsed laser deposition

Mungunshagai Gansukh[1], Jørgen Schou[1], Stela Canulescu[1*]

[1]DTU Fotonik, Technical University of Denmark, DK-4000
Corresponding author: stec@fotonik.dtu.dk

Kesterite structure Cu2ZnSnS4 (CZTS) is a p-type semiconductor material which attracts high interest for solar cells with thin-film absorber layers. It has a direct bandgap of 1.5 eV and a high optical absorption coefficient of 105 cm-1[1]. Compared to other thin film solar cell materials like CdTe and Cu(In, Ga)Se2, it consists of abundant and non-toxic elements. Although Cu2ZnSnS4 is a promising material, the record efficiency is still 9.2% [2], whereas CdTe and Cu(In,Ga)Se2 have efficiencies of 22.6% and 22.1%[2]. The efficiency loss in CZTS is mainly due to the open circuit voltage (VOC) deficit defined as Eg /q- VOC.

Nagaoka et al. [3] reported an increase in hole carrier concentration with increasing Cu content in CZTS. Tajima et al. [4] reported a two-layer structure of CZTS that consists of a Cu-poor (low carrier concentration) between the p-n junction and a stoichiometric composition between p-type CZTS and molybdenum back contact. This structure resulted in a better band alignment between the p-CZTS, n-CdS and window layers (Fig 1.).

Our previous studies on laser ablation of CZTS have shown that the composition of the films can be controlled in-situ by tuning the laser fluence [5]. The as-deposited films exhibit a Cu/(Zn+Sn) metallic ratio varying from 0 to 1.0 by changing the laser fluence from 0.2 J/cm2 to 0.7 J/cm2 on the target material. This suggests that pulsed laser deposition is a flexible method of controlling the hole concentration in the CZTS material. In this study, we will deposit Cu-graded CZTS films from Cu/(Zn+Sn) ≈0.7 at the p-n junction and stoichiometric (Cu/(Zn+Sn) ≈1.0) at the back contact. The as-deposited films of Cu-Zn-Sn-S are annealed at a temperature of 5750C in a sulfur atmosphere. Our initial results on two-layer deposition formed two distinct layers of CZTS after sulfurization. The optical and electric properties of solar cells made by Cu-poor, stoichiometric and Cu graded samples will be discussed in detail.

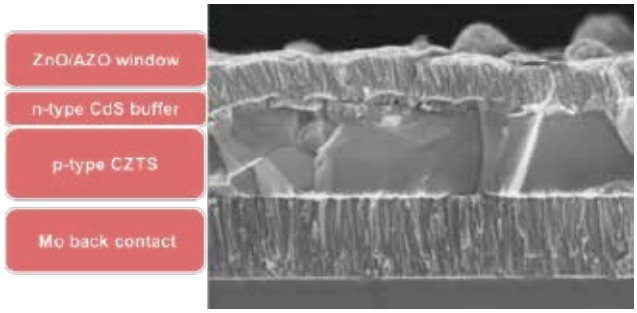

Fig. 1 Solar cell structure containing a p-type absorber layer deposited by PLD[5].

[1] W. Wang *et al.*, "Device Characteristics of CZTSSe Thin-Film Solar Cells with 12.6% Efficiency," *Advanced Energy Mater.*, vol. 4, no. 1301465, 2014.
[2] M. A. Green, Y. Hishikawa, E. D. Dunlop, D. H. Levi, J. Hohl-Ebinger, and A. W. Y. Ho-Baillie, "Solar cell efficiency tables (version 51)," *Prog. Photovoltaics Res. Appl.*, vol. 26, no. 1, pp. 3–12, Jan. 2018.
[3] A. Nagaoka, H. Miyake, T. Taniyama, K. Kakimoto, and K. Yoshino, "Correlation between intrinsic defects and electrical properties in the high-quality Cu2ZnSnS4 single crystal," *Cit. Appl. Phys. Lett*, vol. 103, 2013.
[4] S. Tajima, H. Katagiri, and K. Jimbo, "Improvement of the open-circuit voltage of Cu 2 ZnSnS 4 solar cells using a two-layer structure Temperature Dependence of Cu 2 ZnSnS 4 Photovoltaic Cell Properties."
[5] A. Cazzaniga *et al.*, "Ultra-thin Cu2ZnSnS 4 solar cell by pulsed laser deposition," *Sol. Energy Mater. Sol. Cells*, vol. 166, pp. 91–99, 2017.

P4

An optical method for determination of the mass thickness of thin gold films with arbitrary morphology

Sergey V. Starinskiy[1*], Alexey I. Safonov[1], Veronica S. Sulyeva[2], Alexey A. Rodionov[1], Yuri G. Shukhov[1], Alexander V. Bulgakov[1,3]

[1]S.S. Kutateladze Institute of Thermophysics SB RAS, Lavrentyev Ave. 1, 630090 Novosibirsk, Russia
[2]A.V. Nikolaev Institute of Inorganic Chemistry SB RAS, Lavrentyev Ave. 3, 630090 Novosibirsk, Russia
[3]HiLASE Centre, Institute of Physics of the Czech Academy of Sciences, Za Radnicí 828, 25241 Dolní Břežany, Czech Republic
Corresponding author: starikhbz@mail.ru

The mass thickness of thin metal films is an important parameter determining the film structure, however, a robust routine method for its determination is still missing. Physical methods are numerous but rather complicated and often dependent on the film density and morphology while chemical methods require removing of the film from the substrate. In this work, we have developed a simple optical method for determining the mass thickness of metal films with arbitrary morphology on transparent substrates. The method is based on film spectrophotometry in the far-UV range when the light attenuation is due to interaction with core electrons, and thus the influence of the film morphology is negligible (in contrast to the visible range when light interacts with conduction electrons). The method was tested using gold films produced by nanosecond pulsed laser deposition (PLD) on quartz substrates at different substrate temperatures resulting in different film structures. We demonstrate that the transmittance spectra of films with different morphologies obtained at a fixed deposited flux are different in the visible and near-UV ranges but identical in the 200-240 nm spectral range (Fig. 1*a*) and thus the latter can be used to measure the film mass thickness *h* by analyzing the light transmittance *T*. The calibration was performed at λ = 200 nm for gold films of known thicknesses deposited by the ion beam sputtering (IBS) technique and a good agreement of the *T*(*h*) dependence with the Beer-Lambert law was obtained (Fig. 1*b*). Using this calibration, we have measured the *h* values for PLD-produced films as a function of the laser pulse number *N* and obtained a liner *h*(*N*) dependence, identical for cold and hot substrates (Fig. 1*b*). The method was then applied to investigate the ablation plume expansion under PLD conditions by placing transparent substrates at different orientations to the plume axis.

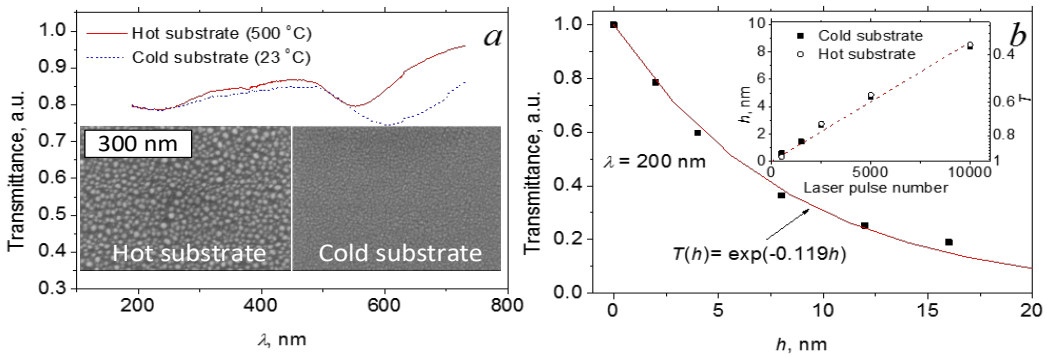

Fig. 1 (*a*) Transmittance spectra and SEM images of gold films obtained by PLD at different substrate temperatures. (*b*) The thickness dependence of the transmittance *T* at λ = 200 nm for IBS-produced gold films. The line is a fit with the Beer-Lambert law. The inset shows the *h*(*N*) dependence measured for Au films deposited by PLD at substrate temperatures of 23 and 500 °C.

P5

In situ laser-induced codeposition of metals for fabrication of non-enzymatic sensor materials

Alexandra Smikhovskaia[1], Ilya Tumkin[1], Maxim Panov[1], Evgeniia Khairullina[1], Vladimir Kochemirovsky[1]

[1]Saint Petersburg State University, St.Petersburg State University, 7/9 Universitetskaya nab., St. Petersburg, lasergroupspb@gmail.com

In the current work, we demonstrate a simple and low-cost method of fabrication of highly developed and electrocatalytically active copper microstructures (microelectrodes) doped with different metals based on *in situ* laser-induced metal deposition technique. The method of laser-induced chemical liquid-phase deposition (LCLD) is an effective tool for chemical reduction of metal on the surface of various dielectrics and semiconductors. [1]. The in situ laser-induced synthesis of conductive copper nano-sized microstructures doped with silver and cobalt was reported. Despite the obvious practical importance of this method, its theoretical background is not well developed so far, and numerous aspects of this process still remain unclear. This fact prevents further development of the technique especially because of the significant difference between the mechanisms of non-equilibrium laser-induced metal deposition and equilibrium chemical and electrochemical depositions. The goal of this work is to reveal the relationship between the structure and stability of metal complexes in parent solutions and structure and electrophysical properties of homogenous and composite metallic nanostructures obtained. As a result, the conditions of the formation of sets of nano- and microstructured metallic materials with different topologies, different porosity and high surface area were optimized (Fig.1.). The complexes formed in solutions are investigated by ATR-FTIR and UV–Vis methods, as well as a chemometric approach for describing the results. The synthesized structures were investigated using scanning electron microscopy, energy dispersive X-ray analysis, atomic absorption spectroscopy, X-ray phase analysis, mass-spectrometry of secondary ions, cyclic voltammetry and amperometry.

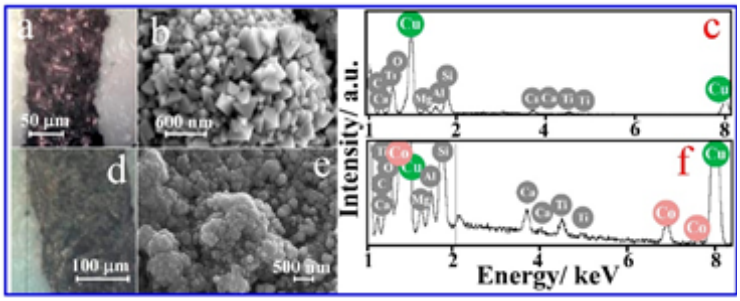

Fig. 1. (a) Optical micrograph, (b) SEM image and (c) EDX spectra of copper structures deposited from solution without additives. (d) Optical micrograph, (e) SEM image and (f) EDX spectra of copper structures deposited from solution containing 0.001 M $CoCl_2$.

All authors acknowledge the Russian Fund for Basic Research (grants 17-03-01266 and 16-03-00436). I.I.T. thanks the Fellowship of President of Russia MK-6153.2018.3.The authors also express their gratitude to the SPbSU Nanotechnology Interdisciplinary Centre, Centre for Optical and Laser Materials Research, Centre for Physical Methods of Surface Investigation, Centre for Geo-Environmental Research and Modelling (GEOMODEL), Centre for X-ray Diffraction Studies and Chemistry Educational Centrer.

[1] M.S. Panov, O.A. Vereshchagina, S.S. Ermakov, I.I. Tumkin, E.M. Khairullina, M.Yu. Skripkin, A.S. Mereshchenko, M.N. Ryazantsev, V.A. Kochemirovsky, Non-enzymatic sensors based on in situ laser-induced synthesis of copper-gold and gold nano-sized microstructures, Talanta. 167, 201–207 (2017).

P6

Influence of ambient gas on microstructure formation on Ni surface by laser-Induced back deposition

Kazuki Koda[1,2], Ryosuke Izumi[1], Hirokazu Imai[1], Masahiro Tsukamoto[3]

[1]Sensor & Semiconductor Packaging R & D Div, DENSO CORPORATION, 1-1 Showa-cho, Kariya, Aichi 448-8661, Japan
[2]Department of Mechanical Engineering, Graduate School of Engineering, Osaka University, 1-1 Yamadaoka, Suita Osaka 565-0871, Japan
[3]Joining and Welding Research Institute, Osaka University, 11-1 Mihogaoka, Ibaraki, Osaka 567-0047, Japan
Corresponding author: kazuki_kouda@denso.co.jp

There are many hybrid structures of polymer and metal in automotive components for lightening or protection of internal components. For cost reduction and downsizing, polymer-metal direct joining method is desired. In addition, for precision products such as devices installed in automotive components, it is also necessary to selectively modify the surface properties. The topography of metal surface is an important factor for adhesion, and it is implied as a possible to selectively fabricate microstructure by back deposition induced by laser plume [1, 2]. Although it has been reported that ambient gas affects shape control of microstructure in addition to laser parameters, sufficient research has not been done. In this report, we investigated the influence of oxygen on the formation of microstructure by changing the oxygen concentration during processing and comparing the microstructure formed at each oxygen concentration. The structures were observed by Scanning Transmission Electron Microscopy (STEM).

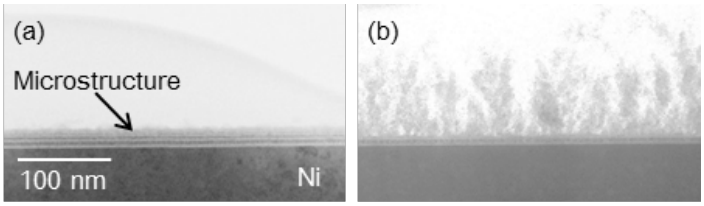

Fig. 1 The cross-section STEM images of microstructure at oxygen concentration of (a) 0.001 % and (b) 21 %.

Fig. 1 shows cross-sectional STEM images on the Ni surface. The wavelength, the pulse duration, the fluence and the number of shots were 1064 nm, 6 ns, 10 J/cm^2, respectively. Fig. 1(a) shows an oxygen concentration of 0.001 % and Fig. 1(b) shows at 21 %. At an oxygen concentration of 21%, a microstructure with large roughness was formed, whereas, at 0.01%, a layered microstructure was formed. Results in this experiment indicated that the oxygen concentration contributes to the morphology of the microstructure.

[1] K.Koda, W. Kobayashi, H. Imai, and M. Tsukamoto, Formation of microstructures on Ni film surface by nanosecond laser irradiation, *Applied Physics A* **124**, 227 (2018).
[2] A. Pereira, P. Delaporte, M. Sentis, A. Cros, W. Marine, A. Basillais, A. L. Thomann, C. Leborgne, N. Semmar, P. Andreazza, and T. Sauvage, *Thin Solid Films* **453**, 16 (2004).

P7

Investigation of optical and electrical properties of Sc-doped ZnO thin films deposited by co-sputtering.

A. Axelevitch[1], M. Shatalov[2]

1. Holon Institute of Technology (HIT), Engineering Faculty, Holon 5810201, Israel
2. Ariel University, Natural Science Faculty, P.O.B. 40700 Ariel, Israel
Corresponding author: alex_a@hit.ac.il

One of the main problems limiting the high-efficient solar cells creation is the well-known Shockley-Queisser restriction. These are various ways which devoted increase the efficiency of the solar cells and circumvent mentioned constraint. One of such ways is the application of up-conversion additional thin-film system attached to the solar cell with the goal to use electromagnetic waves with the large wavelength, not absorbed by the solar cell. For this goal, the large bandgap semiconductors with dissolved ionized rare-earth elements may be applied.

Zinc oxide is a unique material representing a wide bandgap semiconductor of the A_2B_6 group with the direct bandgap of 3.4 eV, transparent in the visual range and conductive enough to substitute indium tin oxide films in various applications as a very promising optoelectronic material. At last time, it was found that ZnO doped by rare-earth elements can be applied as a hosting material in the thin film structures enabling anti-Stokes photoluminescence or up-conversion.

In our work, ZnO thin films doped by scandium were prepared by magnetron co-sputtering from two different targets, zinc oxide and pure scandium. We used various combinations of DC and RF sputtering supplies. Thin films were grown in the atmosphere of pure argon at a low pressure of 3-15 mTorr and at a different temperature, RT to 300^0C. The effects of deposition parameters on the electrical and optical properties of grown thin films were studied. Special attention was paid to photoluminescent properties of prepared samples.

P8

Tailoring diamond's optical properties via direct femtosecond laser nanostructuring

M. Martínez-Calderon[1], J. J. Azkona[1], N. Casquero[1], A. Rodríguez[1], Matthias Domke[2], M. Gómez-Aranzadi[1], S.M. Olaizola[1], and E. Granados[1]

[1]Ceit, Manuel Lardizabal 15, 20018 Donostia / San Sebastián, Spain
[2]Josef Ressel Center for Material Processing with Ultrashort Pulsed Lasers, Vorarlberg University of Applied Sciences, Dornbirn, Austria.
Corresponding author: mmcalderon@ceit.es

We demonstrate a rapid, accurate, and convenient method for tailoring the optical properties of diamond surfaces by employing laser-induced periodic surface structuring (LIPSS) [1]. The characteristics of LIPSS-based fabricated photonic surfaces were adjusted by tuning the laser wavelength, a number of impinging pulses, angle of incidence and polarization state. The irradiation parameters for the generation of high-quality LIPSS were identified for three different harmonics of a Ti:Sapphire laser (λ ~ 800, 400 and 267 nm) and also harmonics from a Ytterbium fiber laser at a λ of ~ 520 nm and ~ 1040 nm. Different scanning strategies were identified for fabricating spatially coherent LIPSS-based nanostructures over large areas maintaining a high degree of nanostructure fidelity and optical performance with both, low and high repetition rate lasers. Figure 1, shows how tuning scanning parameters, such as line spacing, diamond nanostructured surfaces almost absolutely coherent were fabricated. Finally, the potential of these structures for its performance as diamond based anti-reflection coatings was analysed by means of simulations and experimental transmission measurements.

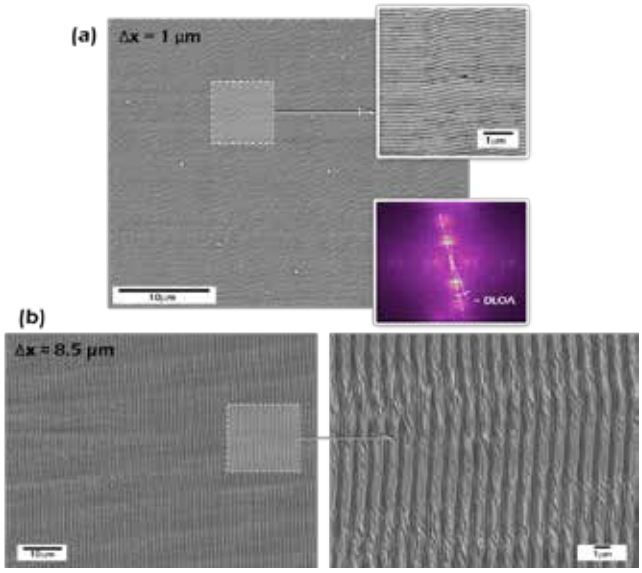

Fig. 1. Example of one of the fabricated surfaces with a LIPSS nanopattern highly coherent and homogeneous with: (a) Ti:Sapphire laser with 1 KHz and (b) Ytterbium fiber laser with 500 KHz.

[1] J. Bonse, S. Höhm, S. V Kirner, A. Rosenfeld, J. Krüger, Laser-Induced Periodic Surface Structures; A Scientific Evergreen, IEEE J. Sel. Top. Quantum Electron. 23 (2017) 1. doi:10.1109/JSTQE.2016.2614183.

P9

Effect of surface roughness on the ultrashort pulsed laser ablation fluence threshold of zinc and steel

H. Mustafa[1], D.T.A. Matthews[1,2], G.R.B.E. Römer[1]

1- Chair of Laser Processing, Department of Mechanics of Solids, Surfaces & Systems (MS³), Faculty of Engineering Technology, University of Twente, P.O. Box 217, 7500 AE, Enschede, the Netherlands

2- Chair of Skin Tribology, Department of Mechanics of Solids, Surfaces & Systems (MS³), University of Twente, P.O. Box 217, 7500 AE, Enschede, the Netherlands

Corresponding author: h.mustafa@utwente.nl

Laser ablation is a subtractive micromachining technique, which can be employed to improve the surface functionality of a product by applying a laser-induced texture to the surface. It is a flexible and precise manufacturing process compared to other techniques like electric discharge texturing, chemical etching, shot blasting and electron beam texturing [1,2]. The absorption of laser light and subsequent heating of the material being machined depends not only on the optical properties of the material but also on its initial surface condition. This means features such as roughness, oxidation or defects etc., of the targeted material, play a major role in the efficiency of material removal and ultimately the resulting quality of the machined surface. For continuous wave (CW) laser processing, a higher surface roughness typically results in better absorption of laser energy through scattering from surface irregularities [3,4,5]. In the case of ultrashort laser pulses, with pulse durations in the picosecond regime, or shorter, the absorption of laser energy (photons) and modification of the material such as ablation take place at different time scales. That is, absorption of photons typically takes place on the femto- to picosecond time scale, whereas modification of material takes place on the nanosecond timescale or longer [6]. To study the effect of surface roughness on the fluence threshold above which ablation occurs in metals in ultrashort pulse regimes, ablation of bulk zinc, galvanized steel and mild steel is performed with single, as well as multiple picosecond laser pulses at wavelengths of 1030 nm and 515 nm and at different preliminary surface roughness (R_a) values ranging from 0.03 µm to 1.5 µm. Using confocal laser scanning microscopy (CLSM) and scanning electron microscopy (SEM), the morphologies and crater dimensions of thousands of ablated craters is studied, by varying the laser fluence over a wide range, as well as varying the number of pulses (*N*) on the same location between *N*=1 and *N*=50. From the analysis, it can be concluded that, within the boundaries of our experimental (laser) conditions, the ablation threshold increases with increasing surface roughness. In addition, the surface roughness of the underlying substrate of a coated material (galvanized steel) also affects the crater morphology and ablation threshold.

[1] D. Zhang and L. Guan, “Laser Ablation” in Comprehensive Materials Processing, S. Hashmi, G. F. Batalha, C. J. van Tyne, B. S. Yilbas, ed. (Elsevier, 2014)

[2] H. Costa and I. Hutchings, “Some innovative surface texturing techniques for tribological purposes,” Proc. Inst. Mech. Eng. Part J: J. Eng. Tribol. 229, 429–448 (2015).

[3] Bergström, David. The absorption of laser light by rough metal surfaces. Diss. Luleå Tekniska Universitet, 2008.

[4] Xie, J., and A. Kar. “Laser welding of thin sheet steel with surface oxidation.” WELDING JOURNAL-NEW YORK- 78 (1999): 343-s.

[5] Auinger, M., et al. “Effect of surface roughness on optical heating of metals.” Journal of the European Optical Society-Rapid publications 9 (2014).

[6] Zhigilei, Leonid V., Zhibin Lin, and Dmitriy S. Ivanov. “Atomistic modeling of short pulse laser ablation of metals: connections between melting, spallation, and phase explosion.” The Journal of Physical Chemistry C 113.27 (2009): 11892-11906.

P10

Effects of the repetition rate on femtosecond laser-induced periodic surface structures on silicon

Jijil JJ Nivas[1,2*], Elaheh Allahyari[1,2], Mohammadhassan Valadan[1], Antonio Vecchione[3],

Rosalba Fittipaldi[3], Riccardo Bruzzese[1,2], Carlo Altucci[1], Salvatore Amoruso[1,2]

[1]Dipartimento di Fisica Ettore Pancini, Università di Napoli Federico II, Complesso Universitario d Monte S. Angelo, Via Cintia, 80126 Napoli, Italy

[2]CNR-SPIN UOS Napoli, Complesso Universitario d Monte S. Angelo, Via Cintia, 80126 Napoli, Italy

[3]CNR-SPIN UOS Salerno, Via Giovanni Paolo II 132, 84084 Fisciano, Italy

Corresponding author: salvatore.amoruso@unina.it, amoruso@fisica.unina.it

Femtosecond (fs) laser-induced periodic surface structures (LIPSS) attract considerable attention due to their intriguing features and increasing importance in various scientific and technological applications [1]. Typically, LIPSS are induced by multipulse laser irradiation either in static or scanning target configuration, at laser repetition rates not larger than 1 kHz. Recently, LIPSS produced in scanning configuration by irradiation at a high repetition rate of several hundred kHz or even MHz have been reported [2-3], addressing a higher regularity of the produced sub-wavelength ripples. However, an experimental investigation with a variable repetition rate in static irradiation configuration is still rather scarce. Here, we report on the effects of the repetition rate on LIPSS formed on a (100) silicon target (intrinsic, > 200 Ωcm) irradiated with 1030 nm fs laser pulses at a repetition rate variable in the range 10 Hz- 200 kHz, in the air. Silicon is selected as a target since it is a case study material with a wide range of applications (e.g., in mechanical, optical and electronic devices) and because various periodic as well as random surface structures forms on it depending on the laser excitation level.

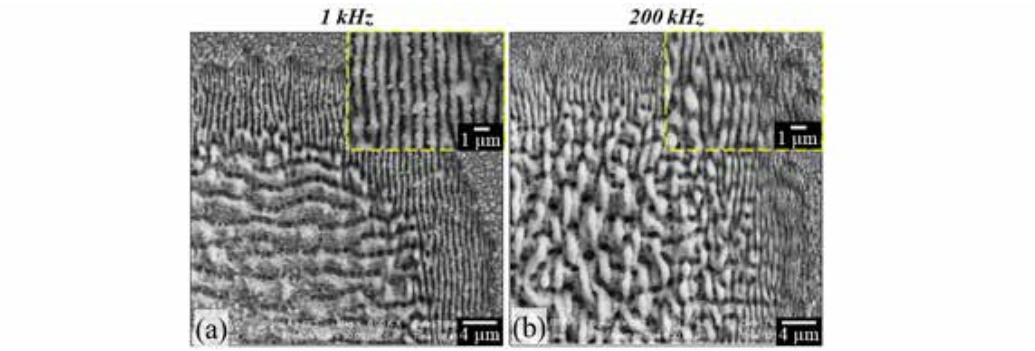

Fig. 1 SEM images of the silicon surface for irradiation with a sequence of *N*=200 laser at an energy of 10 μJ per pules for two different repetition rates: (a) 1 kHz; (b) 200 kHz. The upper-right corners show zoomed view of the subwavelength ripples.

In this communication, we discuss the changes induced by the repetition rate on the features of the surface structures, namely subwavelength ripples and suprawavelength grooves, at a fixed number of pulses *N* delivered at a variable repetition rate.

[1] J. Bonse, S. Höhm, S.V. Kirner, A. Rosenfeld, and J. Krüger, *Laser-Induced Periodic Surface Structures—A Scientific Evergreen*, IEEE J.Sel. Top. Quantum Electron. **23**, 9000615 (2017).

[2] X. Lin, X. Li, Y. Zhang, C. Xie, K. Liu, Q. Zhou, *Periodic structures on germanium induced by high repetition rate femtosecond laser*, Opt. Laser Techn. **101**, 291–297 (2018).

[3] I. Gnilitskyi, T.J.-Y. Derrien, Y. Levy, N.M. Bulgakova, T. Mocek, and L. Orazi, *High-speed manufacturing of highly regular femtosecond laser-induced periodic surface structures: physical origin of regularity*, Sci. Rep. **7**, 8485 (2017)

P11

Control of femtosecond laser-induced periodic surface structures on Ni

Hyun Uk Lim[1], Jeongjin Kang[1], Chunlei Guo[2,3], Taek Yong Hwang[1*]

[1]Molds & Dies R&D Group, Korea Institute of Industrial Technology, Bucheon 14441, South Korea
[2]The Institute of Optics, University of Rochester, New York 14627, USA
[3]The Guo China-US Photonics Laboratory, Changchun Institute of Optics, Fine Mechanics, and Physics, Changchun, China

Corresponding author: taekyong@kitech.re.kr

Various types of low spatial frequency laser-induced periodic surface structures (LSFLs) have been investigated on metals in the past decades by using femtosecond (fs) laser pulse irradiation [1,2]. In general, the formation mechanism of LSFLs on metals has been explained by the interference between the incident laser beam and surface plasmon polaritons (SPPs) [3,4]. According to the interference mechanism, at off-normal incidence, LSFLs can have two structural periods depending on the propagating direction of SPPs, and these periods can be easily changed with the incident beam angle [3,5]. To fully make use of the incident beam angle as a variable to control the period, it is essential to understand how to select one of two possible periods at a certain incident angle.

In this work, by simply adjusting the number of irradiating pulses at a relatively large incident angle of 65°, we observe the period variation of small- to dual- to large-scale period as shown in Fig. 1, where all scales of periods are consistent with the predicted periods by the interference mechanism. Therefore, with this period variation, it is expected that the incident beam angle can be one of the most important parameters to control the period of LSFLs.

This work was supported by the Ministry of Planning and Budget, Korea Institute of Industrial Technology (EO180024).

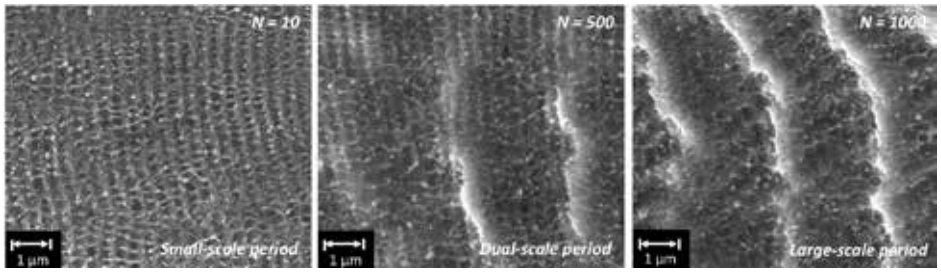

Fig. 1 SEM images of LSFLs with small-, dual-, and large-scale periods.

[1] J. Bonse, S. Höhm, S. Kirner, A. Rosenfeld, J. Krüger, Laser-induced Periodic Surface Structures (LIPSS) - A Scientific Evergreen, Conf. Lasers Electro-Optics. 23, STh1Q.3. (2016).
[2] A.Y. Vorobyev, V.S. Makin, C. Guo, Periodic ordering of random surface nanostructures induced by femtosecond laser pulses on metals, J. Appl. Phys. 101, 34903 (2007).
[3] J.E. Sipe, J.F. Young, J.S. Preston, H.M. van Driel, Laser-induced periodic surface structure. I. Theory, Phys. Rev. B. 27, 1141 (1983).
[4] A.M. Bonch-Bruevich, Surface electromagnetic waves in optics, Opt. Eng. 31 (1992) 718. doi:10.1117/12.56133.
[5] T.Y. Hwang, C. Guo, Angular Effects of Nanostructure-Covered Femtosecond Laser Induced Periodic Surface Structures on Metals, J. Appl. Phys. 108, 73523 (2010).

P12

Investigation of large-area femtosecond laser-induced periodic surface nanostructuring of metals

Marek Stehlík[1,2*], Juraj Sládek[1,2], Mindaugas Gedvilas[3], Inam Mirza[1], Nadezhda Bulgakova[1], Gediminas Račiukaitis[3]

[1]HiLASE Centre, Institute of Physics of the Czech Academy of Sciences, Za Radnicí 828, 25241 Dolní Břežany, Czech Republic
FNSPE, Czech Technical University in Prague, Břehová 7, 115 19 Prague 1, Czech Republic
[3]Center for Physical Sciences and Technology, Savanoriu Ave. 231, LT-02300 Vilnius, Lithuania
Corresponding author: stehlikm@fzu.cz

Nanostructuring of surfaces is of great scientific interest due to enabling surface functionalization and controlling their properties. Ultrashort laser processing is an attractive method for surface nanostructuring because of the simple, one-step irradiation process. The laser-induced periodic surface structures (LIPSS) show a clear correlation with incident laser light properties (polarization, pulse duration and wavelength) [1]. For many scientific and industrial application, it is desirable to have regular LIPSS over a large area with nm-scale periodicity. In recent years, few studies have been performed to produce regular LIPSS on high-quality metallic surfaces using laser scanning methods [2, 3]. The phenomenon of LIPSS regularity has been addressed in terms of coherent excitation of material due to scanning direction parallel to LIPSS and the decay length of the excited surface electromagnetic wave [2, 3]. In this work, we will present results on large-area LIPSS fabrication on Ti and Mo surfaces of different initial roughness by IR fs-laser pulses (1030 nm, 290 fs). A systematic study was performed first using single-to-multi laser shots at a fixed place, where LIPSS are formed due to local excitation of material. Then we studied the evolution of the LIPSS morphology by scanning the sample under focused, linearly polarized laser light with different overlaps between the focal spots (typical images are shown in Fig. 1). The evolution, morphology, bifurcation, and effects of surface roughness in large-area LIPSS fabrication will be discussed.

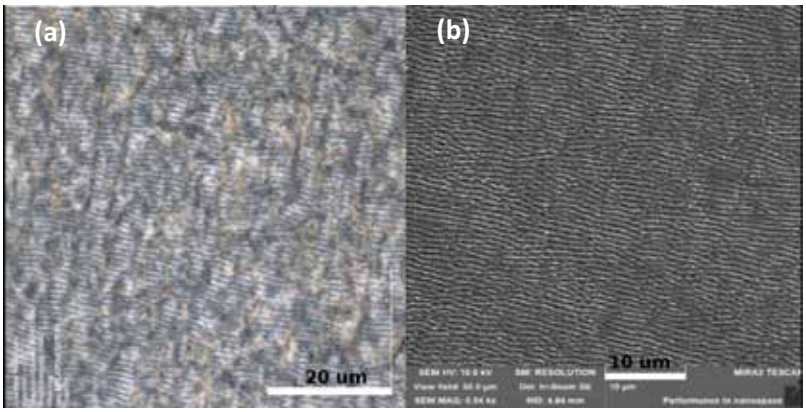

Fig. 1 LIPSS on (a) Mo and (b) Ti fabricated using IR femtosecond laser at peak fluence of 0.84 and 0.63 J cm^{-2} by scanning a linearly polarized laser over the sample surface at an overlap of 90 and 75% between the focal spots, respectively.

[1] J. Bonse, S. Höhm, S. V. Kirner, A. Rosenfeld, J. Krüger, Laser-Induced Periodic Surface Structures – A scientific evergreen. *IEEE J. Sel. Topics Quantum Electron.* **23**, 900615 (2017).
[2] I. Gnilitskyi, T.J.-Y. Derrien, Y. Levy, N.M. Bulgakova, T. Mocek, L. Oeazi, High-speed manufacturing of highly regular femtosecond laser-induced periodic surface structures: Physical origin of regularity. *Sci.Rep.* **7**, 8485 (2017).
[3] A. Ruiz de la Cruz, R. Lahoz, J. Siegel, G. F. de la Fuente, J. Solis, High speed inscription of uniform, large-area laser-induced periodic surface structures in Cr films using a high repetition rate fs laser. *Opt. Lett.* **39**, 2491-2494 (2014).

P13

ULTRASHORT LASER NON-GAUSSIAN PULSE INDUCED TEMPERATURE FIELD DYNAMICS

Alexander Fedotov, Yaraslau Okrut, Yana Tsitavets

Belarusian State University, Physics Faculty, Nezalezhnasci Ave. 4, BY-220030 Minsk, Belarus
Corresponding author: fedotov.alehandro@gmail.com

The heat transfer simulations are one of the most useful tools for the study of transient heat conduction in laser-matter interaction problems. In the present work, we describe the propagation of heat field caused by pulses with different spatial shapes: Gaussian and tubular.

We show that heat energy deposited by a single tubular pulse in gold (Au) with pulse length τ_p=100 fs, beam radius *R*=10 μm does not spread inside the volume under the center of axial symmetry of the pulse for a time comparable to $10\tau_p$ (Fig,1). Temperature under symmetry center of incident pulse changes slightly, but it was established that collapsing region exists at depth $2 \cdot 10^1$ nm below the surface. Such a feature of temperature field propagation is of interest for the studies of nanostructured surfaces and advanced probe application.

Simulations were performed by means of custom finite-differences code and finite-element software COMSOL Multiphysics. It was established that COMSOL allows quick calculations in terms of a two-temperature model showing divergence approximately 4 % in comparison to Crank-Nicolson finite difference scheme in a moment of maximum electronic subsystem temperature. The same accuracy as in COMSOL can be achieved with Dufort-Frankel finite differences scheme with three times acceleration.

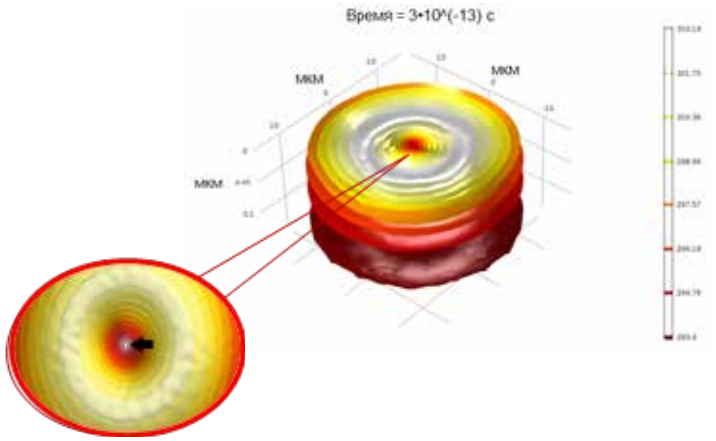

Fig. 1 – Isothermal surfaces (ring shape) at the time 300 fs

[1] E. Stankevicius, M. Garliauskas, M. Gedvilas, N. Tarasenko, and G. Raciukaitis Structuring of Surfaces with Gold Nanoparticles by Using Bessel-Like Beams Ann. Phys. (Berlin), 1700174 1-5 (2017)

[2] V.P. Zhukov, A. M. Rubenchik, M. P. Fedoruk, and N. M. Bulgakova Interaction of doughnut-shaped laser pulses with glasses *Journal of the Optical Society of America* B Vol. 34, 020463-09 (2017)

P14

Electron-Phonon Coupling after ultrashort laser-excitation in gold

Sebastian T. Weber*, Baerbel Rethfeld

Department of Physics and Research Center OPTIMAS, Technische Universitaet Kaiserslautern, Germany
Corresponding author: weber@physik .uni-kl.de

Laser-driven material processing is one of the most important topics in today's manufacturing. The most crucial points are the timescale and strength of energydeposition in the different subsystems of the material. For ultrashort laser-excitation, the electronic system is driven out of thermal equilibrium. Electron-Electron interactions thermalize the electrons again towards a Fermi-distribution at an elevated. Additionally, energy is transferred to the cold phonons. The electron-phonon coupling parameter is often referred to as "coupling-constant". However, it depends not only on the excitation strength, but also on the nonequilibrium state of the system.

We trace the time-dependent electron and phonon nonequilibrium dynamics, using full Boltzmann-type collision integrals. Our approach allows us to extract electron-phonon coupling parameters in dependence on the different time-dependent nonequilibrium states during and after laser-matter interaction. We show results for gold comparing equilibrium and nonequilibrium electron-phonon coupling parameters and their influence on the relaxation processes.

P15

The resolution study of the 3D printer EOSINT M280 for iron-based powders

Ada Steponavičiūtė, Ruslan Travkin, Gediminas Račiukaitis and Genrik Mordas

Center for Physical Sciences and Technology, Savanoriu Ave. 231, LT-02300 Vilnius, Lithuania
Corresponding author: genrik.mordas@ftmc.lt

The EOSINT M280 is based on the innovative DMLS (Direct Metal Laser Sintering) technology. The applied DMLS has a 200 W 1030 nm built-in Yb fibre laser and a high-speed (7 m/s) scanner comprising precision galvanometer (11 µrad) with temperature compensation. The F-theta objective focuses a laser beam at a building area in 100 µm. That allows sintering the metal particles (from 10 to 80 µm in size) at a layer thickness of 20 - 40 µm in inert (nitrogen or argon) environment. So, ultra-fine layers of metal powders are selectively sintering together and with the previously formed layer. As a result, there are produced metal parts, which properties are determined on the DMLS process parameters (laser energy, laser scanning speed) and powder characteristics (particles size, melting temperature and thermal diffusion coefficient) [1]. Thus, it is possible to fix DMPS parameters for commercial EOS powder and to use them for other same-base powders. However, the resolution limits should be different. The aim of our study was to determine the EOSINT M280 limits using commercial EOS and LPW iron-based powders.

We selected two iron-based powders (EOS 316L and LPW GP1). They are characterised by different chemical composition (62.1 and 73.8% of iron resp.) and different particles size distribution (20-120 µm and 10-80 µm resp.). Using both powders, we produced duplicate parts (Fig. 1a), which had holes, columns and building angles of different sizes. The microstructure study of the produced parts was performed using SEM (Fig. 1b). It allowed determining the EOSINT M280 limits for commercial EOS and LPW powders and showing application possibilities of both powders.

a)

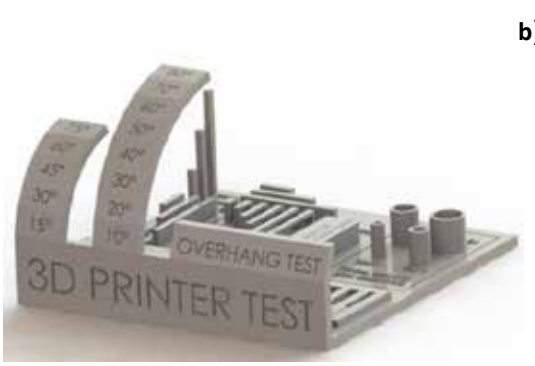

b)

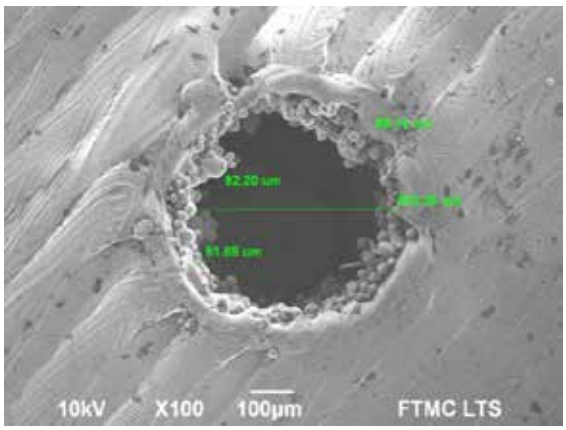

Fig. 1 (a) CAD model for 3D testing part [2] and (b) SEM image of 500 um hole.

[1] M.D.Viramgama, M.C.Karia. Study and investigation of influence of process parameters for selective laser melting. *IJEDR* 4(1), pp. 578-585 (2016).
[2] https://www.thingiverse.com/thing:2656594

P16

Design of fs-laser writable borate glasses for photonic devices

A. Dias[1], F. Muñoz[2], A. Álvarez[1], P. Moreno[3], J. Atiénzar[1], A. Urbieta[4], P. Fernandez[4], M. García[1], R. Serna[1], J. Siegel[1], J. Solis[1*]

[1] Laser Processing Group, Institute of Optics (IO, CSIC), Serrano 121, 28006 Madrid, Spain)
[2] Ceramics and Glass Institute (ICV, CSIC), Kelsen 5, 28049 Madrid, Spain
[3] Engineering School, Tepexi Higher Technological Institute, Av. Tecnológico S/N, 74690, Tepexi de Rodríguez, Mexico
[4] Department of Materials Physics, Faculty of Physics, University Complutense of Madrid, Madrid 28040, Spain

Corresponding author: j.solis@io.cfmac.csic.es

It has recently been shown that fs-laser induced ion-migration effects can be used for producing extremely efficient photonics devices, like waveguides [1], optical amplifiers, and lasers [2]. A comprehensive review on fs-laser induced ion-migration phenomena in commercial glasses is given in Ref.[3]. Previous works [1], have shown that specific modifiers of the glass network generate positive refractive index contrast waveguides (Δn>0) by fs-laser induced ion-migration. Δn values > 10^{-2} can be easily achieved by this mechanism. Still, the design and performance of samples specifically designed for efficient fs-laser writing via compositional changes have not been so far reported.

In this work, borate glass samples were ad-hoc modified by adding different concentrations of La_2O_3 and Na_2O. The performance of these samples for photonic devices was analyzed in the two samples (~28.4Na_2O-3.2La_2O_3-68.0B_2O_3 mol.% and ~22.8-Na_2O-5.5La_2O_3-71.4B_2O_3 mol.%) [4]. Waveguides were laser-written by using 350 fs-laser pulses, at 500 kHz rep rate in conditions similar to those in Ref.2. EDX analysis of the structures reveals La-enrichment and Na-depletion in the guiding region. The refractive index contrast of the waveguides was estimated through numerical aperture measurements providing values consistent with the EDX-determined local La-enrichment in the guiding region, and a linear dependence of n with the La content. An index contrast of 10^{-2} was achieved in a glass sample with just 5.5 mol% of La_2O_3. It is worth noting that the maximum achievable Δn values increase with the initial La concentration in the sample, enabling further optimization of the material response.

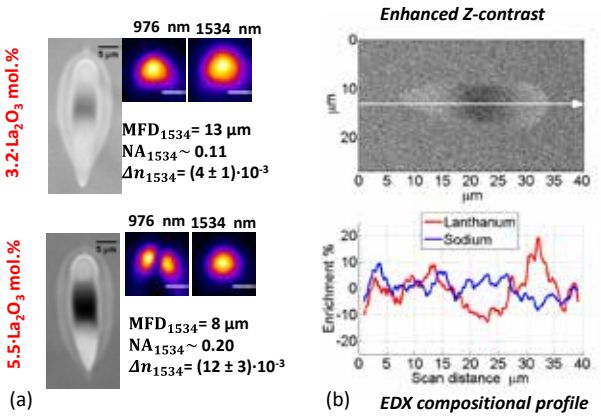

Fig. 1 (a) Optical images of the cross-section of waveguides written into samples with different La concentration under the same irradiation conditions and the propagated modes at 976 and 1534 nm (scale bars are 5 µm long). (b) SEM micrograph and EDX-compositional profile of the waveguide produced in the 5.5 La_2O_3 mol.% borate glass sample.

[1] T. Toney Fernandez, et al.; Opt. Lett. 38 (2013) 5248–51 and J. Del Hoyo, et al.; Appl. Phys. Lett. 105 (2014) 131101
[2] J. del Hoyo, et al.; J. Light. Technol. 35 (2017) 2955–2959.
[3] T.T. Fernandez, et al.; Prog. Mater. Sci. 94 (2018) 68–113.
[4] A. Días, et al.; Opt.Lett. (in press)

P17

Selective surface modification on PEDOT:PSS films for planar heater fabrication using short and long laser wavelengths

Wen-Tse Hsiao[1*], Yu-Chen Hsieh[1], Ching-Ching Yang[1], Yi-Cheng Lin[1], Ming-Wei Hung[1], Donyau Chiang[1], Kuo-Cheng Huang[1], Shih-Feng Tseng[2], Tien-Li Chang[3], Keh-Moh Lin[4]

[1]Instrument Technology Research Center, National Applied Research Laboratories, Hsinchu 300, Taiwan
[2]Department of Mechanical Engineering, National Taipei University of Technology, Taipei 106, Taiwan
[3]Department of Mechatronics Engineering, National Taiwan Normal University, Taipei 106, Taiwan
[4]Department of Mechanical Engineering, Southern Taiwan University of Science and Technology, Tainan 710, Taiwan
Corresponding author: wentse@narlabs.org.tw

Recently, due to the transparent conductive oxide and its compound films (i.e. ITO, graphene, PEDOT:PSS, and AgNW) has excellent properties, such as optical transmittance, electrical conductivity, and flexibility properties; therefore, there are now widely used to fabricate the electronic devices, including electrodes, sensors, and heaters applications [1-3]. Especially, in gas sensor devices with a heating function for environmental pollution monitoring also necessary that can accelerate the detection response time; moreover, they can reduce sensor power consumption and enable the temperature modulation under gas sensing processes. This study investigated the selective surface modification characteristics on PEDOT:PSS films using short and long laser wavelengths that combined with the galvanometric scanning unit with varying parameters, including laser fluence, pulse repetition frequency, and scanning speed (Fig. 1 (a)). The PEDOT:PSS films with a 300 nm thick were deposited on soda-lime glass substrates by wet coating (Fig. 1 (b)) with sheet resistance was approximately 100 Ω/□. To analyze the properties of the modified and non-modified PEDOT:PSS films, the Hall-effect measurement instrument and the four-point probe were used for verification of electronic properties. X-ray diffraction, a field emission scanning electron microscope was used to measure the surface morphologies, crystalline grain size, and surface roughness. Moreover, the infrared thermographer was used to evaluate the planar heater temperature under different driving current (Fig. 1 (c)). From the above results lead to further explore the resistivity, carrier concentration, degree of crystallinity, mobility, energy gap and then verify the interactions between PEDOT:PSS films at short and long laser wavelengths performance.

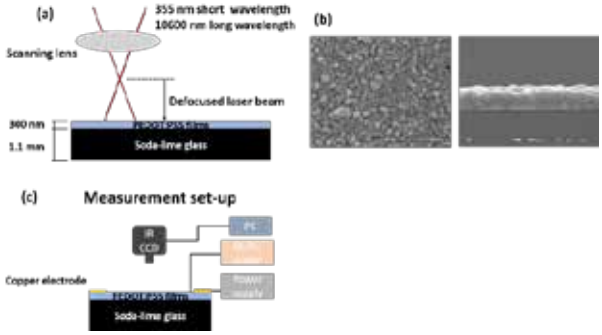

Fig. 1 (a) Experiment set-up for surface modification on PEDOT:PSS films, (b) PEDOT:PSS films morphologies, and (c) planar heater performance characteristics evaluation.

[1] J. Ouyang, "Secondary doping" methods to significantly enhance the conductivity of PEDOT:PSS for its application as a transparent electrode of optoelectronic devices. *Displays* **34**, 423-436 (2013).
[2] S. An, Y.I. Kim, H.S. Jo, M.W. Kim, M.T. Swihart, A.L. Yarin, S.S. Yoon, Oxidation-resistant metallized nanofibers as transparent conducting films and heaters. *Acta Mater.* **143**, 174-180 (2018).
[3] X. Wang, F. Meng, T. Wang, C. Li, H. Tang, Z. Gao, S. Li, F. Jiang, J. Xu, High performance of PEDOT:PSS/SiC-NWs hybrid thermoelectric thin film for energy harvesting. *J. Alloys Compd.* **734**, 121-129 (2018).

P18

A micro sensor fabricated on bipod structure using 355 nm pulsed UV laser for evaluating the deformation by scattering light

Hsin-Yi Tsai, Fang-Chi Su, Chih-Chung Yang, Kuo-Cheng Huang*, Wen-Tse Hsiao
Instrument Technology Research Center, National Applied Research Laboratories, 20, R&D Rd. VI, Hsinchu Science Park, Hsinchu 30076, Taiwan
Corresponding author: huangkc@narlabs.org.tw

Deformation evaluation is critical processing for the optical components supporting bipod structure; especially, the large diameter lens module or reflected mirror [1]. As the bipod structure of gradually deformed, the surface performance of the reflected mirror lens will evidently drop. Conventionally, the strain gauge [2] was used to estimate the deformation of the component, but the adhesive process should be fixed, and the attached force should be controlled to obtain the correct measuring results. Hung et al. [3] attached a strain gauge on the tube wall and analyzed the flow rate according to the resistance and intensity of scattered light of strain gauge when the liquid flow through the sensor. Therein, the small variation of liquid flow could be analyzed from the evident effect of scattered light when the flow of liquid was adjusted slightly.

In the study, we present micro sensor fabricated using 355 nm pulsed UV laser to directly ablate on the bipod structure with a comb pattern and develop a high accuracy and non-contact measuring method to detect the micro-deformation of the structure. The linewidth of the comb pattern ranged from 100 to 500 µm, the scanning rate of the laser was adjusted from 800 to 1200 mm/s, and the power and frequency of laser employed in the experiment were 14 W and 100 kHz, respectively. The experimental process and the results can be divided into three parts; 1) the laser spot was focused on the ablated pattern and relationship between the intensity of scattered light and the exerted force on the bipod structure was build, 2) the pattern position on the bipod structure will evidently deform and the better linewidth of comb pattern which could cause the largest scattered light was determined, 3) the contour of ablated pattern by laser with different parameters and its intensity of scattered light was analyzed to investigate the suitable processing parameter. In the future, the comb pattern would be marked on the bipod structure to monitor the deformation of bipod according to the intensity of scattered light and then evaluating the effect on the surface performance of the reflected mirror of the lens module.

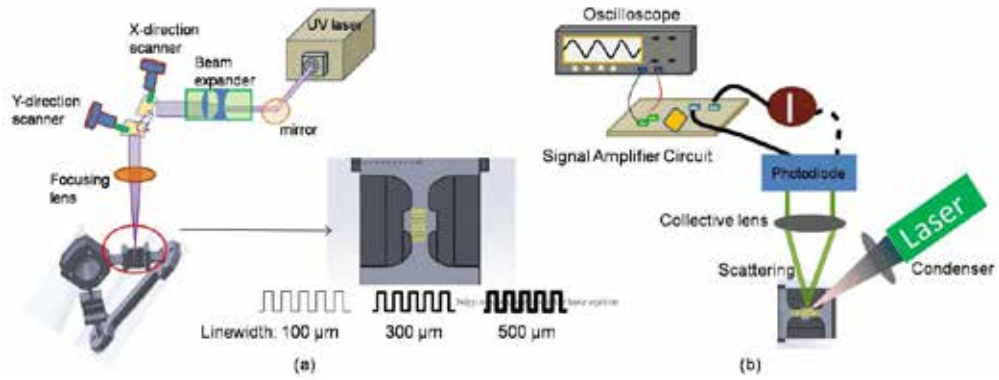

Fig. 1 (a) Schematic of the micro sensor fabricated by UV laser system on bipod structure. (b) The intensity of scattered light from micro sensor the induced by different exerted forces.

[1] C. Y. Chan, Z. T. You, B. K. Huang, Y. C. Chen, T. M. Huang, Analysis investigation of supporting and restraint conditions on the surface deformation of a collimator primary mirror, Proc. SPIE Optomechanical Engineering, 95730V (2015).
[2] P. Lv, K. Yu, X. Tan, R. Zheng, Y. Ni, Z. Wang, C. Liu, Super-elastic graphene/carbon nanotube aerogels and their application as a strain-gauge sensor, RSC Advances, **6**, 11256-11261 (2016).
[3] M. W. Hung, K. C. Huang, Y. H. Lin, H. Yi Tsai, C. C. Yang, Development of plug-in laser scattering module for measurement of flow rate, IEEE Sensors Applications Symposium (SAS), 1-6 (2018).

P19

Laser surface texturing of copper and variation of the wetting response with the laser pulse fluence

Elaheh Allahyari[1,2], Jijil JJ Nivas[1,2], Stefano L. Oscurato[1], Marcella Salvatore[1], Giovanni Ausanio[1,2], Antonio Vecchione[3], Rosalba Fittipaldi[3], Pasqualino Maddalena[1], Riccardo Bruzzese[1,2], Salvatore Amoruso[1,2]

[1]Dipartimento di Fisica Ettore Pancini, Università di Napoli Federico II, Complesso Universitario d Monte S. Angelo, Via Cintia, 80126 Napoli, Italy
[2]CNR-SPIN UOS Napoli, Complesso Universitario d Monte S. Angelo, Via Cintia, 80126 Napoli, Italy
[3]CNR-SPIN UOS Salerno, Via Giovanni Paolo II 132, 84084 Fisciano, Italy

Corresponding author: salvatore.amoruso@unina.it; amoruso@fisica.unina.it

Irradiation of solid surfaces with ultrashort laser pulses offers a flexible, robust and direct technique to alter various materials properties, as, e.g. enhanced optical absorption and improved wetting, and fabricate multifunctional surfaces [1-2]. In many cases, the final functional properties are achieved by further chemical treatments of the laser structured surfaces. The functional properties depend on the kind of structures formed on the surface as well as on their features at the nano- and micro-scale and often involve a hierarchical organization of the textured surface. Here we report on structures produced on the surface of a copper target by single step femtosecond laser processing in the air, addressing the final wetting response of the sample to water droplets. In particular, micro-trenches with a period of 50 mm were formed on the copper surface at different laser pulse energy and the morphological features of the samples were addressed by AFM and SEM analyses.

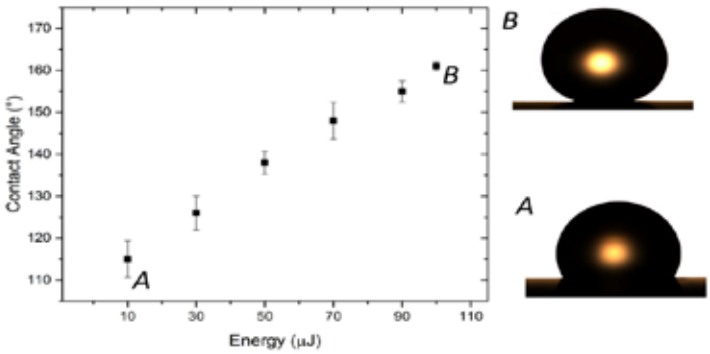

Fig. 1 Variation of the contact angle with the laser pulse fluence. The two insets on the right show images of the water droplets for case A and B as indicated.

Ripples and nanostructures are present both within the micro-trenches and on the surface. The surface morphology of the samples is characterized by a hierarchical organization of periodic trenches, ripples and nanostructures. Their wetting properties are analysed and correlated with their surface texture, addressing an important effect of the laser energy which progressively enhances the sample superhydrophobicity, as shown in Fig. 1, through a progressive change of the surface texture.

[1] F.A. Müller, C. Kunz and S. Gräf, *Bio-Inspired Functional Surfaces Based on Laser-Induced Periodic Surface Structures*, Materials **9**, 476 (2016).
[2] A.Y. Vorobyev and C. Guo, *Multifunctional surfaces produced by femtosecond laser pulses*, J. Appl. Phys. **117**, 033103 (2015).

P20

Optimization of P3 Laser Process in CIGS Thin-Film Solar Cells

Edgaras Markauskas*, Paulius Gečys

Center for Physical Sciences and Technology, Savanoriu Ave. 231, LT-02300 Vilnius, Lithuania
Corresponding author: edgaras.markauskas@ftmc.lt

CIGS technology demonstrates high power conversion efficiency and can compete with silicon-based solar cells in the case of small-scale devices [1]. However, full-scale devices still fall behind the record efficiencies of the minicells [2]. This is primarily due to the CIGS film nonuniformities and dead areas caused by serial interconnects. A laser is a promising tool to realise large area thin-film scribing. However, non-optimized laser processes can cause additional efficiency losses due to the laser-induced shunts during the scribing processes. Laser-induced thermal damage can lead to the absorber composition changes and severe shirt circuiting of the cells. Isolation scribes become the most challenging one since it must ensure high electrical isolation of the neighbouring cells for a highly efficient device.

P3 laser scribing experiments were realised in a CIGS thin-film cells. Direct and front-contact lift-off layer ablation techniques were used to perform P3 isolation scribe. A wide range of parameters was investigated involving pico-, nanosecond laser pulses, and five radiation wavelengths (355 nm, 532 nm, 1064 nm, 1342 nm, and 2.5 µm). High-speed scribing of up to 25 m/s was investigated.

The quality of the scribes was evaluated with a scanning electron microscope and the electrical measurements of the cells. Based on the experimental results mini-module efficiency simulations were conducted. Additionally, simulations of laser-induced temperature distributions in CIGS solar cell structure were performed.

According to our experiments, the top-contact lift-off process resulted in lowest P3 scribe conductivity, and the simulations showed the highest mini-module efficiencies.

[1] E. Markauskas, P. Gečys, A. Žemaitis, M. Gedvilas, G. Račiukaitis, Validation of Monolithic Interconnection Conductivity in Laser Scribed CIGS Thin-Film Solar Cells, *Solar Energy* **120**, pp. 35-43, (2015).

[2] S. Dongaonkar, M.A. Alam, In-Line Post-Process Scribing for Reducing Cell to Module Efficiency Gap in Monolithic Thin-Film Photovoltaics, *{IEEE} J. Photovolt.* **4**, pp. 324-332, (2014).

P21

New laser-assisted method for copper circuit fabrication on dielectrics

Karolis Ratautas*, Aldona Jagminienė, Ina Stankevičienė, Eugenijus Norkus, Gediminas Račiukaitis

Center for Physical Sciences and Technology, Savanoriu Ave. 231, LT-02300 Vilnius, Lithuania
Corresponding author: karolis.ratautas@ftmc.lt

New technology for circuit traces production: Selective Surface Activation Induced by Laser (SSAIL) enables to fabricate a fine metallic structure on dielectric materials – polymers and glass. SSAIL contains three main steps: The first step is surface modification by laser, second – chemical activation of modified areas and the last step is metal deposition by electroless plating. Both picosecond and nanosecond lasers were used for writing. The method has been investigated in detail for a wide window of laser processing parameters. XPS spectroscopy and scanning electron microscope images were used to analyse the activation step. The technology has been upscaled for fast laser writing process (up to 4 m/s). Therefore, spatial plating pitch is kept narrow.

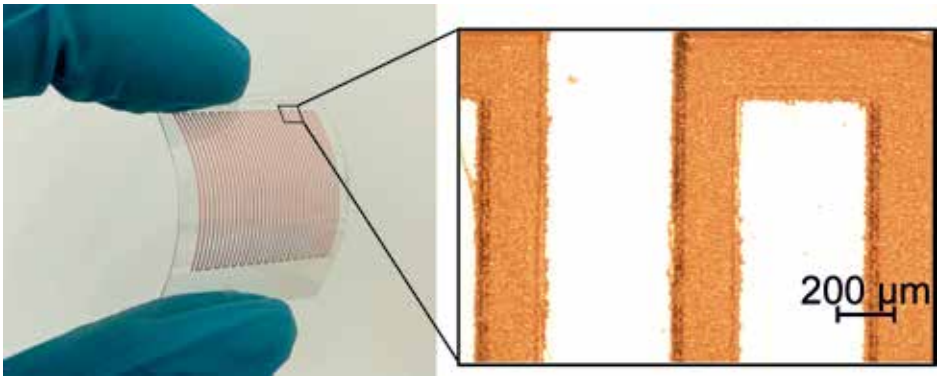

Fig. 1 (a) Circuit traces on flexible PET polymer produced using SSAIL technology

State of the art LDS [1,2] technology uses additives in polymers matrix, which increases the polymer price at least three times compared with raw material. SSAIL use standard polymers, and no special additives are necessary to the process. Therefore this new technique can reduce the production cost of circuit traces for moulded interconnect devices, electronics on the glass, or even flexible electronics as shown in Fig. 1.

[1] J. K. M. Huske, J. Mller, G. Esser, Laser Supported Activation and Additive Metallization of Thermoplastics for 3D-MIDs, *Proc. of LANE 2011*, (2001).

[2] K. Ratautas, M. Gedvilas, I. Stankevičiene, A. Jagminienė, E. Norkus, N. L. Pira, S. Sinopoli, G.Račiukaitis, Laser-Induced Selective Metallization of Polypropylene Doped with Multiwall Carbon Nanotubes, *Appl. Surf. Sci.*, **412**, 319–326 (2017).

P22

Delamination of GaN coating from sapphire substrate using femtosecond laser lift-off technique

Domas Paipulas, Simas Butkus, Valdas Sirutkaitis

[2]Vilnius University, Faculty of Physics, Laser Research Center, Sauletekio Ave. 10, Vilnius, Lithuania
Corresponding author: domas.paipulas@ff.vu.lt

Gallium nitrate (GaN) is direct band gap semiconductor material extensively used in electrooptics applications. Bulk GaN substrates are rarely used for widespread applications due to extensive cost, however thin functionalized GaN coatings can be epitaxially grown on dissimilar substrates such as sapphire. A presence of a rigid substrate with high refractive index hampers GaN device efficiency and flexibility, therefore in many application, it is necessary to disattach GaN coating. One of the most promising separation technique is Laser Lift Off (LLO) pioneered by Wong [1] and Kelly [2]. Method relays on different band gaps between substrate and GaN which allows direct UV light absorption at the intersection and subsequent thermal decomposition of the bonding layer. As method relays on the localized increase of intersection temperature, nanosecond UV lasers (excimers) are the primary choices as light sources. In contrast, ultrafast lasers were never applied for this task. Due to short pulse duration, thermal diffusion length in the absorbing material becomes limited which minimizes heat effected zone (HEZ). This could expand flexibility in control of thermal decomposition of the bonding layer and sufficiently improve coating quality.

In this work, we present a feasibility study of the LLO method on GaN coatings using ultrafast UV laser pulses. A parametrical analysis consisting of laser exposure, focusing conditions and patterning algorithm influence on LLO quality will be presented. We demonstrate that using femtosecond lasers, it is possible to achieve sufficient thermal decomposition of GaN interface and successfully delaminate the coating (Fig.1). Moreover, a different delamination regime could be attained with fs pulses, where separation is realized using stress-induced peeling without thermal decomposition. Later case could meet industry demands as delamination process speed reach up to 0.5 cm^2/s with the sufficiently simple optical setup. We demonstrate that this technique can be realized for thin (up to 3 µm) or thick (>20 µm) GaN coatings.

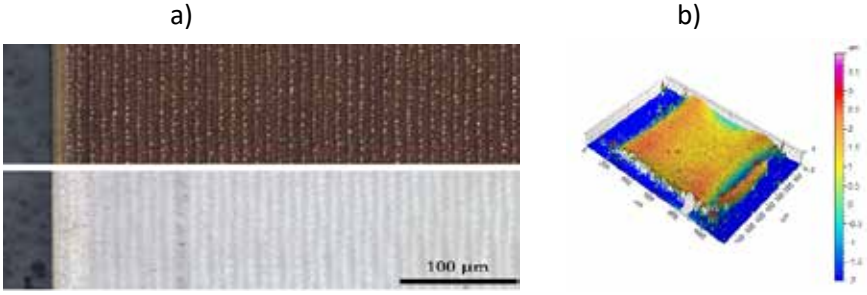

Fig. 1 (a) Delaminated 4 µm thickness GaN coating using two regimes: top – GaN thermal decomposition, bottom – stress induced peeling; b) topography of delaminated free–standing 3 µm GaN coating.

This research was supported by the Research Council of Lithuania under grant agreement LAT 01/2016.

[1] W. S. Wong, T. Sands, and N. W. Cheung, Damage-free separation of GaN thin films from sapphire substrates, Appl. Phys. Lett. **72**, 599 (1998)

[2] M. K. Kelly, R. P. Vaudo, V. M. Phanse, L. Gorgens, O. Ambacher, and M. Stutzmann, Large Free-Standing GaN Substrates by Hydride Vapor Phase Epitaxy and Laser-Induced Liftoff, Jpn. J. Appl. Phys. **38**, L217 (1999)

P23

Graphene formation in wood by 1064 nm laser irradiation

Romualdas Trusovas, Karolis Ratautas, Gediminas Račiukaitis, Gediminas Niaura
Center for Physical Sciences and Technology, Savanoriu Ave. 231, LT-02300 Vilnius, Lithuania

Corresponding author: romualdas.trusovas@ftmc.lt

The laser is a proven valuable tool for modification and formation of graphene [1]. Recently, the laser-induced formation of graphene in commercial polymers and different types of wood was discovered by utilizing CO_2 infrared laser [2,3]. Production of graphene from renewable resources can be helpful for electronics applications. We present experimental results of laser-induced formation of graphene structures in pinewood. Experiments were conducted using nanosecond and picosecond lasers with a pulse duration of 10 ns and 10 ps, respectively, at the irradiation wavelength of 1064 nm and 100 kHz pulse repetition rate in the hermetic chamber with a nitrogen atmosphere. Raman spectroscopy measurements showed the formation of high-quality few-layer graphene structures with I(2D)/I(G) ratio of 1.10 obtained at an irradiation dose of 662 J/cm^2 utilizing nanosecond laser pulses (Fig. 1).

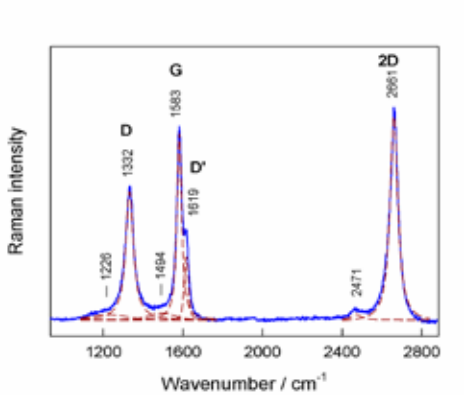

Fig. 1 Raman spectrum of the pinewood surface treated by a nanosecond 1064 nm laser at the irradiation dose of 662 J/cm^2 with the fitted Lorentzian-Gaussian form components.

Sheet resistance measurements showed a correlation with Raman spectroscopy data and revealed a significant decrease in electric resistance for the sample with highest I(2D)/I(G) Raman bands ratio using nanosecond laser irradiation.

Acknowledgements

This research is funded by the Lithuanian Research Council via measure "Towards Future Technologies", Project No. LAT 11/2016.

[1] R. Trusovas, G. Raciukaitis, G. Niaura, J. Barkauskas, G. Valusis, R. Pauliukaite, Recent advances in laser utilization in the chemical modification of graphene oxide and its applications, *Adv. Optical Mater*. **4** 37–65 (2016)

[2] J. Lin, Z. Peng, Y. Liu, F. Ruiz-Zepeda, R. Ye, E.L.G. Samuel, et al., Laser-induced porous graphene films from commercial polymers, *Nat. Commun*. **5** 5714 (2014).

[3] R. Ye, Y. Chyan, J. Zhang, Y. Li, X. Han, C. Kittrell, et al., Laser-induced graphene formation on wood, *Adv. Mater.* 1702211 (2017).

P24

Dynamic Optical Properties of Graphene Layers with Different Preparation and Morphology

Erika Rajackaitė[1], Domantas Peckus[1], Asta Tamulevičienė[1,2], Tomas Tamulevičius[1,2], Rimas Gudaitis[1], Šarūnas Meškinis[1], Sigitas Tamulevičius[1,2]

[1]Kaunas University of Technology, Institute of Materials Science, K. Baršausko Str. 59, LT-51423 Kaunas, Lithuania

[2]Kaunas University of Technology, Department of Physics, Studentų Str. 50, LT-51368 Kaunas, Lithuania

Corresponding author: erika.rajackaite@ktu.edu

Graphene is coming on strong for widespread applications such as photovoltaic devices, field-effect transistors, supercapacitors, sensors due to its unique properties as well as atomically thin, transparent, and flexible structure, ultrafast carrier dynamics, wavelength-independent absorption, tunable optical properties via electrostatic doping, low dissipation rates and high mobility [1, 2].

In the current research, graphene films were formed on single and double copper foils (catalyst) as well as directly on quartz using microwave plasma enhanced chemical vapor deposition technique (IPLAS, Germany). In the sequel, the transfer of synthesized in vacuum graphene layers on different substrates (quartz, amorphous glass, SiO_2/Si) was performed via etching copper foil in different etchants at room temperature.

Employed Raman scattering spectroscopy (532 nm, inVia, Renishaw, UK) results confirmed that the graphene films of one and more layers were successfully transferred. Atomic force microscope (NanoWizard, Germany) analysis revealed the changes of graphene films morphology and uniformity depending on the preparation method. The electrooptical properties of graphene mono and several layers deposited on quartz or transferred was compared.

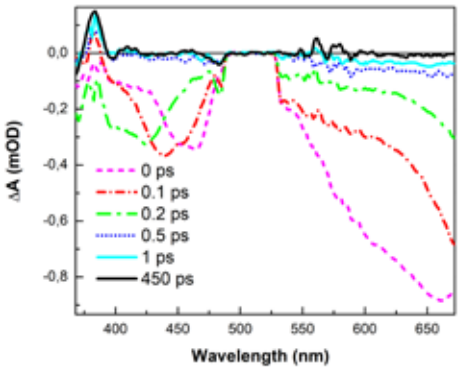

Fig. 1 TAS spectra of graphene on quartz.

Ultrafast excited state relaxation dynamics in graphene formed directly on quartz (Fig. 1) or transferred was investigated by means of transient absorption spectroscopy (TAS). The samples were excited using a Pharos ultrafast Yb:KGW laser (Light Conversion) with a regenerative amplifier at a 66.7 kHz repetition rate and 290 fs duration pulses at 1030 nm wavelength. The pump beam wavelength was tuned with an Orpheus collinear optical parametric generator and harmonic generator Lyra to 350 nm and an energy density of 20.8 μJ/cm^2. The samples were probed with a white light supercontinuum generated using a 2 mm thickness sapphire plate excited with the fundamental laser wavelength (1030 nm). The detailed analysis and comparison of morphological and electrooptical properties of graphene layers dependence on preparation method were done.

[1] M. Li, D. Liu, D. Wei et al., Controllable Synthesis of Graphene by Plasma-Enhanced Chemical Vapor Deposition and Its Related Applications, *Adv. Sci.* **3**, 1600003 (2016).

[2] K. J. Tielrooij, L. Piatkowski, M. Massicotte et al., Generation of photovoltage in graphene on a femtosecond timescale through efficient carrier heating, *Nature Nanotech.* **10**, 437-443 (2015).

P25

Analysis of ultrafast optical properties and morphology of diamond-like carbon nanocomposites with aluminum nanoparticles

Domantas Peckus, Andrius Vasiliauskas, Tomas Tamulevičius, Mindaugas Andrulevičius, Šarūnas Meškinis, Sigitas Tamulevičius

Institute of Materials Science, Kaunas University of Technology, K. Baršausko St. 59, LT-51423, Kaunas, Lithuania
Corresponding author: domantas.peckus@ktu.lt

Recently, the study of the electronic and optical properties of metallic nanoparticles became one of the most active areas of nanoscience and technology [1]. In this research, more complex materials of amorphous diamond-like carbon thin films containing Al nanoparticles (DLC:Al) were analysed. Each of these two materials individually shows unique properties. DLC is well known for its mechanical properties, chemical inertness and optical transparency [2]. The unique optical properties of Al nanoparticles attract attention because of their plasmonic effects in UV region - localized surface plasmon resonance (LSPR) - in other words, the collective oscillations of electrons in the conduction band. The plasmonics in UV region is of great interest in numerous applications; for example, most organic molecules have a strong absorption in the ultraviolet, allowing for ultrasensitive chemical sensing, UV light can be used for photocatalysis and it is as well efficient in breaking organic bonds, which could be used for sterilization processes [1].

DLC films with different Al content were synthesized employing unbalanced reactive magnetron sputtering of Al target with argon ions and using acetylene as a reactive gas. Direct current (DC) magnetron sputtering was applied [2]. The size of nanoparticles and chemical composition of the films were determined by employing Raman, XRD, XPS, SEM-EDS and AFM. Optical properties were analyzed with UV-VIS-NIR steady-state absorption spectrometer while ultrafast processes - employing transient absorption spectrometer (HARPIA, Light Conversion Ltd.).

Several different samples of DLC:Al nanocomposites with different Al content were deposited and their electro-optical properties were investigated by the methods mentioned above. The structure analysis revealed that Al_2O_3 has a large share in DLC:Al nanocomposites. In order to decrease oxidation of Al nanoparticles additional layer of DLC deposition on top of DLC:Al was suggested, and its influence was explored in detail.

This research is funded by the European Social Fund under the No 09.3.3-LMT-K-712 “Development of Competences of Scientists, other Researchers and Students through Practical Research Activities” measure.

[1] M. J. McClain, A. E. Schlather, E. Ringe, Aluminum Nanocrystals. Nano Lett. **15**, 2751-2755 (2015).
[2] D. Peckus, T. Tamulevičius, Š. Meškinis, Linear and nonlinear absorption properties of diamond-like carbon doped with Cu nanoparticles. Plasmonics **12**, 47-58 (2017).

P26

Formation of laser-induced periodical surface structures on multilayer graphene with femtosecond pulses

O. Fedotova[1,2], O. Khasanov[1], T Smirnova[2], A. G. Kovačević[3], A.S. Fedotov[2], Ya. Okrut[2] and G. Rusetsky[1]

[1] Scientific-Practical Material Research Centre, NAS of Belarus, Brovki 19, Minsk 220072, Belarus
[2] Belarusian State University, Nezalezhnasci Ave. 4, Minsk 220030 Belarus
[3]Institute of Physics, University of Belgrade, Pregrevica 118, Belgrade 11080, Serbia

Corresponding author: smirnova@iseu.by

Graphene, both single-layer and multi-layer, is known as a unique novel material with outstanding electronic, optical and mechanical features with high potential for fundamental studies and numerous applications. Its ability to controllably form patterns is very important for flexible electronics and energy devices. Due to this property as well as high transparency it is a desirable material for the formation of laser-induced periodic surface structures (LIPSS) by femtosecond laser beams [1].

In this work, we study the formation of LIPSS on multilayer graphene samples (from 3 to 15 layers) generated by the action of femtosecond laser with 840 nm excitation wavelength, 150 fs pulse duration, 76 MHz repetition rate and 4.3-4.4 mJ/cm^2 fluence, presented in work [1]. The orientation of LIPSS is related to the polarization direction of the laser radiation, and their spatial period depends on the laser wavelength and the number of pulses delivered. Experimental results concerning LIPSS period and some other peculiarities can be treated consistently by use of the plasmon-polariton mechanism. However, some questions are still open. In order to understand and explain experimental results, we propose a theoretical model based on equations describing the nonlinear interaction of an ultrashort pulse with graphene sample and the substrate, electron density evolution, heat conduction, and thermo-elasticity.

Financial support of the BRFFR (project: F16SRBG-003) is gratefully acknowledged.

[1] Angela Beltaos, Aleksander G. Kovačević, Aleksandar Matković, Uroš Ralević, Svetlana Savić-Sević, Djordje Jovanović, Branislav M. Jelenković, and Radoš Gajić. Femtosecond laser induced periodic surface structures on multi-layer graphene. *Journ. Appl. Phys*., 116, 204306-1-6 (2014)

P27

Comparative single-shot femtosecond laser ablation of solid surfaces in the air and liquid environments

Sergey Kudryashov[1,2,*] Irina Saraeva[2], Vasily Lednev[3], Sergey Pershin[3], Andrey Rudenko[2], Andrey Ionin[2]

[1] ITMO University, 49 Kronverksky prospect, 191107 St. Petersburg, Russia
[2] Lebedev Physical Institute, 53 Leninsky prospect, 119991 Moscow, Russia
[3] A.M. Prokhorov General Physics Institute, 38 Vavilova st., 119991 Moscow, Russia
* Corresponding author: sikudryashov@corp.ifmo.ru, sikudr@sci.lebedev.ru

Dynamics of ablative plumes from a gold surface in ambient air and liquid isopropyl alcohol were studied by time-resolved optical emission spectroscopy in single-shot IR femtosecond-laser ablation regimes, typical for non-filamentary and non-fragmentation laser production of nanoparticles sols. Despite one order of magnitude shorter (few nanoseconds) lifetimes and almost two orders of magnitude lower intensities of the ablative plume emission in the alcohol ambient at the same peak laser fluence, nanofoam-like spallative crater topographies appeared rather similar for the dry and wet conditions [1]. These facts envision the underlying surface spallation as one of the basic ablation mechanisms relevant for both dry and wet advanced femtosecond laser surface nano/micro-machining and texturing, as well as for femtosecond laser ablative production of nanoparticle sols by MHz femtosecond-laser pulse trains via their direct nanojetting in the air and fluid environments [2].

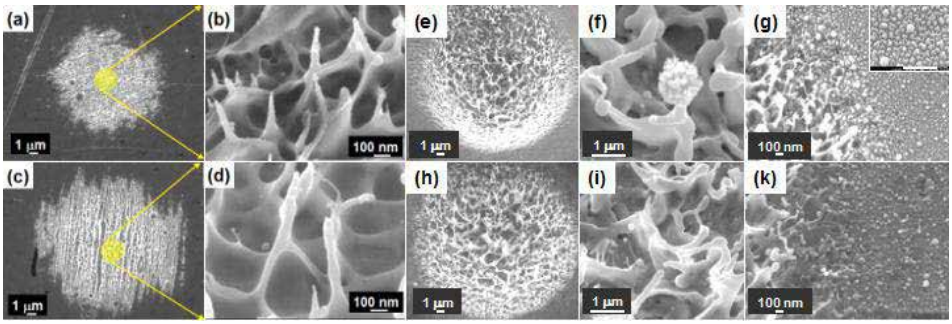

Fig. 1 Typical side-view SEM images (view angle – 35^0) of general crater views, their central parts and edges, produced on gold surface in air (a-b,e-g) and IPA (c-d,h-k): (a-d) single shot per spot, $F_0 \approx 4.6$ J/cm^2, (e-k) 100 shots per spot, $F_0 \approx 5$ (air) and 3.2 (IPA) J/cm^2. Inset: nanoparticle deposit around the crater edge in (g), scale bar – 500 nm.

Filament-free, single-shot femtosecond laser ablation of gold surface in ambient air and liquid isopropyl alcohol at variable laser fluences demonstrated similar spallative removal of the top melt layer and the final fluence-dependent, tunable nanorough crater topography. Upon the spallation, the driving vapor pressure in the sub-surface melt cavity tends to the atmospheric one, yielding in the strong vapor plume confinement by the liquid and faster kinetics of its recondensation, as visualized by the fast damping and strong broadening of atomic gold lines in the optical emission spectra of the confined plumes. The post-spallative nanojetting in the sub-surface nanofoam and sub-threshold nanoparticle ejection via sub-surface boiling appear as sources of directly ejected, potentially weakly-modified colloidal nanoparticles, while the re-solidified crater nanoroughness demonstrates enhanced nanosensing and anti-fouling properties.

This work was supported by Russian Science Foundation (grant #18-15-00220).

[1] S. Kudryashov, I. Saraeva, V. Lednev, S. Pershin, A. Rudenko, A. Ionin, Single-shot femtosecond laser ablation of gold surface in air and isopropyl alcohol environments: nanotopographic and optical emission studies, *Applied Physics Letters* **112** (accepted, 2018).

[2] A. Ionin, A. Ivanova, R. Khmel'nitskii, Yu. Klevkov, S. Kudryashov, N. Mel'nik, A. Nastulyavichus, A. Rudenko, I. Saraeva, N. Smirnov, D. Zayarny, A. Baranov, Milligram-per-second femtosecond laser production of Se nanoparticle inks and ink-jet printing of nanophotonic 2D-patterns, *Applied Surface Science* **436**, 662-669 (2018).

P28

Single- shot pulse ablation of silicon by ultrashort laser pulses of varying duration

Nikita Smirnov[1], Pavel Danilov[1], Sergey Kudryashov[1,2], Alena Nastulyavichus[1], Sophia Umanskaya[1,3], Andrey Ionin[1]
[1]P. N. Lebedev Physical Institute of the Russian Academy of Sciences, Moscow, Russia
[2]ITMO University, St. Petersburg, Russia
[3]National Research Nuclear University MEPhI, Moscow, Russia

Corresponding author: cna1992@mail.ru

Installations with ultrashort laser pulses are widely used for various technological operations to modify the surface of materials. In this case, for different pulse durations, the material ablation thresholds can significantly vary, which in turn are one of the key parameters for laser processing [1,2]. Silicon was chosen as a target, which is widely used in opto- and microelectronics due to its unique properties. In this paper, the ablation thresholds for the silicon wafer were experimentally obtained [2]. In the course of the experiment, laser ablation of the surface of a silicon single-crystal wafer with a variable pulse duration was carried out. Figure 1 shows the optical image of craters with different energies for one of the durations (a), and also the visualization of one of the craters using a scanning electron microscope (SEM) (b). Laser irradiation of the target surface areas was carried out by single pulses of a fiber laser Satsuma (Amplitude Systems) with an active medium on ytterbium ions with the wavelength of the first harmonic of 1030 nm and with a frequency doubling of -515 nm. The pulse duration was varied with the help of an output compressor in the interval 0.3-9 ps. The radiation was focused by a lens with a numerical aperture of 0.25 into a focal spot measuring (1 / e-diameter) 4 μm. The crater profile was obtained using a scanning probe microscope. Then the dependencies of the depth of the crater on the energy density for different durations were constructed.

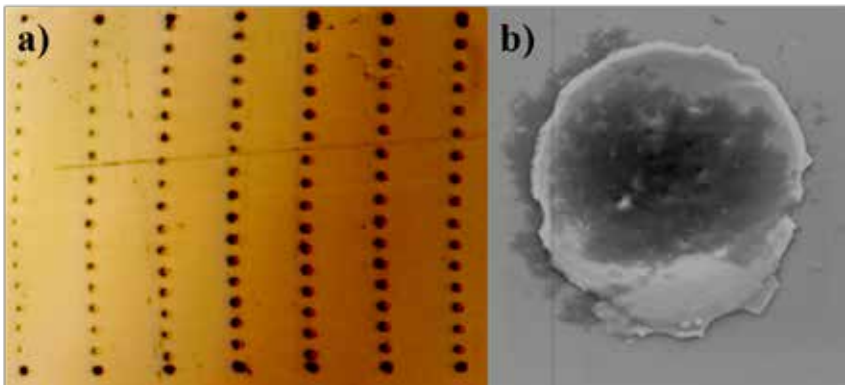

Fig. 1 (a) Optical picture of obtained craters with different energy for one duration; (b) SEM visualization of the crater (0.3 ps 1 μJ)

[1] B. Neuenschwander, B. Jaeggi, M. Schmid, G. Hennig Surface Structuring with Ultra-short Laser Pulses: Basics, Limitations and Needs for High Throughput, Physics Procedia, Vol 56, pp. 1047-1058 (2014)
[2] D. Zayarny, A. Ionin, S. Kudryashov, S. Makarov, A. Kuchmizhak, O. Vitrikand and Y. Kulchin Pulse-width-dependent surface ablation of copper and silver by ultrashort laser pulses, Laser Physics Letters, Vol 13, no. 7,p. 076101 (2016)

P29

Laser ablation of material surfaces by ultrashort pulses of varying duration

Nikita Smirnov[1], Pavel Danilov[1], Sergey Kudryashov[1,2], Alena Nastulyavichus[1], Sophia Umanskaya[1,3], Andrey Ionin[1]

[1]P. N. Lebedev Physical Institute of the Russian Academy of Sciences, Moscow, Russia
[2]ITMO University, St. Petersburg, Russia
[3]National Research Nuclear University MEPhI, Moscow, Russia

Corresponding author: cna1992@mail.ru

Pulsed laser ablation by ultrashort laser pulses is one of the most effective methods of surface treatment of materials. High temperature gradients and heating rates of the surface in comparison with the relaxation time of the system are characteristic for nonequilibrium processes, which can be considered the effect of pulsed laser radiation on the surface of solids. The processes of ablation depend on many factors, which include, firstly, the type of the material itself, secondly the environment, and also the parameters of the laser radiation with which ablation is performed play an important role [1]. One way to obtain information about the dynamics of the interaction of laser radiation with matter is to study the ablation thresholds of the material surface. This topic is very interesting since there is still no complete understanding in this matter. In the study, laser irradiation of fresh surface areas of different materials of optical quality was carried out. The targets were mounted on a three-axis motorized computer-controlled platform [2]. The irradiation was carried out by single pulses of a fiber laser with an active medium on ytterbium ions: the wavelength of the first harmonic was 1030 nm (the second harmonic with a frequency doubling was 515 nm), the repetition rate was 0-2 MHz. The pulse duration (at half-maximum) was varied via an output compressor in the interval 0.3-9 ps. The radiation was focused by a lens with a numerical aperture of 0.65 in a focal spot measuring (1 / e-diameter) of 1.5 µm. The profile of the craters was obtained with the help of a scanning probe microscope (SPM), the visualization of which is shown in Fig.1. Then the dependences of the depth of the crater on the energy density for different durations were constructed and analyzed.

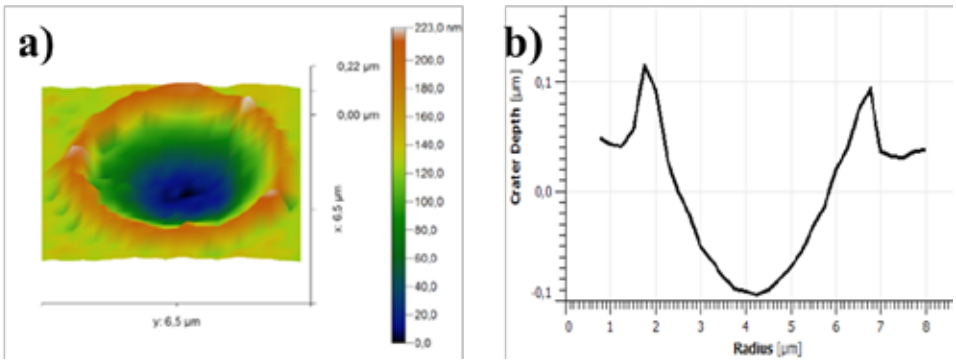

Fig. 1 Visualization of the crater by the SPM method (a), crater profile (b)

[1] A. Zazhogin, A. Fadaian Dynamics of ablation and development processes surface laser plasma of aluminum alloys double laser impulses, Bulletin of BSU. Series 1. №3, pp. 15-18 (2008)
[2] D. Zayarny, A. Ionin, S. Kudryashov, S. Makarov, A. Kuchmizhak, O. Vitrik, Y. Kulchin Surface ablation of aluminum and silicon by ultrashort laser pulses of variable width, JETP Letters, Vol. 103, no. 12, pp. 752-755 (2016)

P30

Femtosecond laser micro-processing of thin films using diffractive optical elements

Pavel A. Danilov[1], Sergey I. Kudryashov[1], Alexander A. Kuchmizhak[2], Oleg B. Vitrik[2], Svetlana N. Khonina[3], Alexey P. Porfirev[3], Sofia F. Umanskaya[1,3,4]

[1]P.N. Lebedev Physical Institute of RAS, 119991, Russia, Moscow, 53, Leninskiy Prospect
[2]Institute of Automation and Control Processes, Far Eastern Branch, Russian Academy of Sciences, 690041, Russia, Vladivostok, 5, Radio st
[3]Samara National Research University, 443086, Russia, Samara, 34, Moskovskoe shosse
[4]National Research Nuclear University MEPHi, 115409, Russia, Moscow, 31, Kashirskoe shosse

Corresponding author: sfumansk@sci.lebedev.ru

Femtosecond laser impact with a tightly focused laser beam induces hydrodynamic flows of the molten material, which redistribute the metal in the target. As a result, microstructures are obtained in the form of holes, cones and nanocrowns [1]. Recently, the attention of researchers is attracted by the interaction of laser radiation structured by a change in polarization or amplitude and phase modulations with matter [2,3]. Broadband diffractive optical elements (DOE) change the shape of the laser beam, which provides fabrication of plasmonic structures unusual forms.

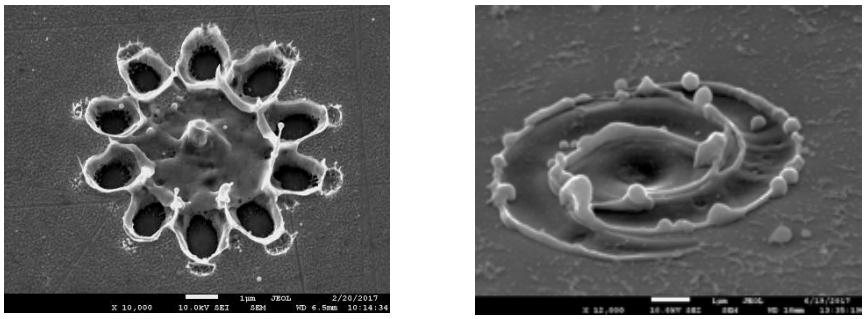

a) b)

Fig. 1 Side-view SEM images of single-shot fs-laser structures on the 500-nm thick Ag-film (NA=0.25). (a) The 10-points structure produced by broadband 20-sector DOE (b) The structure produced by the broadband spiral DOE.

Tightly focused femtosecond laser beam structured with DOE provide single-shot printing of complex plasmonic micro- and nanostructures with significantly increased focal depth. Femtosecond laser with the MHz-repetition rate in combination with multiplexing efficiency makes DOE very useful for high-performance laser fabrication of mm-scale plasmonic devices.

The experiments were supported by the Russian Science Foundation (grant no. 16-12-10165)

[1] P. Danilov; D. Zayarny; A. Ionin, S. Kudryashov, A. Rudenko, A. Kuchmizhak, O. Vitrik, Yu. Kulchin, V. Zhakhovsky, N. Inogamov, (2016). Redistribution of a material at femtosecond laser ablation of a thin silver film. JETP letters, 104, 11, 759-765.
[2] N. M. Litchinitser Science 337 (6098), 1054-1055
[3] J. Hamazaki, R. Morita, K. Chujo, Y. Kobayashi, S. Tanda, and T. Omatsu, Opt. Exp. 18, 2144 (2010).

P31

Temporally and spatially resolved investigations on resonant-infrared ablation of organic materials caused by ultrafast mid-IR laser radiation

Theo Pflug[1]*, Markus Olbrich[1], Roland Rösch[2], Ulrich S. Schubert[2], Harald Hoppe[2], and Alexander Horn[1]

[1]Laserinstitut Hochschule Mittweida, Schillerstraße 10, 09648 Mittweida, Germany
[2]Center for Energy and Environmental Chemistry Jena (CEEC Jena), Friedrich-Schiller-Universität Jena, Philosophenweg 7a, 07743 Jena, Germany
Corresponding author: pflug@hs-mittweida.de

In order to achieve the necessary structure resolution of devices like integrated circuits consisting of organic materials, the microstructuring is increasingly realized by laser radiation. Microstructuring with pulsed UV laser radiation enables high ablation rates, but the photochemical ablation damages the molecular structure of organic compounds and limits their functionality and lifetime [1]. On the other hand, modification using laser radiation in the mid-IR spectrum allows a direct excitation of molecular vibrational modes, so-called resonant-infrared absorption (RIA). Owing to the lower photon energy, molecular compounds are not photo-ionized, thus avoiding excessive material damage. Beside the mentioned benefits of RIA compared to processing using laser radiation within the UV-spectrum, the thermal load of the material is increased [2], but might be reduced by using ultrafast laser radiation due to the short interaction time with the material.

In regard of gaining a better understanding of resonant excitation of organic materials, and finally, to use ultrafast mid-IR laser radiation for processing of devices in organic electronics, fundamental investigations on the ablation and modification of the material have to be performed. Therefore, several organic polymers (PA, PC, PI and PMMA) are irradiated with ultrafast mid-IR laser radiation (40 fs – 4 ps) in dependence on the applied fluence and by varying the wavelength (3.0 – 3.8 µm) of the laser radiation, wherein 3.4 µm represents the excitation of C-H stretching modes. The differences between resonant excitation of vibrational modes and non-resonant excitation of the electron system are identified in terms of the obtained ablation structures [3] as well as temporally and spatially revolved measurements of the relative changes of reflectance [3, 4] and complex refractive index [5], respectively (Fig. 1). Applying ultrafast laser radiation within the femtosecond range with photon energies below the band gap evokes non-linear absorption as the dominant excitation process, since only slight differences between using resonant and non-resonant wavelengths in regard of the derived complex refractive index are determined. In contrast to that, non-linear processes are reduced by extending the pulse duration up to the picosecond range, as no excitation is obtained for non-resonant wavelengths [5].

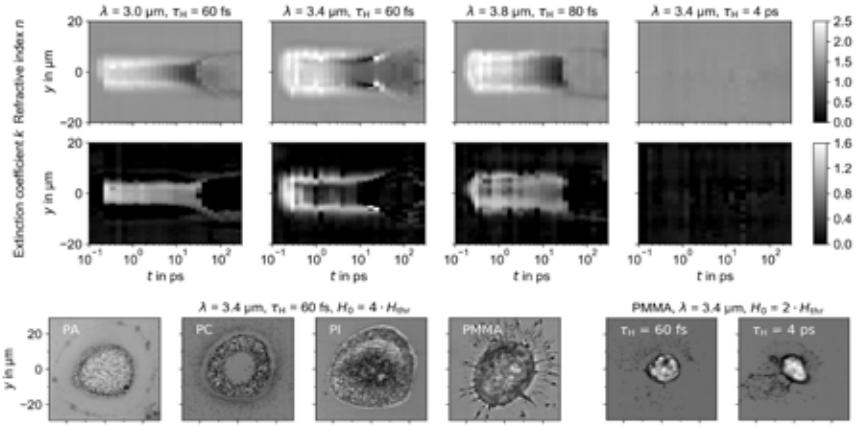

Fig. 1 *Top*: Optical micrographs of the obtained ablation structure for PA, PC, PI, or PMMA using ultrafast laser radiation; determined temporally and spatially resolved refractive index (*middle*) and extinction coefficient (*bottom*) for PMMA as well

[1] C. Faber, I. Duchemin, T. Deutsch, C. Attaccalite, V. Olevano, X. Blase, *J Mater Sci* **47**, 7472 (2012)
[2] S.L. Johnson, *Resonant-infrared laser ablation of polymers*. Dissertation (Vanderbilt University, 2008)
[3] T. Pflug, M. Olbrich, R. Roesch, H. Hoppe, A. Horn, *App. Surf. Sci., in preparation*
[4] T. Pflug, J. Wang, M. Olbrich, M. Frank, A. Horn, *Appl. Phys. A* **124**, 17572 (2018)
[5] T. Pflug, M. Olbrich, R. Roesch, H. Hoppe, A. Horn, *Phys. Chem. Chem. Phys, in preparation*

P32

Case study on the dynamics of ultrafast excitation of gold thin films and bulk PMMA by ultrafast pump-probe reflectometry and ellipsometry

Theo Pflug*, Markus Olbrich, and Alexander Horn

Laserinstitut Hochschule Mittweida, Schillerstraße 10, 09648 Mittweida, Germany
Corresponding author: pflug@hs-mittweida.de

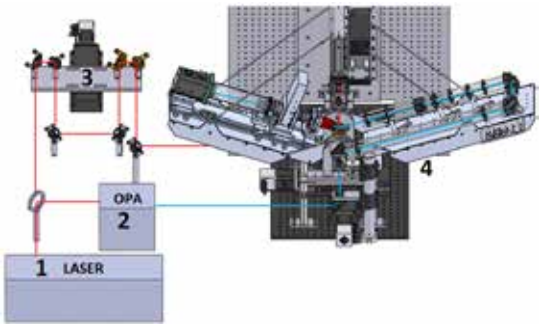

Fig. 1 Experimental setup: 1) laser emitting pump radiation at 800 nm; 2) optical parametric amplifier emitting probe radiation at 250 nm 20 µm; 3) delay line; 4) ellipsometer

To increase the comprehension of the dynamics of ultrafast excitation, here gold and PMMA as a representative of a metal and an organic material respectively, the process of the excitation and the subsequent relaxation has to be portrayed with sufficient temporal resolution. For example, the temporal and spatial modification of the complex refractive index of a sample material after irradiation with ultrafast single pulsed laser radiation (40 – 60 fs) is measured, combining an ellipsometer with a pump-probe setup. This work describes the construction and the validation of a pump-probe setup (Fig. 1) enabling spatially, temporally and spectroscopically resolved ellipsometry with rotaa ting compensator and rotating analyzer [1, 2]. The self-constructed ellipsometer is validated by comparative measurements of the spectroscopically resolved complex refractive index of gold thin films (200 nm, 3 nm) and bulk PMMA at rest with a commercial ellipsometer (nanofilm_ep4, Accurion Inc.), resulting in a deviation less than 10 %.

First temporally and spatially resolved reflectometric measurements at 800 nm and 440 nm are performed on gold for 1 – 7 J/cm² as well as at 3.0 – 3.8 µm and 800 nm are performed on PMMA for

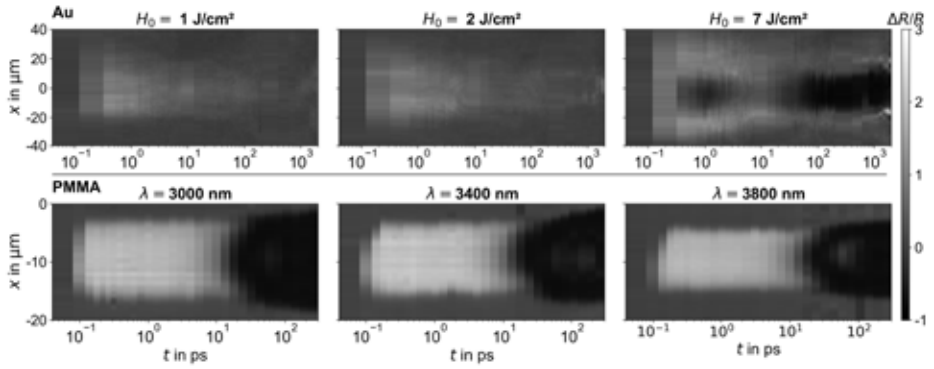

Fig. 2 cross section on the x-axis of the spatially resolved change of the relative reflectance plotted as a function of the delay time for gold (top) for different fluences of the pump radiation and for PMMA (bottom) for different wavelengths of the pump radiation

(Fig. 2) [2, 3]. The change of relative reflectance for gold demonstrates an increase for a fluence of 1 J/cm² and 2 J/cm², whereas a decrease of at the center is obtained for 7 J/cm².

[1] H. Fujiwara, *Spectroscopic Ellipsometry*, John Wiley & Sons, Ltd, Chichester, UK (2007)
[2] T. Pflug, J. Wang, M. Olbrich, M. Frank, A. Horn, *Appl. Phys. A* **124**, 17572 (2018)
[3] T. Pflug, M. Olbrich, R. Roesch, H. Hoppe, A. Horn, *App. Surf. Sci., in preparation*

P33

Efficient picosecond laser ablation on cylindrical surfaces

Mantas Gaidys*, Andrius Žemaitis, Paulius Gečys, Mindaugas Gedvilas

Center for Physical Sciences and Technology, Savanoriu Ave. 231, LT-02300 Vilnius, Lithuania
Corresponding author: mantas.gaidys@ftmc.lt

Machining using ultrashort laser pulses is vastly used in science, technology and medicine. However, how to use the expensive laser irradiation efficiently is an important and open question. Using laser ablation, it is possible to drill, cut and form threedimensional structures off various materials [1]. In this work, optimal parameters for efficient laser ablation were found experimentally on a cylindrical surface using a confirmed theoretical model [2].

Spinning cylindrical copper samples were ablated using a picosecond laser at various fluences. The laser fluence was varied by controlling the average laser power. The experiment was repeated at different pulse repetition rates. The changes of the ablation depth and processed surface roughnesses were measured using a stylus profiler. Ablation efficiency and surface roughness versus laser fluence are presented in Fig. 1.

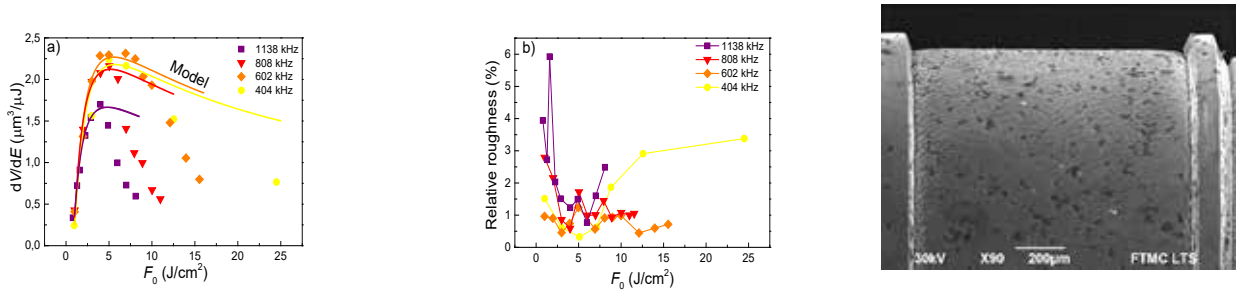

Fig. 1 (a) Ablation efficiency and (b) relative roughness (surface roughness divided by ablated depth) at different pulse repetition rates on a cylindrical copper sample. (c) SEM photo of efficient laser ablation using 602 kHz, 36 μJ, 1080 mm/s laser parameters.

According to the theoretical model, there is a fluence window where the material is removed most efficiently. In this experiment, the highest ablation efficiency was in the fluence range of 4 – 7 J/cm^2. The relative roughness (the ratio of surface roughness and ablated depth) was also lowest in this interval. Experimental results fit well with the theoretical model in the low fluence range F_0 < 10 J/cm^2. However, faster than anticipated ablation efficiency decrease was observed for fluences above 10 J/cm^2. The main cause of this efficiency drop was particle shielding [3]. Laser irradiation was scattered, reflected and absorbed by the ablated particles.

[1] S. Hou, S. Qi, D. A. Hutt, J. R. Tyrer, M. Mu, and Z. Zhou, Three dimensional printed electronic devices realised by selective laser melting of copper/high-density-polyethylene powder mixtures, J. Mater. Process. Technol., **254**, 310–324 (2018).
[2] B. Lauer, B. Jäggi, B. Neuenschwander, Influence of the pulse duration onto the material removal rate and machining quality for different types of steel, Phys. Procedia, **56**, 963–972 (2014).
[3] J. König, S. Nolte, A. Tünnermann, Plasma evolution during metal ablation with ultrashort laser pulses, Opt. Express, **13**, 10597–10607 (2005).

P34

Fabrication of scanned three-dimensional object by efficient laser ablation

Augustinas Skirsgilas*, Andrius Žemaitis, Paulius Gečys

Center for Physical Sciences and Technology, Savanoriu Ave. 231, LT-02300 Vilnius, Lithuania

Corresponding author: augustinas.skirsgilas@ftmc.lt

Ultrashort laser micro-machining is a very attractive technology for micro-structuring due to minimal heat affected zone and almost melt-free surface. The ablation process has to be investigated in order to achieve high processed surface quality and maximum ablation efficiency [1] since complicated laser-matter interaction, and many adjustable laser processing parameters have to be considered. To create a three-dimensional (3D) structures, a representative 3D model must be created. Creating a 3D model of complicated structures such as the human face can become time-consuming and skill requiring task.

In this work, an experimental study was carried out to find the optimal processing parameters for the efficient copper ablation. Also, the simplest and quickest method to scan a three-dimensional object was investigated. To find the optimal parameters for the highest efficiency, a matrix of cavities with dimensions of 1.5 x 1 mm2 were ablated using various processing parameters (pulse repetition rate and pulse energy). The depths of the cavities were measured, and calculations were made to identify the ablation efficiency of each parameter combination. Results were similar to the theoretical model proposed by Furmanski et al. [2] and had a peak of efficiency at fluences in the range of 3-9 J/cm2 (Fig. 1a).

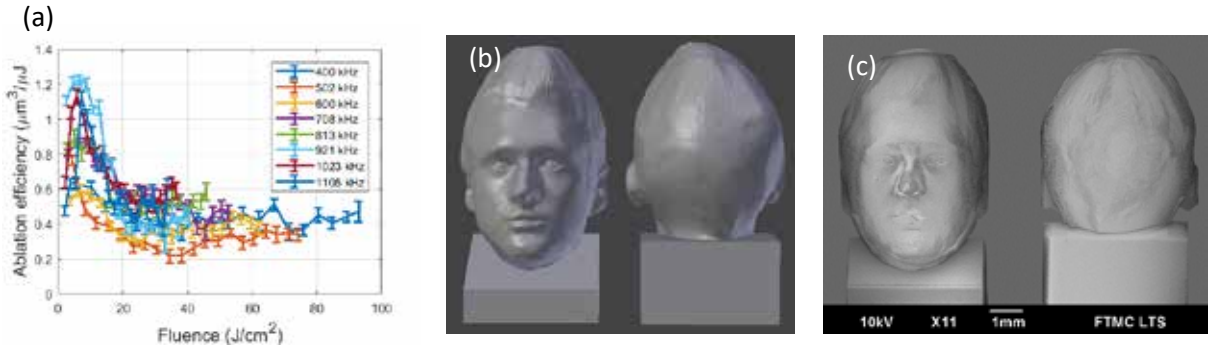

Fig. 1 (a) Ablation efficiency dependence on fluence for different pulse repetition rates. (b) Human face scanned by photogrammetry technique. (c) SEM image of 6 x 11 mm^2 laser sculpted bust front (left) and back (right) from a copper plate.

The simplest method to scan a human face was to use photogrammetry. For this method, a number of photographs around the object have been made. With the help of the software, photographs were converted to a 3D model (Fig. 1b). Using photogrammetry technique a human face was scanned, the 3D model was created and improved. This model was used to fabricate a 3D bust from a copper plate by the efficient laser ablation utilising optimal processing parameters (Fig. 1c).

[1] G. Račiukaitis, M. Brikas, P. Gečys, B. Voisiat, M. Gedvilas, Use of High Repetition Rate and High Power Lasers in Microfabrication: How to Keep the Efficiency High?, *J. Laser Micro Nanoeng*. **4**, 186–191 (2009).

[2] J. Furmanski, A. M. Rubenchik, M. D. Shirk, B. C. Stuart, Deterministic processing of alumina with ultrashort laser pulses, J. Appl. Phys., **102**, 073112 (2007).

P35

Rapid and high-quality 3D fabrication by efficient ultrashort laser ablation

Andrius Žemaitis*, Paulius Gečys, Gediminas Račiukaitis, Mindaugas Gedvilas

Center for Physical Sciences and Technology, Savanoriu Ave. 231, LT-02300 Vilnius, Lithuania
Corresponding author: andrius.zemaitis@ftmc.lt

The high interest of scientific and industrial societies in additive manufacturing has shown that fabrication of three-dimensional (3D) objects is a needed task. Mostly, the 3D printing technology is based on matter melting and solidification, which changes the physical properties of the material, giving the undesirable layer-by-layer appearance, also, void formation [1]. To overcome these issues, ultrashort pulse laser ablation can be used instead of 3D printing. Due to confined laser-matter interaction during ultrashort pulse duration, minimal heat affected zone and melt-free treatment are achieved leading to advanced processing precision [2].

To form a 3D object, with the help of laser pulses, layer-by-layer the unwanted material was removed from a bulk sample plate. To fabricate efficiently, the process had to be optimised [3]. In this work ablation efficiency, ablation rate and surface roughness (Ra) were investigated by varying processing parameters: laser fluence, pulse repetition rate, beam scanning speed and distance between scanned lines (hatch) (Fig. 1a, b, c).

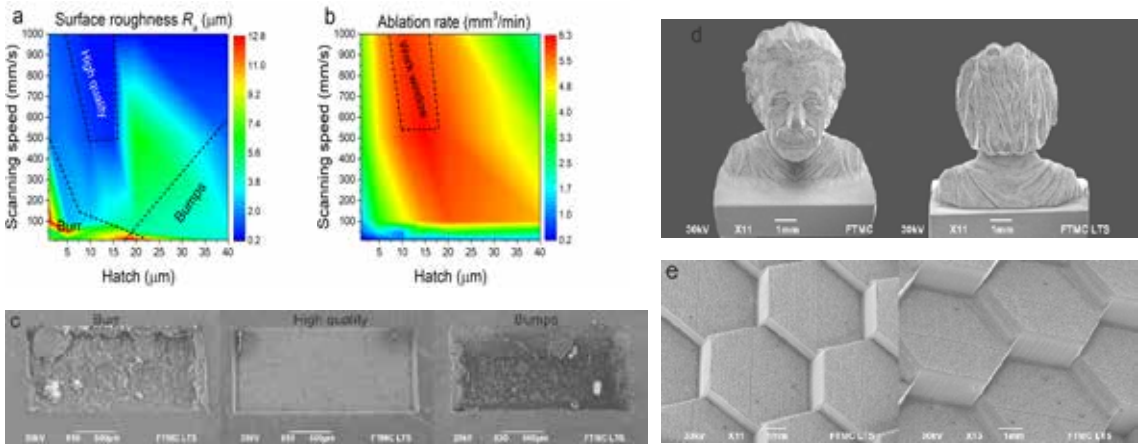

Fig. 1 (a) Surface roughness of the bottoms of laser ablated cavities in copper dependence on scanning speed and hatch distance with indicated three quality regions: burr; high quality; bumps. (b) Ablation rate dependence on scanning speed and hatch distance with indicated working window. (c) Typical SEM images of three quality regions. (d) SEM images of both-sided laser sculpted Albert Einstein's bust. (e) SEM image of the fish skin-like structure. Ablation rate 6.3 mm^3/min, peak fluence F_0 = 3.5 J/cm^2, pulse repetition rate f = 1138 kHz, pulse duration τ = 10 ps, laser wavelength λ = 1064 nm, average power P = 40 W.

It was shown that surface roughness could be automatically enhanced if optimal laser processing parameters for the highest ablation rate and efficiency are used. By using optimal parameters representative 3D objects were created: Einstein's bust was laser sculpted from the bulk copper plate (Fig. 1d). Also, a copper plate was textured with fish skin-like structure (Fig. 1e).

[1] T. D. Ngo, A. Kashani, G. Imbalzano, K. T. Q. Nguyen, D. Hui, Additive manufacturing (3D printing): A review of materials, methods, applications and challenges, *Compos. Part B* **143**, 172–196 (2018).
[2] K. Sugioka, Y. Cheng, Ultrafast lasers - reliable tools for advanced materials processing, *Light Sci. Appl.* **3**, e149 (2014).
[3] G. Račiukaitis, M. Brikas, P. Gečys, B. Voisiat, M. Gedvilas, Use of High Repetition Rate and High Power Lasers in Microfabrication: How to Keep the Efficiency High?, *J. Laser Micro Nanoen*. **4**, 186–191 (2009).

P36

Photosensitive naturally derived resins toward optical 3D printing

Edvinas Skliutas[1], Sigita Kašėtaitė[2], Linas Jonušauskas[1,3], Miglė Lebedevaitė[2], Jolita Ostrauskaitė[2], Mangirdas Malinauskas[1]

[1]Vilnius University, Faculty of Physics, Laser Research Center, Sauletekio Ave. 10, Vilnius, Lithuania
[2]Kaunas University of Technology, Department of Polymer Chemistry and Technology, Radvilėnai Rd. 19, Kaunas, Lithuania
[3]Femtika Ltd., Sauletekio Ave. 15, Vilnius, Lithuania

Corresponding author: edvinas.skliutas@ff.vu.lt

Recent advances in material engineering have shown that renewable raw materials, such as plant oils or glycerol, can be applied for synthesis of polymers due to ready availability, inherent biodegradability, limited toxicity, and existence of modifiable functional groups and eventually resulting to a potentially lower cost. After additional chemical modifications (epoxidation, acrylation, double bonds metathesis, etc.), they can be applied in such areas as direct write stereolithography [1] and dynamic projection lithography [2], which allows fabrication of three-dimensional (3D) objects. “Autodesk’s” 3D optical printer “Ember” using 405 nm light was implemented for dynamic projection lithography. It enabled straightforward spatio-selective photopolymerization on demand, which allows development of various photosensitive materials. The bio-based resins’ photosensitivities were compared to standard materials like “Autodesk” “PR48” and “Formlabs” “Clear”. Submillimeter range 2.5D and 3D objects of various geometries including internal architectures were successfully produced (Fig. 1). It was revealed that a higher exposition dose results in a linear increase in the formed structures height, proving controllability of the undergoing process.

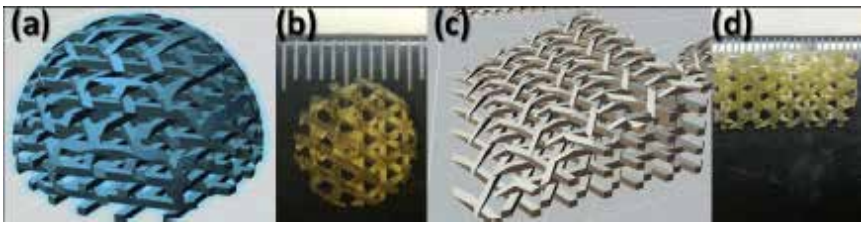

Fig. 1. (a,c) CAD models of half-sphere and prism scaffolds having internal architectures, (b,d) 3D printed objects out of acrylated epoxidized soybean oil (AESO). Scale interval – 1 mm. Concluding, the provided results prove that naturally derived resins are suitable candidates for tabletop optical 3D printing as well as direct laser writing 3D nanolithography (currently ongoing research).

[1] S. Miao, W. Zhu, N.J. Castro, M. Nowicki, X. Zhou, H. Cui, J.P. Fisher, L.G. Zhang, 4D printing smart biomedical scaffolds with novel soybean oil epoxidized acrylate. Sci. Rep. 6(1), 27226 (2016).
[2] E. Skliutas, S. Kasetaite, L. Jonusauskas, J. Ostrauskaite, M. Malinauskas, Photosensitive naturally derived resins towards optical 3D printing. Opt. Eng. 57(4), 041412 (2018).

P37

Large-Scale 3D Microstructured Scaffolds Fabricated by Direct Laser Writing out of Biocompatible Polymers

Sima Rekštytė[1], Edvinas Skliutas[1], Justinas Mačiulaitis[2,3], Romaldas Mačiulaitis[2], Sergei Kostjuk[4], and Mangirdas Malinauskas[1]

[1]Laser Research Center, Faculty of Physics, Vilnius University, Saulėtekio Ave. 10, LT-10223 Vilnius, Lithuania
[2]Institute of Physiology and Pharmacology, Medical Academy, Lithuanian University of Health Sciences, A. Mickevičiaus 9, LT-44307 Kaunas, Lithuania
[3]Institute of Sports, Medical Academy, Lithuanian University of Health Sciences, Kalniečių 231, LT-50108 Kaunas, Lithuania
[4]Research Institute for Physical Chemical Problems, Belarusian State University, Leningradskaya str. 14, Minsk 220030, Belarus
Corresponding author: sima.rekstyte@gmail.com

Direct laser writing in pre-polymers (DLW-PP) employing ultrashort pulses is a well-known and established a technique for the creation of complex geometry 3D microstructured scaffolds suitable for *in vivo* and *in vitro* cell studies [1,2]. Various throughput-augmenting techniques are being investigated [2-4] in order to make this technique even more attractive for tissue engineering applications as a large number of identical samples for statistically significant results is required.

We present the results on high-throughput (>50 000 $\mu m^3/s$) fabrication of mm-to-cm sized scaffolds, maintaining 15-25 µm structural resolution (Fig. 1). An ultrafast amplified femtosecond laser system Pharos (ν=200 kHz, τ=300 fs, λ=515 nm) was used, and synchronized motion of linear stages and galvoscanners was employed for the positioning of the focused laser beam inside the pre-polymer. This allowed combining the stage's wide working area with the scanner's high-speed beam scanning capabilities. Thus, the inherent disadvantages of using these positioning methods separately could be overcome.

The materials that we used were a non-biodegradable hybrid SZ2080 pre-polymer and biodegradable chemically modified poly(D, L-lactide). Both photosensitized and pure versions of these materials were structured, demonstrating the versatility of the DLW-PP technique. The optimal fabrication parameters were found as well as the possibility to scale the pore size depending on the mechanical properties of the material was investigated.

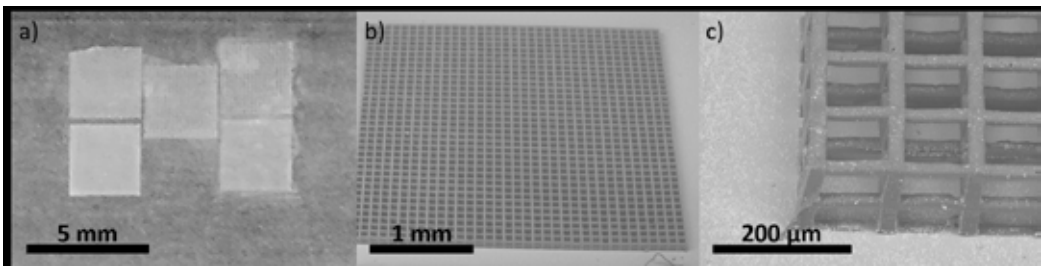

Fig. 1 (a) an optical and (b-c) SEM images of 3x3mm^2 3D scaffolds, fabricated out of biodegradable chemically modified poly(D, L-lactide). The fabrication time for the scaffolds ranges from 1 to 2.5 hours, depending on the chosen pore size.

[1] J. Mačiulaitis, M. Deveikytė, S. Rekštytė, M. Bratchikov, A. Darinskas, A. Šimbelytė, G. Daunoras, A. Laurinavičienė, A. Laurinavičius, R. Gudas, M. Malinauskas, R. Mačiulaitis, Preclinical study of SZ2080 material 3D microstructured scaffolds for cartilage tissue engineering made by femtosecond direct laser writing lithography. *Biofabrication* **7,** 015015 (2015).
[2] D. Ricci, M.M. Nava, T. Zandrini, G. Cerullo, M.T. Raimondi, R. Osellame, Scaling-up techniques for the nanofabrication of cell culture substrates via two-photon polymerization for industrial-scale expansion of stem cells. *Materials* **10**, 66 (2017).
[3] S.D. Gittard, A. Nguyen, K. Obata, A. Koroleva, R.J. Narayan, B.N. Chichkov, Fabrication of microscale medical devices by two-photon polymerization with multiple foci via a spatial light modulator. *Biomed. Opt. Express* **2**, 3167-3178 (2011).
[4] A. Trautmann, M. Rüth, H.-D. Lemke, T. Walther, R. Hellmann, Two-photon polymerization based large scaffolds for adhesion and proliferation studies of human primary fibroblasts. *Opt. Laser. Technol*. **106,** 474-480 (2018).

P38

3D polymeric microstructures for micro-actuation and environmental sensing fabricated by direct laser writing technique

Mae Nishimura[1], Sima. Rekštytė[2], Vygantas Mizeikis[1]

[1]Research Institute of Electronics, Shizuoka University, 3-5-1 Johoku Hamamatsu 432-8011, Japan
[2]Laser Research Center, Vilnius University, Saulėtekio Ave. 10, Vilnius 10223, Lithuania

Corresponding author: mizeikis.vygantas@shizuoka.ac.jp

We report utilization of 3D polymeric microstructures fabricated by direct laser writing in polymeric photoresist for application as smart materials capable of exhibiting solvent-sensitive, reversible volume change. We have designed 3D microstructures consisting of sub-micrometre-thick photoresist features and fabricated them using Direct Laser Write (DLW) technique in hybrid organic-inorganic photoresist SZ2080[1]. Upon immersion to various solvents, the sub-micrometer thick features are permeated by the solvent, leading to their volume and length change. This phenomenon can be used to build microstructures that exhibit solvent-controllable deformations (shrinkage or swelling). Photoresist SZ2080 was found to exhibit swelling (shrinkage) upon immersion in ethanol (water). We report several kinds of structures that reveal and amplify these deformations, thus acting as micro-mechanical actuators or environmental sensors. Fig. 1(a) depicts schematically a mechanical lever structure whose orientation angle is controlled by the length of thin solvent-sensitive photoresist lines. We demonstrate lever structures exhibiting total angle change as large as 45 degrees upon immersion in water and ethanol. Fig. 1(b) compares optical microscope images and orientation of the same lever structure in ethanol and water, illustrating the above claim. Structures with other geometries that are also applicable as environmental sensors with purely optical readout will be demonstrated.

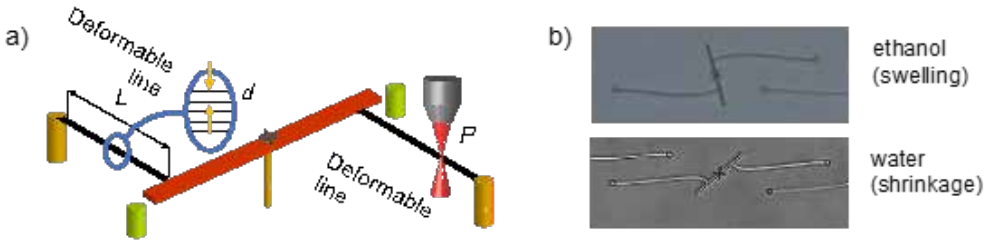

Fig. 1 Schematic image of a lever consisting of a hard pivoted arm, attached to the substrate via two deformable lines (a), comparison of different lever orientation in ethanol and water, representing swelling and shrinkage of the lines, respectively.

[1]. S. Rekštytė, D. Paipulas, M. Malinauskas, V. Mizeikis, "Microactuation and sensing using reversible deformations of laser-written polymeric structures", Nanotechnology **28,** 124001 (2017).

P39

Lithography of True 3D Ceramic Structures on the Microscale

Viktorija Padolskytė[1,2], Darius Gailevičius[1,2], Linas Jonušauskas[1,2], Lina Mikoliūnaitė[3], Tomas Katkus[4], Roaldas Gadonas[1,2], Simas Šakirzanovas[3], Vygantas Mizeikis[5], Kestutis Staliunas[6,7], Saulius Juodkazis[4,8], Mangirdas Malinauskas[1]

[1]Laser Research Center, Vilnius University, Sauletekio Ave. 10, LT-10223, Vilnius, Lithuania
[2]Femtika Ltd., Sauletekio Ave. 15, Vilnius, LT-10224, Lithuania
[3]Faculty of Chemistry and Geosciences, Vilnius University, Naugarduko Str. 24, LT-03225, Vilnius, Lithuania
[4]Swinburne University of Technology, John St., Hawthorn 3122 Vic, Australia
[5]Research Institute of Electronics, Shizuoka University, 3-5-1 Johoku, Naka-ku, Hamamatsu, 432-8561, Japan
[6]Nonlinear Dynamics, Nonlinear Optics and Lasers, Universitat Politecnica de Catalunya, Rambla Sant Nebridi 22, 08022, Terrassa, Spain
[7]Institució Catalana de Recerca i Estudis Avançats Passeig Llu ís Companys 23, 08010 Barcelona, Spain
[8]Melbourne Centre for Nanofabrication, the Victorian Node of the Australian National Fabrication Facility, 151 Wellington Rd., Clayton 3168 Vic, Australia
Corresponding author: viktorija.padolskyte@ff.stud.vu.lt

Ceramics are widely used in today's science and industry as it can withstand immense thermal and mechanical and other hazards [1]. Stereolithographic 3D printing of hybrid organic-inorganic photopolymer and subsequent heat-treatment was demonstrated to be capable of providing ceramic [2] and glass structures [3] in addition to improved resolution and reduced dimensions of the structures [4,5]. In this work, we explore a possibility to apply ultrafast 3D laser nanolithography followed by heat-treatment to acquire ceramic 3D structures in micro-/nano-scale [6,7].

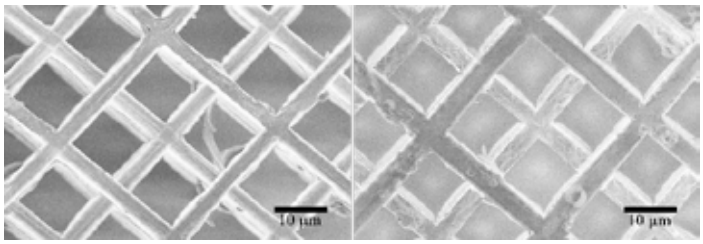

Fig. 1. Image of a 3D laser fabricated and heat-treated scaffold before (left) and after (right) plasma etching. The scaffold has miniscule changes on the surface, whereas the material when it is not heat-treated tends to have deep gaps after the procedure.

In our case, we use direct laser writing (DLW) technique to obtain initial 3D structures out of hybrid organic-inorganic material SZ2080. Then, during heating at temperatures up to 1500 °C in an air atmosphere, the organic part evaporates, which results in the glass-ceramic material. Additionally, heat-treatment of the structures provides an extra route for size control down to 60 % (Fig. 1). We show this can be applied to bulk, periodic and free-form objects. Sintered structures have proven to be more resilient to wet and dry etching, high temperatures. Also, Raman spectroscopy and X-ray diffraction proved that heated SZ2080 structures have ceramic-like material properties.

[1] J. Bauer, *et al.*, *Approaching theoretical strength in glassy carbon nanolattices*, Nat. Mater. **15**(4), 438–443 (2016).
[2] Z. C. Eckel, *et al.*, *Additive manufacturing of polymer-derived ceramics*, Science **351**(6268), 58–62 (2015).
[3] F. Kotz, *et al., Three-dimensional printing of transparent fused silica glass*, Nature **544**(7650), 337–339 (2017).
[4] J. Li, B. Jia, and M. Gu, *Engineering stop gaps of inorganic-organic polymeric 3D woodpile photonic crystals with post-thermal treatment*, Optics Express **16**(24), 20073 (2008).
[5] G. Seniutinas, A. Weber, C. Padeste, I. Sakellari, M. Farsari, C. David, *Beyond 100 nm resolution in 3D laser lithography - post-processing solutions*, Microelectron. Eng. **191**, 25-31 (2018).
[6] L. Jonušauskas, *et al., Optically Clear and Resilient Free-Form μ-Optics 3D-Printed via Ultrafast Laser Lithography*, Materials, **10**(1), 12 (2017).
[7] V. Padolskytė, D. Gailevičius, L. Jonušauskas, L. Mikoliūnaitė, T. Katkus, R. Gadonas, S. Šakirzanovas, V. Mizeikis, K. Staliūnas, S. Juodkazis, M. Malinauskas, *3D Opto-Structuring of Ceramics at Nanoscale*, Proc. SPIE **10675**, 106750U (2018).

P40

Investigation of mechanical properties of polymeric microstructures using glass microcantilevers

Titas Tičkūnas[1], Mangirdas Malinauskas[1], Roaldas Gadonas[1], Yves Bellouard[2] and Domas Paipulas[1]

[1]Laser Research Center, Vilnius University, Saulėtekio Ave. 10, LT-10223 Vilnius, Lithuania
[2]Ecole Polytechnique Fédérale de Lausanne (EPFL), Galatea Lab, Rue de la Maladière 71b, 2002 Neuchatel, Switzerland
Corresponding author: *titas.tickunas@gmail.com*

We present an investigation of the mechanical properties of polymeric microstructures fabricated by additive two-photon polymerization (2PP) technique and examined through glass micromechanical sensor produced by subtractive laser-assisted etching [1]. Ultrashort laser pulses provide the ability to modify transparent material within the focal point of the laser beam. By spatially moving the laser focus trajectory, pre-programmed algorithms can be written in the volume of the material. With this direct laser writing 2PP technique, we can additively grow 3D structures out of a wide range of polymeric materials. Alternatively, glass microstructures could be fabricated out of glass substrate with laser illumination followed by a chemical etching step. The combined used of both these techniques could find new applications and open new functionalities, which are inaccessible to make with only one technique [2,3].

Structures made by 2PP distinguish the feature that during the wet development and drying processes, the structures result in geometrical distortions. The polymerized material becomes denser, and structure dimensions turn out smaller than expected. On the other hand, polymeric structures can swell after rinsing in solvents after (or during) developing process. In most cases, these polymer shrinkage/swelling are an undesired effect, but it is demonstrated that this phenomenon could be a potentially be applied for chemical sensing applications [4].

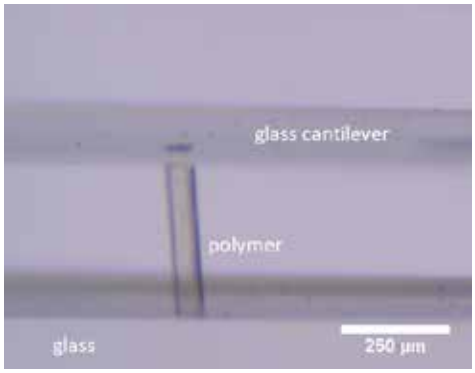

Fig. 1 Subtractively made glass cantilever with an integrated rectangular-shape polymeric beam structure via 2PP technique.

Here, we present a subtractive fabrication of a cantilever out of glass substrate with an integration of a polymeric beam *via* the 2PP technique. We demonstrate that the glass-polymer micromechanical sensor could be used to investigate the elastic properties of polymeric microstructures. Glass cantilever acts as an amplification system and tester for the quantitative investigation of the polymeric beam properties. We present the polymeric beam length change due to the shrinkage/swelling phenomena, as well as Young's modulus estimation results of the 2PP polymer in different ambient surroundings. Additionally, we have investigated polymer change in length over the total exposure dose. By changing focusing and exposure conditions, we can alter polymeric structure mechanical properties.

[1] T. Tičkūnas *et al*., "Combination of additive and subtractive laser 3D microprocessing in hybrid glass/polymer microsystems for chemical sensing applications". Opt. Express, **25**(21), pp. 26280-26288 (2017).
[2] K. Sugioka, "Progress in ultrafast laser processing and future prospects". Nanophotonics, **6**(2), pp. 393-413 (2016).
[3] L. Amato *et al*.,"Integrated three-dimensional filter separates nanoscale from microscale elements in a microfluidic chip". Lab Chip, **12**, pp. 1135-1142 (2012).
[4] S. Rėkštytė *et al*., "Microactuation and sensing using reversible deformations of laser-written polymeric structures". Nanotechnology, **28**, pp. 124001 (2017).

P41

Fabrication and Surface Engineering of Silicon Nanocrystals by Laser-Induced Processes in Liquid

Natalie Tarasenka[1], Andrei Butsen[1], Alena Nevar[1], Lizaveta Shustava[1], Nikolai Tarasenko[1], Evaldas Stankevičius[2], Paulus Gečys[2], Gediminas Račiukaitis[2]

[1]B.I. Stepanov Institute of Physics, 68 Nezalezhnasti Ave. 220072 Minsk, Belarus
[2] Center for Physical Sciences and Technology, Savanoriu Ave. 231, LT-02300 Vilnius, Lithuania
Corresponding author: n.tarasenko@ifanbel.bas-net.by

Silicon nanocrystals (Si NCs) have recently attracted much attention due to a unique combination of their size-dependent optoelectronic properties and biocompatibility, which have great potential for use in photovoltaics, optoelectronics, biological imaging and diagnostics applications [1]. In this paper, we demonstrate the use of pulsed laser ablation in liquid (PLAL) with additional laser processing for preparation of Si NCs in colloids with pre-determined surface chemistry, desired characteristics and tunable photoluminescence. Additional laser processing of the colloidal solution can be an effective technique capable of engineering the surface of NCs. The formation of chemical groups on the surface of the Si NCs by the laser-based process depends on the laser parameters and laser-induced processes in colloid leading to the production of radicals suitable for surface functionalization. The focused beam of an Nd:YAG laser (1064 nm, 10 ns pulse width, 20-80 mJ/pulse) was used for ablation of Si target in ethanol, distilled water, DMSO and 0.008 M aqueous DTPA solution. The phase composition, morphological, structural, and optical properties of the synthesised NCs have been investigated. The TEM image of a sample prepared in ethanol (Fig.1a) displays ultrafine and well-dispersed Si NCs with an average diameter of about 7 nm. HRTEM image revealed that the prepared Si NCs have the crystalline cubic Si structure confirmed by the observed interplanar spacing of 3.1 Å corresponded to the (111) plane.

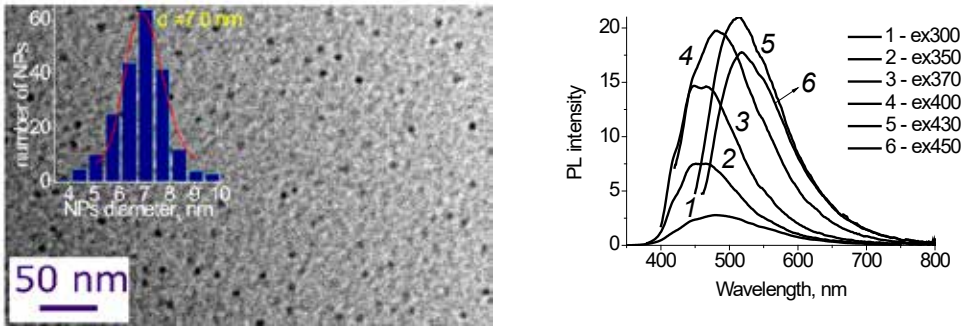

Fig. 1 (a) TEM microphotograph of Si NCs prepared by laser ablation in ethanol. (b) Photoluminescence spectra of Si NCs prepared by laser ablation in DTPA/DMSO solution at indicated excitation wavelengths

Si NCs prepared by laser ablation in ethanol and water exhibited a relatively weak PL in the blue region the origin of which is typically assigned to the formation of oxygen-related defects. The Si NCs-DTPA/DMSO colloid exhibited good photoluminescence stability in the green-orange spectrum region. As it can be seen in Fig. 1b, the resulting SiNCs show excitation wavelength-dependent emission when maximum wavelength ranges from ~450 to ~600 nm under excitation wavelengths in the range 300 – 450 nm.

[1] Y. He, C.H. Fan, S.T. Lee, Silicon nanostructures for bioapplications. *Nano Today*, **5**, 282 - 295 (2010).

P42

Photocatalytic TiO_2-Based Fine Particles Synthesized by Pulsed-Laser Ablation in $SrCl_2$ Solution

Shu Kaiya[1], Takuya Sagara[3], Satoshi Kurumi[2], Ken-ichi Matsuda[2] and Kaoru Suzuki[2]

[1]Graduate School of Electrical Engineering, College of Science and Technology, Nihon University
[2]*Department of Electrical Engineering, College of Science and Technology, Nihon University* (*1-8-14 Kannda-Surugadai, Chiyoda-ku Tokyo 101-8308 Japan*)
[3]*Tokyo Metropolitan College of Industrial Technology*(*1-10-40 Higashi-Ohi, Shinagawa-ku Tokyo 140-0011 Japan*)

cssh18007@g.nihon-u.ac.jp

TiO_2-based materials, which have the Honda-Fujishima effect, have attracted much attention as a hydrogen generator in hydrogen fuel cells without exhausting CO_2 under their photocatalytic reaction.[1] This photocatalytic reaction occurs at the surface of the catalyst, and thus the reaction strongly depends on the surface area of the catalyst. Therefore, we aimed to improve the reaction efficiency by increasing the catalyst surface. In this study, we examined to the synthesis of $SrTiO_3$ photocatalytic fine particles by pulsed-laser ablation in liquid (PLAL) using Ti target and $SrCl_2$ solution as a dopant. A Ti plate (10 × 10 × 0.5 mm) as an ablation target was dipped into the solution, and the focused Nd:YAG laser beam (LOTIS, LS2147, wavelength: 355 nm, power: 0.18 J, pulse width: 20 ns, repetition frequency: 10 Hz) was irradiated to the plate for 30 min. Ablation plumes were observed from the laser beam spot, and Ti fine particles were produced in the solution. The solution including the fine particles was dropped on a Si substrate. The fine particles in the solution were taken on the substrate by drafter evaporation.

Scanning electron microscope image of the substrate is shown in Fig. 1. This indicated the fine particles whose size were about 1.0 µm in diameter was existence. Fig. 2 shows the result of energy dispersive x-ray measurement. This suggested that fine particles were composed of Cl, Sr, Ti and O atoms.

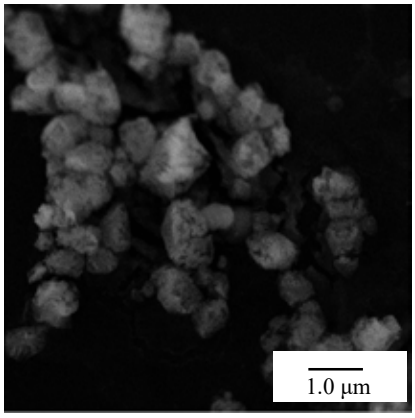

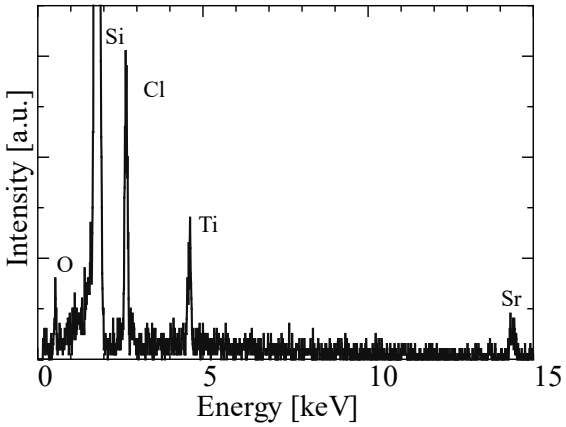

[1] A. Fujishima and K.Honda:"Electrochemical photolysis of water at a semiconductor electrode", Nature, **238**, 37 (1972).

P43

Laser Generation of Photoactive Nanoparticles

Ilie Alina Georgiana[1, 2], Scărișoreanu Monica[1],Vasile Eugenia[3], Elena Duțu[1], Cristi Mihailescu[1], Dumitrache Florian[1], I. Fort[4], Mihăilescu Ion[1]

[1] National Institute for Lasers, Plasma and Radiation Physics, 409 Atomistilor Street, 077125, Bucharest-Magurele, Romania;

[2] University of Bucharest, Faculty of Physics, 405 Atomistilor Street, 077125, Magurele, Romania;

[3] University Politehnica of Bucharest, 313 Splaiul Independenței, 011061, Bucharest, Romania.

[4] Babes-Bolyai University, Faculty of Chemistry and Chemical Engineering, 11 Arany Janos Str., Cluj-Napoca, 400028, Romania;

Corresponding author: ilie.georgiana@inflpr.ro

Laser pyrolysis (LP) is a well-established synthesis method for a wide range of top nanomaterials[1]. It is based upon the resonant absorption of laser radiation by a gaseous precursor- in our case C_2H_4. High selectivity reactions are induced by the resonant process, which promotes material nucleation and growth, while selected experimental parameters allow for easy tailoring of characteristics and high purity.

Our selection was focused to TiO_2-based nanocomposites [2]: mixed phase titania [3], noble metal support anatase nano-TiO_2 (Figure 1a), or metal-doped TiO_2 nanoparticles, synthesized by laser pyrolysis from $TiCl_4$ vapours, with air as an oxidizing agent, under CW CO_2 laser radiation (λ=10.6 μm). LP TiO_2-based nanoparticles exhibit fast photodegradation rates, up to 28.74 x10^{-3} min^{-1} in UV and 16.78 x10^{-3} min^{-1} in VIS, and diminished bandgaps (Figure 1b), while core-shell C titania nanoparticles show high thermal stability.

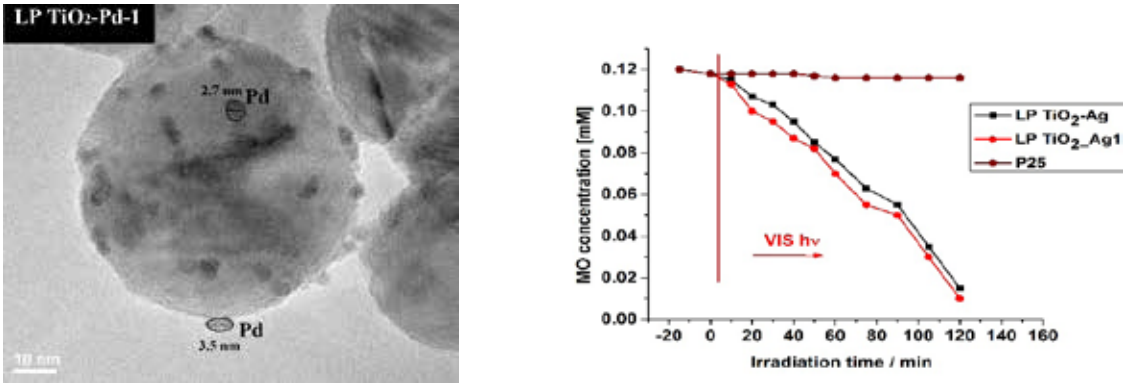

Fig. 1 (a) TEM image of LP titania as support for nano-Pd decorations; (b)TiO_2 nanoparticles absorbance in UV and VIS.

We conduct a parallel study regarding various LP TiO_2-based nanomaterials with respect to synthesis parameters, morphology, crystalline phase behaviour and photocatalytic efficiency, by Raman spectroscopy, XRD, TEM and XPS analysis. High quality photoactive TiO_2 nanoparticle generation is an important step towards a clean environment via eco-friendly techniques for pollutant degradation.

Different stages of the pollution process and various areas of application imply targeted characteristics. Laser pyrolysis versatility opens a promising alternative in respect to today ecological requirements.

[1] R. Alexandrescu, F. Dumitrache, et al., Nanotechnology 15, 537–545 (2004).

[2] M. Scarisoreanu, A.G. Ilie, et al., Appl. Surf. Sci. 418, 491-498 (2017).

[3] A.G. Ilie, M. Scarisoreanu, et al., Appl. Surf. Sci. 427, 798-806 (2018).

P44

Laser ablative hybrid Si-Au nanoparticles

Anastasia Ivanova[1,2], Andrei Ionin[1], Sergey Kudrayshov[1], Irina Saraeva[1], Alena Nastylayvichus[1]

[1] P.N. Lebedev Physical Institute of the Russian Academy of Sciences, 53, Leninskiy Prospekt, Moskow, Russia
[2] National Research Nuclear University MEPhI (Moscow Engineering Physics Institute), 31, Kashirskoe shosse, Moskow, Russia
Corresponding author: mephynastya@gmail.com

In this paper, hybrid metal-insulator silicon-gold nanoparticles were synthesized by laser ablation with nanosecond pulses surface of a solid target consisting of a single-crystal silicon wafer with a deposited gold film about 50 nm in thickness. The object of the work was to study the effect of laser radiation parameters, such as the laser radiation density and scanning speed, on the configuration of nanoparticles by varying them with the development of colloidal nanoparticle solutions. The energy density obviously affects the heating and fusion of materials. The scanning speed actually determines the interaction time of the laser radiation with the target surface. An increase in the radiation density increases the concentration of colloidal solutions of nanoparticles. With an increase in the scan rate, it is possible to observe the optimum value at which the effective production of nanoparticles with sizes of 60-80 nm takes place depending on the radiation density.

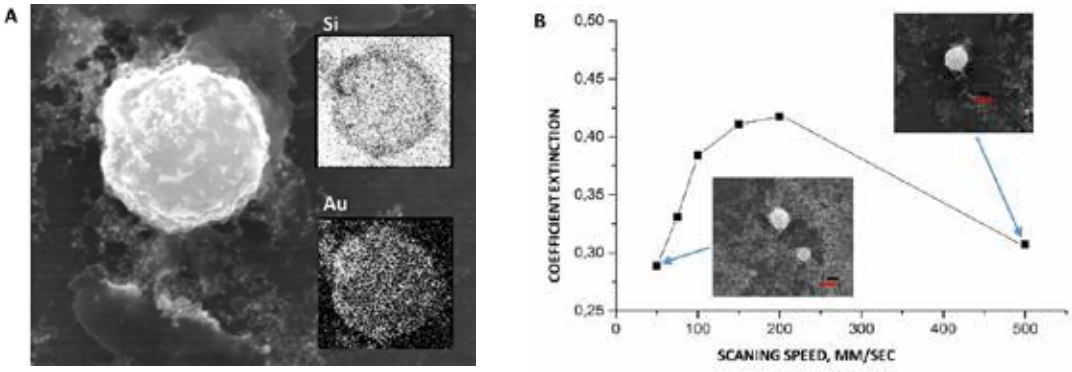

Fig. 1 (a) SEM image hybrid Si-Au NP with elemental composition. (b) Extinction coefficient at wavelength 520 nm from laser scanning speed. At the inset SEM image hybrid, Si-Au NP dried.

This work was financially supported by the Russian Ministry of Science and Education (agreement no. 18-15-00220).

P45

Fs/ps pulsewidth-dependent yield of Au, Ag and Si nanoparticles

I. N. Saraeva,[1*] A. A. Ionin,[1] A. A. Rudenko,[1] S. I. Kudryashov[1,2]

[1] Lebedev Physical Institute, Leninskiy prospect 53, 119991 Moscow, Russia
[2] ITMO University, Kronverkskiy prospect 49, 197101 St. Petersburg, Russia
Corresponding author: insar@lebedev.ru

The dependence of silver, gold and silicon NPs yield on laser pulsewidth τ = 0.3 - 10 ps during IR (λ = 1030 nm) multi-shot laser ablation of solid targets in deionized water or isopropyl alcohol, was studied by measuring the optical transmission of their hydrosols in the UV – near IR range. The extinction coefficient spectra exhibited a non-monotonous dynamics versus τ in case of water medium use and were correlated to SEM analysis of corresponding ablated surface spots and resulting NP size distributions, as well as with the single-shot ablation threshold values and 1/e-radii of ablated spots.

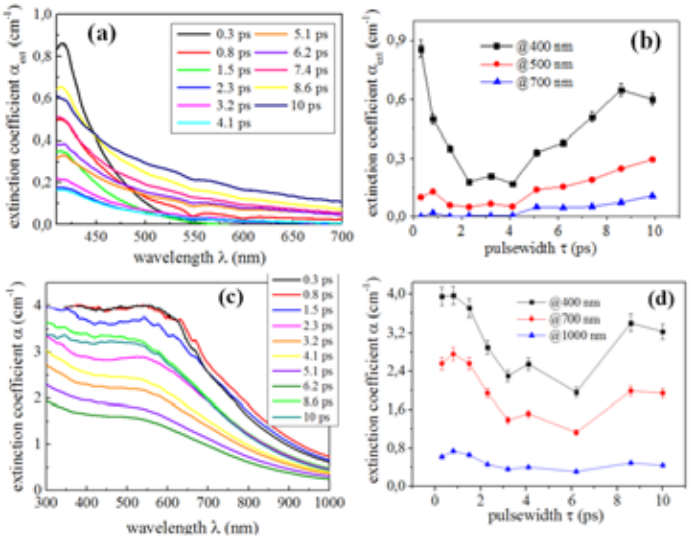

Fig. 1 Experimental extinction coefficient spectra of Ag (a) and Si (c) colloids, fabricated at different pulsewidths in water; the corresponding extinction coefficient αext as a function of τ (b, d).

The observed phenomenon may be explained by (1) the increase of ablation thresholds for the growing τ values; (2) laser filamentation in the liquid layer [1]; (3) ultrafast boiling of intact water layer near the target surface [2] at near-critical temperatures for water [3] on ps timescale. Different subsequent – nucleate and surface film boiling – temporal stages can differently perturb laser energy deposition into the target, with longer (> 4 ps) ps laser pulses providing energy deposition slow enough to yield in film boiling stage, more favourable for laser beam delivery to the ablation spot. However, laser pulses with intermediate τ, providing heating of the surface until the critical temperature of the water during their duration, can exert optical perturbation during the nucleate boiling stage.

This work was supported by the Russian Science Foundation (project no. 18-15-00220).

[1] A. A. A. Ionin, S. I. Kudryashov, S. V. Makarov, L. V. Seleznev, D. V. Sinitsyn, JETP Lett., 2009, 90, 423–427
[2] V. Kotaidis, C. Dahmen, G. von Plessen, F. Springer, A. Plech, J. Chem. Phys., 2006, 124, 184702.
[3] A. M. Lindenberg, S. Engemann, K. J. Gaffney, K. Sokolowski-Tinten, J. Larsson, P. B. Hillyard, D. A. Reis, D. M. Fritz, J. Arthur, R. A. Akre, M. J. George, A. Deb, P. H. Bucksbaum, J. Hajdu, D. A. Meyer, M. Nicoul, C. Blome, Th. Tschentscher, A. L. Cavalieri, R. W. Falcone, S. H. Lee, R. Pahl, J. Rudati, P. H. Fuoss, A. J. Nelson, P. Krejcik, D. P. Siddons, P. Lorazo, J. B. Hastings, Phys. Rev. Lett., 2008, 100, 135502.

P46

Micro-Sampling of Biological Tissue by Substrate-Mediated Laser Ablation: Toward Spatially-Resolved Proteomics at µm Scale

Tony MAULOUET[1,2], Cristian FOCSA[2], Michel SALZET[1], Isabelle FOURNIER[1], Michael ZISKIND[2]
[1]Laboratoire PRISM INSERM U1192, Université Lille 1, Villeneuve d'Ascq, France
[2]Laboratoire PhLAM-CNRS UMR 8523, Université Lille 1, Villeneuve d'Ascq, France

Contact: tony.maulouet@ed.univ-lille.fr

Since the pioneering works of R. Caprioli in 1997, conventional mass spectrometry imaging (MSI) tools resulting from Matrix-Assisted Laser Desorption/Ionization (MALDI) is widely used in various fields of -omics research (e.g. lipidomics, proteomics, metabolomics...) because of its high spatial resolution and detection sensitivity. However, due to the inherent complexity of the biological tissue, it has certain limitations. One of the major drawbacks of the technique is the limited capability of detecting and identifying minority compounds, notably proteins, directly on tissue. Various strategies have been developed to overcome this issue. All require a micro-sampling step. Different techniques have explicitly been applied for this purpose like laser capture microdissection, liquid extraction or parafilm assisted microdissection (PAM) [1]. However, the spatial resolution of these techniques is typically about 1mm, and it is a real challenge to develop a tool with sufficient yield to reduce the size of the sampled area.

We have explored the potential of a new micro-sampling technique based on an indirect substrate-mediated laser ablation (SMLA) mechanism which permits the use of low deposited energy while preserving the biological content. Taking advantage of this effect, analyses of micro-sampled tissue was performed, demonstrating the identification of a significant number of proteins [2]. Furthermore, SMLA was confronted with PAM in order to show its efficiency.

Our objective is now to increase the spatial resolution up to µm scale. This requires the characterization of the SMLA mechanism to optimize the ablation yields. We present here recent advances in this field including systematic studies taking into account the physicochemical parameters of various substrates who highlight the role of the ablation of the substrate in the SMLA mechanism and the study of the plume dynamic by shadowgraphy used to improve the capture yield of the ablated material.

[1] Quanico J *et al.* Integrated mass spectrometry imaging and omics workflows on the same tissue section using grid-aided, parafilm-assisted microdissection. Biochim Biophys Acta. 2017 Jul;1861(7):1702-1714. DOI: 10.1016/j.bbagen.2017

[2] Fatou, B. *et al.* **Substrate-Mediated Laser Ablation under Ambient Conditions for Spatially-Resolved Tissue Proteomics.** *Sci. Rep.* **5**, 18135; DOI: 10.1038/srep18135 (2015).

P47

Contact laser surgery of oncological tumors with a minimum of dissemination of tumor in the operating field on the basis of the technology of the absorbing layer at the tip of quartz fiber

Vladislav Kamensky*, Vladimir Bredikhin, Vadim Elagin, Nikita Bityurin
Institute of Applied Physics of the Russian Academy of Sciences

Corresponding author: vlad@ufp.appl.sci-nnov.ru

We have developed a new technique for bloodless resection of biological tissue in a contact mode, in which cutting is performed by the lateral edge of a strongly heated multi-mode silica fiber [1]. The fiber tip is heated due to absorption of laser radiation in a special (resistant to mechanical loads at high temperatures) layer deposited onto the fiber's tip. We have developed a theoretical model of the laser cutting process of biological tissue by a silica fiber tip, including a fiber tip with a strongly absorbing coating (SAC) [2]. This theoretical model is different from the laser ablation model in that in our case a softened (due to high temperature) tissue is mainly separated by the silica fiber tip, not ablated, as is the case with the laser ablation. A strong dependence of the cutting speed on the angle of inclination of the scalpel relative to the tissue surface was shown experimentally and theoretically in highly scattering media when scattering exceeds absorption in biological tissue. The main purpose was an experimental assessment of the possibility to use the "indirect" contact laser surgery for tumor excision under fluorescence image guidance. Mouse colon adenocarcinoma CT-26 cells stably expressing fluorescent protein mKate-2 were used as a tumor model. The resection of the tumor node was performed with a laser scalpel with a SAC on the fiber tip. The presence of tumor in the surgical field was evaluated by fluorescence imaging system IVIS® Spectrum using the fluorescence band mKate-2. Fluorescence imaging of the tumor bed performed after resection to assess the presence of tumor cell clusters is sufficiently effective only with a bloodless resection. The bloodless tumor resection in mice was obtained by using the SAC fiber tip. When using the technique for tumor removal with the contact laser scalpel and intraoperative fluorescence control, cancer recurrence occurred in one of five cases.

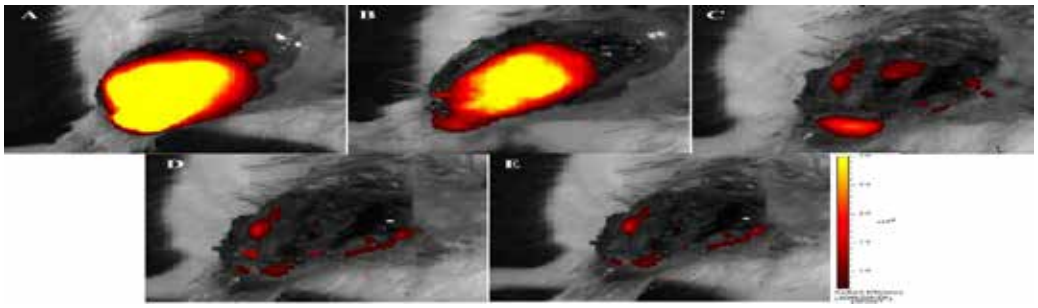

Fluorescence images of the tumor during resection using a laser scalpel with SAC: a – before resection, b – surgical field after the first resection, c – surgical field after the second resection

The work was supported by the RSF grant No. 14-15-00840

[1] V Bredikhin, V Kamensky, N Sapogova, V Elagin, M Shakhova, N. Bityurin. Indirect laser surgery Applied Physics A 122 (3)
[2] N Sapogova, V Bredikhin, N Bityurin, V Kamensky, V Zhigarcov, V.Yusupov. Model for indirect laser surgery Biomedical Optics Express 8 (1), 104-111

P48

2D mesoscale colloidal crystal patterns on polymer substrates due to control of wettability of materials by UV treatment

Vladimir I. Bredikhin*, Nikita Bityurin
Institute of Applied Physics RAS, Nizhny Novgorod, Russia
Corresponding author: bredikh@appl.sci-nnov.ru

It was shown [1] that the wettability of hydrophobic materials (in particular, polymetilmeta-acrylate (PMMA)) may be controlled by UV (ultra violet) λ<240 nm treatment. In experiments, the contact angle θ was decreased down to ~ 30 degrees after irradiation of the material surface either by a UV lamp or by the fifth harmonic of an Nd:YAG laser (λ=213 nm). UV stimulated hydrophilicity of PMMA after UV irradiation is connected with the surface oxidation.

The possibility of hydrophilicity control can be used in various technologies, such as liquid coating, printing, spray quenching, nanolithography, pharmacology and others.

In the present work, we use the above phenomenon for producing 2D mesoscale colloidal crystal patterns of monolayer colloidal crystals of micro size particles on polymer substrates. Until now, there were known technologies for a continuous uniform monolayer on hydro filling materials only.

UV irradiation of the PMMA surface through a mask allows creating 2D patterns consisting of mesoscale cells of different wettability. We present a new method [2] of deposition of a monolayer of colloidal particles on the substrate that provides formation of a two-dimensional array of self-assembled microparticles (polystyrene microspheres 1 μm) only on the irradiated (hydrophilic) parts of the surface, leaving unirradiated (hydrophobic) ones intact.

The example of the obtained 2D mesoscale colloidal crystal pattern is shown in Fig.1. This approach can be useful in different applications of nanosphere lithography.

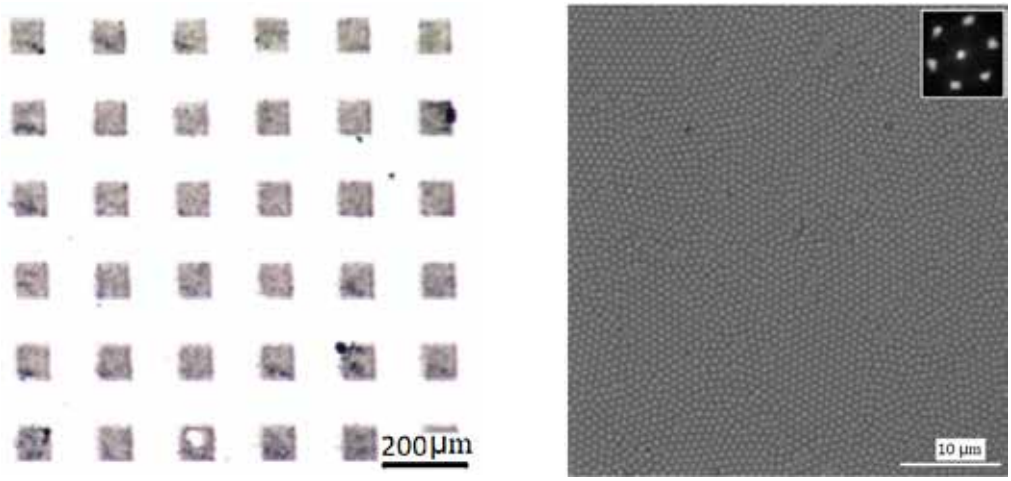

a) b)

Fig. 1. (a), (b). 0.96 μm PS microspheres on PMMA substrate: a) the microspheres are deposited only on the UV irradiated parts of the surface, microphotograph; (b) microstructure of the structure elements (the total area of the structure is ~ 5 cm^2). The inset: diffraction of a focused beam λ=0.532 μm on a monolayer of microspheres.

The research was supported by the RFBR (grants 16-02-00792 and 18-02-00806).

[1] VI Bredikhin, NM Bityurin, International Journal of Engineering Research & Science (IJOER) 3 (11), 82-87, 2017. DOI 10.1007/978-3-642-34243-1_1.
[2] VI Bredikhin, N Bityurin, Materials Research Express 5, 05536, 2018. https://doi.org/10.1088/2053-1591/aac1e9.

P49

Patterning of Photoinduced Nanocomposites by Focused Laser Beam: a Model

Alexander Pikulin*, Anton A. Smirnov, Nikita Bityurin
Institute of Applied Physics of the Russian Academy of Sciences, 46 Ul'yanov Str, 603950, Nizhny Novgorod, Russia

Corresponding author: pikulin@ufp.appl.sci-nnov.ru

Metal or semiconductor nanoparticles (NPs) can be instantly generated in photoinduced nanocomposite polymers under the irradiation by light. The light causes the photodestruction of the precursor molecules dissolved in the matrix. As a result, some elementary species (such as atoms of metal) are released and then precipitate into the NPs right within the polymer. Recently, we have shown theoretically that by inducing inhomogeneities within the matrix, one can tailor the spatial distributions of the generated NPs even under the spatially-uniform light irradiation.[1] Another way to pattern such materials is the local irradiation by the laser light. For that, either focused beams or near-field optics can be employed. In this work, we consider the kinetics of the localized NP generation theoretically under the prolonged irradiation by the focused continuous-wave or pulsed laser light. The NP concentration and size spatial distributions are studied. The locally generated elementary species tend to leave the irradiated zone due to the diffusion. However, if the precursor concentration is high enough, the growing NPs act as traps for elementary species thus impeding this delocalization effect.[2] It is found that the optimal beam power is determined by the balance between the depletion rate of the precursor within the irradiated spot and its diffusion flux from the surrounding volume. The variation of the beam power around the optimum determines the shape of the domain where the precursor molecules are destructed, and the NPs are formed. For instance, one can populate the hollow volume with NPs, leaving the center untouched. This can be useful for the fabrication of core-shell systems. This work was supported by the Russian Science Foundation (RSF) under project No. 14-19-01702.

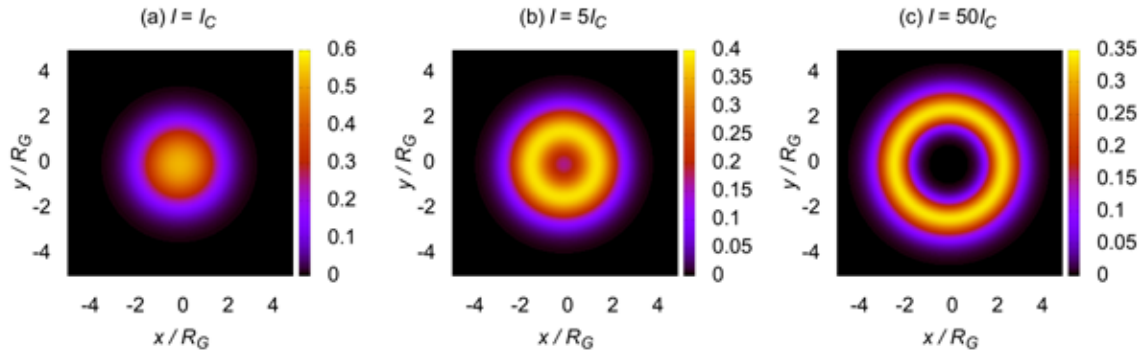

Fig. 1 (a) Stationary rate (in dimensionless units) of the elementary species generation calculated for a dynamical balance between the precursor depletion under the local laser irradiation and its diffusion from the surrounding volume. The spatial coordinates are normalized by the radius of the irradiated domain. The beam intensity I is set at the optimal level I_c (a) and above the optimal level (b,c).

[1] N. Sapogova, A. Pikulin, A. A. Smirnov, N. Bityurin, Diffusion-controlled alteration of inhomogeneous materials: tailoring of the spatial distribution of nanoparticles in nanocomposites. *Phys. Chem. Chem. Phys.* **18**, 32921–32930 (2016).
[2] A. A. Smirnov, A. Pikulin, N. Bityurin, Spatial localization of nanoparticle growth in photoinduced nanocomposites. *Appl. Phys. A* **124**, 117 (2018).

P50

In-situ monitoring of the evolution of optical properties of UV LED irradiated polymer-based photoinduced nanocomposites

Anton A. Smirnov[1*], Andrey Kudryashov[1], Andrey Afanasiev[1], Nickolai Ermolaev[1], Nadezhda Agareva[1], Sergey Gusev[2], Dmitry Tatarskiy[2], and Nikita Bityurin[1]

[1] Institute of Applied Physics of Russian Academy of Sciences, 46 Ul'yanov Street, 603950 Nizhny Novgorod, Russia

[2] Institute for Physics of Microstructures of Russian Academy of Sciences, GSP-105, 603950 Nizhny Novgorod, Russia

Corresponding author: antonsmirnov@ufp.appl.sci-nnov.ru

Photoinduced nanocomposites are initially transparent polymeric materials possessing the specially designed precursor molecules. UV irradiation leads to the destruction of the precursor followed by the nanoparticles growth within the initially homogeneous media.

In the present work, we use UV-LED (365 nm) for the irradiation [1]. Current LED production technologies to provide light sources, which are stable, cheap, compact and very often are suitable to replace mercury lamps and lasers. A specially designed experimental setup allows UV and thermal treatment of a sample film simultaneously [2]. We monitor the evolution of the absorbance spectra in all visible range using the combination of a white LED, and UV LED. The presence of polymer and high thickness of a sample make it difficult to observe in situ the nanoparticle formation in the material by means of TEM and XRD techniques. Optical properties monitoring seems to be the only non-destructive method for that. We study the UV induced formation of different kinds of nanoparticles using different kinds of precursors. They are a good soluble CdS precursor, an Ag precursor, an Au precursor, and composites containing a combination of the Au and CdS precursors. The detailed study of absorbance evolution during UV irradiation of these materials can shed light upon the mechanisms of nanoparticles formation. Fig. 1 shows the evolution of absorbance spectra of the material containing a CdS precursor (a) and an Ag precursor (b). The red shift of the spectrum in the former case corresponds to semiconductor nanoparticle growth. The evolution of the spectra in the latter case corresponds to the growth of plasmonic nanoparticles. Additional a posteriori TEM and HR TEM investigations help to interpret the experimental data obtained in situ.

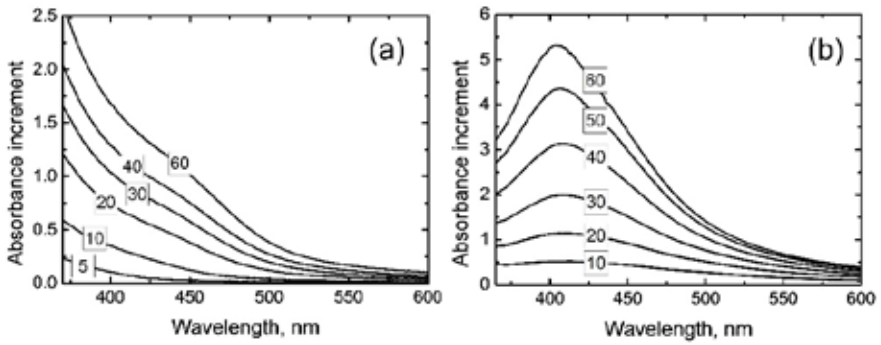

Fig. 1 (a) The evolution of the absorption spectra of the polymer film with the precursor chosen for CdS nanoclusters formation during UV irradiation at 90 ^{0}C. (b) The evolution of the absorption spectra of the PMMA film with the silver trifluoroacetate during UV irradiation at 70 ^{0}C. The exposure time (minutes) is indicated on the plots.

The work is supported by Russian Science Foundation (Grant No. 14-19-01702)

[1] A.A. Smirnov, A. Afanasiev, N. Ermolaev and N. Bityurin, LED induced green luminescence in visually transparent PMMA films with CdS precursor, Opt. Mater. Express. **6**(1), 290-295 (2016)

[2] A.A. Smirnov, A. Afanasiev, S. Gusev, D. Tatarskiy, N. Ermolaev and N. Bityurin, Exposure dependence of the UV initiated optical absorption increase in polymer films with a soluble CdS precursor and its relation to the photoinduced nanoparticle growth, Opt. Mater. Express (2018) in print

P51

Nanopattern formation by local laser annealing of diblock copolymer (BCB) films

Klaus Zimmer[1], Joachim Zajadacz[1], Andre Mayer[3], Christian Steinberg[3], Hui-Fang Chang[2], Ji-Yen Cheng[2], Hella-Christin Scheer[3]

[1] Leibniz Institute of Surface Engineering *(IOM)*, Permoserstr. 15, D-04318 Leipzig, Germany
[2] Research Center for Applied Sciences, Academia Sinica, Taipei 11529, Taiwan
[3] Department of Electrical and Information Engineering, University of Wuppertal, Rainer-Gruenter-Str. 21, D-42119 Wuppertal, Germany
Corresponding author: klaus.zimmer@iom-leipzig.de

The nanopatterning of surfaces to achieve pattern less than 100 nm is challenging in particular for direct laser writing techniques. Self-assembly processes, however, provide a mechanism of pattern generation in this dimensional range, enabling an alternative fabrication route that is also suitable for large-area, low-cost fabrication.

The current work focuses on studies of laser-annealing of BCP films to achieve self-assembly into vertical lamellas with periods in the range of 50 nm. For the study of this high-temperature, short-time process ~60 nm thick BCP films are prepared by a standard process onto fused silica that was irradiated after that by a CO_2-laser studying the impact of the laser power and the scanning speed on the self-assembly process. The experimental results were analysed in relation to already known processes that can be induced by laser irradiation. Combining the relevant one a mechanism of the laser annealing process will be proposed.

Thermal simulations of the laser heating and additional involved processes were used for discussion the experimental results. Combining local heating by laser beams can provide a tool for direct writing of hierarchical nano-microscale patterns that can be utilized for different applications.

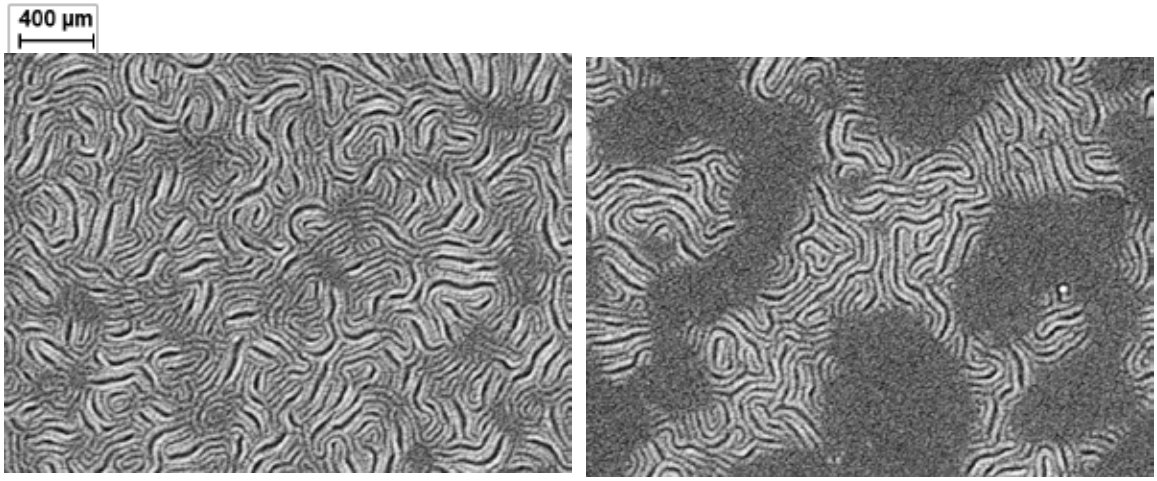

Fig. 1: SEM images of laser-annealed BCP films featuring the vertical lamellas that result from microphase separation at neutral fused silica substrates.

P52

Control of wettability on PLLA surface by femtosecond laser irradiation for development of advanced implant devices

Yuji Sato[1], Keisuke Takenaka[2], Masahiro Tsukamoto[1], Kensuke Murai[3]
[1]Joining and Welding Research Institute, Osaka University, (11-1 Mihogaoka, Ibaraki, Osaka 567-0047, Japan)
[2]Graduate School of Engineering, (Osaka University, 1-1 Yamadaoka, Suita, Osaka, 565-0871, Japan)
[3] AIST Kansai4, (1-32 Higashikagatsumemachi Kanazawa Ishikawa 920-0209, Japan)

Corresponding author: sato@jwri.osaka-u.ac.jp

A poly-L- lactic acid (PLLA) film, which has been clinically applied for a bioabsorbable suture and a bone fixation material, because of its excellent properties, such as biocompatibility, processability and biodegradability. However, it takes time to form a fibrous tissue for bone due to cell adhesion of random direction on PLLA surface. Bone tissue formation may be enhanced if cell spreading direction of an osteoblast can be controlled in the orientation of bone formation. Thus, periodic nanostructures were formed on the interface between the PLLA film and a titanium (Ti) plate surface by using the femtosecond laser at the wavelength of 800 nm. A Ti:sapphire laser of which wavelength, pulse duration and repetition rate were 800 nm, 150fs and 1 kHz, respectively, was employed in our experiments. The PLLA which was 1mm thickness was contacted with Ti plate by using a contact jig at a pressure of 1800 kN/m^2. Then the laser beam was focused on the Ti plate passing through the PLLA film using a plano-convex lens with a focal length of 100mm. The Gaussian laser beam has a diameter of 110 µm at the 1/e^2 intensity point. Fig.1 shows scanning microscope images for (a) before and (b) after laser irradiation. The bare surfaces of the PLLA film are smooth and do not exhibit periodic structures. After laser irradiation at the laser fluence of 0.25 J/cm^2 and scanning speed of 3.0 mm/s in Fig.1 (b), the nanostructures at a periodicity of 415 nm and depth of 50 nm, were exhibited on the PLLA surface. In order to investigate wettability, a contact angle with water on the PLLA surface was measured. As the results, the contact angle with water on the PLLA film with periodic nanostructures became 91 degrees from 71 degrees of non-treated PLLA surface.

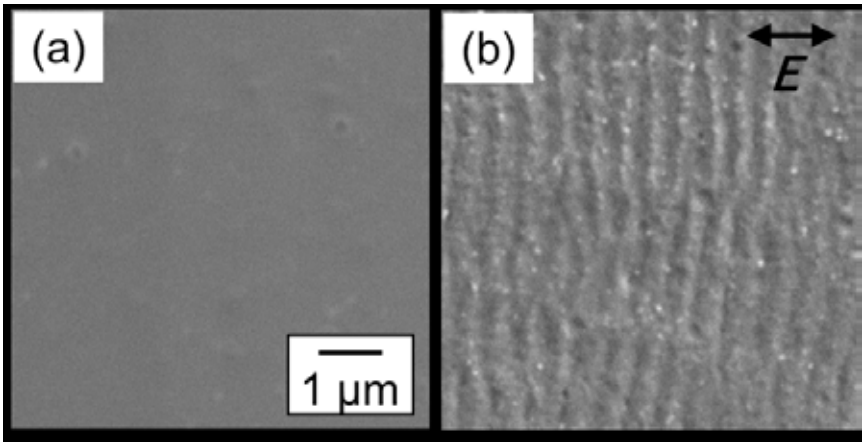

Fig. 1 SEM images (a) before and (b) after laser irradiation at the laser fluence of 0.25 mJ/cm2, scanning speed of 3.0 mm/s.

P53

Fabrication of Elastomeric Structures via Stereolithography and Optimization of their Biocompatibility

Giedrė Grigalevičiūtė1, Daiva Baltriukienė2, Linas Jonušauskas1 and Mangirdas Malinauskas1

1Vilnius University, Laser Research Center, Sauletekio Ave. 10, Vilnius, Lithuania
2Vilnius University, Life Sciences Center, Sauletekio Ave. 7, Vilnius, Lithuania
Corresponding author: giedre.grigaleviciute@gmail.com

Recently diverse 3D printing technologies have received a lot of attention in the areas of science and industry. Differently from traditional processes of manufacturing, 3D printing allows fabrication of arbitrary geometry objects, using computer aided design and spatial formation of the structures layer-by-layer. It can be applied in various fields. One of them is medicine, where 3D printed objects have already made a great influence in such areas as orthopedics [1], face and skull reconstruction, plastic, teeth and mouth surgeries [2], etc.

Cells can be seeded into 3D printed structures and artificial tissue or organ can be grown and implanted into human body. Currently, there is a lack of elastomeric photostructurable resins that would fit for tissue engineering requirements for scaffolds [3]. However, optimizing biocompatibility of existing commercial resin would make a great influence.

In this work the biocompatibility tests of photostructured commercial elastomeric resin Formlabs Flexible were investigated [4]. 3D printer Autodesk Ember was used as a photopolymerization setup. Fabricated structures were soaked in isopropanol and methanol for different conditions (temperature, duration) in order to leach out unpolymerized monomers. Also printed structures were additionally UV exposed. Post-processed structures were seeded with cells and the number of live cells was evaluated as an indicator for the material biocompatibility.

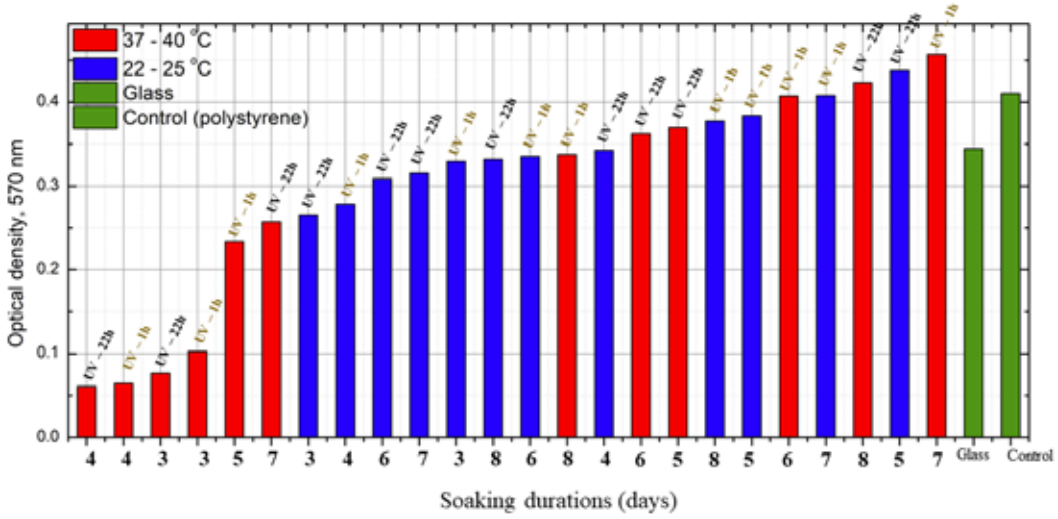

Fig. 1 (a) Biocompatibility tests results with different soaking conditions (temperature, duration) and different UV post-exposure durations.

Acknowledgments. Financial support by a project “ReSoft” (SEN-13/2015) from the Research Council of Lithuania. Giedrė Grigalevičiūtė acknowledges the Research Council of Lithuania and EU Investments Fund (grant No. 09.3.3-LMT-K-712-03-0064).

[1] F. Auricchio et al, EFORT Open Reviews 1(5), 121–127 (2016).
[2] Y. Wang et al, Biomed. Res. Int. 2017, 1–8 (2017).
[3] Samand Pashneh-Tala et al, Front. Phys., 6:41, 08 May (2018).
[4] G. Grigalevičiūtė et al, Proc. SPIE 10544, 105441E (2018).

P54

Nanometric z-profiling of Bio-chromophore layers by DRLS

Aaron Peled* and Simona A. Popescu

Photonics Laboratory, Engineering Faculty, Holon Institute of Technology, Holon 5810210, Israel
*Corresponding author: peled@hit.ac.il

In this work, the previously developed DELI evanescent technique [1] is upgraded to a more general optical microscope technique named differential back-scattering of light intensity (DRLS) for evaluating optically the nanometric layers profiles deposited onto any optically flat substrate. The sample is illuminated preferentially with a p-polarized light beam with a top x-y plane projected spatial intensity $I_z(x,y,0)=I_0$. At a critical angle from the normal to the x-y plane, an optimized z-profile optical density contrast is achieved. Similar to the DELI case, the z-axis differential *backscattered* light intensity element $dI_z(x,y,z)$ collected from the nanolayer particles by the microscope objective is assumed proportional to $\gamma\cdot[I_0(x,y,0)-I_z(x,y,z)]$. The light intensity also decays through the layer along the z-axis with a total absorption coefficient α, providing the following differential equation:

$$\frac{\partial I_z(x,y,y)}{\partial z}=\gamma\cdot[I_0\cdot e^{-\alpha z}-I_z(x,y,z)] \quad (1)$$

Solving the differential equation (1) by integration through the deposited layer from $z=0$ to its film depth contour profile $h(x,y)$ at any projected point (x,y) on the substrate, with the top *backscattered* border value of $I_z(x,y,0)=0$ gives the following analytic solution for the collected intensity by the microscope objective:

$$I_z(x,y)=I_0(x,y)\frac{\gamma}{\gamma-\alpha}\left(e^{-\alpha h(x,y)}-e^{-\gamma h(x,y)}\right) \quad (2)$$

The scattering constant γ is sought either theoretically, or otherwise experimentally by calibration, enabling then the mapping of the nanolayer thickness z-profile on the substrate plane i, e., $h(x,y)$. For negligible optical absorption in the layer, a condition often met in thin semitransparent bio-nanometric layers, one obtains:

$$h(x,y)=-\frac{1}{\gamma}\ln\left[\left(1-\frac{I_z(x,y)}{I_0}\right)\right] \quad (3)$$

A synthesized 3D profile image using the DRLS formalism for a bio-chromophore grating sample with a top mean height of 80 nm is given in the figure below.

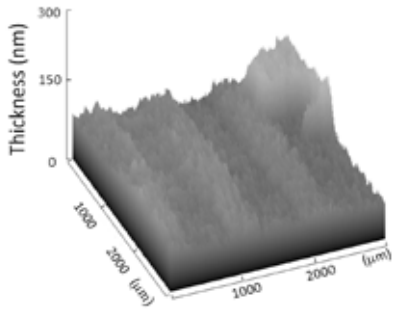

[1] N. Mirchin and A. Peled, Journal of Advanced Microscopy Research **7**, 1–6, (2012).

P55

Antibacterial effect of nanostructured silicon

Alena Nastulyavichus[1], Irina Saraeva[1], Sergey Kudryashov[1,2], Etery Tolordava[3], Nikita Smirnov[1], Andrey Rudenko[1], Andrey Ionin[1], Dmitryi Zayarny[1],Yuliya Romanova[3]

[1] Lebedev Physical Institute, Leninskiy prospect 53, 119991 Moscow, Russia

[2] ITMO University, Kronverkskiy prospect 49, 197101 St. Petersburg, Russia

[3] N.F. Gamaleya Federal Research Centre of Epidemiology and Microbiology, Gamalei street 18, 123098 Moscow, Russia

Corresponding author: ganuary_moon@mail.ru

Biofilms represent a great threat due to resistance to many methods of dealing with them, including the action of antibiotics. Artificial nanoimprinted structures formed under the action of laser radiation on the surfaces of a wide variety of materials - metals, semiconductors, polymers, in recent years have shown the high effectiveness of preventing from biofilm formation on nanostructured surfaces [1]. It is known that crystals of black silicon very effectively destroy various microbes, including deadly Staphylococcus aureus.

In this paper, the nanosheets were obtained by laser ablation of a silicon wafer in carbon disulphide (Fig.1a). The source of radiation was a Yb-fiber femtosecond laser with a wavelength of 1030 nm, an FWHM of a pulse of 200 fs, a maximum pulse energy of 10 μJ, and a repetition rate of 0–2 MHz.

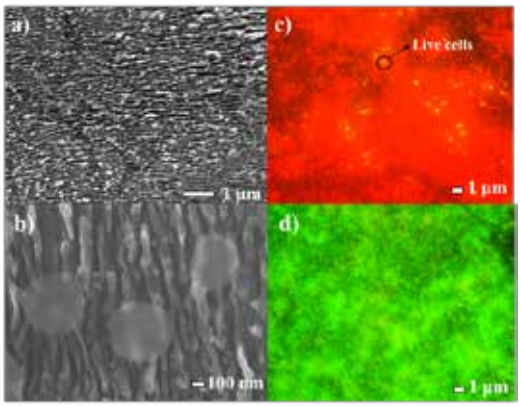

Fig. 1 (a) SEM-image of silicon nanosheets. (b) SEM-image of silicon nanosheets+bacteria. (c) Optical images of assays of live (green) and dead (red) cells in bacterial biofilms. (d)bare silicon slide.

Received samples were tested regarding their antibacterial impact on Gram-positive (Staphylococcus aureus) bacteria biofilms. A coloration set «Live/Dead Biofilm Viability Kit» allows the differentiation between viable and non-viable bacteria in the biofilms [2]. The staining method is based on the ability of the two different dyes to penetrate into the bacterial cells. Green corresponds to living cells, red-dead.

This work was supported by Russian Science Foundation (grant #18-15-00220).

[1] E.Ivanova, J. Hasan, H. Webb, Vi. Truong, G. Watson, J. Watson, V. Baulin, S. Pogodin, J. Wang, M. Tobin, Ch Löbbe, R. Crawford. Natural bactericidal surfaces: mechanical rupture of Pseudomonas aeruginosa cells by cicada wings. *Small* V8 (16) 2489-2494 (2012)

[2] A.A. Ionin, A.K. Ivanova, R.A. Khmel'nitskii, Yu.V. Klevkov, S.I. Kudryashov, A.O. Levchenko, A.A. Nastulyavichus, A.A. Rudenko, I.N. Saraeva, N.A. Smirnov, D. A. Zayarny, S.A. Gonchukov, E.R. Tolordava, Antibacterial effect of the laser-generated Se nanocoatings on S. aureus and P. aeruginosa biofilms, Laser physics letters, 15(1), (2018).

P56

Nanosecond and femtosecond laser ablation of silver films of variable thickness

Alena Nastulyavichus[1], Sergey Kudryashov[1,2], Nikita Smirnov[1], Irina Saraeva[1], Andrey Rudenko[1], Alexander Kharin[3], Andrey Ionin[1], Dmitryi Zayarny[1]

[1] Lebedev Physical Institute, Leninskiy prospect 53, 119991 Moscow, Russia

[2] ITMO University, Kronverkskiy prospect 49, 197101 St. Petersburg, Russia

[3] National research nuclear university MEPhI (Moscow Engineering Physics Institute), Kashirskoe shosse 31, 115409 Moscow, Russia

Corresponding author: ganuary_moon@mail.ru

At present, pulsed laser ablation in a liquid is a popular method for obtaining nanoparticles because it has a number of advantages [1-3]. The choice of the regime has a great influence on the characteristics of the produced particles.

Colloidal solutions of silver nanoparticles were generated in water from silver films of variable thickness at different intensities both of a nanosecond fiber laser marker (Bulat) on Yb3+ ions and a Yb-fiber femtosecond laser. For comparison, different scanning speeds were chosen. Silver thin films were produced by magnetron sputtering in an argon atmosphere on SiO_2 substrates. The target was arranged in a glass beaker with deionized water of a volume ≈2.5 ml (height above the target ≈ 1 cm). The laser beam was focused through the liquid layer onto the target surface (Fig. 1a). The obtained colloidal nanoparticles were characterized by scanning electron microscopy (Fig.1b), optical transmission spectroscopy, and dynamic light scattering. The chemical composition was confirmed by energydispersive x-ray spectroscopic chemical microanalysis (EDS) using the INCA module (Oxford Instruments, England) of the electron microscope.

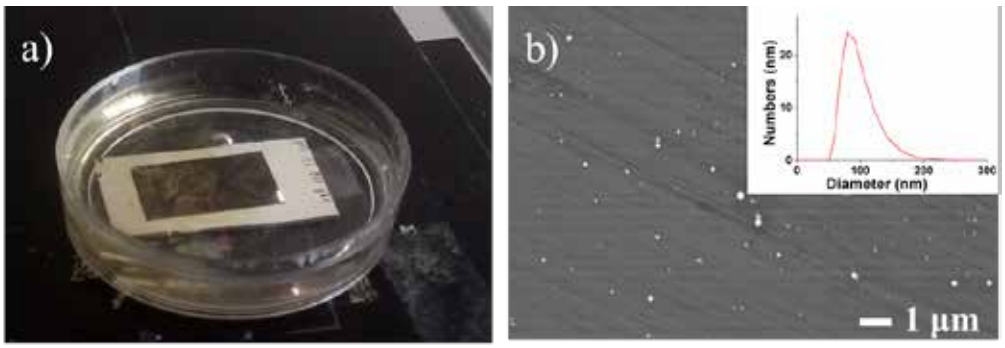

Fig.1 (a) Image of the ablation region in the course of laser exposure (b) SEM-image of deposited nanoparticles and the particle size distribution function

This work was supported by Russian Science Foundation (grant #18-15-00220).

[1] A. Hahn, S. Barcikowski, and B. Chichkov, Influences on Nanoparticle Production during Pulsed Laser Ablation, JLMN-Journal of Laser Micro/Nanoengineering. 3, No. 2 73-77 (2008)

[2] J. Pfleger, P Smejkal, B. Vlckova, M. Slouf, Preparation of Ag nanoparticles by two-wavelength laser ablation and fragmentation, Proc. SPIE. 5122 198-205 (2003)

[3] A. Ionin, A. Ivanova, R. Khmel'nitskii, Y. Klevkov, S. Kudryashov, N. Mel'nik, A. Nastulyavichus, A. Rudenko, I, Saraeva, N. Smirnov, D. Zayarny, A. Baranov, D. Kirilenko, P. Brunkov, A. Shakhmin, Milligram-per-second femtosecond laser production of Se nanoparticle inks and ink-jet printing of nanophotonic 2D-patterns, Applied Surface Science, vol. 436, pp. 662-669, (2018).

P57

Femtosecond laser fabrication, spectral characterization and modeling of plasmonic nanostructures

Nikolay Busleev[1,3], Pavel Danilov[1], Irina Saraeva[1,3], Sergey Kudryashov[1], Andrey Ionin[1], Sophia Umanskaya[1,3], Dmitry Zayarny[1,3], Alexey Porfirev[2,3], Alex Kuchmizhak[3], Svetlana Khonina[2,3]

[1]Lebedev Physical Institute, 53 Leninskiy Prospekt, 119991 Moscow, Russia
[2]IPSI RAS – Branch of the FSRC "Crystallography and Photonics" RAS, 443001 Samara, Russia
[3]Samara National Research University, 443086 Samara, Russia

Corresponding author: nbusleev@lebedev.ru

A number of methods for generating laser beams, which allowed solving the problem of laser fabrication of "two-dimensional" structures in the form of rings on the surface of a substrate with a nanoparticle located in the center, were proposed and investigated [1-4]. One of the proposed methods is to use the S-wave plate, an element that allows the formation of a radially or azimuthally polarized laser beam with a circular intensity distribution. Using a laser beam formed by such an element, various types of nanoparticles were created by single-pulse laser ablation regime. Azimuthally polarized pulses create on the surface of a substrate with a deposited silver film a nanoneedle with a very small tip curvature radius. Radially polarized pulses create on the surface of a substrate with a deposited gold film a nanodisk surrounded by an annular region with the removed film material. Vortex pulses create on the surface of a substrate with a deposited either gold or silver film a twisted "nanoneedle". The effect of the energy flux magnitude in the initial radiation on the parameters of the formed structures was investigated. It was shown that the increase in the energy flux magnitude leads to an increase in the aspect ratio of the nanoneedles formed by azimuthally polarized pulses. In the case of radially polarized pulses, under the same conditions, the characteristic sizes of the formed nanodisks decrease.

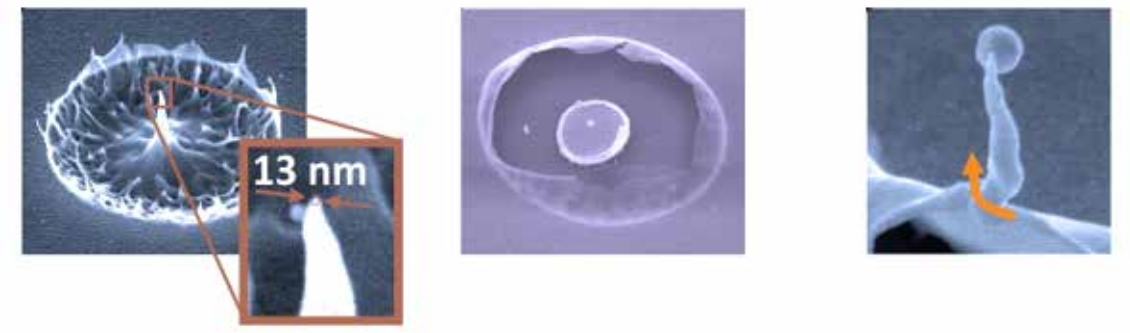

Figure 1: Examples of fs-laser ablation of thin metal films. (a) Azimuthally polarized laser beam. (b) A radially polarized laser beam. (c) Vortex laser beam.

The difference in the distribution of electric and magnetic near fields for such structures depending on the type of metal was investigated by numerical methods.

This work was supported by Russian Science Foundation (grant #17-12-01258).

[1] P. Danilov et al., Polarization-selective excitation of dye luminescence on golden film by structured ultrashort laser pulses. *JETP Letters* **vol. 107**, pp. 18-22 (2018). DOI: 10.7868/S0370274X18010046
[2] S. Syubaev et al., Direct laser printing of chiral plasmonic nanojets by vortex beams. *Optics Express* **vol. 25**, pp. 10214-10223 (2017). DOI: 10.1364/OE.25.010214
[3] A. Kuchmizhak et al., Multi-beam pulsed-laser patterning of plasmonic films using broadband diffractive optical elements. *Optics Letters* **vol. 42**, pp. 2838-2841 (2017). DOI: 10.1364/OL.42.002838
[4] S. Syubaev et al., Zero-orbital-angular-momentum laser printing of chiral nanoneedles. *Optics Letters* **vol. 42**, pp. 5022-5025 (2017). DOI: 10.1364/OL.42.005022

P58

High-efficiency Fabrication of Geometric Phase Spiral Phase Plates by Femtosecond Laser

Jian-Guan Hua[1], Zhen-Nan Tian[1], Qi-Dai Chen[1*]
[1]State Key Laboratory of Integrated Optoelectronics, College of Electronic Science and Engineering, Jilin University, Changchun 130012, China
Corresponding author: chenqd@jlu.edu.cn

The vortex beam has a wide range of applications in the field of optical manipulation and optical communication due to the helical phase plane and the orbital angular momentum. One important way to create a vortex beam is through a spiral phase plate. Geometric phase spiral phase plates have caused extensive research due to their polarization characteristics. In this paper, the geometric phase spiral phase plates with different topological charge numbers were efficiently fabricated on the surface of 50 nm thick gold film by femtosecond laser direct writing technology. The phase was controlled by the direction of the sub-wavelength grating in each sector. The sub-wavelength grating period is 800 nm. The diameter of the entire phase plate is 400 *m*m. At the same time, the helical phase distributions were obtained by optical interference test with a 633 nm laser, which verified the optical performance of the phase plate. The femtosecond laser galvanometer processing system enables the efficient preparation of the phase plate elements, with a single device processing time of less than one minute.

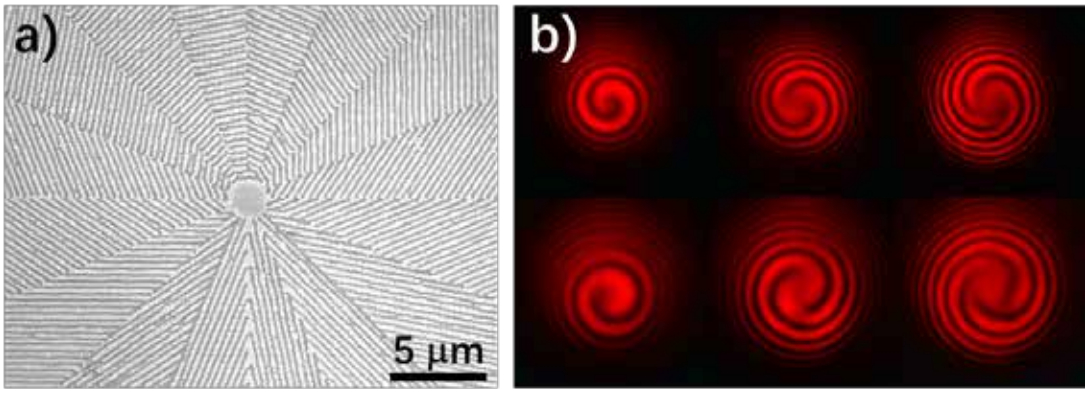

Fig. 1 (a) The SEM photograph of the geometric phase spiral phase plate. (b) Wavefront testing pictures of spiral phase plates.

In conclusion, the geometric phases spiral phase plates with topological charge numbers of ±1, ±2, and ±3 were efficiently fabricated by femtosecond laser direct writing. The optical properties of the elements were verified by the optical test, and the vortex beam can be generated. With the femtosecond laser galvo processing system, the average processing time for a device was 40 s or so. Compared with other processing technologies, the processing efficiency has been significantly improved. In addition, this method would actively promote the application of the element.

[1] X. W. Wang, A. A. Kuchmizhak, E. Brasselet, S. Juodkazis, Dielectric geometric phase optical elements fabricated by femtosecond direct laser writing in photoresists, *Appl. Phys. Lett.* 110, 181101 (2017).
[2] D. Wu, J. N.Wang, S. Z. Wu, Q. D. Chen, S. Zhao, H. Zhang, H. B. Sun, L. Jiang, Three-level biomimetic rice leaf surfaces with controllable anisotropic sliding, *Adv. Funct. Mater.* 21, 2927-2932 (2011)
[3] Y. L. Zhang, Q. D. Chen, H. Xia, H. B. Sun, Designable 3D nanofabrication by femtosecond laser direct writing, *Nano Today* 5, 15-20 (2010).

P59

High-throughput ablative pulsed-laser pattering of various nanoplasmonic films.

Pavel A. Danilov[1], Sergey I. Kudryashov[1], Alexander A. Kuchmizhak[2], Andrey A. Rudenko[1], Svetlana N. Khonina[3], Alexey P. Porfirev[3,4], Sofia F. Umanskaya[1,3,5]

[1]P.N. Lebedev Physical Institute of RAS, 119991, Russia, Moscow, 53, Leninskiy Prospect
[2]Institute of Automation and Control Processes, Far Eastern Branch, Russian Academy of Sciences, 690041, Russia, Vladivostok, 5, Radio st
[3]Samara National Research University, 443086, Russia, Samara, 34, Moskovskoe shosse
[4]Image Processing Systems Institute of the RAS branch of FSRC "Crystallography&Photonics" of the RAS, 443001, Russia, Samara, 151 Molodogvardeyskaya st.
[5]National Research Nuclear University MEPHi, 115409, Russia, Moscow, 31, Kashirskoe shosse
Corresponding author: pavel-danilov2009@yandex.ru

Single tightly focused short and ultrashort laser pulses are used to fabricate different types of nanostructures: microbumps, nanojets, nanocrowns, micro – and nanoholes and their regular arrays. The ability to control the intensity distribution, phase distribution and polarization of the laser beam are very important for creating metacoatings or metasurfaces [1-3].

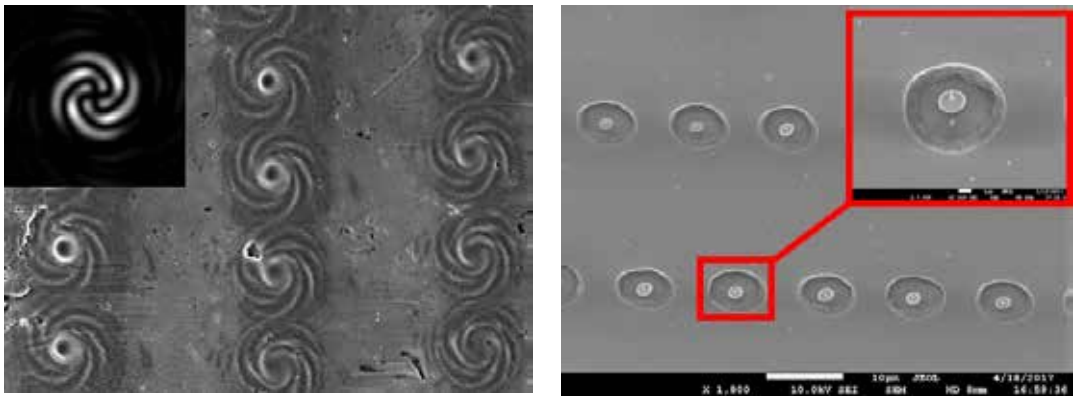

a) b)

Fig. 1 Side-view SEM images of single-shot fs-laser structures: (a) the spiral structure on the 500nm thick Se-film (NA=0.65); (b) the complex structures produced by S-plate with radial polarization.

In this work, we formed structured laser beams with given two- and three-dimensional configurations of light fields using elements of diffractive optics. We made laser nanofabrication of individual nanoelements and their ordered arrays, and also performed spectroscopic analysis of the structures obtained.

The experiments were supported by the Russian Science Foundation (grant no. 17-12-01258)

[1] Hnatovsky, C., Shvedov, V., Krolikowski, W., & Rode, A. (2011). Revealing local field structure of focused ultrashort pulses. Physical Review Letters, *106*(12), 123901.

[2] Porfirev, A. P., & Khonina, S. N. (2017). Generation of azimuthally modulated circular superlinear Airy beams. JOSA B, *34*(12), 2544-2549.

[3] Syubaev, S., Porfirev, A., Zhizhchenko, A., Vitrik, O., Kudryashov, S., Fomchenkov, S., Khonina S., Kuchmizhak, A. (2017). Zero-orbital-angular-momentum laser printing of chiral nanoneedles. Optics Letters, *42*(23), 5022-5025.

P60

Colloidal particle lens arrays-assisted surface nano-patterning by two-colored femtosecond pulses. The effect of delay time between the pulses of different frequences

A. Afanasiev*, V. Bredikhin, I. Ilyakov, B. Shishkin, R. Akhmedzhanov, and N. Bityurin

Institute of Applied Physics of Russian Academy of Sciences, 46 Ul'yanov Street, Nizhny Novgorod 603950, Russia
Corresponding author: ava@ufp.appl.sci-nnov.ru

We consider femtosecond laser nanostructuring of the material surface by means of a colloidal particle lens array. Here, the monolayer of dielectric micro- or nanospheres placed on the surface acts as an array of near-field lenses that focus the laser radiation into the multitude of distinct spots, allowing the formation of many structures in a single stage. Previously, it was shown that conversion of a small part of the energy of the fundamental frequency (FF) femtosecond beam into the second harmonic (SH) is an efficient way to decrease the modification threshold and to increase the surface density of obtained nanostructures.[1,2].In the present communication, we investigate the effect of delay time between the FF and SH pulses on the efficiency of the nanostructuring.

The result depends on the position of the edge of the absorption band of the substrate with respect to the photon energy of the third harmonic (TH). If the TH photon energy is larger than the band gap, then the minimal modification threshold corresponds to the zero delay time between the pulses because the two-photon absorption FF+SH dominates the material alteration process (see Fig 1). When the delay time is larger than the pulse duration that is the two-photon absorption is excluded, then the threshold is smaller when the SH pulse comes first. It can be explained by the different role of the FF and SH in multiphoton ionization that is responsible for the transparent materials alteration by femtosecond pulses. We also consider the two-pulse (FF and SH) interactions with the substrates with the band gap larger the TH photon energy. When the TH photon energy is close to the band gap, then the frequency chirp obtained by the both FF and SH femtosecond pulses influence the delay time dependence of the threshold. The results shed light onto the features of the interaction of two-colored femtosecond impulses with the transparent dielectrics. We discuss the advantages of employment of a colloidal particles lens array for the study of light-matter interaction in this case.

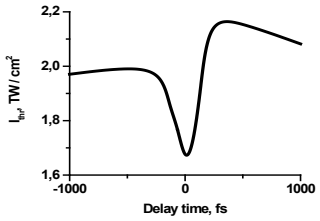

Fig. 1. Surface structuring threshold dependence on the SH pulse delay time relative to the FF pulse.

The work is supported by RFBR (Grant No. 16-02-00792).

[1] N. Bityurin, A. Afanasiev, V. Bredikhin, A. Alexandrov, N. Agareva, A. Pikulin, I. Ilyakov, B. Shishkin, and R. Akhmedzhanov, Colloidal particle lens arrays-assisted nano-patterning by harmonics of a femtosecond laser, Optics Express, 21(18), 21485- 21490 (2013)
[2] A. Afanasiev, V. Bredikhin, A. Pikulin, I. Ilyakov, B. Shishkin, R. Akhmedzhanov, and N. Bityurin, Two-color beam improvement of colloidal particle lens array assisted surface nanostructuring, Applied Physics Letters, 106, 183102 (2015)

P61

How uniform is uniform – Characterisation and Optimisation of structures fabricated by Direct Laser Interference Patterning

Mikhael El-Khoury[1], Tobias Steege[1], Alfredo Ismael Aguilar-Morales[1], Sabri Alamri[1], Andrés Fabián Lasagni [1,2], Tim Kunze[1]

[1]Fraunhofer Institute für Werkstoff- und Strahltechnik IWS, Winterbergstraße 28, 01277 Dresden, Germany
[2]Institute for Manufacturing Technology, Technische Universität Dresden, George-Baehr-Str.3c, 01069 Dresden, Germany
Corresponding author: mikhael.el-khoury@iws.fraunhofer.de

Surface topographies with well-defined microstructures and uniform distribution of contact points are required in many applications to obtain or optimize the desired surface functionality. Laser surface texturing technologies have shown to be capable of providing these well-defined surface structures with a high degree of flexibility and productivity. Within these methods, Direct Laser Interference Patterning (DLIP) has emerged as a disruptive fabrication technology capable of producing high-resolution structures with extremely high throughput. In general, DLIP employs the interference of laser beams to produce periodic structures on surfaces by transferring the periodic pattern directly to the material [1]. Interference patterns are generated by splitting a coherent laser beam into multiple sub-beams which are superposed on the sample surface in a well-defined manner. The structure quality on the surface is directly dependent on laser processing parameters, which needs to be optimized.

In this work, periodic surface microstructures fabricated by DLIP are characterised and optimized by design of experiments (DoE) with respect to pattern homogeneity. Through this DoE, the impact of various DLIP process parameters such as laser fluence, pulse-to-pulse overlap, hatch distance and spatial period on surface uniformity was investigated. Large-area analysis of microstructures was performed by white light interferometry and scanning electron microscope. A 3D-characterization method based on morphological filtering [2], which allows a holistic view of the surface properties, was applied and a new qualification scheme for DLIP surface structures was introduced.

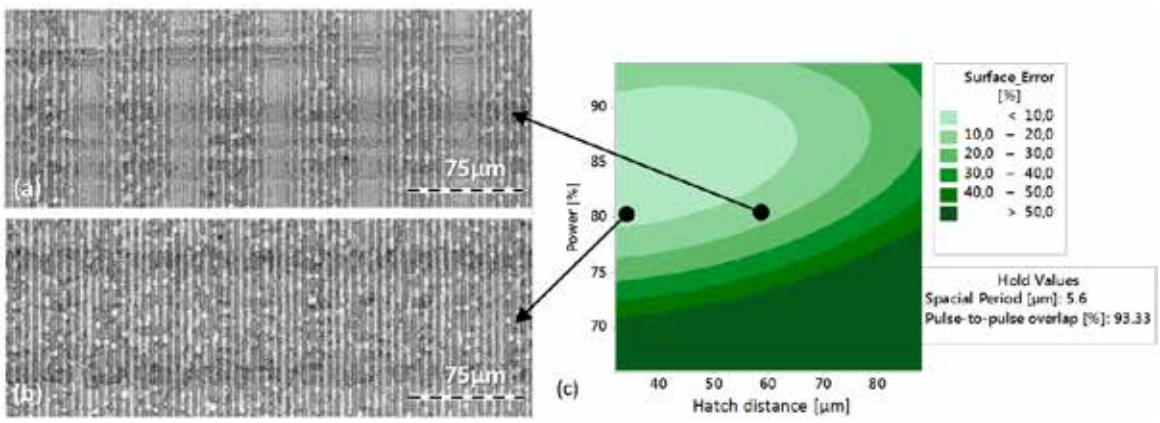

Fig. 1 White light interferometry picture of the microstructure produced with nanosecond DLIP on 100Cr6 bearing steel using the spatial period of Λ= 5.6 µm, hatch distance of (a) 61.6 µm and (b) 33,6 µm, F= 3.22 J/cm² and 93,33 % overlap, and (c) contour plot of the structure homogeneity as a function of laser power and hatch distance.

[1] F. A. Lasagni, A. F. Lasagni, *Fabrication and Characterization in the Micro-Nano Range*, Chapter 1 (Springer, 2011).
[2] S. Lou, X. Jiang, P. J. Scott, Applications of Morphological Operations in Surface Metrology and Dimensional Metrology, *Journal of Physics: Conference Series, Volume 483, conference 1* (2014)

P62

Laser fabrication of optical components for THz radiation

Simonas Indrišiūnas[1*], Milda Tamošiūnaitė[1], Ramūnas Šniaukas[1], Vincas Tamošiūnas[1,2], Linas Minkevičius[1,2], Andrzej Urbanowicz[1], Irmantas Kašalynas[1], Gintaras Valušis[1,2], Gediminas Račiukaitis[1]

[1]Center for Physical Sciences and Technology, Savanoriu Ave. 231, LT-02300 Vilnius, Lithuania
[2]Vilnius University, Faculty of Physics, Sauletekio Ave. 9, Vilnius, Lithuania
Corresponding author: simonas.indrisiunas@ftmc.lt

In the THz applications, spherical lenses may be replaced by the diffractive lenses to make the setup more compact and lightweight. Such elements can be fabricated using laser ablation, which allows flexible fabrication and is a relatively simple single-step process [1].

The fabrication speed is the crucial factor for the cost-effectiveness of such product. Therefore, the fabrication speed of the several machining setups was compared. Diffractive lenses for the 0.58 THz (Fig. 1a) and 4.75 THz wavelengths were fabricated using polygon and galvoscanners. Influence of the fabrication parameters such as scanning strategy, laser fluence and spot size for the fabrication quality and speed of the diffractive structures were investigated.

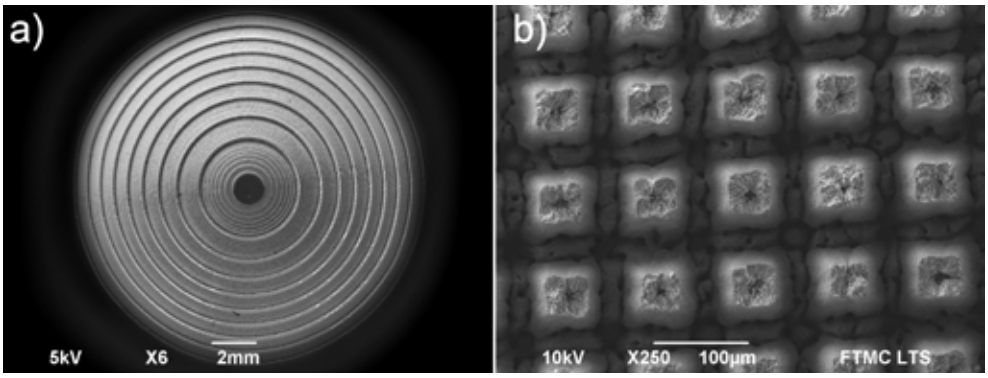

Fig. 1 (a) SEM image of the 8-level laser fabricated diffractive lens (focal length 5 mm) for the 0.58 THz radiation. (b) Laser-fabricated antireflective structure for the 0.58 THz radiation.

Bare silicon exhibits over 30% reflection losses in the THz range [2]. Therefore, to ensure the efficiency of the diffractive lenses, antireflective surface structures are needed. Such structures for the 0.58 THz region, suitable for laser fabrication, were designed and incorporated in the laser fabricated diffractive lens (Fig. 1b).

[1] L. Minkevičius, S. Indrišiūnas, R. Šniaukas, B. Voisiat, V. Janonis, V. Tamošiūnas, I. Kašalynas, G. Račiukaitis and G. Valušis, Terahertz multilevel phase Fresnel lenses fabricated by laser patterning of silicon. *Opt. Lett*. **42**, 1875-1878 (2017).
[2] C. Brückner, T. Käsebier, B. Pradarutti, S. Riehemann, G. Notni, E.-B. Kley and A. Tünnermann, Broadband antireflective structures applied to high resistive float zone silicon in the THz spectral range. *Opt. Express* **17**, 3063-3077 (2009).

P63

Direct Laser Writing and Etching of High Aspect Ratio Structures in Fused Silica Using Different Etchants

S. Butkus[1], M. Rickus[1], R. Sirutkaitis[2], D. Paipulas[1] and V. Sirutkaitis[1]

[1]Vilnius University, Faculty of Physics, Laser Research Center, Saulėtekio Ave. 10, Vilnius, Lithuania
[2]Vilnius University, Institute of Biochemistry, Mokslininkų str. 12c, Vilnius, Lithuania
Corresponding author: simas.butkus@ff.vu.lt

High depth to width ratio channels made in glass are important for manufacturing microfluidic devices, micromechanical applications, etc. [1-2]. These devices are used widely: chemical synthesis and drug development, high-throughput medical and biochemical analysis, micro mechanics and various sensors. Though femtosecond bulk writing and chemical etching enable the above-outlined applications, due to the high spatial resolution which is required when using this method, producing large and complicated structures becomes time consuming (writing and etching steps are required which total in several hours of fabrication), therefore optimization of the process is important.

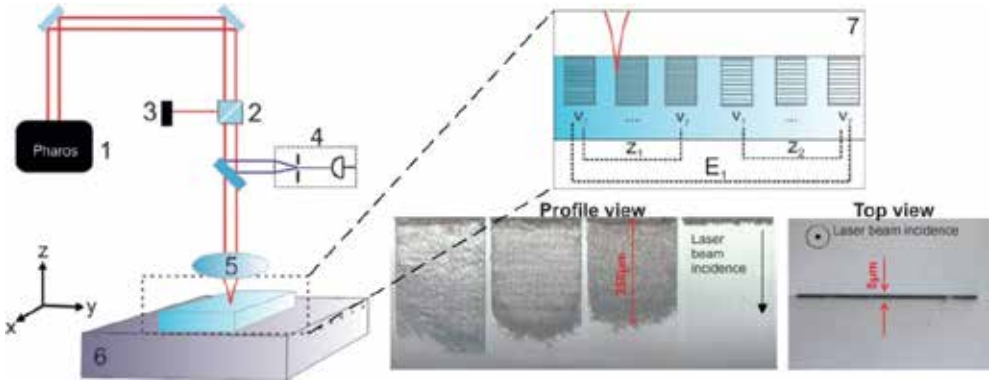

Fig. 1 (a) Used fabrication setup and experiment description. 300 µm deep, 0.2 mm long channels were written with various experimental conditions in fused silica samples. The samples were later etched in different etchants (HF liquid and vapour, KOH). The etched depth and aspect ratio was inspected multiple times during etching (from 5 minutes to several hours) for all of the samples.

In our experiments we have written 300 µm deep columns in fused silica samples and investigated how various laser (pulse energy, writing speed, axial overlap) and non-laser (etching time, type of etchant) parameters impact the whole femtosecond laser writing and chemical etching process in terms of writing and etching throughput and the selectivity of etching. In our experiments, KOH at different concentrations and temperature settings and HF in liquid and vapour phase were used as the etchants. Our experiments show that given the correct parameter settings it is possible to achieve selective etching at high writing speeds (0.5 mm2/s) while the etching rate is high (0.2 µm/s), e.g. a 0.1 mm deep and 5 mm long trench is fabricated in 1 second and etched in 5 minutes. Such writing and etching throughput values are attractive for rapid prototyping and various other applications.

[1] R. Osellame, H. J. Hoekstra, G. Cerullo, M. Pollnau (2011), Femtosecond laser microstructuring: An enabling tool for optofluidic lab-on-chips, Laser and Photonics Reviews, 5(3), pp. 442-463

[2] T. Tičkūnas, M. Perrenoud, S. Butkus, R. Gadonas, S. Rekštytė, M. Malinauskas, D. Paipulas, Y. Bellouard, and V. Sirutkaitis (2017), Combination of additive and subtractive laser microprocessing in glass/polymer microsystems for chemical sensing applications, Optics Express, 25, pp. 26280-26288

P64

Recording of Diffraction Elements in Fused Silica by the Deep Focused Femtosecond Pulses

Valdemar Stankevič[1,2*], Mindaugas Gedvilas[1], Jonas Karosas[1], Gediminas Račiukaitis[1]

[1]Center for Physical Sciences and Technology, Savanoriu Ave. 231, LT-02300 Vilnius, Lithuania
[2] ELAS, UAB, Savanoriu ave 235, Vilnius, Lithuania
Corresponding author: valdemar.stankevic@ftmc.lt

It is well known that internal modifications laser-induced in fused silica utilising high-NA objectives are affected by spherical aberration. The air-glass interface displaces the geometrical focus position, and the focal volume becomes elongated [1]. Due to the energy dissipation in the case of deep focusing (<1 mm below the surface), the modification can be induced only in the central part of the beam. Consequently, the radial size of the modification drops down. This feature allows recording of a high-density volume gratings and paves the way for the formation of deeply focused diffraction elements.

In this work, the modification length elongation in the wide focusing depth window in the fused silica from 0.5 mm to 5.7 mm was investigated (Fig.1 a), and the energy to depth conditions where only the I type induced modifications were found. The single pass modification length >50 µm was achieved. The induced refractive index change was measured by recording volume gratings of various thickness. The diffraction efficiency of such gratings exceeded the 90% (Fig. 1 b), that shows the significant efficiency increase compared to the results presented in [3] and to our knowledge, this is the highest achieved diffraction efficiency of the gratings recorded with the Gaussian beam.

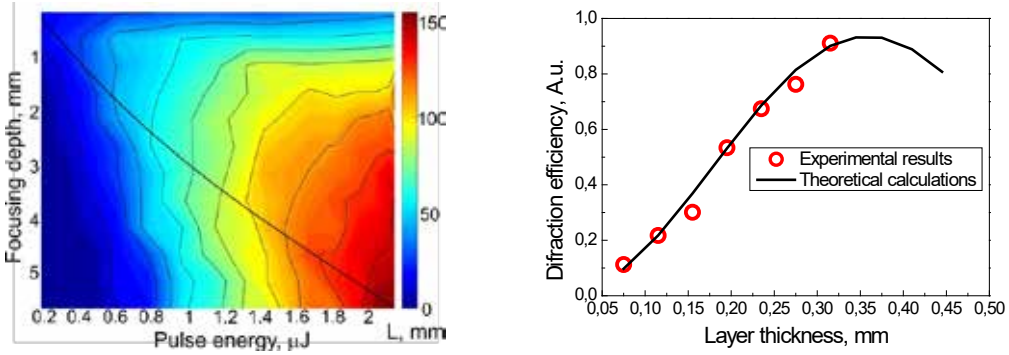

a) b)

Fig. 1 (a) Contour map of the volume modifications length elongation depending on the focusing depth and pulse energy used at constant writing speed – 5 mm/s and repetition rate – 500 kHz; (b) Deep volume gratings diffraction efficiency dependence on the gratings thickness. The measured refractive index change is Δn~0.00088.

The presented results were applied to record the 2 × 1 (50/50% beam splitter) diffraction optical element which demonstrated > 40% diffraction efficiency for each -1 and 1 diffraction orders, consequently almost no radiation to the 0 diffraction order and low propagation losses were demonstrated.

[1] C. Hnatovsky, R. S. Taylor, E. Simova, V. R. Bhardwaj, D. M. Rayner, and P. B. Corkum, High-resolution study of photoinduced modification in fused silica produced by a tightly focused femtosecond laser beam in the presence of aberrations, *J. Appl. Phys.* **98**(1), 013517 (2005).
[2] D. Liu, Y. Li, R. An, Y. Dou, H. Yang, and Q. Gong, Influence of focusing depth on the microfabrication of waveguides inside silica glass by femtosecond laser direct writing, *Appl. Phys., A Mater. Sci. Process.* **84**(3), 257–260 (2006).
[3] C. Voigtländer, D. Richter, J. Thomas, A. Tünnermann, and S. Nolte, Inscription of high contrast volume Bragg gratings in fused silica with femtosecond laser pulses, *Appl. Phys A - Mater. Sci. Process.* **102**, 35 – 38 (2011).

P65

Femtosecond laser micromachining of glass samples in air, water and various solutions (NaCl, KOH)

Lina Mačernytė, Ona Balachninaitė, Simas Butkus, Valdas Sirutkaitis
Vilnius University, Faculty of Physics, Laser Research Center, Sauletekio Ave. 10, Vilnius, Lithuania
Corresponding author: *lina.macernyte@ff.stud.vu.lt*

Lasers with ultrashort pulse durations have demonstrated excellent micromachining quality because pulse widths are shorter than the time for converting the energy of excited electrons into thermal energy [1]. Micromachining performed in liquids can significantly improve the ablation quality and material removal efficiency. Bubbles that form in the liquid during laser heating determine used liquid's movement. Throughout the ablation process removed material particles sink slower in liquids. In this way, sediment can be removed efficiently from laser formed grooves. Also, additional water layer above the material surface performs a cooling function, so sample fractures and cracks are avoided [2].

Usually, water is the most commonly used liquid medium for femtosecond laser micromachining. In this study to increase the machining rate, we tried laser-assisted wet etching using KOH and saline NaCl solutions with different concentrations. *CARBIDE* (Light Conversion) laser with 290 fs pulse duration at 1030 nm wavelength was used for micromachining. The operating pulse repetition frequency was 60 kHz, and average laser power was 5 W. The liquid thickness above the surface was kept constant and equal to approximately 0.6 mm [3]. In order to determine the optimum micromachining parameters, we changed scanning speed, a number of scanning, etc. The aim of this experiment was to investigate the influence of various solutions on depth and quality of the formed grooves.

Performed measurements showed that at small scanning speeds and particular concentrations of solutions the grooves with increased depths could be formed. It was impossible to achieve deeper grooves depths while using KOH solution because of formed hydrogen bubbles [4].

[1] A. H. Hamad, High Energy and Short Pulse Lasers, Effects of Different Laser Pulse Regimes (Nanosecond, Picosecond and Femtosecond) on the Ablation of Materials for Production of Nanoparticles in Liquid Solution, 305-321, (2006).
[2] A. Kruusing, Handbook of Liquids-Assisted Laser Processing, 143-148, (2008).
[3] S. Butkus, D. Paipulas, R. Sirutkaitis, E. Gaižauskas and V. Sirutkaitis: Journal of Laser Micro/Nanoengineering 9(3), (2014).
[4] K. P. Luong, R. Tanabe, Y. Ito, Machining on Rear Surface of Silicon Substrate by an Infrared Femtosecond Laser via Non-linear Absorption Processes, 73-76, (2016).

P66

Application of Asymmetrical Bessel-like Laser Beams for Glass Processing

Juozas Dudutis*, Rokas Stonys, Paulius Gečys

Center for Physical Sciences and Technology, Savanoriu Ave. 231, LT-02300 Vilnius, Lithuania
Corresponding author: juozas.dudutis@ftmc.lt

As conventional methods for glass processing can no longer fulfil the ever-growing industrial requirements for processing speed and quality, nowadays new technologies emerge employing various laser-based techniques. One of the most material and energy efficient glass cutting technique is to locally weaken the material along the cutting path by generating cracks or material modifications and then separate the sheets by applying thermal or mechanical load. This results in a cut with an infinitely thin kerf width and, in most cases, does not require any additional processing [1].

Bessel-Gaussian beams are very appealing for glass processing as they have exceptional properties, such as a long non-diffracting propagation length and rapid reconstruction behind an obstacle. However, glass cutting with symmetrical Bessel-Gaussian beams is not ideal as glass modifications are random and negatively influence speed and quality of the cut.

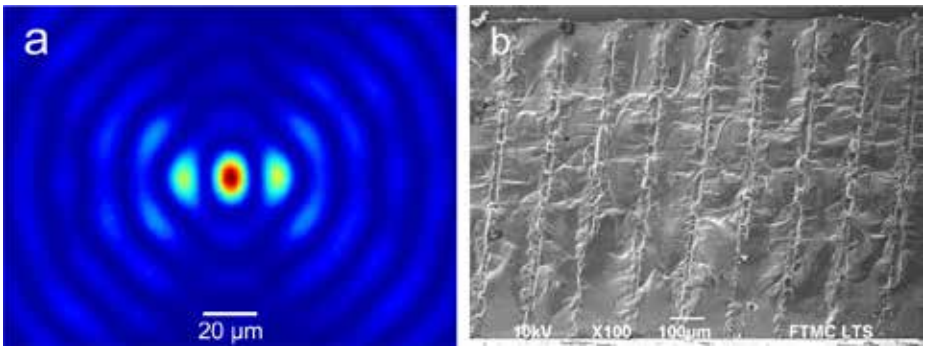

Fig. 1 (a) Asymmetrical Bessel-like beam and (b) a cut of a soda-lime glass sheet as seen with a scanning electron microscope.

It was shown that asymmetrical Bessel-Gaussian beams (Fig. 1 (a)) could be formed by filtering its spectrum of spatial frequencies [2, 3]. We have proven that these beams, in turn, generate directional cracks in the bulk of a transparent material. The direction of the cracks generated using this method can be easily controlled by changing filter's position with respect to the cutting direction. Cracks that are made using asymmetrical Bessel-Gaussian beams can then be employed for fast and high-quality cutting of transparent materials (Fig. 1 (b)).

[1] S. Nisar, L. Li, M. A. Sheikh. Laser glass cutting techniques – A review. *Journal of Laser Applications*, **25**(4), 42010 (2013)
[2] F. O. Fahrbach, V. Gurchenkov, K. Alessandri, P. Nassoy, A. Rohrbach, Self-reconstructing sectioned Bessel beams offer submicron optical sectioning for large fields of view in light sheet microscopy, *Optics Express*, **21**(9), 11425 (2013).
[3] R. Meyer, M. Jacquot, R. Giust, J. Safioui, L. Rapp, L. Furfaro, F. Courvoisier. Single-shot ultrafast laser processing of high-aspect-ratio nanochannels using elliptical Bessel beams. *Optics Letters*, **42**(21), 4307 (2017).

P67

Direct Laser Writing of Photonic Microstructures for Spatial Light Filtering using Gaussian and Bessel beams

Vytautas Purlys[1,2*], Darius Gailevičius[1,2], Roaldas Gadonas[1,2], Kestutis Staliunas[3,4]
[1]Vilnius University, Faculty of Physics, Laser Research Center, Saulėtekio al. 10, Vilnius, Lithuania
[2]Femtika LTD, Saulėtekio al. 15, Vilnius, Lithuania
[3]Departament de Física i Enginyeria Nuclear, Universitat Politècnica de Catalunya, Colom 11, 08222 Terrassa, Spain
[4]Institucio Catalana de Reserca i Estudis Avançats (ICREA), Passeig Lluis Companys 23, 08010 Barcelona, Spain
Corresponding author: vytautas.purlys@ff.vu.lt

Spatial light filtering is a broadly used technique for cleaning the light beams. Commonly, a confocal system of lenses and a pinhole is used for such purpose. However, such systems often suffer from mechanical instability and are relatively large in size, which restricts their usage in micro-optical devices. In addition, their usage is limited in high power optical systems due to laser damage of the pinhole. These limitations can be overcome by using photonic crystals (PhCs), dedicated to spatial filtering applications. The length of such PhC filters are typically around a millimeter, and their operation does not require focusing. Therefore, they are perfect candidates for integration into miniature devices or for high power spatial filtering implementations.

The discussed PhC spatial filters typically have periodicities of micrometer scale and are fabricated in the bulk of glass via point-by-point direct laser writing process, where the glass is locally modified using tightly focused femtosecond laser beam with the Gaussian profile. We demonstrate that the strategy mentioned above allows the precise fabrication of various PhCs geometries, both 2D and 3D, periodic or quasi-periodic, but on the other hand, it has certain limitations, namely limited length of the structures due to limited fabrication lens working distance and irregularities due to spherical aberration.

Fig. 1 (a) Schematic illustration of the direct laser writing process in glass using Gaussian (left) and Bessel (right) beams. (b) Optical microscope image of an example PhC microstructure (top view) fabricated in soda lime glass sample using 350 µm length voxels. The scalebar length is 100 µm and the transversal period of the structure is 3 µm.

As an alternative method, we demonstrate the fabrication of PhCs using Bessel beam. In this case, the point-by-point writing becomes line-by-line writing (Fig. 1a). Such strategy significantly improves the fabrication throughput of 2D PhCs and allows the fabrication of much longer PhCs, which are required for wide angle filters, where chirped or numerically optimized geometries are especially useful.

P68

Fabrication of perfect absorber metasurface structures by direct laser write technique and their post-fabrication tuning

Subhashri Chatterjee[1], Edy Yulianto[1], Ihar Faniayeu[1,2], Vygantas Mizeikis[1]
[1] Research Institute of Electronics, Shizuoka University, 3-5-1 Johoku Hamamatsu 432-8011, Japan
[2]Department of General Physics, Francisk Skorina Gomel State University, 246019 Gomel, Belarus
Corresponding author: mizeikis.vygantas@shizuoka.ac.jp

Electromagnetic (EM) metamaterials based on 3D split-ring resonators (SRR) were designed and realized experimentally for infra-red (IR) spectral range using Direct Laser Write (DLW) technique[1] and metalization by gold sputtering. The fabricated EM structures exhibit perfect absorber (PA) functionality at IR wavelengths of 6-9µm, depending on structural parameters of the dielectric templates, defined during the DLW fabrication. Possibilities to tune the PA resonance after the DLW step via gradual increase of the gold layer thickness were investigated. In the experiments, gold was deposited on dielectric templates using plasma sputtering technique multiple times, and spectral response of the structures was measured after each step. Figure 1 compares the appearance of the structure before the gold sputtering and after the multiple sputtering steps. The same figure also compares absorbance spectra of the structure before and after the sputtering. As can be seen, deposition of an additional ≈ 50 nm thick gold film leads to significant blue-shift of the absorbance peak. This shift can be explained using numerical simulations and is related to the reduction of effective SRR length due to the increase in the gold film. Applications of this mechanism for versatile post-DLW spectral tuning of PA structures will be discussed.

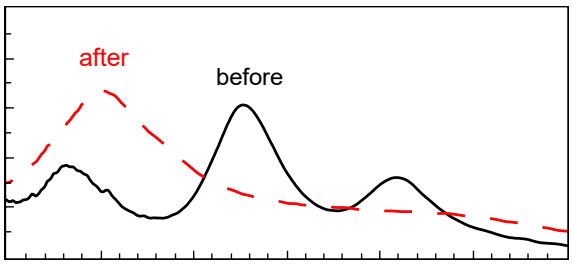

Fig. 1 Comparison between absorbance spectra of a PA structure before and after the Au layer augmentation.

[1] I. Faniayeu and V. Mizeikis, “Vertical split-ring resonator perfect absorber metamaterial for IR frequencies realized via femtosecond direct laser writing,” Appl. Phys. Expr., **10** 062001 (2017).

P69

Numerical Study on Power Absorption Distribution of Powders in Selective Laser Melting

Tomomasa Ohkubo[1], Yuji Sato[2], Toshi-taka Ikeshoji[3], Ei-ichi Matsunaga[1], Masahiro Tsukamoto[2]

[1] Tokyo University of Technology, 1404-1, Katakura, Hachiouji, Tokyo 192-0982, Japan

[2] Joining and Welding Research Institute, Osaka University, 11-1Mihogaoka, Ibaraki-shi, Osaka 567-0047, Japan

[3] Kindai University Fundamental Technology for Next Generation Research Institute, 1 Takaya Umenobe, Higashi Hiroshima, Hiroshima 739-2116, Japan

Corresponding author: ookubotmms@stf.teu.ac.jp

Selective laser melting (SLM) is an additive manufacturing technology to create a 3-dimensional object using high power-density laser to melt and solidified metallic powders. It is necessary to understand what occurs when powders are heated by laser for the optimization of this process. However, simple powder scatters model is not applicable to this technique, and ray tracing which requires too much computational cost was applied to clarify how much power is reflected by powders [1]. Although the reflectivity and absorption distribution of the top surface was discussed, the absorbed power distribution of depth direction was not discussed in that study. In this study, we propose a simple estimation model to calculate absorbed power distribution including depth direction. Figure 1 shows an example of the calculated result of absorbed distribution in r-z geometry: r is the coordinate in the radial direction, and z is the coordinate in the depth direction. As shown in Fig. 1 (a), input power propagated into the deep and wide area when the powder distribution is sparse. On the other hand, dense powder distribution realizes compact absorbed power distribution as shown in Fig. 1 (b). In this study, we will introduce numerical analysis about absorbed power into powders to analyse SLM using blue direct diode lasers [2].

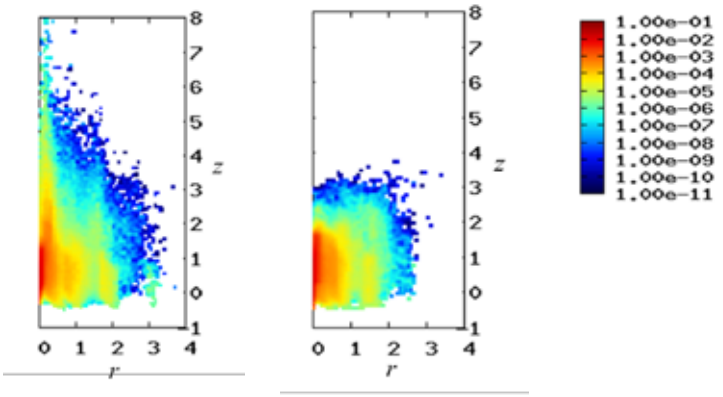

(a) (b)

Fig. 1 Calculated results of absorbed power distribution. The scale is normalized by the size of a particle. (a) the case of filling rate is 58.8%. (b) the case of filling rate is 64.0%.

[1] C. D. Boley, *et al.*, "Calculation of laser absorption by metal powders in additive manufacturing", Applied Optics 54, pp. 2477-2482 (2015)

[2] T. Shibata, *et al.*, "The dependence on laser wavelength of powder melting solidification in selective laser melting", Digest of technical papers, Annual Meeting of the Laser Society of Japan (2018)

P70

In situ X-ray observation of pure-copper layer formation with blue direct diode laser

Yuji Sato[1], Masahiro Tsukamoto[1], Takahisa Shobu[2], Yoshinori Funada[3], Yorihiro Yamashita[3], Takahiro Hara[4], Ritsuko Higashino[1], Yu Sakon[5], Tomomasa Ohkubo[6], Nobuyuki Abe[1]

[1]Joining and Welding Research Institute, Osaka University, (11-1 Mihogaoka, Ibaraki, Osaka 567-0047, Japan)
[2]Japan Atomic Energy Agency, (1-1-1 Kouto, Sayou-cho, Sayou-gun, Hyogo 679-5148, Japan)
[3]Industrial Research Institute of Ishikawa, (2-1 Kuratsuki, Kanazawa, Ishikawa 920-8203, Japan)
[4]Graduate School of Engineering, (Osaka University, 1-1 Yamadaoka, Suita, Osaka, 565-0871, Japan)
[5]Muratani Machine Inc.(1-32 Higashikagatsumemachi Kanazawa Ishikawa 920-0209, Japan)
[6]Tokyo University of Technology, Department of Mechanical Engineering, (1404-1 Katakura, Hachiouji, Tokyo 192-0914, Japan)

Corresponding author: sato@jwri.osaka-u.ac.jp

A blue direct diode laser cladding system, which uses a multi-laser combining method, was developed in order to realize a high-quality cladding layer having a dense, fine and purity. In order to clarify the mechanism of copper layer formation, the layer formation process when forming a copper layer using a blue direct diode laser was observed using in situ X-ray observation. The six-blue diode lasers were guided to focusing head with every optical fiber, which core diameter is 100 µm. Beam profile at the focal point of the combined six lasers was set a spot diameter of 400 µm. The focusing head has a function to supply a pure copper powder at a focal point from a center nozzle. As the results, it was found that the stainless steel 304 substrate was melted and generate some bubble in the molten pool at a laser fluence of 1221 kJ/cm^2, and output power of 92W, as shown in Fig.1(a). At laser fluence of 407 kJ/cm^2, the bubble was disappeared because only a slight molten pool was formed on the surface of the substrate, as shown in Fig.1(d). It was found that amount of bubble and penetration depth was depended on the laser fluence with a blue direct diode laser. By controlling the amount of input energy, the copper coating was produced minutely with no weld penetration

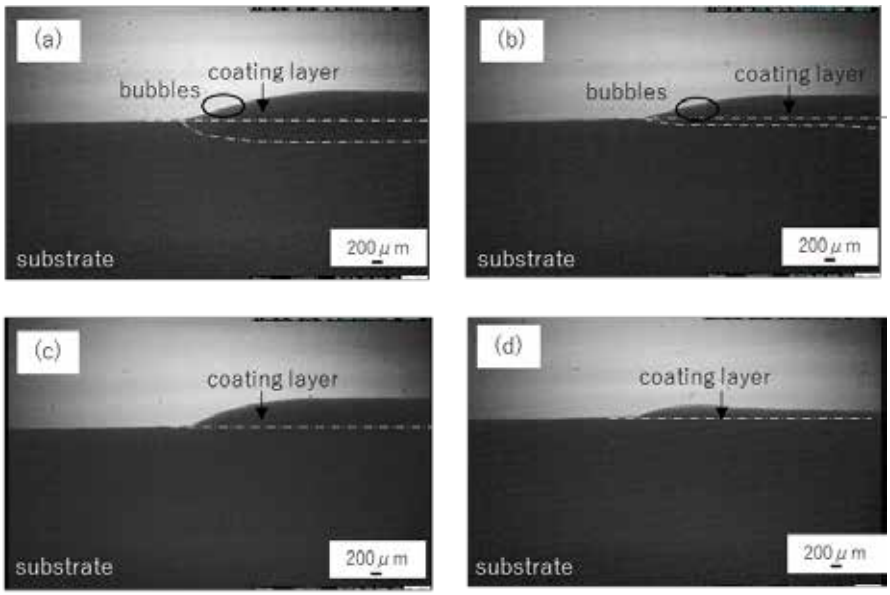

Fig. 1 X-ray observation of laser coating with blue laser fluence at (a) 1221 kJ/cm^2 (b) 732 kJ/cm^2 (c) 523 kJ/cm^2 and (d) 407 kJ/cm^2

P71

Laser microwelding application for wire to flat geometry of dissimilar materials in electromechanical components

Mahdi Amne Elahi, Peter Plapper

University of Luxembourg, 6, rue Coudenhove-Kalergi, 1359 Luxembourg, Luxembourg
Corresponding author: mahdi.amneelahi@uni.lu

In the presented study, the laser welding of wire to flat geometry for miniature electromechanical hybrid components has been investigated. Laser welding offers a variety of advantages compared to the current joining processes for this application, however, considering the geometry of parts to be also welded mechanical properties requirement, accurate spatial modulation of the laser beam should be implemented to achieve a sound joint. Tensile shear test and optical microscopy were employed to represent the mechanical properties and melt pool geometry of the joint. All welds were done by power modulation of the laser beam to better control the energy input at several feed rates and three different beam trajectories. Results show that the shear load of the joint can be controlled by feed rate and the trajectory of the laser beam. The material combination of the study (Nickel and $CuSn_6$), represents solubility in the solid state, therefore, by defining a proper spatial modulation of the laser beam a joint stronger than base wire metal is achievable. Figure 1 represents the schematics of weld components.

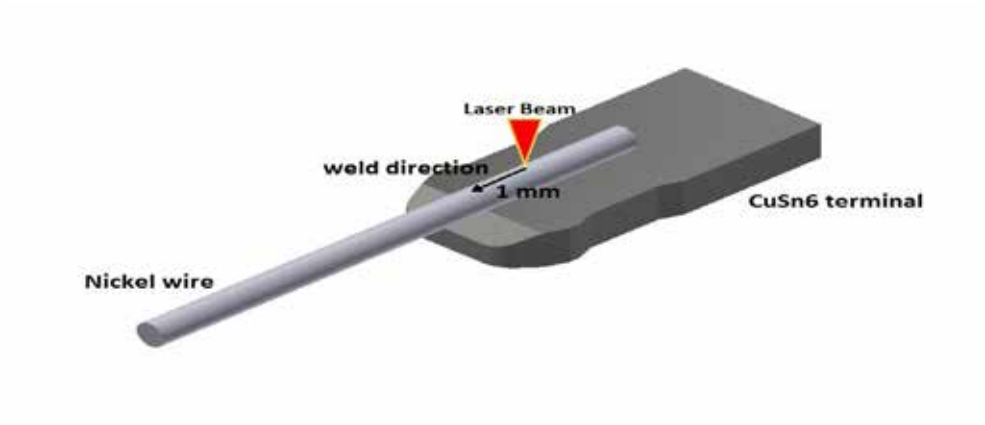

Figure 1. Schematics of weld components geometry and weld position.

There are limited studies on the application of laser beam trajectory [1, 2] however, the application of different trajectories for microwelding has not been systematically studied.

[1] Lamberti Christian, Solchenbach Tobias, Plapper Peter, Possart Wulff. Laser-assisted joining of hybrid polyamide-aluminum structures. *Phys Procedia* 2014;56(C):845–53. Doi: 10.1016/j.phpro.2014.08.103.

[2] Mehlmann Benjamin, Olowinsky Alexander, Thuilot Michael, Gillner Arnold. Spatially modulated laser beam micro welding of CuSn6 and nickel-plated DC04 steel for battery applications. *J Laser Micro Nanoeng* 2014;9(3):276–81. Doi: 10.2961/jlmn.2014.03.0019.

P72

Investigation on autogenous laser welding of copper to aluminium

Karthik Mathivanan[1], Peter Plapper[1]

[1]University of Luxembourg, 6, rue Richard Coudenhove-Kalergie L-1359 Luxembourg the
Corresponding author: karthik.mathivanan@uni.lu

This paper investigates laser joining of copper sheets to aluminium in overlap configuration. Dissimilar Cu-Al connections are widely used in the electrical and electronics applications, e.g. battery and solar panels. Joining these materials is a very critical assembly process. The laser welding from the aluminium surface to copper (Al-Cu) is well described in the literature [1][2][3]. However, there is no data concerning the laser seam welding from the copper side to join with aluminium, i.e. Cu-Al. The selection of aluminium surface to irradiate is mainly because of poor absorption of copper to laser in the IR region. However, high intensities of about 10^7 W/cm^2 allow for initial vaporization of the copper surface. Once the keyhole is generated, absorption of laser light is improved. Thereby high power lasers allow for successful penetration of the copper surface to produce a joint with aluminium.

The main objective is to investigate the approach of dissimilar laser welding starting from the copper surface to aluminium. The effect of process parameters on the shear force (Fig 1), microstructure and weld pool dimensions are studied. An experimental design is realized to see the effect of laser irradiation of copper surface (Cu-Al) in contrast to aluminium surface(Al-Cu). The selection of aluminium or copper surface is mainly dependent on the laser power. With the high power disk laser, the possibility of joining from the copper side was evident, and results of joining copper to aluminium and aluminium to copper are comparable. Therefore welding from a highly reflective surface to achieve a comparable shear strength is demonstrated.

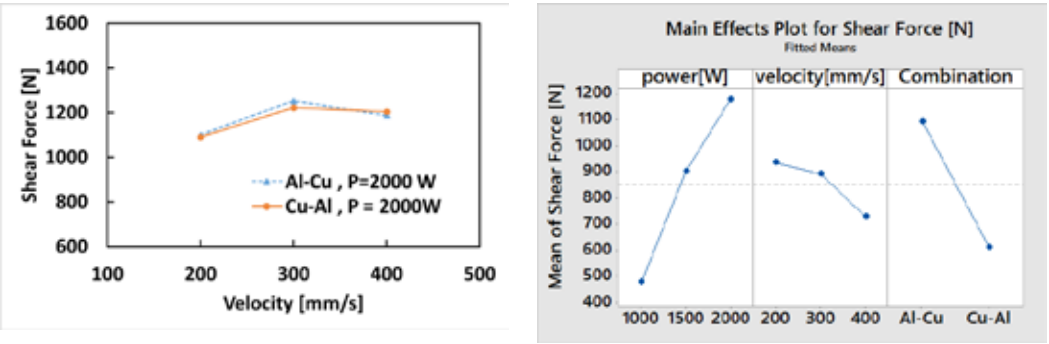

Fig 1(Left) Effect of velocity on the shear force response of welding Al-Cu and Cu-Al with a laser power of 2000 W; (Right) DOE: Main effects plot considering the laser irradiation on the Copper surface(Cu-Al) Vs Aluminium surface(Al-Cu) and the effect of Power and velocity.

[1] T. Solchenbach and P. Plapper, "Mechanical characteristics of laser braze-welded aluminium-copper connections," *Opt. Laser Technol.*, vol. 54, pp. 249–256, 2013.

[2] T. A. Mai and A. C. Spowage, "Characterisation of dissimilar joints in laser welding of steel-kovar, copper-steel and copper-aluminium," *Mater. Sci. Eng. A*, vol. 374, no. 1–2, pp. 224–233, 2004.

[3] M. Naeem, A. Montello, and C. Rasmussen, "Experimental Studies of Fiber Laser Welding of a Range of Dissimilar Material Combinations," 2015.

P73

Pulse length and shape in two-photon excited theranostics

Janez Štrancar[1*], Rok Podlipec[1], Jaka Mur[2], Jaka Petelin[2], Rok Petkovšek[2]
[1]Laboratory of Biophysics, Condensed Matter Physics Department, Jožef Stefan Institute, Jamova cesta 39, Ljubljana, Slovenia
[2]University of Ljubljana, Faculty of Mechanical Engineering, Aškerčeva 6, Ljubljana, Slovenia
Corresponding author: janez.strancar@ijs.si

Traditionally, a femtosecond laser pulsed source is employed in the two-photon excited fluorescence microscopy resulting in superior optical sectioning and a significant reduction in out-of-focus light [1,2]. The implementation of the same concept in medical diagnostics such as for ophthalmic applications is hindered by very high costs of such laser sources. On the other hand, the therapeutic applications in ophthalmology can employ nanosecond laser pulsed sources, due to their higher cost-efficiency. Lacking the two-photon ability of fine optical sectioning, the therapy is, as expected, much less confined in the z-direction.

The challenge is thus to develop a new cost-effective laser source with the pulse length in the picosecond regime that would enable two-photon excitation for theranostic applications, i.e. for both diagnostics and therapy at the same time with much higher optical sectioning ability.

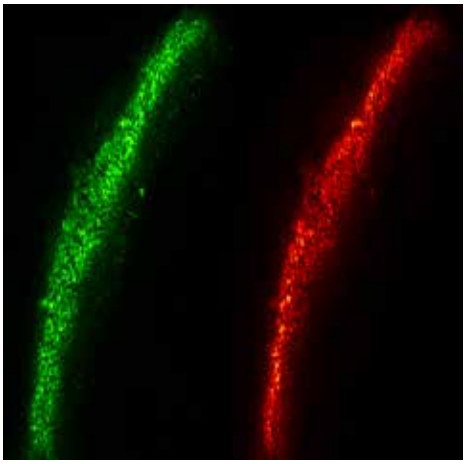

Fig. 1: Retinal epithelium imaged by two-photon excited fluorescence 300 microns deep in the retina at low magnification with NA of only 0.1, a typical value used in the ophthalmic application.

Here we show the implementation of the novel custom-developed 60 picosecond fiber-laser source [3] comparing with a standard Ti-sapphire 100 femtosecond source in a two-photon microscope configuration to enable diagnostic applications in a two-photon excited fashion, avoiding the problems of nanosecond excitation [4]. We test such configuration on imaging of retinal epithelium 300 microns deep in the retinal tissue behind all the retinal visual-light absorbers. We compare the efficiency of both laser sources to characterize this typically biological interface, full of different absorbers [5], which usually makes single-photon deep tissue imaging problematic. We furthermore compare different pulse length and pulse shapes on the efficiency of two-photon excitation.

[1] W. Denk, J. H. Strickler, and W. W. Webb, Science **248**, 73 (1990).
[2] W. R. Zipfel, R. M. Williams, and W. W. Webb, Nat. Biotechnol. **21**, 1369 (2003).
[3] J. Petelin, B. Podobnik, and R. Petkovšek, Appl. Opt. **54**, 4629 (2015).
[4] S. Karpf, M. Eibl, B. Sauer, F. Reinholz, G. Hüttmann, and R. Huber, Biomed. Opt. Express **7**, 2432 (2016).
[5] S. Andjelic, K. Drašlar, A. Hvala, N. Lopic, J. Strancar, and M. Hawlina, Acta Ophthalmol. (Copenh.) **94**, e183 (2016).

P74

Application of Laser-Induced Breakdown Spectroscopy to Femtosecond Laser Micromachining of Glass by use of Single Pulses and Pulse Trains

Julius Skruibis[1], Ona Balachninaitė[*1], Valdas Sirutkaitis[1]

[1]Vilnius University, Faculty of Physics, Laser Research Center, Sauletekio Ave. 10, Vilnius, Lithuania
Corresponding author: ona.balachninaite@ff.vu.lt

Laser-induced breakdown spectroscopy (LIBS) can be used as one of the potential monitoring technologies for laser micromachining with ultrafast laser pulses [1, 2]. This technology stands out by its stability and precision. The primary aim of the investigation was to find the correlation between multiple degrees of freedom in femtosecond specially formed pulse train (burst) laser micromachining and compare it with single pulse femtosecond laser micromachining in compatible conditions of the process. The rapid energy dissipation during the ultrafast laser-material interaction can cause strong shock and a quick heating and cooling cycle. It can produce such harmful effects as microexplosion and microcracks. One promising method to reduce such effects is to use a burst of laser pulses in high-repetition-rate where residual thermal energy does not diffuse out of the laser interaction zone before the next laser pulse arrives [3].

The experiments were carried out using CARBIDE (Light Conversion) laser system with pulse duration 290 fs and average power up to 5 W at 1030 nm wavelength, with a pulse repetition rate of 60 kHz. For all the measurements we used a particularly simple, but practical and functional optical scheme. Moreover, quick assemble and fast alignments granted us the capability to investigate effects on laser micromachining caused by different pulse energy distributions in the pulse train, a variety of different delays between pulses in the train, alterations in target temperature, scanning speed, number of scanning, etc.

After the evaluation of data, the parameters that have the highest contribution to the enhancement of laser micromachining with pulse train were indicated. Noticeable improvements were achieved in quality of the grooves, ablation rate, control of the process and other parameters characterizing laser micromachining.

[1] R. Noll, C. Fricke-Begemann, M. Brunk, S. Connemann, C. Meinhardt, M. Scharun, V. Sturm, J. Makowe, C. Gehlen, Laser-induced breakdown spectroscopy expands into industrial applications. *Spectrochimica Acta Part B: Atomic Spectroscopy* **93**, 41–51 (2014).
[2] A. Baskevicius, O. Balachninaite, M. Karpavicius, S. Butkus, D. Paipulas, V. Sirutkaitis, Monitoring of the Femtosecond Laser Micromachining Process of Materials Immersed in Water by Use of Laser-Induced Breakdown Spectroscopy, *Journal of Laser Micro/Nanoengineering* **11**(3), 381-387 (2016).
[3] P. R. Herman, R. Marjoribanks, and A. Oettl, Burst-ultrafast laser machining method*, U.S. patents,* 6, 552, 301 (2001).

P75

Characterization of latent 3D laser exposure patterns in photoresist using photoluminescence quenching

Edy Yulianto, Subhashri Chatterjee, Vygantas Mizeikis
Research Institute of Electronics, Shizuoka University, 3-5-1 Johoku Hamamatsu 432-8011, Japan
Corresponding author: mizeikis.vygantas@shizuoka.ac.jp

Direct Laser Writing (DLW) is a lithographic technique for the fabrication of three-dimensional (3D) objects and structures with a high spatial resolution [1]. It uses the exposure of photosensitive material (e.g., photoresist) by a focused beam of an ultra-short pulse laser. Using a vector scan of the focus in the bulk of the material, desired 3D exposure pattern can be obtained. Subsequently, exposed (or unexposed) material becomes dissolved in a liquid developer, and after the drying 3D patterned material is obtained. This technology is fruitfully used for the fabrication of 3D photonic crystals, optical metamaterials, diffractive elements, micro-mechanical systems, etc. The possibility to visualize the latent 3D exposure pattern and to determine its various characteristics before the development would be highly advantageous for the development of this technique. Here, we describe *in situ* imaging of photoexposed patterns using the phenomenon of quenching of photoluminescence (PL) intensity in the exposed regions of photoresist. By scanning a low-intensity focused laser beam over previously exposed features (Fig. 1(a)) and recording the induced PL intensity, size and shape of the recorded features can be assessed from the spatial distribution of PL quenching (Fig. 1(b). A significant decrease of the PL intensity at locations of the previously recorded lines can be exploited for pre-development diagnostics of the recorded 3D patterns, determination of the feature size and shape, the threshold exposure dose, and other useful parameters.

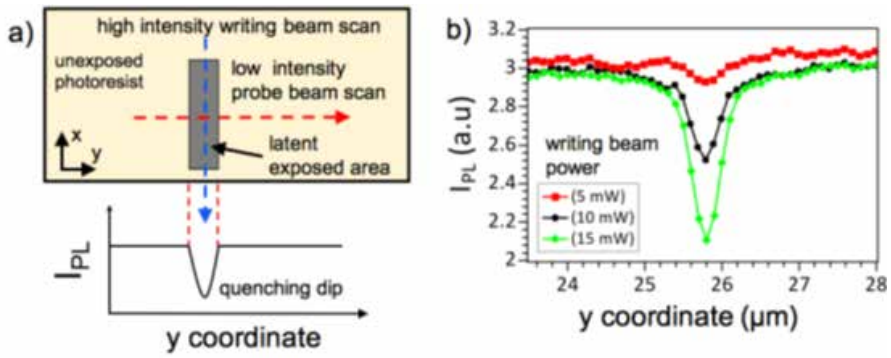

Fig. 1 Schematic layout of the written and scanned lines (a), PL intensity as a function of position along the scan line for three different writing intensities (b) PL intensity as a function of position along the scan line for three different writing intensities, with FWHM of the intensity dips indicated by numbers.

[1] M.Malinauskas, M. Farsari, A. Piskarskas, S. Juodkazis, "Ultrafast laser nanostructuring of photopolymers: A decade of advances", Phys. Reports **533**, pp.02, (2013).

P76

Active tuning of surface plasmon resonance by controlling interparticle distance of gold nanoparticles

Ayana Mizuno[1] and Atsushi Ono[1, 2*]
[1]Graduate School of Science and Technology, Shizuoka University, Hamamatsu 432-8561, Japan
[2] Research Institute of Electronics, Shizuoka University, Hamamatsu 432-8011, Japan

Corresponding author: ono.atsushi@shizuoka.ac.jp

We demonstrated the resonant wavelength shift of surface plasmons by gold nanoparticle array on a stretchable substrate. The resonant wavelength indicates clear wavelength-shift depending on the interparticle distance of the close-packed gold nanoparticle array [1]. Figure 1(a) shows a schematic diagram of the conceptual structure proposed in this research. It is considered that the interparticle distance of close-packed gold nanoparticles is extended by elongating the elastomeric substrate.

Close-packed gold nanoparticle arrays were fabricated by self-organization of colloidal gold nanoparticles due to the intermolecular interaction [2]. Figure 1(b) shows an SEM image of closed packed gold nanoparticle array with a diameter of 50 nm fabricated by the self-assembly method. This gold nanoparticle array was transferred to a stretchable substrate. In this research, PDMS (Polydimethylsiloxane), great in transparency and stretching property, was used as the substrate. Figure 1(c) shows a picture of a gold nanoparticle array on a PDMS substrate elongated to 1.5 times. The gold nanoparticle array exhibits a complementary color of blue because it absorbs red color by interparticle couplings of surface plasmon resonance. Figure 1(d) shows the absorption spectra of the gold nanoparticle array. The peak wavelength shifted from 659 nm to 619 nm before and after elongation of the stretchable substrate. This shorter peak wavelength shift is considered to have changed from interparticle couplings of surface plasmons to a local mode of surface plasmons in isolated nanoparticles. This surface plasmon tuning would be utilized for variable color filters, tunable SERS substrates, and optical strain sensors.

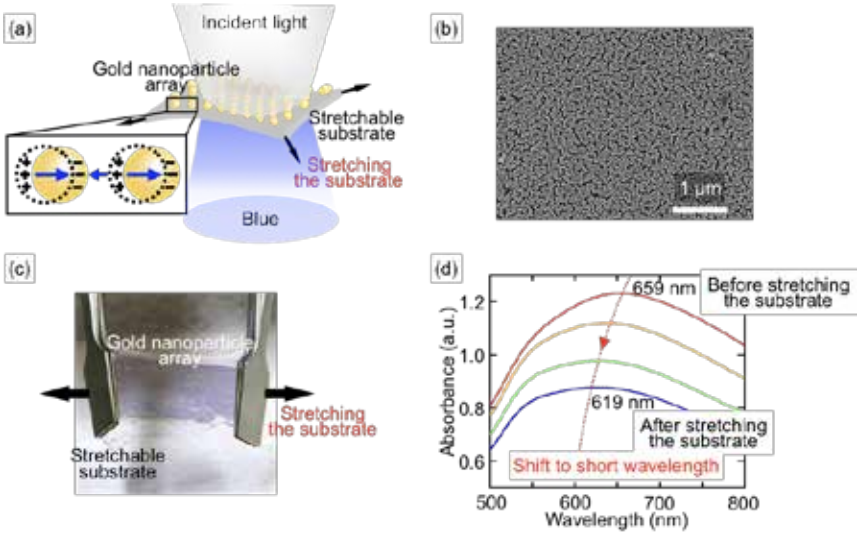

Fig.1 (a) Schematic diagram of gold nanoparticle array on stretchable substrate and surface plasmon oscillation in gold nanoparticles, (b) SEM image of closed-packed gold nanoparticle array, (c) Photo of elongated gold nanoparticle array on PDMS film, (d) Absorption spectra of gold nanoparticle array before and after stretching.

[1] Isabel Romero, *et al*., "Plasmons in nearly touching metallic nanoparticles: singular response in the limit of touching dimers", Opt. Express **14**, 21, 9988-9999 (2006).
[2] Yong-Jun Li, *et al*., "A Universal Approach for the Self-Assembly of Hydrophilic Nanoparticles into Ordered Monolayer Films at a Toluene/Water Interface", Angew. Chem. Int. Ed. **45**, 2537-2539 (2006).

P77

Control of expansion processes by counter shock waves during pulsed laser ablation

Keita Katayama[1], Toshiki Kinoshita[2], Hiroshi Fukuoka[2], Takehito Yoshida[3], Tamao Aoki[4], and Ikurou Umezu[4]
[1]Graduate School of Natural Science, Konan University, Kobe 658-8501, Japan
[2]National Institute of Technology, Nara College, Nara 639-1080, Japan
[3]National Institute of Technology, Anan College, Anan 774-0017, Japan
[4]Department of Physics, Konan University, Kobe 658-8501, Japan
Corresponding author: d1821002@s.konan-u.ac.jp

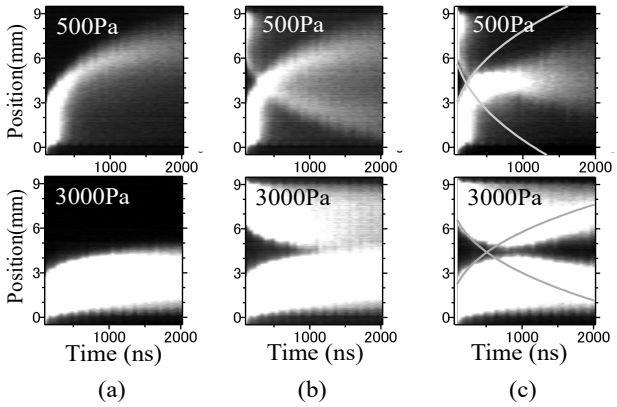

Effect of the shock wave on the expanding laser-induced-plume is very important for pulsed laser ablation in background gas. We have been proposed double pulsed laser ablation (DPLA) with two targets and two lasers in background gas to form complex nanoparticles. The conventional pulsed laser ablation with a target and a laser is named single laser ablation (SPLA) in the present paper. The collision of two expanding plasmas that are plumes is very important not only in the field of laser processing but also in fluid dynamics, plasma physics and astrophysics. Nb_2O_5 and Ni targets were set parallel to each other and irradiated simultaneously by two YAG lasers in He gas under various gas pressures. The contour plots of plume intensity as a function of time and distance from the target is shown in Fig.1. The results of Nb_2O_5 of SPLA are shown in Fig.1(a). The numerical superposition of the results of Nb_2O_5 and Ni plumes during SPLA are shown in Fig.1(b). The results of DPLA are shown in Fig.1(c). The lines in Fig.1(c) show estimated shock fronts. The effect of counter plumes is clearly observed when we compare Figs.1(a), (b) and (c). The plume expansion is suppressed by collision, and backward movement is observed at 3000 Pa. It should be noticed that backward movements of the plumes take place even though the plumes do not collide with each other. This means that collision takes place between plume and background gas and two plumes are immiscible at this background gas pressure. We estimated the effect of counter shock wave from viewpoints of Knudsen number and shock impedance. Below about 500 Pa, Knudsen number is less than 0.01 and plumes penetrate each other without fluid dynamic collision. Above about 500 Pa, Knudsen number is larger than 0.01, and the effect of counter shock should be considered. The velocity of expanding plumes after a collision with counter shock wave is determined by the ratio of shock impedance at ahead and behinds of contact front. The estimated shock impedance well describes experimental results. Our results suggest that control of plume expansion dynamics and design of complex nanoparticles could be possible by controlling Knudsen number and shock impedance.

[1] K. Katayama, Y. Hourai, H. Fukuoka, T. Kinoshita, T. Yoshida, T. Aoki, I. Umezu, Appl. Phys. A. **124**, 045328, 2018

P78

Impact of the Wall Roughness on the Quality of Micrometric Nozzles Manufactured from Fused Silica by Hybrid Laser Processing

Vidmantas Tomkus[1*], Valdas Girdauskas[2], Juozas Dudutis[1], Paulius Gečys[1], Valdemar Stankevič[1] and Gediminas Račiukaitis[1]

[1]Center for Physical Sciences and Technology, Savanoriu Ave. 231, LT-02300 Vilnius, Lithuania
[2]Vytautas Magnus University, Vileikos St. 8, 44404, Kaunas, Lithuania
[*]Corresponding author: vidmantas.tomkus@ftmc.lt

Femtosecond laser-plasma wakefield can accelerate electrons to GeV energies in few centimetres and produce betatron X-ray radiation with harmonics peaking in the range of tens and hundreds of keV [1]. Interest in ultrafast hard X-ray sources requires the formation of high-density gas targets of micrometric dimensions to maintain the laser pulse duration being equal to the time the laser beam is crossing the half of the plasma wavelength of the gas profile [2]. In this report, the impact of the wall roughness on the quality micronozzles with the diameter of 100, 200 and 300 µm on were investigated.

The gas jet concentration profiles of micronozzles were simulated using OpenFOAM® a compressible steady-flow solver rhoSimpleFoam with the basic Reynolds-averaged Navier–Stokes (RANS) ω-SST turbulence model [3]. The cylindrical nozzles were manufactured from fused silica using the nanosecond rear-side processing [4] and the hybrid Femtosecond Laser-assisted Selective Etching (FLSE) technique [5]. The average roughness R_a of the nanosecond rear-side milled surface was in the range of 4-6 µm and the sand roughness R_z = 15-20 µm. Surface roughness of the microchannel, fabricated with the FLSE technology and etched in the 10M KOH for 22 hours, was R_a = 120 nm and R_z = 568 nm.

The transversal gas density profile was determined using a Mach–Zehnder interferometer, continuous wave 632.8 nm He-Ne laser and CCD cameras. The density profiles were reconstructed using the Interferometric Data Evaluation Algorithms (IDEA) [6]. The gas concentration measured at the output of 100 µm cylindrical channel at the distance of 50 µm from the output of the nozzle was at 25 % lower in the channel with the higher sand roughness R_z = 15 µm relatively to the channel with the sand roughness of the wall R_z = 0.5 µm. The measured gas concentrations were $2.2 \cdot 10^{20}$ and $3 \cdot 10^{20}$ cm^{-3} correspondingly. The FSLE technology is preferred where low surface roughness and < 100 µm diameter microchannels are required. It is less effective than nanosecond rear-side processing where machining of high-volume parts is necessary.

[1] S. Cipiccia, M. R. Islam, B. Ersfeld, R. P. Shanks, E. Brunetti, G. Vieux, X. Yang, R. C. Issac, S. M. Wiggins, G. H. Welsh, M. P. Anania, D. Maneuski, R. Montgomery, G. Smith, M. Hoek, D. J. Hamilton, N. R. C. Lemos, D. Symes, P. P. Rajeev, V. O. Shea, J. M. Dias, and D. A. Jaroszynski, "Gamma-rays from harmonically resonant betatron oscillations in a plasma wake," Nat. Phys. **7**, 867–871 (2011).
[2] E. Esarey, C. B. Schroeder, and W. P. Leemans, "Physics of laser-driven plasma-based electron accelerators," Rev. Mod. Phys. **81**, 1229–1285 (2009).
[3] O. C. Ltd., "The Open Source CFD Toolbox, Version v1712," (2017).
[4] P. Gečys, "Nanosecond Laser Processing of Soda-Lime Glass," J. Laser Micro/Nanoengineering **10**, 254–258 (2015).
[5] X. Zhao and Y. C. Shin, "Femtosecond laser drilling of high-aspect-ratio microchannels in glass," Appl. Phys. A **104**, 713–719 (2011).
[6] V. Tomkus, V. Girdauskas, J. Dudutis, V. Stankevic, G. Raciukaitis, and G. Račiukaitis, "Characterisation of Tuneable Gas Target Profiles for Laser Wakefield Acceleration," in *High-Brightness Sources and Light-Driven Interactions* (OSA, 2018), p. EM3B.4.

P79

The approximations of the Boltzmann transport equation for modelling of ultrafast photoconductive terahertz antennas

Gediminas Šlekas[1,2], Raimondas Čiegis[1], Žilvinas Kancleris[2*]

[1]Vilnius Gediminas Technical University, Faculty of Fundamental Sciences, Saulėtekio Ave. 11, LT-10223, Vilnius, Lithuania
[2]Center for Physical Sciences and Technology, Department of Physical Technologies, Saulėtekio Ave. 3, LT-10257 Vilnius, Lithuania
Corresponding author: gediminas.slekas@ftmc.lt

Photoconductive terahertz antennas (PCA) based on a low temperature grown gallium arsenide (LT-GaAs) are one of the most popular and most promising terahertz (THz) wave generators developed so far [1]. Although THz radiation has very broad and substantial application field, all THz antennas, including PCA, have extremely low optical to terahertz power conversion efficiency, which leads to high usage costs and limited usability [1]. This problem has attracted the attention of a significant part of the scientific community, leading to many publications on the investigation of THz phenomena.

Despite many efforts [1-3], the theoretical models of PCA are still quite limited. The models created up to now are based on simplified approximations of Boltzmann's transport equation (BTE) which is coupled with Poisson or Maxwell equations. The most popular carrier transport models are obtained from the moments of BTE, which are obtained integrating the equation with degrees of impulse variable. For obvious reasons, only equations for lowest order moments are solved, which makes the model an approximation. Another problem with this approach is that in the last equation, higher order moment appears as the extra unknown, so the closure relation should be added to the model. The whole information about the remaining higher order equations has to be packed into this closure.

Drift-diffusion (DD) model is the simplest non-trivial carrier transport model which is derived as the zeroth order moment of BTE. The conventional closure relation for the current unknown is drift and diffusion approach. For many decades, DD has been used as a basic tool for simulation of semiconductor devices. However, in the active area of PCA strong electric field creates a velocity overshoot (VO) effect, which can make great impact on the dynamics of photocurrent. VO is not described by DD equations, so higher order transport models are used to include this effect into calculations. However, higher order models still require a lot of fine-tuning and a detailed understanding of the underlying physical phenomena [4].

We investigated the effect of simplified approximations of BTE on the accuracy of the PCA model based on LT-GaAs. We have used Monte Carlo simulation as the golden tool for verification of different approximations of BTE.

[1] X.-Ch. Zhang, J. Xu, *Introduction to THz wave photonics*, (Springer, 2010).
[2] R. Emadi, R. Safian, and A. Z. Nezhad, Theoretical Modeling of Terahertz Pulsed Photoconductive Antennas Based on Hot-Carriers Effect, *IEEE J. Sel. Topics Quantum Electron.*, **23,** 1-9 (2017).
[3] N. Khiabani and Y. Huang and Y. C. Shen and S. Boyes, Theoretical Modeling of a Photoconductive Antenna in a Terahertz Pulsed System, *IEEE Trans. Antennas Propag.*, **61,** 1538-1546 (2013).
[4] T. Grasser, T.-W. Tang, H. Kosina, and S. Selberherr. A review of hydrodynamic and energy-transport models for semiconductor device simulation, *Proceedings of the IEEE*, **91,** 251-274 (2003).

P80

Microstructure and mechanical properties of parts obtained by Direct Metal Laser Sintering

Genrik Mordas, Andrius Šlivinskas, Karolis Stravinskas, and Gediminas Račiukaitis

Center for Physical Sciences and Technology, Savanoriu Ave. 231, LT-02300 Vilnius, Lithuania
Corresponding author: genrik.mordas@ftmc.lt

New manufacturing technologies, such as Direct Metal Laser Sintering (DMLS), allow producing high-quality metal tools and prototypes of extremely complex geometries. The microstructure and mechanical properties of fabricated parts are affected by the DMLS process parameters (laser energy, laser scanning speed) [1] and the powder properties (particle size, shape and chemical composition). This study has been performed to expose an effect of different metal powders on the microstructure and mechanical properties of manufactured parts.

The selected metal powders were EOS MP1, EOS 316L and LPW GP1. They were characterised by different chemical composition (MP1 - cobalt-based (61.8%), 316L and GP1 - iron-based (62,1 and 73,8% resp.)) and different particles size distribution (10-100 µm, 20-120 µm and 10-80 µm resp.). The test samples were manufactured by utilising the DMLS technology applied in EOSINT M280. EOSINT M280 has a 200 W of 1030 nm built-in Yb fibre laser and a high-speed (up to 7 m/s) scanner comprising precision galvanometer (11 µrad) with temperature compensation. The F-theta objective focuses a laser beam at a building area in 100 µm. In this study, the set DMLS parameters were: laser power – 190 W, scanning speed – 7 m/s, layer thickness – 40 µm, gas - nitrogen. They were fixed for all used powders. Within, the produced parts stand out in surface roughness (Fig. 1) and cross-section microstructure. So, the roughness was higher for iron-based parts (EOS 316L - 13.72 µm; LPW GP1 - 11.41 µm) comparison with cobalt-based (EOS MP1 - 3.00 µm). The cross-section of iron-based parts had a higher defect content compared with cobalt-based ones too. It is explained in both iron-based materials have lower thermal conductivity and higher melting temperature than cobalt-based ones. Also, the cobalt-based parts characterised a monolithic microstructure comparing with polycrystalline grain structure of iron-based.

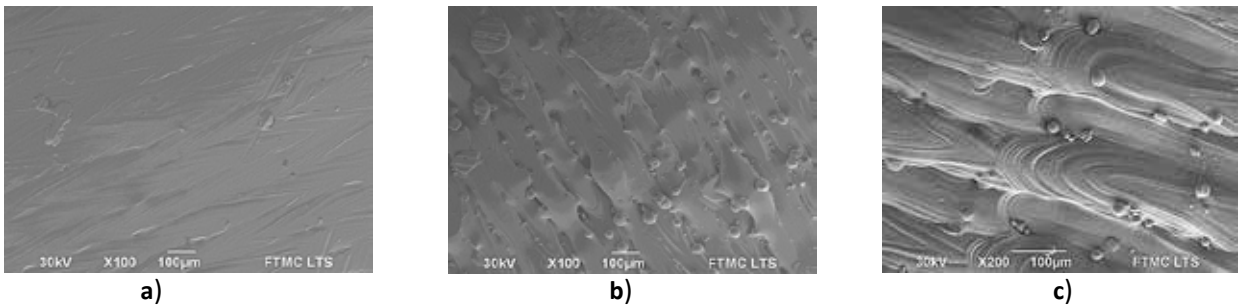

a) b) c)

Fig. 1 The parts surface microstructure produced from (a) EOS MP1 (b) EOS 316L and (c) LPW GP1.

[1] M.D.Viramgama, M.C.Karia. Study and investigation of influence of process parameters for selective laser melting. *IJEDR* 4(1), pp. 578-585 (2016).

P81

Infrared-laser precipitation of Dy-Yb codoped SrF_2 nanocrystals in glass and emission enhancement

Gangseon Ji[1], Chang-hyuck Bae[1], P. Babu[2], Ki-Soo Lim[1]*

[1]Department of Physics, Chungbuk National University, Cheongju, 28644, Republic of Korea

[2]Department of Physics, SVCR Govt. Degree College, Palamaner-517408, India

*Corresponding author: kslim@chungbuk.ac.kr

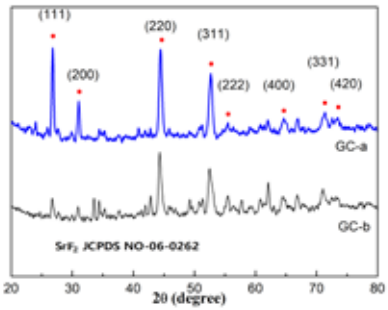

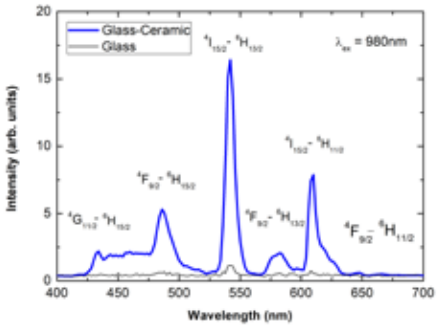

Oxyfluoride glass ceramics are traditionally fabricated using controlled heat treatments in an electric furnace, and nanocrystals are formed in the interior of glass [1]. Rare-earth ion doped glass ceramics may become potentially useful for optoelectronic applications. Recently, laser irradiation of glass has been reported as an alternative method for glass ceramic formation with an advantage of spatially selected structural modification and crystallization inside glass [2]. We present a novel and simple method to enable spatially selective SrF_2 nanocrystal formation on the surface of SiO_2–Al_2O_3–SrF_2-LiF-Dy_2O_3-Yb_2O_3 glass prepared by melt-quenching technique with controlling CO_2 laser power and scan speed. Micro-x-ray diffraction (Fig. 1) and high-resolution transmission electron microscopy revealed the SrF_2 crystal formation and the mean size and morphology. Optimized scan speed and laser power produced nanocrystals with the sizes of less than 10 nm. Energy dispersive spectroscopy mapping analysis showed that Dy^{3+} and Yb^{3+} ions are highly populated inside the nanocrystals. We also report much enhanced down-converted visible emission from the $^4F_{9/2}$ state of Dy^{3+} ions in the glass-ceramics compared with the glass under 365 nm excitation. Enhanced Stark splitting features also support the incorporation of rare-earth ions into crystalline domain. Moreover, the 980 nm laser diode excitation produced strong and additional blue emissions from the $^4I_{15/2}$ and $^4G_{11/2}$ states of Dy^{3+} ions which were not observed in down-conversion emission (Fig. 2). We proposed a model to explain the blue upconverted emissions by energy transfer from efficient sensitizer Yb^{3+} ions to Dy^{3+} ions.

[1] P. P. Fedorov, A. A. Luginina, A. I. Popov, Transparent oxyfluoride glass ceramics, *J. Fluor. Chem*. **172**, 22-50 (2015).

[2] Masaki Kanno, Tsuyoshi Honma, and Takayuki Komatsuw, Two-Dimensional Mapping of Er^{3+} Photoluminescence in CaF_2 Crystal Lines Patterned by Lasers in Oxyfluoride Glass, *J. Am. Ceram. Soc.*, **92**, 825–829 (2009).

P82

Spatial-Temporal Dynamics of Vortex Light Bullet at Femtosecond Filamentation in Kerr Media

O. Fedotova[1,2*], O. Khasanov[1], T Smirnova[2], E.Gaizauskas[3] and G. Rusetsky[1]
[1] Scientific-Practical Material Research Centre, NAS of Belarus, Brovki 19, Minsk 220072, Belarus
[2] Belarusian State University, Nezalezhnasci Ave. 4, Minsk 220030 Belarus
[3] VULRC Universiteto 3, Vilnius 01513, Lithuania

Corresponding author: olfe@physics.by

Spatiotemporal localization of femtosecond high-intensive pulses and related phenomena are key issues for challenging applications like remote sensing, high-precision micro- and nano-machining, communication and transmission systems [1]. We analyze nonlinear spatio-temporal dynamics of the intense femtosecond vortex pulsed beam in Kerr media under anomalous GVD [2] resulting in the formation of topologically charged light bullets. The model exploited is based on the system of modified nonlinear optical Schrödinger equation for the complex envelope of the electric field, and rate equation for the electron plasma density assuming the main ionization mechanism is multi-photon absorption. The two-scaled variational approach allowed us to obtain the system of motion equations for temporal and spatial beam radii in order to estimate possible stability regions for vortex light bullet. Finite-difference numerical simulations confirm the variational analysis results demonstrating more feasible conditions for light bullet formation for input beam transverse and temporal widths. We show that dynamics of temporal *T(z*) and spatial *R(z)* radii under propagation can be reduced to the dynamics of nonlinear coupled oscillators, at this *T(z)* and *R(z)* may oscillate: in phase as well in anti-phase (Fig. 1).

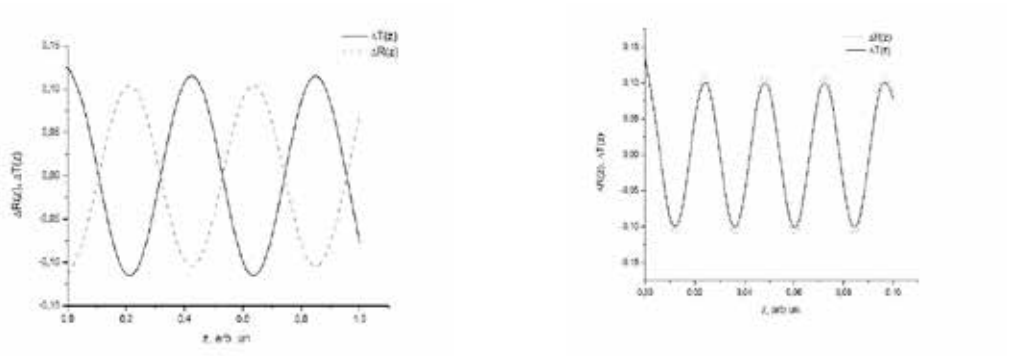

Fig. 1 Dynamics of spatial and temporal radii of the light bullet at their initial values are slightly detuned from the potential energy minimum: left: antiphase oscillations; right: “in-phase” oscillations

The light bullet with input parameters corresponding to the potential function minimum propagates without any oscillations of pulse radii. The threshold condition is established between topological charge *m* and relation α of input pulsed beam power to the critical for self-focusing.

[1] R.Kammel, J. Gotte, S. Skupin, et al., Enhancing precision in fs-laser material processing by simultaneous spatial and temporal focusing, *Light-Science & Applications* 3, e169 (2014).
[2] D.Majus, G.Tamošauskas, A.Dubietis, et al., Nature of Spatiotemporal Light Bullets in Bulk Kerr Media, *Phys. Rev. Lett.* 112, 193901 (2014).

P83

Forming accelerating light beams with phase masks fabricated from glass

Mykolas Karpavičius, Simas Butkus, Domas Paipulas, Valdas Sirutkaitis
Vilnius University, Faculty of Physics, Laser Research Center, Sauletekio Ave. 10, Vilnius, Lithuania
mykolas.karpavicius@ff.stud.vu.lt

Accelerating beams are a novel type of beams that have attracted considerable attention in various applications including optical particle clearing, light-sheet microscopy and laser micromachining [1]. Formation of an accelerating beam requires modulating the wavefront of a Gaussian beam with a specific phase which is most commonly accomplished utilizing a spatial light modulator (SLM). However, SLMs have a low optical damage threshold and thus are not an optimal choice for material processing where large average power settings are involved. In this work, we demonstrate an alternative way of modulating the phase of a Gaussian beam using a binary phase mask fabricated from glass plates by cutting or inducing local refractive index changes.

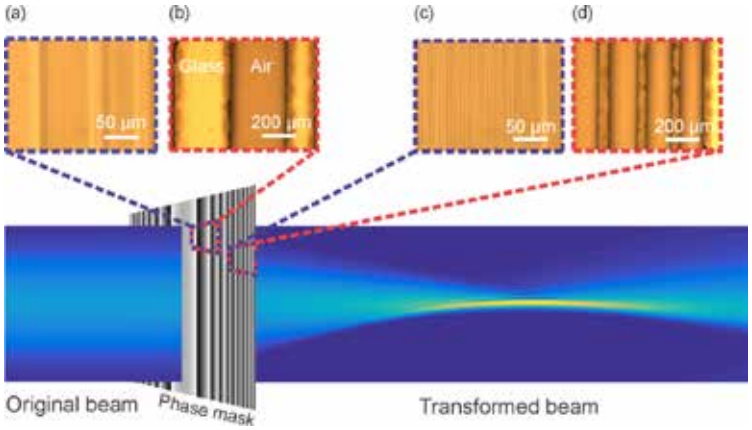

Figure 1: Schematics for forming an accelerating beam. Phase masks were fabricated with two methods - by modifying the refractive index of glass (a, c) and by cutting out parts of the glass plate (b, d).

Two methods of fabricating binary glass phase masks were tested: one 6 mm diameter mask was cut by ablation in water [2] from 0;1 mm thick soda-lime glass using a femtosecond Yb:KGW laser another was fabricated by inducing refractive index change [3] in 1 mm soda-lime glass. Local refractive index changes created by 260 fs pulses with 0.75 µJ energy in single layer amounts to 0.003-0.008 which is not enough to create a phase shift of π. To rectify this a total of 50 layers were written into the glass. The phase masks were tested by passing a Gaussian beam through them and imaging the resulting beams over a set distance using a CCD camera. Both masks formed beams that propagated along the predesigned trajectories. Our experimental results are in good agreement with theoretical modeling results and the phase mask manufactured by inducing refractive index change shows good promise for potential future applications.

[1] A. Mathis, F. Courvoisier, L. Froehly, L. Furaro, M. Jacquot, P. A. Lacourt, J. M. Dudley (2012) Micromachining along a curve: Femtosecond laser micromachining of curved profiles in diamond and silicon using accelerating beams, Appl. Phys. Lett., 101, 071110.
[2] S. Butkus, E. Gaizauskas, D. Paipulas, Z. Viburys, D. Kaskelyte, M. Barkauskas, A. Alesenkov, V. Sirutkaitis (2014) Rapid microfabrication of transparent materials using filamented femtosecond laser pulses, Applied Physics A, 114, 81-90.
[3] V. R. Bhardwaj, E. Simova, P. B. Corkum, D. M. Rayner, C. Hnatovsky, R. S. Taylor, B. Schreder, M. Kluge, J. Zimmer (2005) Femtosecond laser-induced refractive index modification in multicomponent glasses, J. Appl. Phys., **97**, 083102.

P84

Structuring of geometric phase microoptics *via* 3D laser nanolithography

Simonas Varapnickas[1], Etienne Brasselet[2], Rūta Pakalnytė[1], Saulius Juodkazis[3], Mangirdas Malinauskas[1]
[1]Laser Research Center, Faculty of Physics, Vilnius University, Saulėtekio Ave. 10, LT-10223, Vilnius, Lithuania
[2]Laboratoire Ondes et Matière d'Aquitaine, CNRS, Université Bordeaux 1, 351 Cours de la Libération, 33405 Talence, France
[3]Nanotechnology facility, Swinburne University of Technology, John st., Hawthorn, 3122 Vic, Australia

Corresponding author: simonas.varapnickas@ff.vu.lt

The development of novel light structuring methods attracted a huge research effort due to their impactful applications in communications, laser material processing or 3D micromanipulation. For some time bulky spatial light modulators have been a primary choice for tailored light fields generation, but now are being replaced by all-dielectric metasurfaces. Various techniques including e-beam lithography, focused ion beam milling or laser nano-inscription in fused silica for geometric phase micro-optical elements (GPμOE) manufacturing were investigated and reviewed [1]. Even the combination of the additive 3D structuring and the subtractive subwavelength resolution patterning was demonstrated [2].

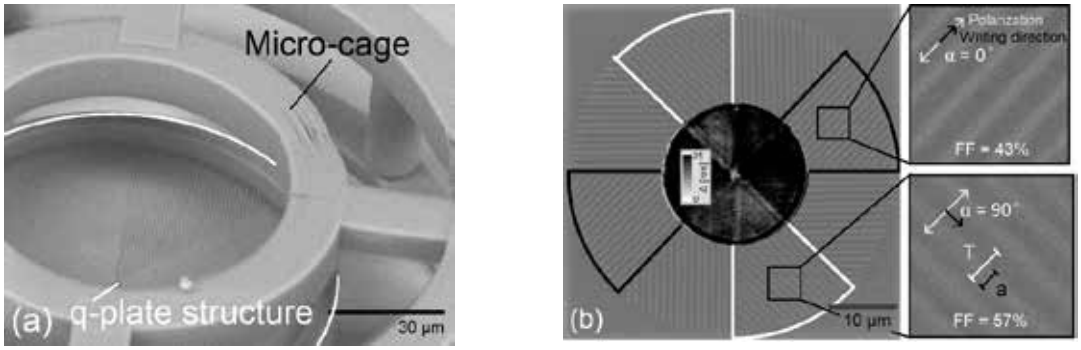

Fig 1 (a) an SEM micrograph of free-floating q-plate element trapped in a polymer micro-cage; (b) the filling factor (FF = a/T) variation on the writing beam polarisation angle (α) with respect to writing direction and its influence to wave retardance (Δ).

We propose fabricating of GPμOE *via* direct laser write (DLW) 3D nanolithography as an efficient way to produce highly integratable micro-devices, since they can be stacked with other polymer optical components, mounted on glass/crystal substrates, dielectric thin film membranes, fiber tips or even left free-floating (as shown in Fig 1 (a)). The possibility to fabricate GPμOE *via* DLW was first time reported by Wang et al. [3]. However, the polarization conversion efficiency of only a few percents was demonstrated as the retardance of single-layered polymer structure is limited by the voxel's aspect ratio, typically around 1:3. In this work, we demonstrate an improvement of the DLW fabrication procedure *via* fine polarization control of the writing beam (Fig 1 (b)) and optimization of the pre-polymer composition. The resin of our choice is a hybrid organic-inorganic prepolymer SZ2080, exhibiting a low shrinkage, broadband optical transparency (0.4 – 2.5 μm) and a decent laser-induced damage threshold [4]. We use a non-photosensitized prepolymer, which is beneficiary due to higher structuring resolution and lower absorption. Using SZ2080 prepolymer doped with polymerization quencher (2(dimethylamino)ethyl methacrylate (20% wt.)) leads to further increase in structuring resolution – up to 24% thinner lines written using same pulse energy for a wide range of exposition regimes (10^2-10^5 pulses/μm).

[1] H. Rubinsztein-Dunlop et al., *J. Opt.* **19**(1) (2017)
[2] A. Balčytis et al., *Opt. Express*, **24**(15) (2016) [
3] X. Wang et al., *Appl. Phys. Lett.* **110**(8) (2017)
[4] L. Jonušauskas et al., *Materials*, **10**(1) (2017)

P85

Direct laser writing of spin-orbital angular momentum coupler microstructures

Ryosuke Shoyama[1], Saulius Juodkazis[2], Vygantas Mizeikis[1]
[1] Research Institute of Electronics, Shizuoka University, 3-5-1 Johoku Hamamatsu 432-8011, Japan
[2] Centre for Micro-Photonics, Swinburne University of Technology, Hawthorn, VIC 3122, Australia
Corresponding author: mizeikis.vygantas@shizuoka.ac.jp

Macroscopic dielectric optical elements for generation of structured light that carries orbital angular momentum are highly sought in micro-photonics, but their fabrication is often problematic since optical anisotropic materials with the precisely controlled orientation of their optical axes are required. Recently, spin-orbital angular momentum coupler microstructures (also known as Q-plates) exploiting shape birefringence in periodically structured media were fabricated using direct laser writing (DLW) technique in photoresist[1]. Such an approach based on 3D laser nano-printing is highly attractive since it allows one to control optical anisotropy via macroscopic structuring of materials rather than modification of their intrinsic properties. However, high spatial uniformity and precise height control of the printing is required in order to improve the efficiency of Q-plates, which is presently too low (on the order of few percents) for practical applications. We have fabricated a series of Q-plate structures in photoresist SZ2080 deposited on a glass substrate using a femtosecond DLW technique, and investigated their structural uniformity and optical properties at visible wavelengths. Optical images of the structures and their height scans performed by Atomic Force Microscopy (AFM) illustrate their high structural quality and nearly-uniform height (Fig. 1 (a,b)). We have imaged the fabricated samples in a polarization optical microscope (POM) to reveal their shape birefringence, which is seen in the images (Fig. 1 (c)) as alternating dark and bright sectors in the Q-plate. These findings allow one to expect higher efficiency and purity of spin-orbital conversion using the fabricated samples. The DLW technique used for fabrication of Q-plates is scalable for writing flat optical elements having a size from micro- to centimeter scale.

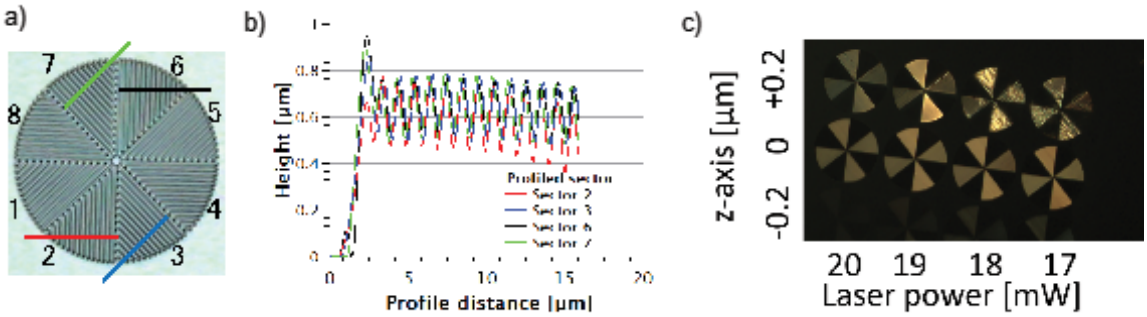

Fig. 1 Optical microscopy image of a Q-plate sample (a), comparison of AFM profiles taken in different sectors, showing height uniformity of the structure (b), optical microscopy image of several samples taken between crossed linear polarizers (c).

[1] X. Wang, A.A. Kuchmizhak, E. Brasselet, S. Juodkazis, "Dielectric geometric phase optical elements fabricated by femtosecond direct laser writing in photoresists," Appl. Phys. Lett. **110**, 181101 (2017).

P86

From Stealth Dicing at 1342 nm to Diamond Nanostructuring at 224 nm: Emerging Opportunities for a New Mode-Locked Laser

Ernestas Kuodys [1], Aleksej M. Rodin [1,2] and Andrejus Michailovas [1,2]

[1] Center for Physical Sciences and Technology, Savanoriu Ave. 231, LT-02300 Vilnius, Lithuania
[2] Ekspla Ltd, Savanoriu 237, LT-02300 Vilnius, Lithuania

Corresponding author: aleksej.rodin@ftmc.lt

Laser emission near 1342 nm wavelength finds applications in stealth dicing, environmental sensing and surgical treatment [1,2]. Wavelength conversion into the red 671 nm or into the blue 447 nm is attractive for laser TV and printing, medical diagnostics and treatment. We describe the development of a high repetition rate, multiple output wavelength mode-locked laser, which covers a wide range of applications with an emphasis on efficient generation of the sixth harmonic at 224 nm. This wavelength is suitable for lithography and microprocessing, such as the manufacturing of fiber Bragg gratings [2]. Besides, the energy of the corresponding quantum of 5.54 eV exceeds the bandgap of the diamond manufactured by CVD, which opens the possibility of laser induced periodic surface structuring (LIPSS) with high throughput and ~ 50 nm scale to reduce Fresnel losses [3] or to enhance absorption in diamond solar cells [4].

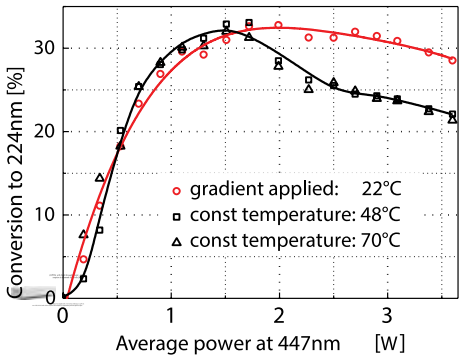

Fig. 1 Mode-locked Nd:YVO4 laser with 1342 nm, 671 nm and 447 nm output wavelength (left). Conversion efficiency to 224 nm versus the average power at 447 nm with (circles) and without (squares and triangles) a temperature gradient applied (right).

To improve the conversion efficiency to 224 nm wavelength at repetition rates 75 – 300 kHz we developed a microprocessor-controlled oven for BBO nonlinear conversion crystal providing the longitudinal temperature gradient. Fundamental 1342 nm radiation of Nd:YVO4 laser with pulsewidth of ~ 13 ps was converted to 224 nm wavelength with an average power of over 1 W. The laser also provides on demand 1342 nm, 671 nm and 447 nm output wavelength with an average power of 10 W, 6 W and 4 W at 300 kHz. Further possibilities will be discussed for a wavelength conversion to 1634 nm and 2089 nm by stimulated Raman scattering (SRS) in diamond.

[1] A.M. Rodin, M. Grishin and A. Michailovas, Picosecond laser with 11 W output power at 1342 nm based on composite multiple doping level Nd:YVO4 crystal, Optics and Laser Technology 76, 46 – 52 (2016). http://dx.doi.org/10.1016/j.optlastec.2015.07.022
[2] P. Koch, J. Bartschke and J.A. L'huillier, Single-mode deep-UV light source at 191.7 nm by seventh-harmonic generation of a high-power, Q-switched, injection-locked 1342 nm Nd:YVO4 laser, Appl.Opt. 55, 1871 – 1877 (2016). http://dx.doi.org/10.1364/AO.55.001871
[3] E. Granados, M. Martinez-Calderon, M. Gomes, A. Rodriguez and S.M. Olaizola, Photonic structures in diamond based on femtosecond UV laser induced periodic surface structuring (LIPSS), Opt.Express 25, 15330 – 15335 (2017). https://doi.org/10.1364/OE.25.015330
[4] D.M. Trucchi, A. Bellucci, M. Girolami, M. Mastellone and S. Olrando, Surface texturing of CVD diamond assisted by ultrashot laser pulses, Coatings 7, 185 – 202 (2017). https://doi.org/10.3390/coatings7110185

P87

Photonic crystals for visible wavelength via physical vapour deposition

Darius Gailevičius[1,2], Lina Grinevičiūtė[3], Vytautas Purlys[1,2], Tomas Tolenis[3], Roaldas Gadonas[1], Kestutis Staliunas[4,5]

[1]Vilnius University, Faculty of Physics, Laser Research Center, Sauletekio Ave. 10, Vilnius, Lithuania
[2]Femtika LTD, Sauletekio Ave. 15, LT-10224, Vilnius, Lithuania
[3]Center for Physical Sciences and Technology, Savanoriu Ave. 231, LT-02300 Vilnius, Lithuania
[4]DONLL, Departament de Física, Universitat Politècnica de Catalunya (UPC), Edifici Gaia, Rambla Sant Nebridi 22, 08222, Terrassa, Spain
[5]Institució Catalana de Recerca i Estudis Avancats (ICREA), Passeig Lluís Companys 23, 08010, Barcelona, Spain
Corresponding author: darius.gailevicius@ff.stud.vu.lt

Spatial (angular) filtering by photonic crystal (PhC) structures [1] has already proven itself as a useful alternative to conventional techniques. It is being implemented in different applications, among others for in-cavity angular filtering for microlasers [2]. The PhC sp. filters so far were fabricated and designed in so-called Laue diffraction regime, where the waves diffract predominantly in the forward direction: no photonic stop-gap present. The lattice constants (along with the optical axis and the transverse direction: a_z ~ tens of microns and $a_{x,y}$ ~ several microns) for Laue regime are well accessible by optical fabrication techniques in organic or inorganic materials [3, 4].

The spatial filtering is, in principle, possible also in the so-called Bragg regime. However, as the a_z must be comparable with half-wavelength λ/2, the optical fabrication techniques can be hardly used. Holographic method, despite successful initial experiments [5], requires ultraviolet sources and complicated optical systems. As an alternative, we propose and consider the possibility of fabricating such spatially filtering photonic structure by Glancing angle deposition method. Note that the spatial filtering structure in the Bragg regime should have $a_{x,y}$ of several microns, and $a_z < \lambda$.

Fabrication procedure is as follows: we use a polymer diffraction grating with a pitch of a_x = 1.67 µm as a geometry template for the PhC, and then we deposit alternating layers of SiO_2 and Al_2O_3. The layers optical thickness is selected to be of a quarter of a He-Ne laser wavelength: $a_z/2 = \lambda/4 \approx 158$ nm.

The structures were characterized with a scanning electron microscope after focused ion beam milling, and by illuminating them with a He-Ne laser. The diffraction patterns show promising results; however, at this early stage, it is still premature to provide the convincing evidence of spatial filtering.

[1] L. Maigyte, K Staliunas, Spatial filtering with photonic crystal, *Appl. Phys. Rev*. **2**, 011102 (2015)
[2] D. Gailevicius, V. Koliadenko, V. Purlys, M. Peckus, V. Taranenko, K. Staliunas, Photonic Crystal Microchip Laser, *Sci. Rep.* **6**, 34173 (2016).
[3] L. Maigyte, T. Gertus, M. Peckus, J. Trull, C. Cojocaru, V. Sirutkaitis, and K. Staliunas, Signatures of light-beam spatial filtering in a three-dimensional photonic crystal, *Phys. Rev. A* **82**, 043819 (2010)
[4] V. Purlys, L. Maigyte, D. Gailevičius, M. Peckus, M. Malinauskas, K. Staliunas, Spatial filtering by chirped photonic crystals, *Phys. Rev. A* **87**, 033805 (2013)
[5] M. Campbell, D. N. Sharp, M. T. Harrison, R. G. Denning, A. J. Turberfield, Fabrication of photonic crystals for the visible spectrum by holographic lithography, *Nature* **404**, 53–56 (2000).

P88

Influence of the third order nonlinearity on the instabilities in the synchronously pumped optical parametric oscillator

Viktorija Tamulienė[1], Adomas Gasperaitis[1]
[1]Vilnius University, Faculty of Physics, Laser Research Center, Sauletekio Ave. 10, LT-10223 Vilnius, Lithuania
Corresponding author: viktorija.tamuliene@ff.vu.lt

Theoretical study of the BBO-based singly resonant synchronously pumped optical parametric oscillator (SPOPO) is presented. In SPOPO, the second-order nonlinearity is utilized for the generation and amplification of the signal wave. The theoretical study usually omits the third-order nonlinearity [1]. In this work, we include the Kerr as well as XPM (cross-phase modulation) terms into the numerical model and demonstrate that these terms are crucial in the oscillatory as well as chaotic regimes of SPOPO. The influence of group delay dispersion and resonator detuning is elucidated, too. In Fig. 1, typical output signal profile dependence on the round-trip number at different resonator detuning is depicted. As we can see, oscillatory and chaotic regimes may appear. When the pump power increases and other parameters are fixed, the chaotic regime is achieved through the period doubling scenario. The structures are known as oscillating and chaotic dissipative solitons [2].

From the practical point of view, the chaos is harmful. In this study, the conditions when the unstable operation of SPOPO could be avoided are found.

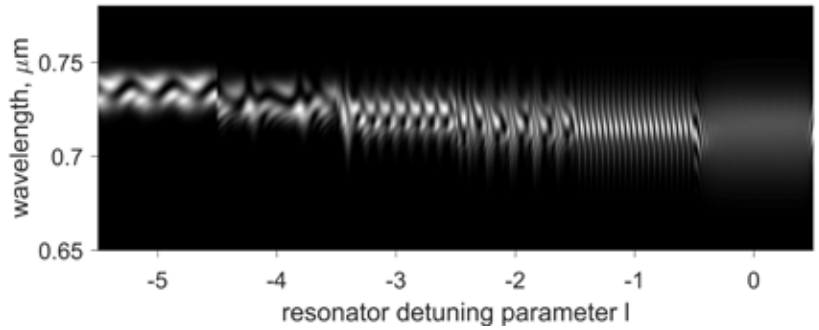

Fig. 1 Dependence of the output signal spectrum on the nondimensional resonator detuning parameter *l*. At each *l*, 600 round-trips are depicted. Negative group delay dispersion.

[1] R. Hamerly, A. Marandi, M. Jankowski, M. M. Fejer, Y. Yamamoto, H. Mabuchi, Reduced models and design principles for half-harmonic generation in synchronously pumped optical parametric oscillators, Phys. Rev. A **94**, 063809 (2016).
[2] N. Akhmediev, A. Ankiewicz, *Dissipative solitons*, (Springer, 2005).

P89

BBO Crystal for Characterization of mid-Infrared Laser Pulses

Gintaras Tamošauskas[1*], Gvidas Beresnevičius[1], Audrius Dubietis[1]

[1] Laser Research Center, Vilnius University, Saulėtekio Ave. 10, LT-10223 Vilnius, Lithuania
*Corresponding author: gintaras.tamosauskas@ff.vu.lt

Owing to its excellent optical properties (broad transparency range, high nonlinear optical coefficients, high damage threshold), beta barium borate (β-BaB_2O_4, BBO) is one of the most popular nonlinear crystals, which provides phase-matching for various second-order interactions almost over its entire transparency range (from 185 nm to 3.3 mm, as deduced from the transmittance measurements using crystal samples of several mm thickness) [1,2]. In this contribution, we demonstrate that thin (of few tens of mm thickness) BBO crystal exhibits reasonable transmittance and phase matching in the 3 − 5.2 mm range [3]. Refined dispersion equations of the ordinary and extraordinary refractive indexes for the 0.188 − 5.2 mm wavelength range indicates that thin (20 mm length) crystal can be phase-matched for sum-frequency generation over an ultrabroad wavelength range. In particular, reference pulse of 720 nm wavelength exhibits simultaneous phase matching over 1 − 5 mm range, see Fig. 1(a). This feature was exploited for simultaneous sum-frequency generation-based frequency-resolved optical gating of the signal and idler pulses from an optical parametric amplifier, and difference frequency pulse with central wavelengths of 1.3, 2.1 and 3.5 mm, respectively, as shown in Figs. 1(b) and 1(c). The crystal was oriented at a fixed θ =24° angle. Transmittance measurements suggest that present and other sum-frequency based techniques operation limit may be as far as 4.8 mm where absorption of BBO reaches 100 cm^{-1}.

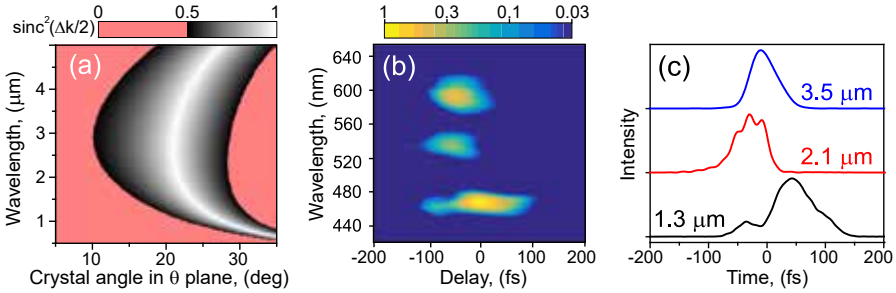

Fig. 1 (a) Phase-matching tolerance for sum-frequency generation with 720 nm wave in 20 mm BBO crystal. (b) Simultaneously recorded XFROG traces and (c) retrieved intensity profiles of the pulses with carrier wavelengths of 3.5, 2.1 and 1.3 mm.

Finally, the refined dispersion equations yield the phase matching for the second harmonic generation with incident wavelengths up to 4.4 mm, suggesting the possibility to characterize the mid-infrared laser pulses by means of self-referenced methods, such as spectral phase interferometry, chirp and dispersion scans, which typically employ very thin BBO crystals for broadband frequency doubling.

[1] D. Eimerl, L. Davis, S. Velsko, E. K. Graham, and A. Zalkin, "Optical, mechanical, and thermal properties of barium borate," J. Appl. Phys. **62**, 1968–1983 (1987).

[2] C. Chen, T. Sasaki, R. Li, Y. Wu, Z. Lin, Y. Mori, Z. Hu, J. Wang, G. Aka, M. Yoshimura, and Y. Kaneda, *Nonlinear optical borate crystals: principles and applications* (Wiley-WCH, 2012)

[3] G. Tamošauskas, G. Beresnevičius, D. Gadonas, and A. Dubietis, "Transmittance and phase matching of BBO crystal in the 3–5 μm range and its application for the characterization of mid-infrared laser pulses," Opt. Mater. Express **8**, 1410-1418 (2018)

P90

Simultaneous ultrabroadband nonlinear interactions in polycrystalline ZnS and ZnSe

Rosvaldas Šuminas, Julius Lukošiūnas, Agnė Marcinkevičiūtė, Gintaras Tamošauskas, Audrius Dubietis

Laser Research Center, Vilnius University, Saulėtekio Ave. 10, LT-10223 Vilnius, Lithuania
Corresponding Author: rosvaldas.suminas@ff.stud.vu.lt

Naturally grown polycrystalline materials consist of a large number of single-crystal domains with random orientations, sizes and shapes [1]. The random orientation of each individual crystallite leads to phase randomization and thus greatly relaxed phase matching conditions, which permit ultra-broadband frequency conversion by simultaneous three-wave interactions [2-4]. Of particular interest are polycrystalline zinc-blende semiconductors such as zinc-sulfide (ZnS) and zinc-selenide (ZnSe), which due to their isotropic nature, large transparency range, high values of the nonlinear refractive index and a nonzero second order-nonlinearity possess an attractive set of properties for use as nonlinear materials in the mid-infrared spectral range.

In this work, we investigate numerous ultrabroadband nonlinear interactions in ZnS and ZnSe samples of various thickness using 3.6 mm, 60 fs mid-infrared laser pulses and 1.33 mm and 2.02 mm near-infrared laser pulses. In the first case, we demonstrate the efficient broadband harmonic generation of up to the seventh order accompanied by a considerable spectral broadening around the fundamental wavelength [see Fig. 1 (a)-(b)]. In the second case, simultaneous sum (λ = 0.8 mm) and difference-frequency (λ = 4.0 mm) generation in 2-mm thick ZnS is demonstrated (see Fig. 1 (c) caption for details). In both cases, the relatively high efficiency of the process is attributed to high intensities reached during the filamentary beam propagation.

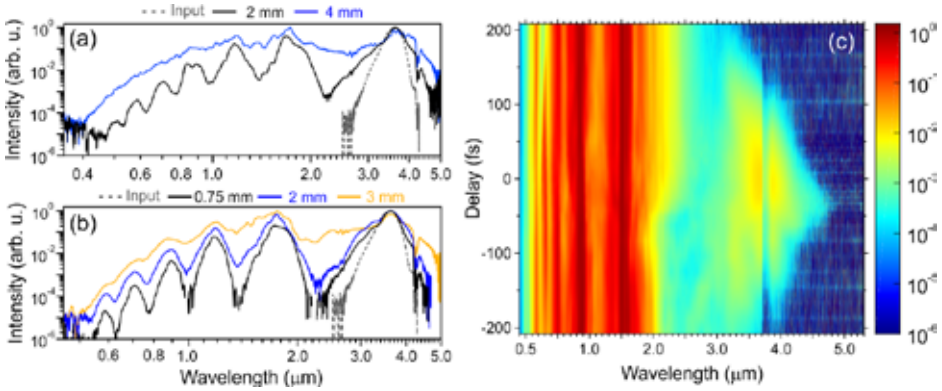

Fig. 1 The output spectra of various length (a) ZnS and (b) ZnSe samples using 3.6 mm, 0.73 μJ laser pulses. The dashed curves show the input pulse spectra. (c) Spectral dynamics obtained in a 2-mm thick ZnS sample using 1.33 mm, 1 μJ and 2.02 mm, 2.3 μJ signal and idler femtosecond pulses from an optical parametric amplifier with respect to the delay between them.

[1] A. Arie, N. Voloch, Periodic, Quasi-periodic, and Random Quadratic Nonlinear Photonic Crystals, *Laser Photonics Rev*. **4**, 355-373 (2010).
[2] M. Baudrier-Raybaut, R. Haïdar, P. Kuepecek, P. Lemasson, E. Rosencher, Random-quasi-phase-matching in Bulk Polycrystalline Isotropic Nonlinear Materials, *Nature* **432**, 374-376 (2004).
[3] X. Vidal, J. Martorell, Generation of Light in Media with a Random Distribution of Nonlinear Domains, *Phys. Rev. Lett*. **97**, 013902 (2006).
[4] R. Šuminas, G. Tamošauskas, G. Valiulis, V. Jukna, A. Couairon, A. Dubietis, Multi-octave Spanning Nonlinear Interactions Induced by Femtosecond Filamentation in Polycrystalline ZnSe, *Appl. Phys. Lett*. **110**, 241106 (2017).

P91

Filamentation of femtosecond mid-infrared pulses in crystalline silicon

Agnė Marcinkevičiūtė, Vytautas Jukna, Rosvaldas Šuminas, Sigita Balandytė, Gintaras Tamošauskas, Audrius Dubietis

Laser Research Center, Vilnius University, Saulėtekio Ave. 10, LT-10223, Vilnius, Lithuania
Corresponding author: agne.marcinkeviciute@ff.vu.lt

Femtosecond filamentation in transparent dielectric materials is a complex phenomenon governed by an interplay of self-focusing, self-phase modulation, multiphoton absorption/ionization and generation of free electron plasma. Possessing a very high nonlinearity, silicon is of particular interest not only for nonlinear photonics [1] but also as a host for femtosecond filamentation and supercontinuum (SC) generation in the mid-infrared [2,3].

In this work, we report on the filamentation and spectral broadening of 100 fs, 3.25 – 4.7 µm laser pulses in a 6.4 mm thick silicon crystal. A considerable boost in spectral broadening is observed as the input pulse wavelength is increased. In particular, more than an octave-spanning SC spectrum is measured with 4.7 µm input pulses spanning from 2.5 to 5.8 µm at the 10^{-4} intensity level (Fig. 1 (a) solid line) with the long-wavelength side being limited by the detection range of our measurement apparatus. Numerical simulations confirm an even more notable infrared extension of the SC spectrum (dash-dotted line). In addition, temporal self-compression of the axial part of the input beam during filamentation is expected due to free electron plasma formation at the trailing part of the pulse [Fig. 1 (b)]. According to the numerical model, during the filamentation of 4.7 µm, 108 fs, 260 nJ pulses, more than three-fold temporal self-compression is achieved yielding two optical cycles (35 fs) pulses [Fig. 1 (c)].

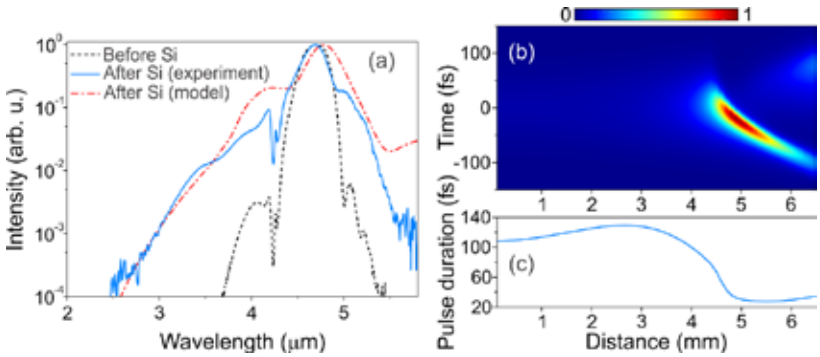

Fig. 1 (a) Normalized measured (solid blue line) and numerically calculated (red dash-dotted line) supercontinuum spectra in 6.4 mm thick silicon crystal. (b) Numerically calculated temporal dynamics and (c) full-width half-maximum (FWHM) pulse duration of the 4.7 µm pulse in a silicon crystal as a function of distance.

[1] J. Leuthold, C. Koos, W. Freude, Nonlinear silicon photonics, *Nat. Photon.*, **4**, 535-544 (2010).
[2] B. Kuyken, T. Ideguchi, S. Holzner, M. Yan, T. W. Hänsch, J. Van Campenhout, P. Verheyen, S. Coen, F. Leo, R. Baets, G. Roelkens, N. Piqué, An octave-spanning mid-infrared frequency comb generated in a silicon nanophotonic wire waveguide, *Nat. Commun.* **6**, 6310 (2015).
[3] A. Blanco-Redondo, C. Husko, D. Eades, Y. Zhang, J. Li, T. F. Krauss, B. J. Eggleton, Observation of soliton compression in silicon photonic crystals, *Nat. Commun.* **5**, 3160 (2014).

P92

Tuneable z-scan setup as a versatile tool to improve the efficiency of PDT and high resolution 3D printing

Wolfgang Steiger[a,c], Peter Gruber[a,c], Agnes Dobos[b,c], Elise Zerobin[b,c], Robert Liska[b,c], Aleksandr Ovsianikov[a,c]
[a] Institute of Materials Science and Technology, TU Wien, Austria
[b] Institute of Applied Synthetic Chemistry, TU Wien, Austria
[c] Austrian Cluster for Tissue Regeneration

The z-scan technique has emerged as a standard methods to characterize nonlinear absorption properties of materials.[1] The highly localized absorption behaviour of these materials has allowed for a wide range of applications such as high resolution 3D printing using two-photon polymerization (2PP) [2] as well as photodynamic therapy (PDT)[3]. However, since most z-scan setups operate at a single wavelength the information about spectral performance of the absorbers is quite limited. Matching the wavelength used in 2PP or PDT processes to the peak absorption of the material leads to a vast increase in performance.

To determine the optimal absorption wavelength we have developed z-scan setup which is completely automated and therefore easy to handle. Based on a tuneable fs laser it can determine the nonlinear absorption spectrum from 690 to 1040 nm. Various photoinitiators (PI), which are required for 2PP, were screened to show that matching the wavelength used for structuring to the absorption maximum of the PI dramatically increases the polymerization performance. Furthermore, we screened various PDT agents to determine their absorbance window for cell culture experiments. To quantify the treatment efficiency cells were encapsulated and irradiated with the optical system operating at the peak absorption wavelength to demonstrate the efficiency of the screened agents.

[1] E. W. Van Stryland and M. Sheik-Bahae, "Z-scan measurements of optical nonlinearities," *Charact. Tech. Tabul. Org. Nonlinear Mater.*, pp. 655–692, 1998.
[2] A. Ovsianikov, V. Mironov, J. Stampfl, and R. Liska, "Engineering 3D cell-culture matrices: multiphoton processing technologies for biological and tissue engineering applications," *Expert Rev. Med. Devices*, vol. 9, no. 6, pp. 613–633, Nov. 2012.
[3] M. Khurana, H. A. Collins, A. Karotki, H. L. Anderson, D. T. Cramb, and B. C. Wilson, "Quantitative In Vitro Demonstration of Two-Photon Photodynamic Therapy Using Photofrin ® and Visudyne ®," *Photochem. Photobiol.*, vol. 83, no. 6, pp. 1441–1448, Nov. 2007.

P93

Nonlinear response of and energy deposition in bulk silicon and germanium driven by intense femtosecond laser

Tzveta Apostolova and Boyan Obreshkov
Institute for Nuclear Research and Nuclear Energy, INRNE-BAS, Sofia, Bulgaria

Femtosecond laser-induced energy absorption and optical breakdown of three single crystal group IV elemental semiconductors – carbon, silicon and germanium, is studied for laser wavelengths in the near- and mid-infrared spectral regions using the Time dependent Schrodinger equation in one electron approximation[1,2]. The dependence of the photoelectron density and deposited energy on the laser intensity and wavelength are obtained. For mid-IR wavelengths and low field strength, material-specific threshold for the onset of energy absorption into the bulk is found, while for near-IR wavelengths the energy transfer to electrons occurs via multiphoton absorption. For high field strength, absorption of energy becomes wavelength independent and increases linearly with increase of the laser intensity. During the irradiation, part of the energy stored in the electronic system is transferred back to the radiation field via high harmonic generation. The dependence of the spectral intensity of the emitted harmonics on the driving laser field strength is obtained[3].

[1] Lagomarsino, S. Sciortino, B. Obreshkov, T. Apostolova, C. Corsi, M. Bellini, E. Berdermann, and C. J. Schmidt, "Photoionization of monocrystalline CVD diamond irradiated with ultrashort intense laser pulse", Phys. Rev. B vol. 93, pp. 085128, 2016
[2] T. Apostolova, B. Obreshkov , A.A. Ionin A.A. , Kudryashov S.I., Makarov S.V., Mel'nik N.N. , Rudenko A.A., "Ultrafast photoionization and excitation of surface-plasmon-polaritons on diamond surfaces", Applied Surface Science, vol. 427, pp. 334, 2018
[3] T. Apostolova, B. Obreshkov, "High harmonic Generation from Bulk Diamond driven by Intense femtosecond laser pulse", Diamond and Related Materials, 82, 165, 2018

P94

Fabrication of carbonaceous pattern based on liquid polymer and laser

Yong-Won Ma[1], Junhan Park[2], Bo Sung Shin[2,3]

[1]Pusan National University, Interdisciplinary Department for Advanced Innovative Manufacturing Engineering, 2, Busandaehak-ro 63beon-gil, Geumjeong-gu, Busan, Republic of Korea
[3] Pusan National University, Department of Cogno-Mechatronics Engineering, 2, Busandaehak-ro 63beon-gil, Geumjeong-gu, Busan, Republic of Korea
[3] Pusan National University, Department of Optics and Mechatronics, 2, Busandaehak-ro 63beon-gil, Geumjeong-gu, Busan, Republic of Korea

Corresponding author: bosung@pusan.ac.kr

It is generally known that carbon materials are produced by laser irradiation due to pyrolysis. Therefore, a number of the studies are made by directly irradiating solid polyimide substrates. However, when the substrates changed to the carbon materials, substrates durability is deteriorated. We report the fabrication of carbonaceous pattern by liquid polyimide (PI) and 355 nm nanosecond laser. The patterns were investigated by scanning electron microscopy (SEM), Fourier-transform infrared spectroscopy (FTIR) and x-ray photoelectron spectroscopy (XPS). The proposed process is directly curing the liquid polymer and it is characterized by making the conductive patterning easily without damaging the substrate.

Author index